NASA TM- 75490

NASA-TM-75490 19800002216

A Reproduced Copy

NASA TM- 75490

Reproduced for NASA

by the

NASA Scientific and Technical Information Facility

FFNo 672 Aug 65

UTTL: Fundamentals of heat measurement ---- heat flux transducers
AUTH: A/GERASHCHENKO, O. A.
CORP: National Aeronautics and Space Administration, Washington, D.C.
        AVAIL.NTIS
SAP: HC A11/MF A01
CIO: U.S.S.R. Transl. by Kanner (Leo) Associates, Redwood City, Calif.
        Transl. into ENGLISH of ""Osnovy Teplometrii"" (Kiev), Naukova Dumka
        Press, 1971 p 1-192
MAJS: /*FLUX DENSITY/*HEAT FLUX/*HEAT MEASUREMENT/*TEMPERATURE MEASUREMENT/*
        TRANSDUCERS
MINS: / CALORIMETERS/ CONDUCTIVE HEAT TRANSFER/ MEDICAL SCIENCE/ RADIATION
        PYROMETERS/ REACTOR PHYSICS
ABA: Author

ABS: Various methods and devices for obtaining experimental data on heat flux
        density over wide ranges of temperature and pressure are examined.
        Laboratory tests and device fabrication details are supplemented by
        theoretical analyses of heat-conduction and thermoelectric effects,
        providing design guidelines and information relevant to further research
        and development. A theory defining the measure of correspondence between
        and development. A theory defining the measure of correspondence between   MORE

  ENTER:

NASA TECHNICAL MEMORANDUM

FUNDAMENTALS OF HEAT MEASUREMENT

O. A. GERASHCHENKO

NATIONAL AERONAUTICS AND SPACE ADMINISTRATION
WASHINGTON, D.C. 20546   AUGUST 1979

1. Report No. NASA TM-75489	2. Government Accession No.	3. Recipient's Catalog No.
4. Title and Subtitle Fundamentals of Heat Measurements		5. Report Date September 1979
		6. Performing Organization Code
7. Author(s) O. A. Gerashchenko		8. Performing Organization Report No.
		10. Work Unit No.
9. Performing Organization Name and Address Leo Kanner Associates Redwood City, California 94063		11. Contract or Grant No. NASw- 3199
		13. Type Report and Period Covered Translation
12 Sponsoring Agency Name and Address National Aeronautics and Space Administration, Washington, D.C. 20546		14. Sponsoring Agency Code

15. Supplementary Notes
Translation of "Osnovy Teplometrii," Naukova Dumka Press, Kiev, 1971, 192 pp. (A72-35495)

16. Abstract Various methods and devices for obtaining experimental data on heat flux density over wide ranges of temperature and pressure are examined. Laboratory tests and device fabrication details are supplemented by theoretical analyses of heat-conduction and thermoelectric effects, providing design guidelines and information relevant to further research and development. A theory defining the measure of correspondence between transducer signal and the measured heat flux is established for individual (isolated) heat flux transducers subject to space and time-dependent loading. An analysis of the properties of stacked (series-connected) transducers of various types (sandwich-type, plane, and spiral) is used to derive a similarity theory providing general governing relationships. The transducers examined are used in 36 types of derivative devices involving direct heat loss measurements, heat conduction studies, radiation pyrometry, calorimetry in medicine and industry and nuclear reactor dosimetry.

17. Key Words (Selected by Author(s))	18. Distribution Statement Unclassified-unlimited

19. Security Classif. (of this report) Unclassified	20. Security Classif. (of this page) Unclassified	21. No. of Pages 233	22. Price

ANNOTATION

The monograph presents basic information on the theory, designs, and applications of devices for measuring heat flows over a wide range of densities and temperatures. Results of studies in a new field of measurement--heat-measurements.

The book is intended for scientific personnel and engineers working in different fields of the national economy. It can serve as a textbook for students in senior courses in institutions of higher learning of the corresponding specialties.

FOREWORD

Measuring the density of heat flows takes on prime impor-
tance for most experimental investigations and industrial pro-
cesses. Successes in building new equipment and methods invar-
iably promoted the appearance of new tasks; solving these tasks
posed new requirements on equipment and theory. This "chain
reaction" led to the advent of an autonomous field of measure-
ment technology--heat-measurements, just as fundamental a method
of experimental physics as thermometry, electrometry, and mag-
netometry, spectroscopy, and thermal dosimetry.

Thermometry unites the methods and means for obtaining
experimental information about the density of heat flows. Heat-
measurement equipment is employed not only for investigation, but
also for monitoring and regulating processes in the most wide-
ranging fields of the national economy.

Usually investigators and practitioners used heat-measure-
ments as an auxiliary means; this led to the dissipation of
manpower and the irrational employment of time with frequent
repetition of developments. Therefore, as long ago as 1955 the
author of this monograph started systematizing accumulated ex-
perience with the aim of preparing the fundamentals for develop-
ing special methods of theoretical and experimental studies,
approaching in standardization, for example, the methods of
electrical measurements. The results of generalizing borrowed
and one's own experience accumulated as of 1964 constituted the
object of exposition in the monograph _Tekhnika teplotekhniches-
kogo eksperimenta_ /Techniques of Heat-Measurement Experiments/,
written by the author together with V. G. Fedorov. In an
abridged version, these materials became part of the reference
handbook _Teplovyye i temperaturnyye izmereniya_ /Thermal and Tem-
perature Measurements/, published in 1965. Both books, judging
from letters received and references in publications were ap-
proved by the scientific and engineering community.

Compared with previous publications, this book heavily
revised and updated the overview section; original investiga-
tions were redescribed. Over the past six years the arsenal of
heat-measurement instruments was significantly renewed; the
temperature range of measurements was extended, supported by
reliable calibration (80-870° K); the number of absolute cali-
bration devices was increased; and measurement accuracy went up.

iii

In parallel with the experimental studies and technological developments, a theoretical analysis was made of the complex of thermal conductivity and thermoelectricity phenomena; this opened up the possibility of determining worthwhile forms of structures and arriving at rational research orientations. The operational characteristics of sensitive elements confirm the theory worked out.

For isolated transducers applied to loads varying in space and in time a theory was formulated that establishes a measure of correspondence of generated signal to the measured flow. All transducer dimensions were optimized.

From an analysis of the properties of battery transducers of different types (sandwich-type, disk-type, and spiral-type) a theory of similarity was derived, for arriving at generalized functions and deducing calculation formulas.

Based on the proposed transducers, 36 types of derived instruments were designed and introduced for direct measurements of heat losses, determining thermal conductivity, radiation pyrometry, biomedical, and technological calorimetric investigations, dosimetry in nuclear reactors, and so on. These instruments are widely used in research and industrial practice. Their use makes it possible to reduce heat losses, lower consumption of thermal insulation, determine heat-physical properties of new substances, correctly estimate the items of heat balance in heat-power and refrigeration installations, to effectively monitor and automate new industrial processes, and so on.

Information gained by heat-measuring units is not confined to heat transport phenomena. For example, a correlation was discovered between thermal conductivity and the strength of fiber glass-reinforced plastics, which makes nondestructive tests possible. When fiber glass-reinforced plastics were tested for fatigue, it was found that over a wide range the dissipation energy in the unit cycle does not depend on the working stress. Generalization of these experiments must foster progress in the autonomous direction of investigations --heat-flow fault detection.

iv

LIST OF SYMBOLS

$A, B, b, C, D, k, k_1, k_2, k_3$ = coefficients; constants

a = coefficient of thermal diffusivity; coefficient of absorption (with subscripts)

f = cross-sectional area

f_t = transducer area

e = electromotive force

l = length

R = electrical or thermal resistance

T, t = temperature

I = strength of electric current

i = density of electric current

P = power

p = perimeter; pressure

$x, y, z, \xi, \eta, \zeta$ = spatial coordinates

κ, ϕ, ψ = dimensionless coordinates

Q = heat flux

q = density of heat flux

α = geometrical angle; heat transfer coefficient; Seebeck thermoelectric coefficient

Δ, δ = thickness

ε = emissivity

λ = coefficient of thermal conductivity

μ = time constant

π = Peltier coefficient; ratio of circumference to diameter

ρ = specific electrical resistance

σ = Stefan's constant; mechanical stress

∂ = dimensionless temperature; geometrical angle

τ = time

$\bar{\tau} = a\tau/l^2$ = dimensionless time

TABLE OF CONTENTS

FUNDAMENTALS OF HEAT MEASUREMENT

O. A. Gerashchenko
Laboratory of Methods of Heat Measurement, Institute of
Engineering Heat Physics, Ukrainian SSR Academy of Sciences

CHAPTER 1: METHODS OF HEAT FLOW MEASUREMENT

This chapter gives information about the development of the /5* main ideas behind existing methods and instruments for measuring heat flows. The fields of knowledge for which thermal measurements are vital are extraordinarily varied. Geothermal studies of regions from permafrost to volcanoes; actinometric investigations of the Earth, Sun, and far-off stars; heat measurements of organisms, organs, and tissues in biology and medicine; technical and physical thermal measurements all the way to measurements in nuclear reactors and on spacecraft--a far from complete list of areas where heat measurements play a considerable role.

Different fields of knowledge have their own specific methods and styles that delineate them from each other. So the classification adopted is largely conditional. Some information is given in a concise form.

Most information centers on instruments and methods; the following chapters expound on these instruments and methods with the fullest continuity. This is especially true of compensation methods and the auxiliary wall method, on which the following chapters are based.

Less attention is given to indirect measurements in different autonomous regions, for example, infrared techniques. Finally, technical problems of instrumental applications are examined in a most compressed way.

1. Use of Energy of Change of State

Calorimetric measurements serve in determining the energy of state changes in matter over a wide range of physical parameters to an accuracy no worse than 1 percent.

Transformations of the solid phase into the liquid phase and back again are especially convenient for physical experiments.

---

* Numbers in the margin indicate pagination in the foreign text.

The line of these transitions for most substances is much removed from the triple point and coincides with the isotherm; the energies of compression are negligibly small for solid and liquid media. So the energy of the change of state is virtually independent of pressure. This fact was noted even by Lavoisier and Laplace, who more than 150 years ago proposed an ice calorimeter, later improved on by Bunsen.

Heat-measuring elements whose basis is the Bunsen calorimeter layout find wide use even at the present time. The F. Ye. Voloshin pyrheliometer /178/ shown in Fig. 1. is one such example.
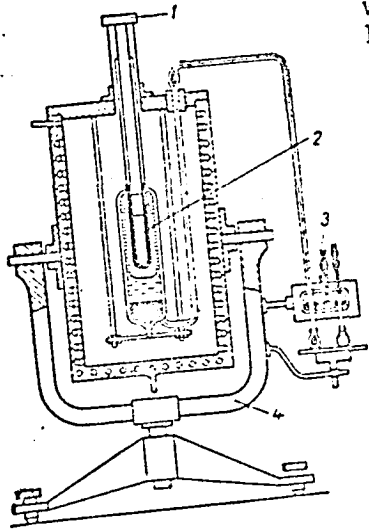
Premised on this same principle is an instrument for determining thermal conductivity; with this instrument heat is brought to a specimen and removed from it using eutectic salt solutions /105/. From the amount of brine formed during the melting one estimates the quantity of heat passing through the specimen. By suitable selection of the composition of the solute substances and the solvents, one can vary the mean temperature of the test specimen over fairly wide limits.

Fig. 1. F. Ye. Voloshin pyrheliometer
1. receiving diaphragm
2. Bunsen chamber
3. measuring unit
4. parallax stand

The heat flows in convective heat transfer can also be conveniently estimated from the amount of melted or sublimated substance. G. N. Kruzhilin and V. A. Shvab described the experiments of Klein: in his work local heat flows were determined from the amount of melted ice as ice cylinders were swept with air /146, 147/. In the air some of the liquid formed is able to evaporate; finding how much this is, is very difficult. So Klein's results cannot be used when determining heat transfer from unmodified surfaces (for example, metal cylinders).

Heat transfer to smooth cylinders from a large volume of liquid (water, benzene, and ethylene-glycol) was investigated by A. G. Tkachev /221/. When he interpreted the experimental data he did not take into account the possibility of the heat fluxes varying along the perimeter of the swept body. Evaporation from the surface was precluded. The appearance of the liquid phase was not taken into consideration. The deviation proved to be the largest for horizontal cylinders.

The heat of melting can obviously be recommended for use in quiescent conditions of measuring weak effects (Lavoisier-Laplace, Bunsen, Voloshin, and Dushin-Nikolayevskiy). But in those cases when unmonitorable mass transport is superimposed on heat transfer (Kleyn and Tkachev), use of the heat of fusion can give only qualititative results.

The advantages of determining the amount of energy from the amount of evaporated or condensed liquid come from the physical property of substances preserving their isobaricity during isothermicity and vice versa. Because of this, by maintaining the same pressure with relatively simple procedures, the identity of temperatures can be achieved; this permits setting up separating partitions with zero thermal flow, that is, insulators that are near-ideal.

One of the first successful attempts in building a steam calorimeter is described in $/\overline{8}/$. To find the heat capacity of different bodies, metals and alloys in particular, a preweighed body is heated for a long time in a high-boiling liquid, then quickly placed in a vessel containing a low-boiling liquid at the boiling point. Ethyl ester and acetaldehyde are used as the low-boiling liquids. The heat of cooling of the test body is estimated from the volume of evaporated liquid.

In 1887 Bunsen proposed a steam calorimeter in which the heat of reaction is determined from the amount of liquid condensed on the body.

Applying the heat of vaporization is widely in practice today. A standardized supply of energy is afforded ordinarily by the condensation of steam. To measure the mean heat flow, the test section is enclosed in two coaxial metal housings. Both housings are fed with gently superheated steam at the same pressure; therefore the walls of the inner housing are isothermal and do not allow heat to escape. The only energy user in this case is the test tube, located in the inner housing. The condensate is removed from it separately and under measurement. From the amount of condensate at known steam parameters we estimate the heat flow.

Superheating the steam a few degrees avoids the chance of the liquid phase falling into the housings. Losses through the structural members owing to thermal conductivity are determined in "dry run" experiments of the installation. This arrangement was used in studying heat transfer to the air within the long tube $/\overline{229}/$ and by studying heat transfer when there is boiling on flat plates heated from within with condensible steam $/\overline{212}/$.

3

Difficulties cropped up because of the need of sectionalizing steam heating to get the local characteristics. Drew and Ryan /146/, in studying heat transfer from the surface of a cylinder transversely swept by air, divided the cylinder into compartments and measured the flow of condensate from each compartment separately. They were able to get the flow values averaged over fairly large areas. Similar methods were applied also by other researchers /15, 97, 99, 276/.

Measurement of the heat flow from the amount of evaporated liquid is used in the instrument described in /237/ for determining the coefficient of thermal conductivity by the plate method (Fig. 2). Housing 4 filled with boiling liquid serves as the chiller in the instrument. The central vessel 5 has separate steam removal; the steam is directed to the removable coil 2. The volume of the condensate formed is measured with graduated cylinder 8. Steam from the circular (guard) part of the vessel condenses on the cooled coil 1 in the top part of the vessel. A similar device was proposed for determining the coefficients of thermal conductivity of vacuum insulation materials with different mechanical loads /90/.

A similar method was used in an investigation of intensifying heat transfer in the tube because of inserts perturbing the air flow and in a study of heat transfer from the air to the tube in the case of large flow rates /99, 107/.

The amount of evaporated liquid was recorded either from the volume flow of the feed liquid or from the volume flow of liquid condensed into steam.

Fig. 2 Steam calorimeter for determining thermal conductivity:
1. internal coil
2. removable coil
3. vessel of removal coil
4. instrument housing
5. central vessel
6. test specimen
7. heated plate
8. graduated cylinder
9. silite heater
10. thermal insulation

The error in heat flow measurements relying on the use of the energy of transformations of the states of matter usually does not exceed 5 percent. Sometimes the error can be lowered to 1 percent in calorimetric measurements.

2. Liquid-Enthalpy Method

This method is based on the fact that when acted on by a measured heat flow a liquid cooling a receiving vessel undergoes a change in enthalpy. It is used just as often as described in the preceding section. The two methods differ in that, for determining the change in the cumulative enthalpy, besides the volume flow of the cooling medium the change in temperature must be measured. Doing the latter invol es sizable difficulties: where the measured heat is supplied (or removed), the temperature is inevitably distributed unevenly in the cooling medium; but if the medium succeeds in being mixed fairly well, losses and perturbations have an effect.
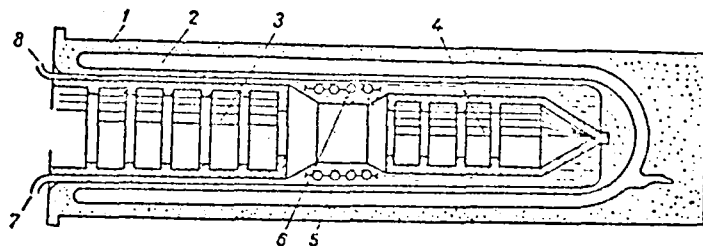
Fig. 3   C. G. Abbot water-jet pyrheliometer:

1. instrument housing
2. Dewar flask
3. calibration section
4. receiving-absorbing section
5. thermometric device at inlet
6. thermometric device at outlet
7. inlet of cooling water
8. outlet of cooling water

When radiant energy is measured in the atmosphere, use is made of the so-called water-jet actinometer that W. A. Michelson proposed in 1900 and that C. G. Abbot (Fig. 3) developed in 1905. The receiver was made in the form of a hollow conical model of an absolute blackbody bathed by water. To reduce the errors of measurement, the temperature of the cooling water is kept at the ambient air temperature.

In the United States and Latin American countries the water-jet instrument is regarded as an absolute instrumeter: all actinometric instruments are compared with it. The accuracy of these measurements made with accuracy customary for astronomers can be judged from the following quotation /10/: "The so-called verified Smithsonian scale of 1913, based on measurements with two absolute instruments--water-jet and water-jacketed

pyrheliometers, provided approximately 2.5 percent overstated
values; this was arrived at by Abbot and Aldrich on a new elec-
trically compensated pyrheliometer in 1932. Comparison with
data of the Angstrom compensation pyrheliometer disclosed yet
another large difference; however, here we must take into ac-
count the correction for thermal conductivity in the Angstrom
pyrheliometer. After allowing for the correction, this differ-
ence will be 2.3-2.4 percent. Measurements by other kinds of
absolute instruments give the same correction values. Thus,   /10
data of the 1913 Smithsonian scale at present must be decreased
by 2.4 percent."

Nonetheless the measurements
of Aldrich and Hoover, made in
1952, differ only by 1.8 percent
from the 1913 data. In 1956 the
"International Pyrheliometric
Scale of 1956" was adopted in
Davos; according to it, data of
the initial Angstrom scale must
be increased by 1.5 percent (the
correction for thermal conducti-
vity), and the data of the 1913
Smithsonian scale must be reduced
by 2 percent.

So the joint efforts of all
actinometrists with a large number
of instruments and observations
taken at many observatories in
the world for more than a century
made it possible to bring the
accuracy of measurement of the
radiant incident flux to 0.5 per-
cent. More exact data are ac-
cepted on agreement. In the
technical measurements the errors
of this method are usually con-
siderably, sometimes by one
order of magnitude, higher. Let
us look at some examples.

In studying heat transfer
from a hot gas jet to a
cooled plate, in various condi-
tions of jet streaming, K. P.

Fig. 4 Perry water-jet
calorimeter:

1. receiving plate
2. calorimeter housing
3. inlet connection for
   cooling water
4. stuffing box of differ-
   ential thermocouple
5. outlet connection of
   cooling water

Perry /3047 used a miniature water calorimeter; its layout is
shown in Fig. 4.

6

The plate swept with the hot jet is cooled with running water. The calorimeter proper (a 16.5 mm diameter metal plug) is inserted into an opening in the plate, on a 0.1 mm thick mica heat-insulating pad. The 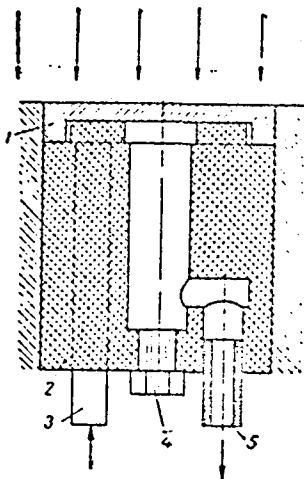rise in the temperature of the water cooling the calorimeter is measured with a chromel-constan battery of 40 thermocouples. In a standard copper-constantan thermocouple the copper is replaced with chromel--to reduce heat losses. The calorimeter body is made of an acrylate plastic--perspeks, which conducts heat poorly. One merit of the unit is that the temperature of the calorimeter surface does not differ from the temperature of the adjoining plate areas. So the calorimeter does not introduce perturbations into the thermal and hydrodynamic patterns of the test phenomenon.

When the heat transfer from the hot air to the cooled tube /11 was investigated for the case of high subsonic velocities by V. L. Lel'chuk, he measured the trend in the cooling water temperature along the tube and from its derivative local heat transfer was estimated /154/. Compressed air was injected into the water for better mixing. The heat balance was reduced to an error of ±5 percent. Taking note of the arduous experimental conditions, the measurement accuracy must be considered as high.

To verify the analytical method of calculating the flows from the readings of two thermocouples embedded at different depths in the wall of a rocket engine nozzle, when determining heat fluxes of approximately 10^5 W/m², A. Witte and E. Harper used a device similar to the Perry calorimeter /332/. The calorimeters were copper shells with envelopes of polyester resin, for organized flow of the cooling medium. The volume flow of water through each calorimeter was measured with a truncated Venturi cavitation nozzle, and the temperature rise--with chromel-constantan differential thermocouples.

Water-jet instruments were used for varied purposes by V. S. Dvernyakov and V. V. Pasichnyy /100/, S. S. Filimonov, B. A. Khrustalev, and V. N. Adrianov /228/, A. B. Willoughby /330/, and others.

3. Electrometric Method

Electric heaters are often used in experimental practice. Their advantages are the simplicity of control, compactness, and high accuracy in measuring the energy supplied. For a monitorable heat flux in the surface area under study there is need for reliable insulation; this can be obtained by using protective and compensation heaters. Organization of effective monitoring of heat losses complicates the experiment and makes the unit cumbersome.

7

One of the first successful proposals is credited to M. V. Kirpichev /129/. In studying heat transfer from a transversely swept cylinder, he had it placed tightly against platinum strips making up a row. Each strip simultaneously functioned as a heater, calorimeter, and resistance thermometer. Since the cylinder was entirely surrounded with heaters, heat loss from the strips into the cylinder-base body could be neglected.

Similar measurements were made by A. S. Sinel'nikov and A. S. Chashchikhin: they lined the porcelain cylinders with nichrome strips /207/.

In studying local heat transfer from plate to air in the case of large subsonic velocities, B. S. Petukhov, A. A. Detlaf, and V. V. Kirillov wound around a framework of delta-wood thin (0.25 mm) constantan ribbon 10 mm wide /180/. The gap (0.5 mm) /12 between the turns was filled with toothpaste. Copper-constantan thermocouples were secured to the ribbon with a thin layer of BF-2 insulating cement. The specific power was estimated from the current passing through the ribbon, and from the voltage drop. Because the resistivity of constantan does not depend on temperature, the voltage drop was adequately measured when done only at two points. The ribbon thermal conductivity was neglected. The measurement errors did not exceed ±2 percent. Of all the methods examined, this one is the most reliable.
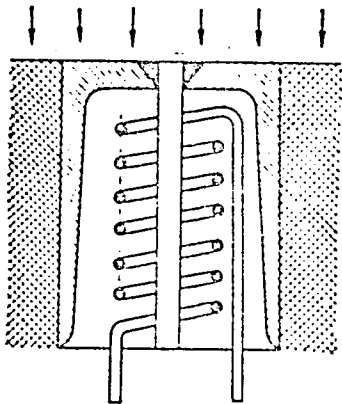
Fig. 5 L. A. Kuznetsov
electric calorimeter

When he investigated heat transfer from a rapidly rotating disk to air sweeping around the disk in pointed jets, L. A. Kuznetsov used a miniature electrical heater, shown in Fig. 5 /151/. Welded into a copper case, 10 mm in diameter, in its center was a constantan rod; around it the electric heater was formed in an insulating compound. From the constantan rod and the copper case stretch the corresponding like-valued conductors of the thermocouple measuring the temperature of the swept surface. The case was pressed into a slab of heat-insulating material; but the losses were found to be so large that they had to be determined in "dry run" experiments as a function of the calorimeter temperature.

8

In studying heat transfer in members of different kinds of machines, T. G. Sergiyevskaya /204/, V. A. Mal'tsev /158/, R. A. Seban /315/, and other investigators made similar measurements. In measuring local heat transfer from a uniformly heated sphere to a forced flow, Brown, Pitts, and Leppert /35/ assembled models of spheres of separately heated sections. The sphere consisted of 11 copper segments all the same in height (3.2 mm), separated with 0.25 mm thick teflon interlayers. Nichrome heater spirals were insulated with magnesium oxide and laid in stainless steel tubes. The heaters were laid tightly in circular grooves in each segment and connected in series with each other. The power values of the heater elements in the segments were the same; for the same lateral segment surfaces this was responsible for the constancy of the flow recorded from the spherical surface (the authors neglected the temperature effect on electrical resistance). To determine the local heat transfer coefficients, an iron-constantan thermocouple was mounted in each segment. /13/ The emf measurement scheme allowed connecting each thermocouple counter to the thermocouple measuring the temperature of the incident flow. The flow interval was $(2.2-12)\cdot 10^4$ W/m². In most of the experiments the error due to axial heat overflow did not exceed 5 percent and only in individual cases did the error climb to 15 percent (for small Reynolds' numbers).

Electric heaters standardized as to power values are used in measuring thermal conductivity in several metrologically legalized methods /186/, in the methods of A. B. Golovanov /90/, Ye. S. Platunov and V. V. Kurepin /184/, B. N. Oleynik, T. Z. Chadovich, and Yu. A. Kirichenko /175/, V. G. Shatenshteyn /239/, and others.

As a rule, electrometric units are used also in compensation circuits, examined in Chapter Nine of this book.

4. Dilato-resistometric and Thermoelectric Methods

In 1800, when investigating the distribution of the density of incident energy in the solar spectrum, Sir William Herschel used a high-sensitivity mercury thermometer /210/.

In 1825 D. Herschel used the blackened receiver of a mercury thermometer in measuring solar radiation--this instrument must evidently be regarded as the first pyrheliometer.

Later, Arago and Davy /9, 13/ proposed pyrheliometer designs in whose basis two thermometers were embodied, differing from each other by the fact that the receiver of one was blackened, and the other was left shiny. The receivers were arranged in a

9

row, the measuring stacks directed downward. Both receivers are simultaneously exposed to the radiation flux measured. The flow value is estimated from the difference in the measurements of the readings of the thermometers occurring during exposure.

The Arago-Davy instrument is convenient and simple so that it is in service at present /119, 120, 196/. N. N. Kalitin gave the thermometer receivers a spherical shape. Capillaries extend from the receivers from the spherical side, and the flat round parts of the receivers serve as receiving areas. The frame bearing the thermometers is placed on a parallax stand.

Poulliet designed a water-filled metal vessel with blackened bottom for receiving radiation; a mercury thermometer was placed in the vessel /209/. From the exposure time and the extent of heating of the unit, we can estimate the flux. Similar pyrheliometers improved by Abbot have been used effectively in the western hemisphere to the present time.
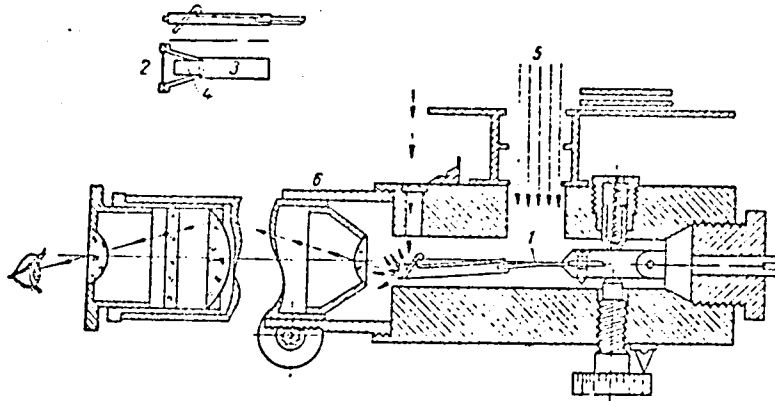
Fig. 6 W. A. Michelson actinometer:

1. bimetal plate
2. quartz filament
3. extension
4. reflecting shield
5. receiving window
6. microscope

In the Abbot actinometer the incident-energy detector is a massive silver body /120/. Its volume is reduced to the minimum necessary for accommodating the receiver of the mercury thermometer. For better contact, the cavity in which the thermometer bead is placed is filled with mercury and for the

0

REPRODUCIBILITY OF THE
ORIGINAL PAGE IS POOR

mercury not to dissolve the silver, the thermometer and the mercury are in an iron capsule dead-end pressed into the silver receiving body. The silver disk, the massive blind with several diaphragms, and a special angular thermometer are mounted on a parallax stand.

Other dilatometric systems, finding service in industrial thermometers, have also been used as thermometric receiving units in radiometers.

Employed quite widely, particularly in the USSR, is the bi-metallic actinometer proposed by W. A. Michelson /168/ and later improved by his students and his successors /120, 246/. Basic to the instrument (Fig. 6) is a thin (several tens of micro-meters) bimetallic (invar-iron) strip 1, located in a copper cylinder with a window 5 through which the exposure is made. By one side the strip is rigidly mounted on the housing, and by the other the extender 3, extruded of approximately 10 μm thin aluminum foil, is mounted by a boxlike cross-section. The detection strip is blackened by one of the accepted methods /187/. At one end the extender has a shield 4 whitened with hydrated magnesium carbonate and a quartz filament 2. During exposure, the bimetal plate is heated and its bending is recorded from the displacement of the quartz filament in the field of the microscope 6 mounted in the copper housing. The theory of the W. A. Michelson was elaborated by S. I. Savinov /198/.

K. Buttner /255/ worked out a version of the Michelson acti-nometer; in it, a panel with a receiving bimetal plate contains two more bimetallic sections, located during the exposure in the shadow and compensated against the receiving plate with change in the temperature of the actinometer as a whole. The scheme of the temperature compensation of the Buttner actinometer was used in the Novogrudskiy actinometer.

Fig. 7 N. N. Kalitin mono-metallic actinometer

Expansion of the monometal plate was used in the N. N. Kal-itin actinometer /118/, schema-tically shown in Fig. 7. Mounted on the invar support is a blackened constantan ribbon. In its middle section this ribbon is stretched toward the side with a spring. When the ribbon temperature rises, its deflection pointer swings over under the action of the pulling force of the

spring. The shift in the deflection pointer is recorded by an indicator. The ribbon is mounted on insulators; because of this the instrument can be calibrated from the power of the electric current passed through it. Given the thin ribbon thickness, the end effects owing to thermal conductivity are insignificant. Constructed on this same principle is the V. D. Tret'yakov mono-metallic actinometer /222/.

With the advent of thermocouples, the dimensions of the receiving bodies of the radiometers have been considerably reduced. The electrode cross-section was gradually brought to several square micrometers; as this was being done, the inertia of the thermocouples began to be measured in microseconds. Series connection of the thermocouples into so-called thermopiles and the considerable improvement in the galvanometers made it possible to raise instrumental sensitivity.

The sensitive thermoelectric elements are widely used in radiometry /120, 126, 246/. In particular, the S. I. Savinov instrument is employed in actinometry /197/; for measuring the heat fluxes passing through the walls of combustion chambers in rocket engines--the radiometers of D. P. Sellers /200/, G. Ye. Ozhigov, V. G. Smirnov, and Yu. A. Sokovishin /173/, and others.

Ordinarily, the receiving strips are blackened; but in some cases the value of the flux measured is so high that its absorption and removal are made difficult. To reduce the absorption, the receiver is sometimes made with high reflectivity.

As an example, we can mention the N. I. Alekseyev-L. M. Shestopalov calorimeter /16/ for measuring laser ray energies.

Boys in 1887 suggested short-circuiting the thermoelectric /16 circuit and, by placing it in a magnetic field, using it as a galvanometer frame /8, 210/. A schematic drawing of this device, which the author called a microradiometer, is shown in Fig. 8. The frame is suspended on a quartz filament; at the same strength the quartz filament is much more elastic than the metal suspensions of galvanometers. Because of the decreased electrical resistance down to a minimum, the microradiometer--given the same area of the receiving plate--has the highest sensitivity of presently known instruments. The large inertia and the capriciousness of instrument handling, as well as the complex manufacturing technology limit its wide application.

By increasing the sensitivity of the mirror galvanometer through focussing the reflected light spot on a secondary differential thermocouple, Moll and Burger in 1925 found the

equivalent sensitivity of the instrument to be approximately 10^{-11} A/mm, with the frame resistance of approximately 100 ohms /289-293/. Later, this idea was applied in photocompensation amplifiers; at present all the most sensitive series-manufactured electrical instruments are equipped with these amplifiers.

In waveguides thermoelectric and calorimetric series devices are used for recording intense long-wave fluxes. Complete and detailed descriptions of thermoelement designs are presented in the monograph of R. Smith, F. Jones, and R. Chesmer /210/ and in extensive articles by L. Geiling /268/ and R. Stair /317/.

Detailed bibliographic references on the sensitive elements of infrared detection systems are given in the reports of R. W. Wolf /333/, R. G. White /329/, and M. Kimmitt /127/.

A radiometric system in which change in temperature under the effect of measured radiation is recorded with a resistance thermometer is called, on Langley's suggestion, a bolometer /139/.

Fig. 8   Boys microradiometer:

1. window
2. mirror
3. circuit-frame
4. magnet
5. housing
6. receiving area
7. thermopile

In addition to thermoelectric systems, resistance thermometers are used successfully and in some temperature ranges the practical temperature scale is metrologically replicated. Since the sensitivity of these systems is sufficient for recording a temperature change of less than 0.001 deg, they are widely used in radiometric and especially spectrometric systems /161, 162, 166, 230/. The advent of thermistors did much to simplify the task of building wideband radiometers /322/.

/17

13

In recent years means of conscious control of the properties of substances have been noted in solid-state physics. As an example, we can mention thermistors: their temperature coefficient is nearly an order of magnitude higher than for wire resistances $\underline{/211, 213/}$.

In the case of independent control of the relationship of resistance with temperature, it becomes possible to use bolometric temperature amplifiers.

The heat balance equation of the bolometric element in vacuum has the following form:

$$P_{e.1} + P_{mea} = k(T^4 - T_0^4),$$ (I.1)

where $P_{e.1}$ is electrical losses, P_{mea} is the measured power of the absorbed radiation, and T_0 is the ambient temperature.

Usually the values of the electrical losses tend, as far as possible, to a minimum. The power of the electrical losses $P_{e.1}$ is expended in raising the receiver temperature. If the released power values are represented mainly in the measured parameter, the incremental heating can be regarded as a kind of thermal amplification of the signal.

When there is material present for which over some temperature range, the resistance can be approximated by the equation

$$R = k_1 T^4 - A,$$ (I.2)

we can select the current I_0 values and the ambient temperatures T_0 so that the equality

$$I_0^2 R = k(T^4 - T_0^4).$$ (I.3)

can be satisfied.

In this case, when the receiver current $I = I_0$, the receiver temperature will be indeterminate. When $I > I_0$, the system is unstable with regard to temperature and receiver is heated in an avalanche-like way to failure or the beginning of deviation from the function (I.2). If $I < I_0$, the system becomes stable and capable of responding in a radiometric bolometer to some incremental (measured) power. When there is a small difference $I_0 - I$, the small power received by the sensitive element causes significant changes in its temperature and resistance. Corresponding to a weak measured signal is the considerable, but

limited, heating of the receiver by means of electrical losses. /18
Unfortunately, Eq. (I.2) can be satisfied only in a very narrow
temperature range, therefore these amplifying circuits have not
yet far found practical application.

5. Evaporographic Method

One of the first attempts at recording images in infrared
illumination by the evaporographic method was successfully
achieved by M. Czerny /259/. Characteristic of the Czerny ex-
periments is the elaborate thought and simplicity of the equip-
ment (Fig. 9). The working chamber is formed in a 50 mm dia-
meter glass tube 2, 150 mm in length. The upper edge of the
tube at the burner is fitted to a cork 1; the lower edge is
polished and a celluloid membrane 5, 0.5 μm thick, coated from
beneath with turpentine black by the Rubens-Hoffman method,
is secured to the lower edge of the tube.
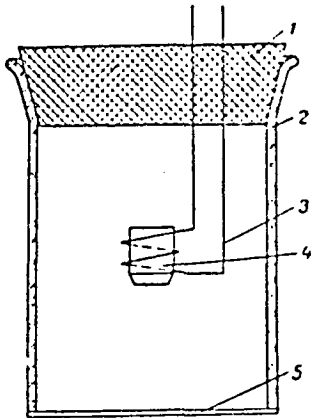
Fig. 9. M. Czerny infra-
ред chamber:

1. cork
2. glass tube
3. heating spiral
4. evaporation vessel
5. receiving membrane

A miniature glass test tube
4 filled with camphor oil, naph-
thalene, or some other heavy hydro-
carbon is suspended in the chamber
on heating spiral 3.

Heating spiral 3 is switched
on to prepare the chamber. The
hydrocarbon filling the test tube
melts, gradually evaporates, and
settles in a thin layer on the
chamber walls and the celluloid
membrane 5. Test tube heating
is ended when the white settled
mattelike layer evenly suppresses
its own interference film pattern.

When the image is exposed on
the blackened side of the film,
from the opposite side of the film
camphor sublimates at a rate that
is proportional to the energy il-
lumination of the section. Thus
the first long-lived visible images
of objects in infrared illumina-
tion were recorded.

In his studies, M. Czerny made mention of D. Herschel, who
in 1840 had recorded a visible image of a pattern in infrared
illumination by exposing it on filter paper soaked with ethanol,
evaporating faster from the more illuminated areas.

15

The technique of making celluloid films blacked with carbon black by the Rubens-Hoffman method, according to M. Czerny's description /258/, amounts to the following. The film is obtained by pouring cellulose nitrate varnish on water; film thickness depends on the water temperature. From the water the film is stripped off with a glass plate so that between the plate and the film remains a bubble-free water interlayer, and the edges are pendent. Then the film is smoked in a turpentine flame. The water interlayer between the film and the glass promotes cooling needed for the carbon black to settle. The evenness of the carbon black coating is monitored visually, and the absolute thickness is determined with reference samples. Sample replicates are dissolved in acetone and the parted carbon black is weighed.

M. Czerny determined the spectral permeability of carbon-black-coated celluloid films /258/. For example, for the case of a coating with a thickness of 34.2 mg/decimeter^2, there is the following transmission spectrum:

Wavelength, μm	0.9	4.4	52	92
Permeability, percent	0.0	1.8	50.7	67.7

When the density of the carbon black coating was increased, so did the wavelength at which transmission begins to considerably increase. Czerny pointed to the possibility of obtaining a narrow-band infrared image with a light filter consisting of two films with different density of carbon black coating. The short-wave region is captured by the first film and the long-wave region, after a narrow absorbed band, is transmitted by the second film.

Later, on the principle of the M. Czerny device, a number of night-vision infrared-illuminated devices /160, 163/ and instruments for spectral analysis of long-wave radiation /102, 211, 224/ were built. Their sensitive element was also a very thin blackened celluloid membrane placed in a chamber at a pressure of about 1 newton/m^2. The pressure in the chamber is determined by the oil vaporizer regime. The thickness of the oil film on the celluloid membrane depends on the pressure of the oil vapor in the evaporograph chamber and the energy illumination of the membrane section. For visual observation of the patterns exposed in infrared illumination, the oil film is illuminated with "cold" visible light. The resolving power extends to 14 lines per mm when the temperature difference is 10 degrees. From the colors of the interference fields, with high accuracy we can estimate the energy illumination of the region, and this means also the density of the incident energy. Some pre-excited phosphors, when acted on by infrared radiation,

begin to glow in the visible region of the spectrum. This property was taken as the basis of a metascope /145, 160/ and can be used for comparative estimates of fluxes of long-wave energy.

6. Pneumatic and Optical Methods

Underlying the instruments classed with the pneumatic method are the gas thermometers, exhibiting the highest sensitivity and accuracy of measurements /186, 274/.
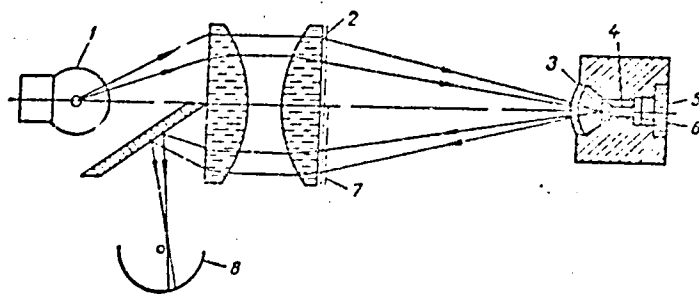
Fig. 10   Golay cell arrangement:

1. light source   4. channel
2, 7. gratings   5. window
3, 6. membranes   8. photocell

In contrast to metrological gas thermometers, the volumes of the receiving chambers of pneumatic indicators of radiant energy usually do not exceed 1 cm^3; the cumulative heat capacity is 10^{-3} J/deg. These small values correspond to the heat capacities of the thinnest (0.02-0.5 μm) film enclosures of the working volumes and make it possible, for large flux values, to achieve decreases in the time constant down to milliseconds. The temperature sensitivity can be brought to 10^{-5} deg. When an instrument is designed for long exposures of the order of 100 s, this makes it possible to record negligibly weak fluxes of the order of 10^{-10} W.

Gases absorb radiant energy only in narrow spectral bands. To extend the absorption spectrum, the receiving chamber is

filled with a fluffy absorber (with the finest down of plant or animal origin) and by subsequent heat treatment it is carbonized. This carbon "down", at moderate heat capacity, exhibits significant absorptivity and its presence increases sensitivity more than inertia in the instrument.

In the widely known Golay cell, the differential thermometric functions are exercised by two gas cavities, each about 3 mm³ in volume, connected to each other with a channel that has a sufficiently large cross-section so that its hydraulic drag does not have a marked effect, and its volume compared with the working chambers is small (Fig. 10) /102, 210/.

The receiving chamber is covered with blackened membrane 6. The measured radiation passes through a halite (rock salt) window 5, is absorbed by membrane 6, and heats together with the membrane the gas enclosed in the receiving chamber. Heated gas, on expanding, causes the mirror membrane 3 to sag.   /21

Information about the membrane construction is contradictory. The indicator membrane is a 0.01 µm thick collodium film, aluminized with a layer such that the resistance of a unit area is 270 ohms. And the membrane remains flexible and adequately reflects light. The receiving membrane is also collodium and is coated with antimony black.
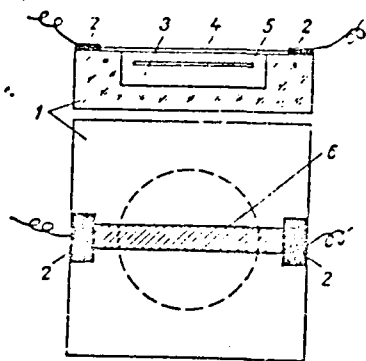
Fig. 11 Pneumatic receiver of radiant energy of A. A. Sivkov and V. V. Gud:

1. glass housing
2. electrodes
3. working chamber
4. membrane
5. absorber
6. strain gage foil

To eliminate the effect of slow change in atmospheric pressure, the instrument cavities are connected to the atmosphere with a capillary of small enough cross-section such that the working pressure in the chambers during the measuring time can be reduced by a negligibly small amount.

The system of photopneumatic amplification is constructed so that, with a plane mirror membrane, the light passing from source 1 through a condenser and openings in grating 2, on being reflected by membrane 3, is incident at the "bars" of grating 7 and does not reach photocell 8. The grating spacing is eight

lines per mm. For the smallest curvatures of the mirror membrane, the light bands reflected by it begin passing through grating 7 to the photocell; its current is recorded with an automatic recorder.

Information about manufactured Golay cells is limited. We can state with good certainty that they are used to record the threshold sensitivity of about $2 \cdot 10^{-9}$ W, for a resolving frequency of about 30 Hz. The data presented on the sensitivity of 10^{-10} W at a frequency of 2 kHz are not reliable and, it appears, were obtained by successive superimposing of extrapolations in which, as we know, information entropy rises significantly. The OAP-1, OAP-2, and OAP-4 radiation receivers are similarly constructed.

A. A. Sivkov and V. V. Gud /206/ (Fig. 11) proposed a simplified design of a pneumatic receiver. Radiant energy heats absorbing body 5, and beyond it also the air in the chamber 3; on expanding, the air presses on membrane 4. This leads to a change in the electrical resistance of the strain-gage foil 6.

In working parameters the first instrument was much inferior to series-manufactured OAP receivers. Still, we can understand the authors' hope of possible improvement in all characteristics, in particular, through combining the strain-gage effect with the bolometric in the strip carried on the membrane. The effectiveness of using the working volume in this instrument must be greater than in the Golay cell.

As the sensitivity increases in pneumatic receivers, the time constant also grows larger. The relations between sensitivity and inertia were explored in detail for these receivers by N. A. Pankratov /176/.

The optical method of investigation proposed by E. Shmidt and carried out by V. S. Zhukovskiy, A. V. Kireyev, and L. P. Shamshev /108/ only indirectly resembles the above-described methods. When light propagates in a compositionally homogeneous medium, its velocity depends on the optical density of the medium; in turn, the optical density is a function of the mass density, and thus, of temperature and pressure. When there is a mass density gradient, any light ray not parallel to the density gradient vector curves toward the side of greater density of the medium.

In all cases when there is convective heat transfer, in immediate proximity to the heat transfer surface there is a laminar sublayer in which heat transfers by means of thermal conductivity. For small projections of the pressure gradient on

a perpendicular to the heat transfer surface, the relative density gradient will equal in magnitude the relative temperature gradient, but is opposite to it in sense.

The relatively short cylinder investigated was illuminated with a narrow circular beam of parallel rays of light. Deviation of the rays was recorded on a film sufficiently distant from the output (for the light rays) face of the cylinder. The angle of deviation of the rays at the output was proportional to the temperature gradient in the sublayer, and thus, to the heat flux passing through the cylinder surface at the given generatrix. The measurement proved to be correct if the rays did not extend beyond the boundaries of the laminar sublayer and if the regions of the end-face perturbations were small. In fact, the heat balance was satisfactorily reduced only for small fluxes. For large fluxes, the heat balance could not be recorded, to a large extent. This is explained by the fact that corresponding to large fluxes is the early exiting of the beam from the boundary sublayer in the region of reduced density gradient.

7. Inertial Calorimeters

The first calorimetric instruments (Lavoisier, Laplace, Bunsen, and others) were intended for determining heat capacities from the amount of heat liberated and from the temperature change. The availability of information about heat capacity lets us measure the amount of absorbed or lost heat from the change in measuring body temperature. For actinometric purposes this instrument was first used by D. Herschel [1, 9], and later Abbot developed instruments that have found application up to the present time [126, 246].

To estimate the field strength of heat flows in steam boiler fireboxes, M. V. Kirpichev and G. M. Kondrat'yev developed a fairly simple device: it consisted of a massive copper cylinder with a thermocouple embedded into it. The amount of heat taken up by the block was measured from the cylinder heating time in a specific temperature range, with a known block heat capacity. Later, this device was used by Bauek and Thring [250], and R. Gase replaced the cylindrical form of the flow receiver with a spherical shape.

One deficiency of the receivers described is that they cannot be used in determining the sense of the vector of the quantity measured. So I. Kazantsev left only one face blackened in an analogous copper cylinder for measuring hemispherical radiation. All the other cylinder surfaces were insulated from the housing with an air gap.
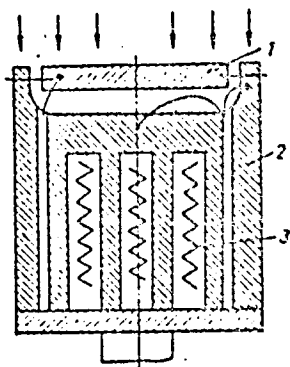
Fig. 12 Maulard inertial
         calorimeter:

1. receiving body
2. housing
3. heater

I. Kazantsev's calorimeters
/236/ are used widely in the inves-
tigation of industrial furnaces.
Particularly effective applica-
tion was found for these calori-
meters by V. S. Kocho /143/--he
proposed simultaneously measuring
with two radiometers that have
different degrees of absorption
by the sensitive surfaces. This
application permits the approxi-
mate estimation of the convective
and radiative heat transfer compo-
nents, on the assumption that there
is no interaction between the com-
ponents.

For measuring fluxes up to
$250 \cdot 10^3$ W/m^2 when the receiver
temperature was as high as 600° C,
Maulard /285/ used an inertial
heat receiver made of technically
pure gold. Gold was the choice
for its high corrosion resistance, its high reflectivity, and
its high thermal conductivity. The receiver (Fig. 12) was
a 25 mm diameter disk, 4 mm in thickness. The irradiated side
was blackened with high-intensity paint capable of service up
to 800° C; the other two surfaces were polished to reduce the
radiation losses and heat leakage. The disk was mounted in the
gilded depression of a massive nichral block of three platinum-
rhodium rod 0.5 mm in diameter. The gap between the disk and
the block was 1.5 mm. Located in the nichral block was a   /24/
heater; with it the block was heated up to the assumed tempera-
ture for a certain period before exposure. Because of this,
the receiving disk was less heated than the housing at the
start of the experiment. During the exposure the behavior of
the absolute disk temperature and of the difference between the
temperatures of the nichral block and the disk was recorded.
The reading was taken at the instant when the disk temperature
equalled the block temperature, which must indicate the absence
of heat losses.

The resultant flux--the difference between the fluxes re-
ceived by and irradiated by the receiving surface--was defined
as the product of the mass heat capacity of the receiving disk
per unit area, by the derivative with respect to disk tempera-
ture at the instant of recording. The latter was determined

graphically, by drawing a tangent to the temperature plot:

$$q = k\frac{dt}{d\tau}.$$

(I.4)

The instrument coefficient k depends linearly on temperature and is 0.241 J/m²·deg at 0° C for the receiver dimensions indicated, and at 600° C--0.250 J/m²·deg. The measurement error, as per Maulard's suggestion, was 5-10 percent.

An inertial receiver similar in design was described in a review article by F. K. Stempel and D. L. Rall /318/. Use of two transducers with different absorption coefficients enabled them to separate the convective and the radiative components of the flux received.

Moran positioned a copper block in a complexly shaped collar machined from fused quartz /294/. The temperature was measured with a thermocouple calked into the block. Its signal was recorded automatically both during exposure and during cooling. The latter was necessary for determining the losses; they were added to the flux calculated by Eq. (I.4).

Musial patented a device for measuring fluxes to 10^7 W/m²: it used the inertia of a receiving plate after brief cessation of cooling /296/.

In shock tubes the duration of the stages in the processes studied was approximately 10^{-4} s. And the thickness of the receiving inertial part must be of the order of 10^{-2} mm. Rose and Start /311/ used for these measurements resistance thermometers in the form of thin (about 0.03 mm) platinum films deposited on a pyrex base. The heat absorbed was expended mainly in raising the film temperature, which was estimated from the change in film resistance. The correction for heat leakage was determined from solving the thermal conductivity equation for the semibounded pyrex base, with fourth-order boundary conditions, as a function of the thickness and material of the deposited film, allowing for the exposure time. Heat leakage in individual cases was 10 percent of the measured quantity.

On the other hand, the inertia of the platinum film lowered the rate of change in the film temperature compared with adjacent sections of the uncoated glass; this introduced appreciable errors in the heat transfer process studied. It was experimentally very difficult to eliminate or allow for the perturbing effect of the metal film. So T. Sprinks /316/ determined the correction for the effect of local nonisothermicity of the surface partially occupied by the transducer from the approximate solution of the boundary layer equations, allowing for the perturbing effect of this nonisothermicity.

8. Instruments Based on Photoelectric and Radiometric Effects

Characteristic of instruments based on photoelectric effects is the direct conversion of the radiant energy of photons to the energy of the liberated electrons. So the nature of the array of the phenomena accompanying this conversion differs widely from the nature of radiant heat transfer, receivers in this group are little used for calorimetric measurements. Their prime drawback is the large spectral inhomogeneity of sensitivity.

Receivers employing the following effects find practical application:

a) external photoelectric effect, in which the absorption of a photon by a thin metal film is accompanied by electron emission in the adjacent vacuum-treated or allowed space filled

b) internal photoelectric effect, in which absorption of radiation quanta is accompanied by the release of free electrons capable of accumulating within a solid in the form of a noticeable difference in electrical potentials

c) internal photoelectric effect, accompanied by a noticeable change in electrical resistance.

Intrinsic to elements in all three subgroups is selectivity of reception, so as a rule they are used with narrow-band light filters, as occurs, for example, in the FEP-3 and FEP-4 series-manufactured pyrometers.

Over the past 20-30 years elements of the third subgroup have been widely employed; they rely on the photoconductivity effect. In some cases sufficiently wideband receivers were made /305/. At the present time formulations have been found that effectively react to radiation at wavelengths longer than 10 μm. Granted, deep cooling to the boiling point of nitrogen, hydrogen, and sometimes even helium must be used /102, 210, 211, 213/.

The threshold sensitivity of photoconductors to monochro- <u>/26</u>
matic radiation is two orders of magnitude greater than for thermopiles and bolometers, and the time constant is measured in microseconds. So lead sulfide photoconductors have a threshold sensitivity, as high as 10^{-14} W when there fluctuations in the signal at a frequency in the 1-17 Hz band.

Therefore, photoconductors are in service most often for measuring the smallest possible fluxes, when the sensitivity of the receiving element becomes the principal desired property /102, 163, 210, 211, 332/.

At first, in instruments of the radiometric subgroup it was suggested to estimate the density of radiant energy from the pressure exerted on the absorbing or reflecting obstacle. The phenomenon of light pressure was noted by J. Kepler as associated with the location of comet tails during travel near the Sun. In 1874 William Crookes designed a torsion balance; on its arm were symmetrically positioned, with respect to the axis, identical mica wafers, deposited on one side with reflecting aluminum, and the other--blackened, evidently with antimony. The wafers were arranged so that during exposure, one of them received the rays with the blackened side, and the other--with the shiny side. The actual force was found to be directed to the side opposite the expected side and in magnitude was much less than the value predicted theoretically.

In 1899 P. N. Lebedev succeeded in measuring the actual light pressure. While relatively weak energy densities had to be dealt with, the designs of instruments using light pressure failed. Only after the appearance of lasers the application of the ponderomotive effect proved to be so effective that it was possible, even without resorting to vacuum treatment, to build torsion balances measuring the energy of a light beam. But the radiometric effect had not yet been given an exhaustive quantitative explanation and took on the significance of a separate problem that had engaged many famous physicists.

M. Knudsen worked out the kinetic theory for gas in cavities whose dimensions are commensurable or less than the mean free molecular path length /280/. This success led him to discover the pressure gradient in fine-porous bodies coincident in direction with the temperature gradient. The new effect enabled Knudsen to be the first to give a qualitative explanation to the appearance of the radiometric moment.

Usually the working rocker arm of the radiometer is in the vacuum-treated space. Between the arm and the aperture through which passes the radiant flux under measurement is form a cavity. For the case when the mean free molecular path length is large compared to the distance between the arm and the aperture, Knudsen worked out a theory analogous to the theory of the effect in /27 porous bodies. When there are no intermediate collisions, the molecules reflected from the more heated side of the wafer carry some excess momentum compared to molecules reflected from the colder side. The blackened side of the arm during irradiation

was found to be more heated and so the pressure on it was higher than on the shiny side. From this theory it follows that the force acting on the arm is directly proportional to its area and to the temperature difference formed on the arms. Theoretical data agree fairly closely with measurements at pressures to 0.3 newtons/m² and the distance between the wafers of more than 0.1 mm.

For the case of intermediate collisions, Peter Debye conceived /260/ of a theory in agreement with the measurements at higher pressures.

In attempting to explain several experimental facts, Albert Einstein /261/ theoretically determined that per unit area of the radiometer arm there must be in action a force

$$N = \frac{1}{2} p \frac{\lambda^2}{T} \frac{dT}{dx},$$

(I.5)

where x is the direction perpendicular to the plane of the arm, and the value of the free path length λ is commensurable with the wafer thickness and is small relative to its transverse dimensions, and p is the pressure of the medium surrounding the radiometer arm.

Later this theory was experimentally validated by P. Schmudde /314/ using a system of balances whose arms had the same areas and different perimeters.

Up to now there has a lack of full clarity in the quantitative manifestations of the radiometric effect. Nonetheless the results of measurements by many investigators agree quite closely with each other.

At high pressures the medium begins to behave as a continuum in which naturally the pressure in all points of the vessel is the same.

Owing to the constancy of the radiometric force at a fixed pressure during a long period many physicists tried to apply the device described in measuring the incident radiation flux. As to design, the instruments were made either as torsion balances in which the radiometric moment twisted an elastic quartz filament, and the measured quantity was estimated from the angle of rotation, or as a miniature turbine with black-shiny arms, freely resting on a fulcrum; its rotational velocity is proportional to the density of the incident flux. A number of purely practical difficulties, in particular the dependence of pressure in the vessel on the wall temperature impeded the building of instru- /28 ments of this type satisfying elementary requirements as to accuracy, sensitivity, and reproducibility of measurements.

9. Compensating Radiometers

Compensating instruments can be classified into one- and two-element types. Usually, thermal compensation is effected by electric heating. In one-element instruments, by compensation heating the element sensitive to the measured flux is periodically calibrated. Viewed from a remote analogy, these instruments are like spring balances, periodically checked with reference standard weights.

Two-element radiometers are constructed on the base of a differential calorimeter. The sensitive arm permits controlling the identicalness of the energy supply. One of the elements receives the flux measured, the other--compensation electric heating. The fundamental basis of these instruments is the same as in a double-arm beam balance, so many principles of weighing theory /103, 165/ are applicable to measurements using compensating instruments, just as to bridge and compensated electrical measurements /123/.

The K. Angstrom pyrheliometer is a typical two-element instrument /248/. The general view and electrical circuit of the instrument are shown in Fig. 13. One of the manganin plates 1 or 2 serves as the receiver of the radiation measured. The plate dimensions are usually 19x2x0.02 mm^3. They are mounted on current lead-ins in an ebonite frame 3 and, on the side facing the radiation source, they are blackened on top with platinum black to a thickness of not more than 0.01 mm. The junctions of the differential thermocouple are soldered with insulating lacquer on the rear, unilluminated, side, to each plate. In some cases the thermocouple junctions are soldered to copper strips, which are cemented to manganin plates. Together with frame 3, the plates are mounted on an ebonite housing 8 using current lead-in rods and are placed in a copper tubular sleeve 14. From the receiving side the sleeve is covered with copper frame 15 with two slitlike opening 23x5 mm^2 in size. The spacing between the frame and the receiving plates exceeds 50 mm. Since the dimensions of the frame slits are larger than the dimensions of the receiving plates, the instrument has a tolerance relative to the placement angle for measurement along the vertical of 13° and along the horizontal--of 5°. In some cases the frames are made with smaller tolerances. Behind the frame 15 is a valve controlled with hook 18. With the valve access can be opened to the measured flux simultaneously at two receiving plates or at one of them separately. Both plates must be closed with a common cover for balancing tests.

The current of the differential thermocouple is monitored /29 with galvanometer 22. In the classical version, only one pair of junctions is used, so the galvanometer sensitivity must be quite high.
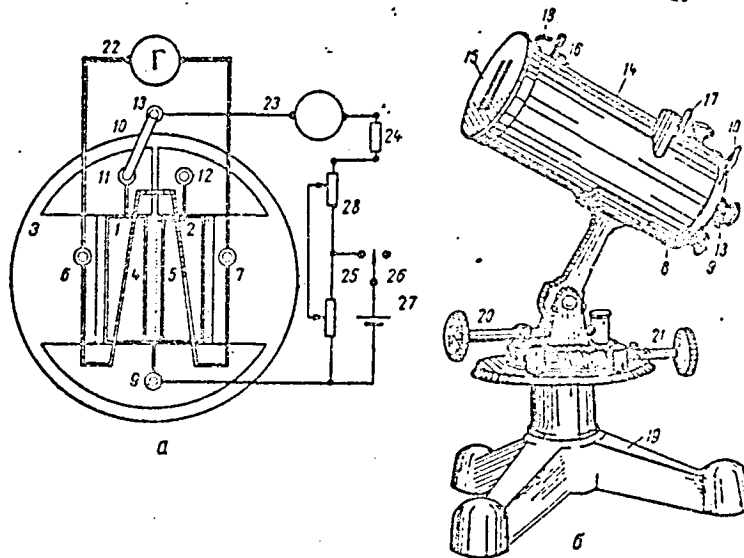
Fig. 13 Scheme (a) and general view (b) of
    Angstrom compensating pyrheliometer:
1, 2. manganin receiving plates
3. ebonite frame
4, 5. junctions of differential thermocouple
6, 7. terminals of differential thermocouple circuit
8. ebonite housing
9. common power terminal
10. selector switch
11, 12, 13. selector switch segments
10, 14. tubular sleeve
15. panel
16, 17. instrument sighting device
18. panel valve hook
19. stand
20, 21. adjusting mechanisms
22. galvanometer
23. ammeter
24. ballast resistance
25, 26. switch
27. battery
28. control rheostat

Power supply to the pyrheliometer comes from a storage battery of a dry cell. The potential difference at the plates must be much less than the battery emf. So ballast resistance 24 is connected to the circuit to prevent scorching. Compensation heating is regulated with double rheostat 28.

The measurements are made by systematically alternating the plates. When there is a deviation in the measurements as between the plates (allowed only in the fourth decimal place), the arithmetic mean is taken as the result.

For faster measurements use is made of incomplete compensation, by first determining the scale division of the galvanometer in an unbalanced state. During later measurements the corresponding correction is introduced, proportional to the deviation of the galvanometer at the instant of reading. In this case it is also customary to alternate the plates.

The compensating power is measured to high accuracy. /30
Using bridge instruments and reference standard resistances, the error in determining the plate heating power can be lowered to 0.01 percent. It is much harder to monitor the geometrical dimensions of the plates and the identicalness of their thermal operating conditions. In particular, the nonidenticalness of the conditions in which energy is removed by thermal conductivity, discovered in 1914 by K. Angstrom--the energy being supplied radiatively and electrically--led to an error of 1.5 percent /10/.

Analogous compensating instruments were developed for measuring the Earth's radiation (a pyrheliometer with four plates) and also scattered and total atmospheric radiation (pyranometer). Later they were somewhat improved on by numerous scientists and students of K. Angstrom.

For higher sensitivity, F. Ye. Voloshin suggested that the number of differential thermocouple junctions in the Angstrom pyrheliometer be increased to three or four.

As applied to heat-engineering radiation measurements under the Angstrom scheme, but in a specific design formulation, the author of the present monograph developed a radiometer for measuring fluxes to 20 kW/m^2 /51/. The D. T. Kokorev radiometer /134/ is constructed on the same principle. Two hollow chambers (Fig. 14), extruded from copper foil, are placed within brass cups, which are cooled externally with running water. The heads of the differential thermocouple are embedded in the walls of the internal copper chambers. The radiative flux enters one of the chambers through a relatively small aperture in a massive

water-cooled partition. Compensating electric heaters in spiral form are placed within the chambers. To compensate for the convective components, the second chamber connects to the ambient space through an angular channel.

The radiometer is calibrated by irradiating with a plane blackened heater with known dimensions and temperature. The density of the incident flux is calculated from the temperatures of radiator and receiver, with allowance for the geometrical factors and the degree of blackness. Essentially, no use is made here of the possibilities of the compensation principle, since substitution of the places and roles of the chambers, as well as verifying identicalness are not provided for. The conditions of ventilation of the working and compensating chambers are dissimilar. Nonetheless, the energy balance is taken with an accuracy of 5.8 percent. The measurement error is apparently of the same error.

For measuring the intense fluxes (to $12 \cdot 10^6$ W/m^2), A. B. /31 Willoughby proposed the design of a radiometer with two hollow models of an absolute blackbody /330/. Fig. 15 presents a schematic drawing of one of them. The chamber is formed of a massive hollow copper cylinder with screw grooves within for the electric heater spiral and externally--for water inflow. On one side the cylinder is closed off with a water-cooled cone, and on the other--with a massive, separately cooled diaphragm. Cooling water from a common tank with constant level upstream of the chambers is divided into two jets identical in volume flow. Downstream of the chambers the water passes through glass tubes in each of whose walls four junctions of the differential thermoelectric battery are embedded. Thus, the radiative and electrical heating are balanced according to the exit water temperature. As a result of testing for chamber identicalness, a marked discrepancy was discovered between their readings when the same flux was measured. Owing to the large inertia of the massive chambers, the duration of each measurement cycle (with two chambers) amounted to 15 min. The flux value was assumed equal to the root-mean-square value of the measurements. The assumed error did not exceed ±2 percent.

One-element compensating calorimeters are much simpler, but less accurate. A typical representative of these instruments is the ORGRES calorimeter (the Trust "Organization of Operations at State Electric Power Stations"), developed by I. Ya. Zalkind, A. V. Anan'in, and I. M. Kormer /109, 110/ (Fig. 16). This instrument was intended for measuring the heat release from the surface because of free or weakly forced convection. The housing of the sensitive element is constructed so that the area of its lateral surface beyond the limits of the
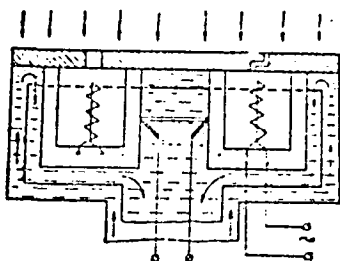
Fig. 14 D. T. Kokorev
radiometer
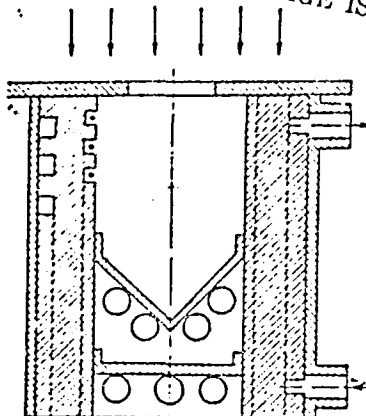
Fig. 15 Chamber of A. B. Wil-
loughby compensating radiometer

central recess is equal to the area of the lower surface placed
against the source of the flux measured. Pad 8 and flat heater
2 are placed in the central recess in successive layers between
two plate resistance thermometers 1.

   In the working regime, the variation in heater power is
chosen so that the flux through the heat insulation is equal to
zero; this can be estimated from the bridge balance; resistance
thermometers are included in the arms of this bridge. Since the
instrument housing is made of material with high thermal con-   /32
ductivity (aluminum); heat sensed from below is transmitted
without substantial thermal resistance to to the cooling medium
through the lateral surfaces. Thus, all the heater energy is
transmitted through the known area of the central recess in the
housing. A method of calculating these calorimeters was worked
out by D. M. Dudnik /104/.

   There are doubtful aspects to the ORGRES instrument; how-
ever, as a whole it satisfies technical requirements and passed
state tests in the All-Union Scientific Research Institute of
Metrology imeni D. I. Mendeleyev (VNIIM). At present these
instruments are manufactured in series of several hundreds of
units a year for monitoring quality of heat insulation. A simi-
lar instrument was patented in the United States by P. Storke
/319/ only by 1963.

)

An instrument for determining thermal conductivity by the stationary flux method was proposed as a special use of the calorimeter described /110/.

In a similar instrument G. G. Schastvlivyy /217, 218/ added one more heater, placing it under the insulating pad (Fig. 17). This made it possible to measure the thermal flux from the upper heater in the case when there is an absence or an insufficiency of the main flux from the body on which the transducer is placed. The temperature was measured with thermocouples. The instruments were used for determining the local coefficients of heat transfer to the cooling medium in the channels of the electric machines without allowing for the nonisothermicity of the heat transfer surface. This procedure evidently can be applied only in clarifying the relative efficiency of heat transfer surfaces.

V. A. Mal'tsev used systems like these in blow-throughs of cold models of electrical machine rotors /158/.

When heat fluxes are measured, an effort must be made to have the thermal conditions on the section occupied by the calorimeter to be the same as before it is placed.

Fig. 16 Design (a) and electric diagrams of ORGRES calorimeter:

1. resistance thermometer
2. heater
3. heater rheostat
4. resistance for varying reading limits
5. milliammeter
6. resistance of bridge circuit
7. null instrument
8. heat-insulating pad
9. calorimeter housing

Compensating calorimeters /33 --especially two-element types-- are absolute instruments of the highest measurement accuracy. So the compensation method is often used in making absolute instruments with which series-manufactured heat fluxes are calibrated (see Chapter 4). But as to sensitivity, generally they are much inferior to thermoelectric, photoelectric and pneumatic instruments, and to bolometers.
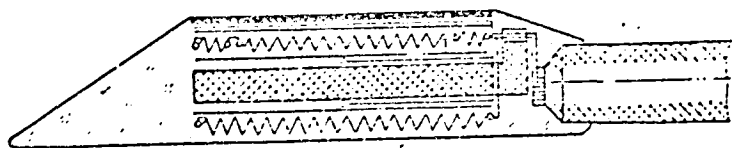
Fig. 17 G. G. Schastlivyy calorimeter

10. Auxiliary Wall Method

Basically the method amounts to placing a wall with known
thermal conductivity on the path of the measured flux. All
that remains is determining the temperature drop and calcula-
ting the flux from the equation

$$q = \lambda \frac{\Delta t}{\delta} .$$
(I.6)

As customary, the effect of the presence of the measuring
part is best minimized, so the auxiliary wall, if possible. must
not be supplementary, as it is sometimes called. But in those
cases when an auxiliary resistance is inavoidable, it is neces-
sary to know not only the absolute magnitude, but also its pro-
portion in the total thermal resistance of the circuit conduc-
ting the measured flux.

One of the first calorimetric instruments based on the
principle of the auxiliary wall and that have been brought to
the stage of series manufacturing is the E. Schmidt ribbon calo-
rimeter /313/. It is widely in service at present for measuring
heat losses through heat insulation. A rubber ribbon 600-650 mm
long, 60-70 mm wide, and 3-5 mm thick is used in making the E.
Schmidt calorimeter. About 200 junctions of a ʰattery of dif-
ferential thermocouples are placed in series on both ribbon
surfaces. Next, the surface is covered with a millimeter layer
of crude rubber and is vulcanized. The current-collecting con-
ductors are extended through terminals embedded in the rubber.
The small ends of the ribbon have accessories with which the
"belt" is fastened with a tightness fit on the convex insula-   /34
tion surface. Owing to the cumbersomeness and large inertia
of the "belts," they are not convenient in use. When the dimen-
sionless values of the time $\bar{\tau}$ are the same, the time of the
actual arrival at the regime of measuring with the "belts" is
two orders of magnitude greater than for sandwich-type trans-
ducers (see Chapter 3), and four orders greater than for iso-
lated transducers (see Chapter 2). Still they are used widely.

Calorimeters developed in the Leningrad Technological
Institute of the Refrigeration Industry are analogous in con-
cept, but somewhat different in design. In this case a battery
of 600-900 pairs of junctions is secured in a rubber disk 300 mm
in diameter and 6 mm in thickness. Because of the increase in
the number of junctions, the sensitivity is two to three times
higher than in the Schmidt "belts."

Disk-calorimeters 60-90 mm in diameter and 3-8 mm thick
were developed in the Moscow Teploproyekt Institute for measur-
ing fluxes to 1000 W/m^2. The number of thermocouple junctions
is increased to 1500-2000, and the thermocouples as such are
made by the galvanic method. The auxiliary wall is assembled
of paronite blocks wound with constantan, each turn being half-
copper-plated. The set of blocks is cemented between two thin
(1 mm) paronite disks. The signal generated with this kind of
transducer is sent to an indicating millivoltmeter.

The Beckman and Wightly company /287/ makes heat flux
transducers differing from those described above by less thick-
ness. The transducer dimensions are 115x115x1.5 mm^3; the ther-
mocouple is constantan-silver constantan; the instrument sensi-
tivity is 19 $W/m^2 \cdot mV$.

The Joyce and Lebl company has been manufacturing since
1956 calorimeters in two type classes--50 and 100 mm in dia-
meter /288/. In these calorimeters the housing of the copper=
constantan calorimeter and the shell of the entire transducer
are made of polyethylene. Owing to the use of polyethylene,
the transducer temperature does not exceed 70° C. This same
calorimeter, with a diameter of approximately 300 mm, was used
in instruments for determining the thermal conductivity of wet
insulating materials /278/. Used for these same purposes was
a structure woven of asbestos cardboard strips (warp) and ribbon
thermopiles (weft) /302/. A bimetallic copper-constantan strip
successively undercut once with the copper side and once with
the constantan side was used in making the thermopile. The
strip thickness was 0.08 mm and its width was 0.6 mm. Exter-
nally the "fabric" was overlaid with asbestos paper, impreg-
nated with phenolic resins, and heat-pressed. Thus, a slab
resulted, 300x300 mm^2 in size, close to asbestos-textolite in
strength and external appearance. In the central part of the
slab was a 150x150 mm^2 measuring section, with about 200 thermo-
pile junctions.

This kind of calorimetric fabric (glass-reinforced ribbon
with bimetallic cut strip) was used by Lawton et al /283/ in
the design of a calorimeter for determining heat transfer and
heat production of animals (Fig. 18). The thickness of the

33

glass-reinforced ribbons was 0.4 mm; the total thickness of the calorimeter shell was about 1 mm. Because of the large area and the small thickness of the fabric covering all the interior surface of the calorimeter chamber, the authors were able to achieve high instrument sensitivity with low inertia.
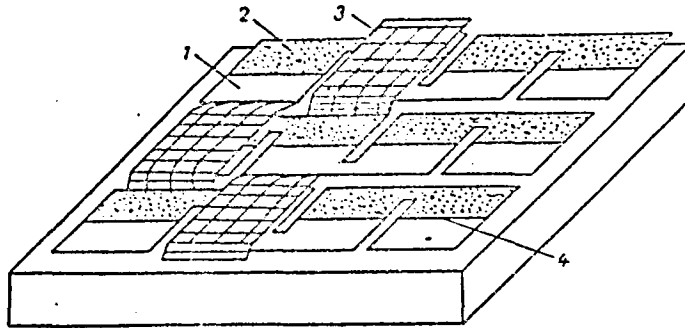
Fig. 18 Lawton fabric calorimeter:

1. copper
2. constantan
3. glass-reinforced ribbon
4. line of junction of copper with constantan

A calorimeter with an auxiliary polymethylmethacrylate wall /136/ was built and used in measuring heat fluxes from the bottom of inland waters. The thermal conductivity of polymethylmethacrylate is close to the thermal conductivity of ice; polymethylmethacrylate has wholly satisfactory electrical insulating, processing, and operational properties. So these transducers are used for measurements of heat fluxes in permafrost regions and areas with high volcanic activity /111, 112, 188/.

To eliminate the perturbations introduced by the presence of the calorimeter, V. V. Shabanov and Ye. P. Galyamin proposed selecting for the auxiliary wall a material that has dispersiveness, porosity, and thermal conductivity similar to these characteristics in the soil in which it is proposed to make the measurements /238/. Yu. L. Rozenshtyuk and M. A. Kaganov proposed making the auxiliary wall composite of materials that are contrasting in thermal conductivity in order to attain a thermal conductivity identical to the ambient value by varying the component thicknesses /194/.

Studies of heat and mass transfer in soil are needed to clarify a number of vital problems in agronomy. Because of this, several calorimeter designs were developed as appropriate to specific experimental conditions. In 1950 measurements of this kind were made by E. L. Dikon, and in 1955 by L. G. Morris et al /295/. The latter, in particular, built calorimeters /36 based on the auxiliary wall method with nickel wire resistance thermometers. For greater water stability, the transducer was coated several times with copper chloride and araldite. In the United States a similar instrument was built by Watts /328/.

For bioclimatic studies in soil, often used are banked thermoelectric transducers with an intermediate wall of glass, for example, the calorimeters of Schacke /312/ and Fransilla and Huovila /264/. The sensitivity of these instruments is approximately $3 \cdot 10^{-6}$ V·m/W. W. Warmbt wrapped a cushion of glass-reinforced fabric partially with copper constantan, impregnated it with araldite, and covered it over with aluminum foil /325-327/. W. Warmbt assumed that araldite-impregnated glass-reinforced fabric has a thermal conductivity that is the same as for soil. For water permeability, along the transducer bed several openings were made until the araldite has completely hardened.

Fig. 19   VNIIMT calorimeter:

1. openings for thermocouples
2. receiving block
3. blind

Similar instruments, described by a number of authors, permit--to a large extent--finding the pattern of heat and mass transfer in the soil layer and the interaction across the surface with the immediate atmosphere at different seasons and on different days /254, 262, 267, 281, 324/.

Measuring the temperature drops involves considerable difficulties, coming from the indeterminacy of the thermal resistances of the elements connected with the auxiliary wall.

For measuring large flux densities the auxiliary wall is made metallic. Fig. 19 shows the VNIIMT (All-Union Scientific Research Institute of Metallurgical Heat Engineering) radiometer with conductive heat removal /236/. A copper or steel

block 2, cylindrical in form, is irradiated from one end, and from the other it is cooled with running water. Thermocouples are embedded through side bored holes along the block axis. The receiving body is protected with blind 3 against lateral heat flows.

The calculated determination of the flow measures is not reliable. Calibration with absolute reference instruments can made the measurements more accurate and simplify instrument design. Single-conductor thermocouples are generally used in the thermal probes, with material of the receiving block serving as the intermediate electrode of the differential thermocouple.

To measure the resultant fluxes in open hearth furnaces, VNIIMT staff members developed a probe with two oppositely /37 oriented receivers /236/. For better sensitivity when weak fluxes are measured, the receiving body was made of two parts with internal bore.

When the thermocouples were used as indicators of temperature difference, it was tempting to merge the functions of auxiliary wall with the functions of intermediate thermo-electrode of the differential thermocouple /49, 113, 262, 271/. For example, E. L. Dikon used cast bismuth as the material for the middle layer of the auxiliary wall in measuring thermal fluxes in soil. One design feature of this transducer is the demarcation of the central measuring part using a thin layer of insulation. Bismuth has a high thermoelectric coefficient and a low thermal conductivity, but a value that is higher than for soil. One drawback is the dependence of the thermoelectric coefficient of bismuth on temperature. So this transducer can be recommended for use only in a narrow temperature range in which calibration is conducted. This is also true for the G. Falkenburg calorimeter, where Wood's alloy was used in place of bismuth /262/. The calibration characteristics of the E. L. Dikon and G. Falkenburg calorimeters differed by 30 percent from the calculated characteristics; this can be explained by the considerable effect of impurities on the thermoelectric properties of bismuth alloys.

Alloys of technically pure (99.0-99.9 percent) tellurium with copper and silver /271/ were used by Hatfield and Wilkins as the auxiliary wall material. In the 15-100° C range an alloy of two parts tellurium and one part pure silver is the most suitable. These transducers were later built by the Joyce and Lebl /287/ and National Instrument Laboratories /272/ companies. For pure tellurium /211/, as a function of temperature the thermoelectric coefficient twice changes sign, attaining the maximum value (800 μV/deg) in the 100-200° K range.

36

One disadvantage of alloys containing semiconductor constituents is the marked dependence of the thermoelectric coefficient on temperature. Materials in thermo-electrodes of standard thermocouples are less sensitive, but more stable and therefore have found wide use.

In measuring high-density fluxes, I. Vrolik used a copper block with constantan current-collecting plates as the auxiliary wall /46/.

As the sensitive element of a total-radiation radiometer, A. A. Piskunov and I. N. El'ke used a single chromel rod with copel current-collecting conductors /182/.

New materials for calorimeters must be sought for not only among conductors and semiconductors, but also among insulators, especially poor insulators (semi-insulators). Good insulators /38 (BeO, MgO, Al_2O_3, and others) are poor choices for use, since their high electrical resistance limits the possibilities of signal measurement.

In Table 1, characteristics of several oxides and their mixtures are presented, based on the measurements of Fischer et al /263/. From Table 1 we can see that some mixtures with large short-circuit current values can be entirely suitable for the intermediate wall. In those cases when the thermal resistance of transducers does not have significance, they will generate signals exceeding the signals of tranducers made of other materials. One disadvantage of semi-insulators is their high thermal resistance and the temperature dependence of the thermal properties. So semiconductors and semi-insulators find practically no use in heat-measuring components.

11. Calorimeters with Transverse Flow Component

In these instruments the flux received passes entirely or in part through an auxiliary part, changing its initial direction. Designs of these instruments were described by R. Gardon /265, 266/, A. S. Sergeyev /202, 203/, and Stempel /318/.

A diagram of the R. Gardon instrument is shown in Fig. 20. An opening in the copper block 2 is covered with constantan plate 1, soldered to the block along the periphery. Energy received by the constantan foil partially streams radially to /39 the copper block and is partially lost to the ambient medium. The heated junction is formed in the center of the plate with the soldered copper wire 3. The constantan plate is usually thinner than 0.3 mm. So the stationary mode sets in relatively

Table 1

(a) Состав материала стенки	(b) Температура на гранях образца, °C		(c) Ток короткого замыкания, ма	(d) Термоэлектрический коэффициент, мкв/град	(e) Мощность режима короткого замыкания, вт	(f) Толщина образца, мм
	(g) верхняя	(h) нижняя				
CdO	595	9	200	—84	0,01000	2,7
Cr₂O₃	752	84	1,2	437	0,00040	2,0
V₂O₅	595	19	0,18	—652	0,00007	3,6
Co₃O₄	747	54	13	290	0,00300	2,0
CuO	767	80	16	276	0,00300	2,0
NiO	750	57	2,7	180	0,00300	2,0
Cr₂O₃+10% CuO	640	255	0,84	150	0,00050	2,3
V₂O₅+20% CuO	570	20	15	—180	0,00150	2,0
CdO+50% MgO (несеребреный) (i)	752	48	470	—159	0,05000	2,0
CdO + 50% MgO (серебреный) (j)	750	42	1970	—154	0,21500	2,0
Co₃O₄+10% CuO+5% Bi₂O₃	759	67	710	311	0,15800	2,1
Co₃O₄+10% CuO+5% Bi₂O₃+2% Ta₂O₅+2% MgO	751	51	2550	234	0,41800	2,1

Key:
a. Composition of wall material
b. Temperature at specimen faces, °C
c. Short-circuit current, milliamperes
d. Thermoelectric coefficient, μV/deg
e. Short-circuit mode power, W
f. Specimen thickness, mm
g. upper
h. lower
i. unsilvered
j. silvered

fast. A plot of the temperature change along the foil radius is shown in the right side of Fig. 20. The maximum temperature t_1 corresponds to the center, and the minimum temperature t_2 -- to the block. The temperature difference $\Delta t = t_1 - t_2$ is measured with a differential thermocouple made up of a central copper wire, constantan foil, and copper block; from the temperature difference we estimate the intensity of the energy flux received. Given in the study /265/ is a solution to the thermal conductivity equation for the foil on the condition that the flux received q is constant along the foil radius. As a result, the following expressions were derived for transducer sensitivity and inertia:

3

$$\frac{e}{q} = a\frac{R^2}{\delta}; \quad \tau = a_1 R^2. \qquad\qquad (I.7)$$

where R and δ are the dimensions of the working section of the foil; a and a_1 and transducer constants.

Gardon found the values of a and a_1 and plotted a nomogram of the solution to Eqs. (I.7).

The working temperature of the calorimeters is bounded by the softening point of the solders tested. As the temperature goes up, the linearity of the relationship between incident flux and signal is disturbed. So the upper limit of measurement is best increased through thickening of the foil, tending to make the radiative component in heat removal from the foil small compared with the conductive and the convective components.

Fig. 20 Diagram of R. Gardon transducer:

1. receiving plate
2. copper block
3. current-collecting conductor

Relying on handbook data, R. Gardon also found that for the copper-constantan pair the dependence of the thermoelectric coefficients on temperature is practically entirely compensated by the dependence of constantan thermal conductivity on temperature. Thus, the transducer proves to be insensitive to the temperature level at which the measurement is taken.

Using these transducers, R. Gardon measured fluxes at a power of $(0.02-4)\cdot 10^6$ W/m^2. Measurements were made of thermal fluxes from the heated plate swept by air; the air exited from /40 3.2 mm diameter openings arranged in unstaggered fashion with a 50.8 mm spacing, at a flow rate corresponding to a volume flow of 0.2 kg/s per m^2 of plate area; the measurements are in Fig. 21 /266/.

Usually the dimensions of the transducers with a foil disk are small (the diameter of the opening in the block is often less than 1 mm). It is difficult to make them strictly identical with each other. The deviation of the actual transducer properties from the calculated values is as high as 30 percent; because of this each transducer needs individual calibration.

39
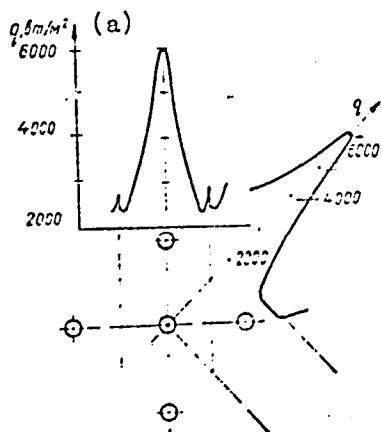
Fig. 21 Measurements of heat fluxes made with the R. Gardon transducer as plate is swept by jets

Key:
a. W/m^2

The part of the heat lost to the ambient space is small compared with the part transferred along the foil because of thermal conductivity, therefore when radiative fluxes are measured there is no need for vacuum treatment; this does much to simplify carrying out the experiments. Usually in radiometric measurements the transducer is surrounded with a shield, reducing the nonuseful absorption of energy by the copper block and protecting the foil from mechanical damage.

In short-term measurements the experimenter is limited to heat removal through inertia of the block, which is many orders of magnitude higher than foil thermal inertia. In the case of long-term measurements of intense fluxes, the block is cooled with running water. G. G. Blau used this kind of cooling in determining the thermal conductivity of zirconium oxide for temperatures higher than 1000° C. F. Stempel /310, 318/ indicated the possibility of separating the radiative and convective components with two transducers; one receives the incident flux directly, while the other is shielded with a sapphire window, which is protected against overheating with a gaseous covering.

Signal strength can be boosted by joining the radiometers with a circular foil in electrical series. And the cooled copper foil naturally must be divided into electrically insulated sections. Thus, A. S. Sergeyev proposed a radiometer of six series-connected sections /202/. This radiometer was improved through the placement of the device on one of the baffle sections; by rotating it the output signal can be regulated and thus in calibrations the device sensitivity is kept constant /203/.

An original instrument, transverse type, for measuring /41 relatively weak radiative fluxes was designed and built by B. G. Tanmor /323/ (Fig. 22). This instrument was used for investigating radiative heat transfer between structures and the ambient medium. A galvanic banked thermocouple was wound on a

perspex plate, 85x50x3 mm in size. The plate thus shaped is inserted into recesses in copper half-disks (Fig. 22). The recesses in each half-disk, 85x26x6 mm in size, are filled ahead of time with molten paraffin, in which a perspex plate with wound thermocouples is immersed. A thin paraffin layer insulates the half-disks from each other. The current-collecting conductors extend through openings on both sides of the disks. Each half-disk is assembled on solder from two identical halves in which cavities are milled out. One end side of each half-disk is polished, gilded, and polished again, and the other is blackened by one of the known methods. The disk is assembled so that each of its planes receives half the reflecting and half the absorbing radiation. The disk is mounted on four strings in a large-diameter collar.
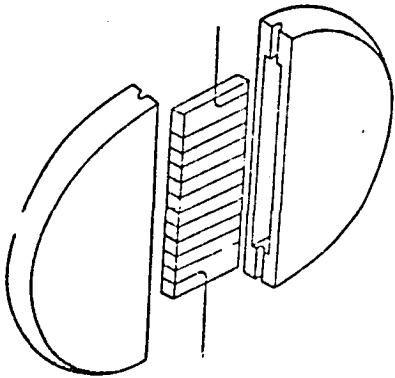
Fig. 22 S. G. Tanmor radio-meter
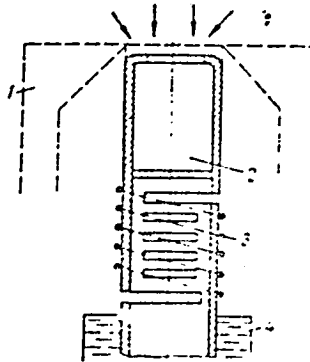
Fig. 23 Radiometer of I. D. Semikin, V. S. Kostogryzov, and O. L. Tsygankov:

1. enclosure blind
2. receiving in form of an absolute blackbody model
3. bank of differential thermocouples
4. cooling sleeve

41

The different degree of half-disk blackness upon exposure to the measured flux accounts for the temperature difference recorded with the bank of differential thermocouples. The signal of the thermocouples then serves as a measure of the resultant flux.

A radiometer with the model of an absolute blackbody and a transverse measuring part was developed by I. D. Semikin, V. S. Kostogryzov, and O. L. Tsygankov [201] (Fig. 23). The receiver in the form of a model of an absolute blackbody is inscribed by design in the end of a brass tube and is inserted in the enclosure sleeve. In its lower part the tube is cooled with water circulating in the sleeve. In the interval between the receiver and the outflow the tube is cut so that the heat flux received is displaced initially to the left, then along the circumference it passes over to the right part and is transmitted to the cooling water.

Wound in the middle part of the intermediate body is the galvanic differential thermocouple, recording the transverse temperature head. The radiometer described is marked by an absence of selectivity and a sensitivity that is quite high for industrial measurements.

The nonlinearity of losses of this kind and the heat-physical properties of the device elements leads to the dependence of sensitivity and measurement accuracy on the temperatures of the cooling water and the ambient air.

To reduce the measurement errors, with this instrument it is necessary to keep the cooling water temperature at the level of the ambient air temperature and to make the heat-conducting tube out of constantan.

A simply manufactured low-inertia thermoelectric radiant energy receiver was proposed by S. Ye. Burav [37].

12. Analytical Methods

As applied to phenomena of thermal conductivity, the differential equation, boundary and initial conditions unambiguously describe the temperature of a given body at any point at an arbitrary instant of time. Since this relationship is unambiguous, knowing the temperature, for example, the flux or the temperature at the boundaries). This approach to the solution is customarily called the inverse thermal conductivity problem [219].

From the temperature values at two points we reconstruct the temperature field of the k-dimensional body that has a cavity; from this temperature field we determine the heat fluxes that the body exchanges with the external medium, and the values of the heat transfer coefficient. At the same time we can calculate the coefficients of thermal conductivity and thermal diffusivity of materials filling the region in question.

For a practical judgement of how effective this method is let us look at an article by R. Kh. Mullakhmetov and L. A. Khorn /170/.

The thermal conductivity equation for an unbounded plate /43 has the form:

$$\frac{\partial t(x, \tau)}{\partial \tau} = a \frac{\partial^2 t(x, \tau)}{\partial x^2}.$$
$$(I.8)$$

The boundary conditions are determined by the fact that the surface temperature $t(x_0, \tau)$ is measured in the experiments, and in the plate midsection owing to the symmetry of the thermal action

$$\frac{\partial t(0, \tau)}{\partial x} = 0.$$
$$(I.9)$$

The coordinate x is read off from the plate midsection.

At the initial instant of time, the plate temperature at all points is the same and all temperatures $t(x, 0) = 0$ are subsequently read off from it.

The desired flux at the external plate boundaries is found in the form of a polynomial

$$q(\tau) = \sum_0^m A_i \tau^i.$$
$$(I.10)$$

Applying the principle of superpositioning, we can represent the temperature at any point in the form of the total of the results of partial actions of each member of the polynomial (I.10):

$$t(x, \tau) = \sum_0^m A_i T_i(x, \tau).$$
$$(I.11)$$

Applying the expansion formula, R. Kh. Mullakhmetov and Ye. A. Khorn found the calculation formulas for $T_i(x, \tau)$ when $i = 0, 1, 2, 3$. With the $m + 1$ measurements, we can set up the same number of equations (I.11) and find the $m + 1$ coefficients A_i.

With absolutely accurate measurements and $m \to \infty$, the solution turns out to be wholly rigorous.

But actually the measurements contain some errors, and the number of measurements is restricted. To make the solution found most probable, the authors of the study /170/ require that the sum of the squares of the differences between the desired solution and the measurements be a minimum (least-squares method). From the components of the normal equations they calculated the coefficients A_i and then, by differentiating the temperature with respect to the coordinate, they found the flux equation.

By this method A. Witte and E. Harper determined fluxes received by the walls of different sections of uncooled combustion chambers and rocket engine nozzles /332/. Each representative area in the chambers and the nozzles had two thermocouples embedded in it; the thermocouple readings are recorded continuously. The junction was deepened by 0.5 mm. The problem was assumed to be one-dimensional. The temperature distribution was approximated with a polynomial of fifth degree. A method for analytical processing of measurement data and a computation program for an IBM 7090 computer were developed by W. B. Powell et al /306, 307/.

The measurements were made on nozzles with exit cross-sectional area in a ratio of 20:1 with respect to the minimum area and with the working pressure in the combustion chamber from 0.7 to 2.0 meganewtons/m². The thrust was brought to 25 kilonewtons. A stoichiometric mixture of hydrazine and nitrogen peroxide was the fuel. To verify the method, simultaneous measurements were made of the flow using a water-jet calorimeter similar to the Perry calorimeter /304/. The measurements agreed satisfactorily. The authors do not give a numerical estimate of possible errors.

In cases like these, many investigators used foil and thin-film resistance thermometers secured to the surfaces of a semi-bounded body /19, 172, 270/. For better sensitivity the exposures were periodically interrupted. Sometimes it is better to use methods of analogy /62/.

Boussinesq /253/, working out Fourier's ideas in the solution of the thermal conductivity equation, showed that the general solution can be represented in the form of the series

$$ t = \sum_{i=0}^{\infty} A_i U_i e^{-m_i \tau}, \qquad (I.12) $$

where U_i stands for the functions of the coordinate of the point with temperature t.

Since with increase in time τ , the total of the series
members, beyond the first member, dwindles rapidly and becomes
small, in many cases only the first member in the expansion
(I.12) is important. The regimes in which this is valid were
investigated at length by G. M. Kondrat'yev /I37, 138/ and
called regular regimes.

13. Pyroelectric Calorimeters

The state of electrical polarity caused by temperature
change and coinciding with optical polarity is called pyroelec-
tricity. This phenomenon was first observed in tourmaline min-
erals; for these minerals, the principal axis of crystal sym-
metry is the principal pyroelectrical axis. A temperature
change of 1 deg along this axis leads to charge of up to 10^{-5}
coulombs/m^2 appearing.

The quantum theory of pyroelectricity was elaborated by
M. Born /252/.

A distinction is made between the primary effect seen in   /45
crystals forcibly deprived of the possibility of expanding
thermally, and the secondary effect, observed in free crystals
/303/. The primary effect at its basis is piezoelectric in
nature and is proportional to the absolute temperature squared.
The nature of the secondary effect is independent; it is pro-
portional to the fourth power of the temperature. Applying
pyroelectricity, a temperature change of 0.01 deg was measured
/13/.

The sensitive elements, based on pyroelectricity, react to
a change in temperature under the effect of the radiation mea-
sured. The elements are usually a plate of pyrosensitive
material coated on both sides with the thinnest metal linings,
serving as current-collecting electrodes (Fig. 24). The current
generated with this device is

$$I = \gamma \frac{q}{\delta c \rho} .$$

where the coefficient of proportionality γ depends on tempera-
ture and only in a relatively narrow range can it be assumed
constant.

B. Meyts and T. Pyorls used pyroelectric calorimeters to
determine the heat effects of Polaris missiles on surrounding
objects during flight /171/. A sensitive element (100 mm in
diameter and 5 mm in thickness) was placed in a metal housing
on glass wool cushions protected against shock, vibration, and
heat loss. Polarized ceramic of barium titanate oxide and lead
zirconate-titanate was the material used. For barium titanate

oxide the working temperature must not exceed 90° C, and for
lead zircontate-titanate--300° C. An increase in the pyro-
electrical coefficient with rise in temperature, in the view
of the authors of the study /171/, is compensated by increas-
ing the heat losses at the receiving surface through back rad-
iation and convection. The instrument error does not exceed
±10 percent.
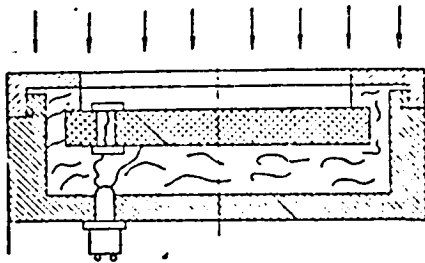
Fig. 24 Pyroelectrical
radiometer

A similar, but miniature unit
was employed in measuring laser
radiation energy /20/.

Radiometric properties of pyro-
sensitive crystals were investigated
in detail by L. S. Kremenchugskiy,
A. F. Mal'nev, and V. B. Samoylov
/144/. The elements studied were
a barium titanate oxide plate and   /46
triglycinesulfate plates in the
form of monocrystals and ceramic
plates 100+3 μm thick and 100 mm^2
in area. Silver 0.1 μm in thick-
ness was deposited in vacuo on the
current-collecting electrodes; the
receiving electrode, for a uniform spectral characteristic, was
covered with gold black /18, 214/. The zonal sensitivity of
the instrument was determined by measuring the pyroelectrical
effect when the light ray-probe was dropp--; its diameter was
varied, starting at 0.15 mm, in the direction of increasing
values. When a small-diameter ray transited the receivers,
nonuniformity was detected in the values of the pyroelectrical
coefficient, reaching 75 percent for the monocrystals. The non-
uniformity was less for the ceramics than for the monocrystals.
When the ray diameter was enlarged to 1 mm, the nonuniformity
dropped to 3 percent.

＊　　＃　　ェ

The methods examined above are based on a relatively small
number of physical phenomena. Searching for new methods of
measurements is oriented mainly at involving previously unused
effects /279, 324/.

In a dielectric bolometer /324/ a celluloid film (its pre-
parative method is described in section 5 of this chapter) is
coated in vacuo with an approximately 0.1 μm gold layer, on
both sides. The capacitor thus obtained is exposed to an inci-
dent flux. The instruments were named as above owing to their
use of a temperature dependence of the dielectric constant.

After exposure to the measured flux, the electrical capacitance
of the sensitive element was varied. In this sense ferroelec-
trics are very promising, as are new polymeric materials that
have a well-defined temperature dependence of the dielectric
constant.

Ferroelectric films prepared on foil surfaces of electro-
lytic capacitors are mechanically weak. In this receiver the
correct exposure across the electrolyte of metal bearing the
dielectric film is difficult.

Among the known diversity of semiconductor thermistors,
classed in a special group are ferrite thermistors; they are
thermosensitive not only as to electrical resistance, but also
magnetic permeability /30/. These sensitive elements are al-
ready in service for measuring incident flux in the UHF range
/29/ and there are no reasons blocking the extension of the
range to infrared and optical frequencies.

Characteristic of dielectric and ferrite transducers is
the variation in the reactive components of the resistances;
highly effective methods have been developed for measuring
these components /123/.

Relatively numerous measurements are made in hygienic and
physiological studies /43, 96/. In several cases, when measure- /47
ments are made of tissues with the probe method, from the rela-
tive change in thermal conductivity it was found possible to
estimate the relative change in blood flow; in turn this yielded
information about the physiological condition of the vital acti-
vity of the organ and the organism as a whole /251, 269, 275,
284/.

To record weak fluxes from functioning transistors, the
authors of the study /21/ used a well-defined dependence of the
rate at which exposed photoemulsion develops on the developing
temperature. Very sensitive and accurate instruments for mea-
suring radiative thermal fluxes can be evidently built on the
basis of the thermosensitivity of chemical reactions.

In conclusion, we can state that measuring heat flux density
is an urgent need for most scientific investigations and indus-
trial processes. Information that these measurement afford is
interesting both in the primary form as well as, often, in indi-
rect secondary manifestations. Developing methods of thermal
measurements and the steadily mounting need for these methods
in science and manufacturing allows us to single out these
methods in an autonomous field--heat-measurement.

A basic task in heat-measurement is designing and building miniature transducers of heat flux density that have high localization of measurements, low thermal resistance, high sensitivity, and good reproducibility of measurements, made possible by reliable absolute calibration.

CHAPTER 2: SELF-CONTAINED HEAT FLUX TRANSDUCERS

The low sensitivity of self-contained transducers is compen-
sated, to a large extent, by design simplicity, reliability, and
stability. Combining these qualities led to the use of these
transducers being involved with highly forced heat transfer char-
acteristic of many fields of technology.

The transducers described are intended mainly for measur-
ing fluxes with a density of 10^3-10^6 W/m^2. The lower limit of
density is due to the sensitivity of the electrical instruments,
and the upper--to the possibilities of correct calibration. If
extrapolating the calibration is allowed, the self-contained
transducers in general do not have an upper limit as to the
magnitude of the flux measured.

The present chapter gives the general design and techno-
logical features of self-contained transducers, as well as an
analysis of the nature of the transducer signal when there is
nonuniform distribution of the measured flux over the transducer
field.

A qualitative analysis is given for the group of phenomena
whose nature is not clear enough to quantitatively allow for
their effect and ways of reducing interference are outlined.

It is shown that noise at the electronic and molecular
levels does not affect measurements. Since knowing the distor-
tions introduced by the presence of transducers is important for
measurement practice, we present the formulas for determining
the corresponding corrections. Features of measuring nonsta-
tionary fluxes are described.

1. Designs of Self-Contained Heat Flux Transducers (S.H.F.T.)
and Problems of Their Manufacture

A self-contained transducer is a unique flattened differ-
ential thermocouple whose intermediate electrode acts as an

auxiliary wall (Fig. 25). When the transducer is positioned
on an isothermal surface of the body studied at the faces of
an intermediate layer with thickness δ_2 a temeprature differ-
ence is induced, proportional to its penetrating flux being
measured. This temperature difference induces the correspon-
ding thermal emf; it is sent by the current-collecting wires
to the measuring instrument. The theoretical value of the
transducer signal e, corresponding to some flux q, can be
determined by the formula

$$e = \frac{(\alpha_1 - \alpha_2)\delta_2}{\lambda} q.$$ (II.1)

from which we find the transducer sensitivity

$$\frac{e}{q} = \frac{(\alpha_1 - \alpha_2)\delta_2}{\lambda}.$$ (II.2)
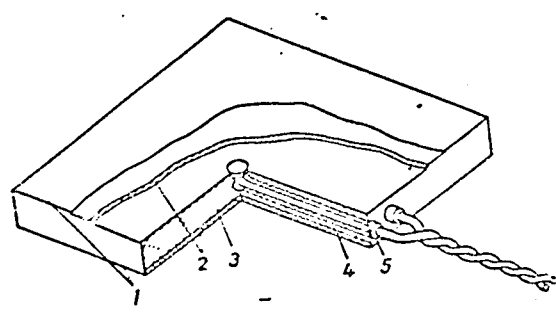
Fig. 25 Self-contained
heat flux transducer:

1. nickel coating
2. copper thermoelectrodes
3. intermediate thermo-
   electrodes
4. current-collecting wires
5. insulating bushings

Since all quantities on the
right-hand side of Eq. (II.2)
depend on temperature, sensi-
tivity must also be a function
of temperature.

The properties of several
thermoelectrode materials were
analyzed in selecting trans-
ducer materials. The results
of the calculations based on
literature data /7, 11/ are
presented in Fig. 26; in it,
the working temperature of the
transducer is plotted along the
y-axis, and along the x-axis--
the change in the working coef-
ficient relative to its value
at 50° C. Assumed as the work-
ing coefficient here and in the
following is a quantity that is
the inverse sensitivity, that
is, the flux inducing a signal
equal to 1 V:

$$k = \frac{q}{e}.$$ (II.3)

As we can see from the plot, most promising are the pairs
copper-constantan /265/ and especially constantan-nichrome.
The changes in the heat-physical characteristics proved to be

such that almost total mutual compensation is achieved for the effect of changes in the thermal conductivity and thermoelectric properties. From handbook data (see Fig. 26), this full compensation does not occur. The reason apparently lies in the considerable scatter of the properties of materials in different samples.
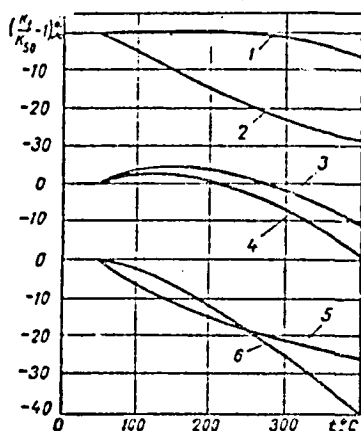
Fig. 26 Dependence of transducer coefficients on temperature (from handbook data):

1. constantan-nichrome
2. nickel-nichrome
3. copper-constantan
4. nichrome-constantan
5. alumel-chromel
6. iron-constantan

In the first series, copper-constantan transducers were made round. The blanks were stamped out of sheet material: clean constantan disks 0.6 mm thick and copper disks, 0.1 mm thick, with current-collecting projections (Fig. 27). The current-collecting plates were welded to the base plate with a capacitative welding machine. For measurement at high temperatures about 40 transducers were made with platinum current-collecting plates and conductors.

One deficiency of transducers with the pickup of signal at the periphery is the large scatter in the data of calibrations made one after the other. The following experiment was especially revealing. A transducer of this design was soldered to the bottom of an open vessel; the vessel was filled with cold water and placed on a heated electric plate. Water temperature and transducer signal were recorded in the experiments. Results of multiple measurements, using different transducers, are shown in Fig. <u>/51</u> 28. When the water boiled, the transducer signal was weakened generally down to one-fifth the initial value, while the density of the heat flux stayed the same. The reason for this significant reduction in signal strength was that at the place where the lower projection exited and along the entire perimeter of the transducer was formed an oblong depression in which materials differing in chemical activity alternated (tinplate, solder, copper, and constantan). Here there were favorable conditions for the growth of vaporization centers, intensively removing heat. Close to the lower projection and along the perimeter heat removal into the liquid occurred from the lower current-collecting plate, by-passing the intermediate plate. In this way the flux

measured took part only slightly in generating the transducer signal. The experimental results showed the need to make a detailed theoretical analysis of the complex of thermal and thermoelectrical effects in determining the best ways of designing monolithic transducers.
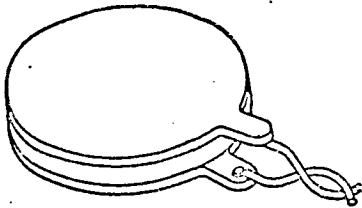
Fig. 27 Round transducer with current-collecting projections
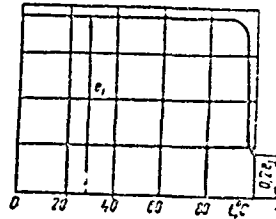
Fig. 28 Plot of change in readings of transducer with peripheral current-collection while liquid boils

2. Signal Formation in Self-Contained Heat Flux Transducers When The Measured Flux Is Nonuniformly Distributed

When taking measurements, we often encounter instances during which, even when the transducers are small, the plot of the measured flux turns out to be nonuniform (for example, the distribution of fluxes at a transversely swept cylinder or sphere).

Warping leads to the nonuniformity of distribution of the thermal emf generated at the middle plate by its penetrating flux; this causes short-circuited loops of electric current to appear, with the corresponding decreases in the electrical potentials. The latter indistinguishably superimpose on the thermal emf generated by the flux at the place where the current-collecting conductors are mounted. So the problem can be reduced to finding the perturbation induced by the imposed difference of electrical potentials in the short-circuited loops and determining the zone and nature of the effect of local perturbation that is limited in extent.

Solving these two problems lets us answer a number of questions, in particular the best dimensions of the transducer in which the signal at the central part is free of the effect of perturbations inevitable at the edges.

52

A qualitative pattern of the distribution of isotherms and heat-flux lines was established by making measurements on electrothermal models using a Fil'chakov-Panshin EGDA-9/61 integrator.

Since ordinarily in working conditions the transducer is placed on an isothermal surface, when the study was made with models, we can justifiably require that one of the transducer faces (upper or lower) be isothermal, that is, an equipotential. At the opposite face the condition of the second kind was replaced with a condition of the first kind by a method similar to that proposed in the study /242/ for converting from conditions of the third kind to a condition of the first kind. For this to be done, on the model surface was cemented an area cut by parallel slices and having a geometry such that when the potential difference was imposed, the pole resistances modeled the boundary conditions.

The results from paper models can be regarded only as a first approximation. The point is that inhomogeneity in the model paper leads to appreciable local perturbations. Solutions were revised by a method adopted in the theory of potential currents. It is based on the orthogonality property of the current lines and the equipotentials (Cauchy-Riemann):

$$\frac{\partial^2 \varphi}{\partial x^2} + \frac{\partial^2 \varphi}{\partial y^2} = 0; \quad \frac{\partial^2 \psi}{\partial x^2} + \frac{\partial^2 \psi}{\partial y^2} = 0;$$

$$\frac{\partial \varphi}{\partial x} = \pm \frac{\partial \psi}{\partial y}; \quad \frac{\partial \psi}{\partial x} = \mp \frac{\partial \varphi}{\partial y}. \qquad \text{(II.4)}$$

where φ and ψ are current function and potential

Plots of temperature and heat flux fields, recorded for the linear and parabolic laws of distribution of the incoming flux, are presented in Figures 29 and 30. The approximating properties of the straight line and the parabola are used widely in approximation analysis. As we can see from the resulting field plots, the horizontal flux components make up not more than 16 percent of the maximum value of the vertical flux components.

We must consider that the horizontal component by itself does not generate at the transducer a signal and, thus, is not a direct source of interference in the signal. It indirectly affects the change in the vertical projections of the heat fluxes.

53

At small angles, when the expansions of trigonometric functions in series can be limited to the first members, we have

$$\frac{1-\cos \alpha}{\lg \alpha} \approx \frac{\alpha}{2}.$$ (II.5)

So the vertical projections of the heat flux generating signals can be varied by no more than 1.5 percent of the maximum change in the flux based on the transducer.

Because localized measurements can be made with miniature transducers, the variations in the measured flux using the transducer are usually much smaller than the mean of the measured parameter to which, ultimately the measurement error must be related.

So in the analysis we can be limited to the one-dimensional inhomogeneity of the measured flux and take into account thermal and electroconductivity only in the actual direction for the measured flux--perpendicular to the transducer plane. In this case the intermediate plate can be represented as a continuous set of thin rods thermally and electrically insulated from each other heightwise and connected to each other with current-collecting plates.
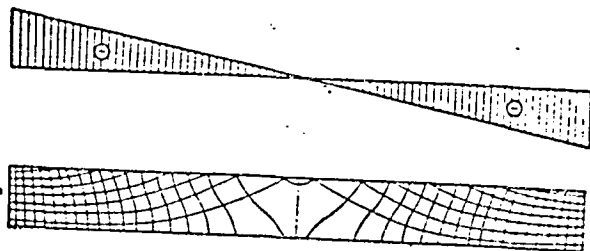
Fig. 29   Plot of flux and temperature fields when the flux varies linearly along trans=ducer

When electroconductivity is determined in a thin current-collecting plate, it is sufficient to allow for the resistance to the flow of electric current only along the plate and neglect the transverse resistance. The latter can be explained by the fact that in current-collecting plates, thickness differs from length by two orders of magnitude, and this leads to a corresponding difference in the longitudinal and transverse electrical resistances of four orders of magnitude. The symbols for the model described are shown in Fig. 31. The dimension is assumed equal to unity in the direction perpendicular to the plane of the figure.

The variation in flux based on the transducer is not limited, but naturally must be specified as a function of the

the coordinate x. The distribution of the incident flux is   /54
somewhat decreased owing to thermal conductivity in the extreme
transducer plates. Signal formation is affected by the flux
distribution at the intermediate plate, which thereafter is
taken into account. Converting from the distribution of the
flux incident at the external surface to the distribution in
the intermediate plate can be achieved in analytical form by
methods of thermal conductivity theory /124/ or using analog
equipment /131/ with the graphical or numerical specification
of conditions.

To derive the dif-
ferential equation that
describes the correla-
tions of the formation
of the thermoelectric
signal in self-con-
tained heat flux trans-
ducers, let us look at
the loop a-b-c-h, con-
sisting of two adjoining
columns of the interme-
diate layer bridged by
joined sections of the
current-collecting plates
(see Fig. 31).
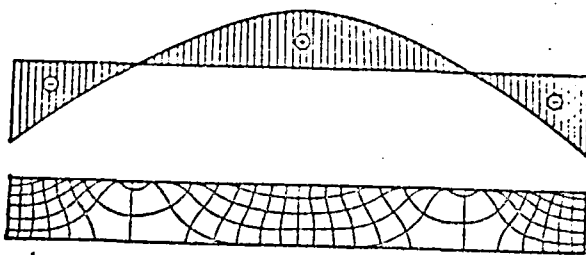
Fig. 30 Plot of flux and tempera-
ture field when the flux varies
parabolically along the transducer

Given the thickness δ_2 = 0.9 mm, we find that the intrin-
sic resistivity of the copper-constantan transducer is approxi-
mately $5 \cdot 10^{-6}$ ohms·cm². This calculated value agrees with the
results of direct measurements of voltage drop in transducers
when strong electric currents were (1-10 A) were passed through
them. Agreement of calculated data with measurements is evidence
of good contact between the current-collecting and intermediate
plates and the practically complete absence of contact resis-
tances. The effective total resistance of the outgoing-signal
conductors and the measuring instrument (load) usually exceeds
10 ohms. So the resistances for a 1 cm² transducer differ by
more than six orders of magnitude. Because of this, the load
current cannot be allowed for in the study made of large short-
circuited thermoelectric currents.

Under Kirchhoff's first law, in each vertical section the
current in the lower plate must equal in magnitude and be oppo-
site in direction to the current in the upper plate.

The current strength along the plate can occur only because
of current leakage into the intermediate plate with the density

55

$$i = -\frac{dl}{dx}. \qquad (II.6)$$
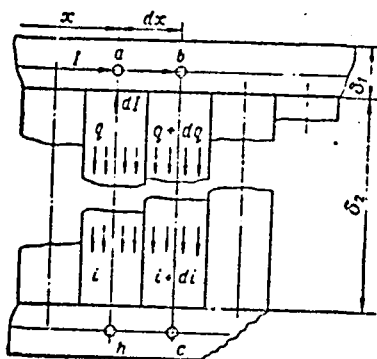
In each section the heat flux received is transmitted owing to thermal conductivity and the Peltier effect /39, 89, 135/:

$$q = \frac{\lambda_2}{\delta_2}\Delta t + \pi i = \frac{\lambda_2}{\delta_2}\Delta t + (\alpha_1 - \alpha_2)Ti, \qquad (II.7) \quad \underline{/55}$$

from which we have

Fig. 31 Model of self-contained heat flux transducer

$$\Delta t = \frac{\delta_2}{\lambda_2}[q - (\alpha_1 - \alpha_2)Ti]. \qquad (II.8)$$

The Seebeck thermal emf induced under the effect of this temperature difference is

$$e = \frac{\alpha_1 - \alpha_2}{\lambda_2}\delta_2[q - (\alpha_1 - \alpha_2)Ti]. \qquad (II.9)$$

Under Kirchhoff's second law, for the loop a-b-c-h we have

$$2l\frac{\varrho_1}{\delta_1}dx + \varrho_2\delta_2 di = (\alpha_1 - \alpha_2)\frac{\delta_2}{\lambda_2}[dq - (\alpha_1 - \alpha_2)Tdi]. \qquad (II.10)$$

whence, by referring to Eq. (II.6), we get

$$-\frac{d^2l}{dx^2} + l\frac{2}{\delta_1\delta_2\left[\frac{\varrho_2}{\varrho_1} + \frac{(\alpha_1-\alpha_2)^2 \cdot T}{\varrho_1\lambda_2}\right]} = \frac{(\alpha_1 - \alpha_2)\frac{dq}{dx}}{\varrho_1\lambda_1\left[\frac{\varrho_2}{\varrho_1} + \frac{(\alpha_1-\alpha_2)^2 T}{\varrho_1\lambda_2}\right]}. \qquad (II.11)$$

Let us introduce the dimensionless quantities

$$x = \frac{x}{\delta_2}; \quad k_\delta = \frac{\delta_2}{\delta_1}; \quad k_\varrho = \frac{\varrho_2}{\varrho_1}; \quad \gamma = \frac{(\alpha_1-\alpha_2)^2 T}{\varrho_2\lambda_2};$$

$$l = \frac{l}{l_0}; \quad \bar{q} = \frac{q}{q_0}; \quad L = \frac{l}{\delta_2}; \quad i = \frac{i\delta_2}{l_0}$$

and let us write Eq. (II.11) in dimensionless form:

$$-\frac{d^2 I}{dx^2} + 2I\,\frac{k_\delta}{k_0\,(1-\gamma)} = \frac{d\bar{q}}{dx}\cdot\frac{q_0(\alpha_1-\alpha_2)\delta_2}{I_0\lambda_2 C_2(1-\gamma)}.\tag{II.12}$$

If I_0 is chosen as equal to the current of the short-circuited transducer loaded with flux q_0, the second cofactor in the right-hand side of Eq. (II.12) will be equal to unity:

$$\frac{q_0(\alpha_1-\alpha_2)\delta_2}{I_0\lambda_2 C_2(1-\gamma)} = 1.\tag{II.13}$$

By denoting

$$\frac{2k_\delta}{k_0\,(1-\gamma)} \cdot k^2$$

and by substituting it together with Eq. (II.3) in Eq. (II.12), <u>/56</u> we get

$$\frac{d^2 I}{dx^2} - k^2 I = -\frac{d\bar{q}}{dx}\tag{II.14}$$

The general integral of Eq. (II.14) has the following form:

$$I(x) = C_1 e^{kx} + C_2 e^{-kx} - \frac{e^{kx}}{2k}\int_a^x \frac{d\bar{q}}{d\xi}e^{-k\xi}d\xi + \frac{e^{-kx}}{2k}\int_a^x \frac{d\bar{q}}{d\xi}e^{k\xi}d\xi\tag{II.15}$$

Here the choice of the lower limit of integration is totally unrestricted. When a = 0, the manipulations and the calculations turn out to be the simplest.

We find the values of the constants C_1 and C_2 from the following boundary conditions. At the transducer ends, when $\kappa = 0$ and $\kappa = L$, under Kirchhoff's first law we have

$$I(0) = I(L) = 0$$

From the first condition we find that $C_2 = -C_1$, and from the second:

$$C_1 = \frac{1}{e^{kL}-e^{-kL}}\left[\frac{e^{kL}}{2k}\int_0^L \frac{d\bar{q}}{d\xi}e^{-k\xi}d\xi - \frac{e^{-kL}}{2k}\int_0^L \frac{d\bar{q}}{d\xi}e^{k\xi}d\xi\right]\tag{II.16}$$

57

By substituting the values found for the constants into Eq. (II.15), we find the solution to Eq. (II.14) as applied to transducer boundary conditions:

$$I(\varkappa) = \frac{e^{-k\varkappa}}{2k} \int_0^{\varkappa} \frac{d\overline{q}}{d\xi} e^{k\xi} d\xi - \frac{e^{k\varkappa}}{2k} \int_0^{\varkappa} \frac{d\overline{q}}{d\varkappa} e^{-k\xi} d\xi +$$

$$+ \frac{sh\,k\varkappa}{sh\,kL} \left[\frac{e^{kL}}{2k} \int_0^L \frac{d\overline{q}}{d\varkappa} e^{-k\varkappa} d\varkappa - \frac{e^{-kL}}{2k} \int_0^L \frac{d\overline{q}}{d\varkappa} e^{k\varkappa} d\varkappa \right] \qquad (II.17)$$

The solution retains its value when κ is replaced with $(L - \kappa)$, that is, it does not depend on the direction in which the coordinate of the instantaneous section is read off from the edge of the transducer.

The values of the transverse current density are arrived at by differentiating Eq. (II.17) with respect to κ. The general expression for the current density in the intermediate plate is cumbersome and therefore is presented only for the special cases examined below.

1. When the transducer thermal load is uniform (q = const; $\frac{d\overline{q}}{d\varkappa} = 0$; $I(\varkappa) = 0$; $i(\varkappa) = 0$) there are no electrical perturbations whatever. The signal is the same over the entire transducer field and corresponds to the uniform measured flux.

2. The flux varies linearly within the transducer: /57

$$\overline{q} = 1 + m\varkappa; \quad \frac{d\overline{q}}{d\varkappa} = m. \qquad (II.18)$$

In this case the current in the collecting plate is

$$I(\varkappa) = \frac{m}{k^2} \left[\frac{ch\,kL - 1}{sh\,kL} sh\,k\varkappa - ch\,k\varkappa + 1 \right]; \qquad (II.19)$$

and the current density is

$$i(\varkappa) = \frac{m}{k} \left[\frac{1 - ch\,kL}{sh\,kL} ch\,k\varkappa + sh\,k\varkappa \right]. \qquad (II.20)$$

Graphical interpretations of Eqs. (II.18)-(II.20), shown in Fig. 32, like all the analogous preceding interpretations, were constructed on the assumption that k = 1, which is close to the actual conditions.

We must note that given the linear nature of flux variation perturbations show up only along the transducer edges. In the middle part of a large enough transducer linear variation in the measured flux does not introduce perturbations. In a transducer that is unbounded with respect to the coordinate x the perturbations are absent--a signal corresponding to the flux at the point of attachment is recorded in the current-collecting conductors.

3. The case when the measured flux within the transducer varies according to the law of quadratic parabola is interesting because the parabolas closely approximate diverse monotonic functions.

Let us postulate that

$$\bar{q}(x) = 1 + a\left[1 - \frac{4}{L^2}\left(x - \frac{L}{2}\right)^2\right] \qquad (II.21)$$

Then we have

$$\frac{d\bar{q}(x)}{dx} = -\frac{8a}{L^2}\left(x - \frac{L}{2}\right) \qquad (II.22)$$

By substituting Eq. (II.22) in Eq. (II.17), we get

$$I(x) = \frac{4a}{kL^2}\left\{\frac{\operatorname{sh} kx}{\operatorname{sh} kL}\left[e^{-kL}\int_0^L\left(x - \frac{L}{2}\right)e^{kx}dx - e^{kL}\int_0^L\left(x - \frac{L}{2}\right)e^{-kx}dx\right] + \right.$$

$$\left. + e^{kx}\int_0^x\left(\xi - \frac{L}{2}\right)e^{-k\xi}d\xi - e^{-kx}\int_0^x\left(\xi - \frac{L}{2}\right)e^{k\xi}d\xi\right\}. \qquad (II.23)$$

from whence, by integration and simplification, we find the cur- /58
rent in the sections of the collecting plates

$$I(x) = \frac{8a}{k^2L}\left[\frac{\operatorname{sh} k\frac{x}{2}}{\operatorname{sh} k\frac{L}{2}}\operatorname{ch} k\left(\frac{L}{2} - \frac{x}{2}\right) - \frac{x}{L}\right] \qquad (II.24)$$

59
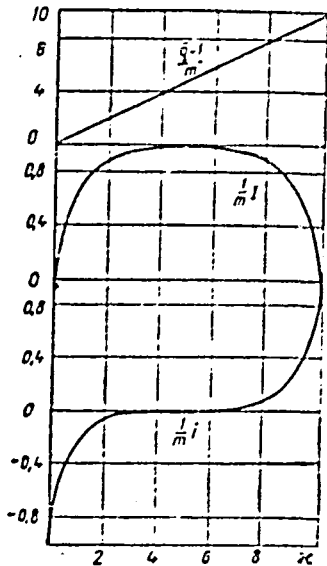
Fig. 32 Plots of transducer when flux varies linearly
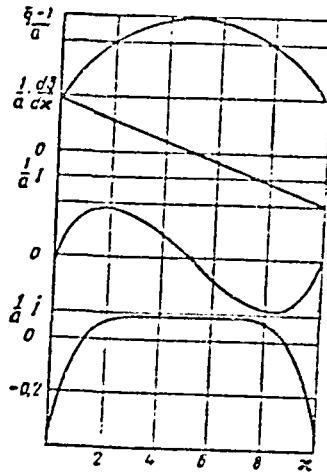
Fig. 33 Plots of transducer current when flux varies parabolically

and the current density in the intermediate plate is

$$i(x) = \frac{8a}{k^2 L}\left[\frac{1}{L} - \frac{k\,\mathrm{ch}\left(x - \frac{L}{2}\right)}{2\,\mathrm{sh}\,k\frac{L}{2}}\right] \qquad (II.25)$$

Plots of current for the case of a symmetric parabola in accordance with Eqs. (II.21), (II.24), and (II.25) are presented in Fig. 33.

Since the phenomena of thermal and electroconductivity, as well as thermoelectrical phenomena exhibit the property of superpositioning, therefore, by combining the two solutions derived, we can approximate various practical cases with them over a considerable range.

4. Further exposition and solution of a number of practical /59 problems requires that we look at the case of stepwise transition from one constant flux value to another. With a fairly

large number of these steps we can effectively approximate an arbitrary flux distribution in the transducer. At the same time the solution for this case allows us to estimate the nature and the region of influence of local perturbation. With a single step, the condition of approximation can be described as follows:

$$\bar{q}(x) = \bar{q}_1 \quad \text{when} \quad 0 \leqslant x < x_1$$

$$(II.26)$$

$$\bar{q}(x) = \bar{q}_2 \quad \text{when} \quad x_1 < x \leqslant L$$

Let us use the Fourier expansion that is customary for the δ-function /220/. Since the region of transition diminishes without limit, we can limit ourselves only to the first term of this expansion and assume that the transition occurs along a sinusoidal curve in the section from $\kappa_1 - \varepsilon$ to $\kappa_1 + \varepsilon$:

$$\bar{q}(x) = \frac{\bar{q}_1 + \bar{q}_2}{2} + \frac{\bar{q}_2 - \bar{q}_1}{2} \sin\left(\frac{x - x_1}{\varepsilon} \cdot \frac{\pi}{2}\right)$$

$$(II.27)$$

$$\frac{d\bar{q}(x)}{dx} = \frac{\bar{q}_2 - \bar{q}_1}{2} \cdot \frac{\pi}{2\varepsilon} \cos\left(\frac{x - x_1}{\varepsilon} \cdot \frac{\pi}{2}\right)$$

where ε can take on arbitrarily small values. Beyond the limits $\kappa \pm \varepsilon$ the flux values are constant, conditionally, and the derivatives are equal to zero. Taking this into account, let us examine the integrals appearing in Eq. (II.17):

$$\int_0^L \frac{d\bar{q}(x)}{dx} e^{kx} dx = \int_0^{x_1 - \varepsilon} \frac{d\bar{q}(x)}{dx} e^{kx} dx + \int_{x_1 - \varepsilon}^{x_1 + \varepsilon} \frac{d\bar{q}(x)}{dx} e^{kx} dx +$$

$$+ \int_{x_1 + \varepsilon}^L \frac{d\bar{q}(x)}{dx} e^{kx} dx.$$

$$(II.28)$$

The integrand functions are equal to zero in the right-hand side, in the first and third members. So, for any arbitrarily small ε

$$\int_0^L \frac{d\bar{q}(x)}{dx} e^{kx} dx = \frac{\bar{q}_2 - \bar{q}_1}{2} e^{kx_1} \int_{x_1 - \varepsilon}^{x_1 + \varepsilon} \frac{\pi}{2\varepsilon} \cos\left(\frac{x - x_1}{\varepsilon} \cdot \frac{\pi}{2}\right) dx =$$

$$= (\bar{q}_2 - \bar{q}_1) e^{kx_1}.$$

$$(II.29)$$

Similarly, it is easy to find that

$$\int_0^L \frac{d\bar{q}(x)}{dx} e^{-kx} dx = (\bar{q}_2 - \bar{q}_1) e^{-kx_1}.$$

since

$$\int_0^{\varkappa} \frac{d\bar{q}(\xi)}{d\xi} e^{\pm k\xi} d = 0 \quad \text{when} \quad \varkappa < \varkappa_1 \tag{II.30}$$

$$\int_0^{\varkappa} \frac{d\bar{q}(\xi)}{d\xi} e^{\pm k\xi} d\xi = (\bar{q}_2 - \bar{q}_1) e^{\pm k\varkappa_1} \quad \text{when} \quad \varkappa > \varkappa_1 \tag{II.31}$$

By substituting Eqs. (II.29)-(II.31) into Eq. (II.17), after cancellations we find the current in the collecting plates for the conditions of stepped transition:

$$I(\varkappa < \varkappa_1) = \frac{\bar{q}_2 - \bar{q}_1}{k} \cdot \frac{\operatorname{sh} k(L-\varkappa_1)}{\operatorname{sh} kL} \operatorname{sh} k\varkappa$$

$$\tag{II.32}$$

$$I(\varkappa > \varkappa_1) = \frac{\bar{q}_2 - \bar{q}_1}{k} \cdot \frac{\operatorname{sh} k\varkappa_1}{\operatorname{sh} kL} \operatorname{sh} k(L-\varkappa)$$

and the current density in the intermediate plate

$$I(x < \varkappa_1) = -(\bar{q}_2 - \bar{q}_1) \frac{\operatorname{sh} k(L-\varkappa_1)}{\operatorname{sh} kL} \operatorname{ch} k\varkappa;$$

$$\tag{II.33}$$

$$I(x > \varkappa_1) = (\bar{q}_2 - \bar{q}_1) \frac{\operatorname{sh} k\varkappa_1}{\operatorname{sh} kL} \operatorname{ch} k(L-\varkappa).$$

A graphical interpretation of the foregoing is presented in Fig. 34.

5. Let us examine two transition steps between three values of the constant fluxes $\bar{q}_1$, $\bar{q}_2$, and $\bar{q}_3$. We let κ_2 stand for the coordinate of the second step. Let $\kappa_2 > \kappa_1$. For the isolated action of the second jump, on analogy with Eqs. (II.32) and (II.33), we can write

$$\left. \begin{array}{l} I(\varkappa < \varkappa_2) = \dfrac{\bar{q}_3 - \bar{q}_2}{k} \cdot \dfrac{\operatorname{sh} k(L-\varkappa_2)}{\operatorname{sh} kL} \operatorname{sh} k\varkappa; \\[2mm] I(\varkappa > \varkappa_2) = \dfrac{\bar{q}_3 - \bar{q}_2}{k} \cdot \dfrac{\operatorname{sh} k\varkappa_2}{\operatorname{sh} kL} \operatorname{sh} k(L-\varkappa); \\[2mm] I(\varkappa < \varkappa_2) = -(\bar{q}_3 - \bar{q}_2) \dfrac{\operatorname{sh} k(L-\varkappa_2)}{\operatorname{sh} L} \operatorname{ch} k\varkappa; \\[2mm] I(\varkappa > \varkappa_2) = (q_3 - q_2) \dfrac{\operatorname{sh} k\varkappa_2}{\operatorname{sh} kL} \operatorname{ch} k(L-\varkappa). \end{array} \right\} \tag{II.34}$$

Based on the superposition property, when there are combined actions, the two steps of the solution can be represented as the sum of particular solutions:

$$I(\varkappa < \varkappa_1 < \varkappa_2) = \frac{sh\, k\varkappa}{k\, sh\, kL} [(\bar{q}_2 - \bar{q}_1)\, sh\, k(L - \varkappa_1) +$$
$$+ (\bar{q}_3 - \bar{q}_2)\, sh\, k(L - \varkappa_2)];$$

$$i(\varkappa < \varkappa_1 < \varkappa_2) = -\frac{ch\, k\varkappa}{sh\, kL} [(\bar{q}_2 - \bar{q}_1)\, sh\, k(L - \varkappa_1) +$$
$$+ (\bar{q}_3 - \bar{q}_2)\, sh\, k(L - \varkappa_2)];$$

$$I(\varkappa_1 < \varkappa < \varkappa_2) = \frac{sh\, k(L - \varkappa)}{k\, sh\, kL} (\bar{q}_2 - \bar{q}_1)\, sh\, k\varkappa_1 +$$
$$+ \frac{sh\, k\varkappa}{k\, sh\, kL} (\bar{q}_3 - \bar{q}_2)\, sh\, k(L - \varkappa_2); \qquad\qquad \text{(II.35)}$$

$$i(\varkappa_1 < \varkappa < \varkappa_2) = \frac{ch\, k(L - \varkappa)}{sh\, kL} (\bar{q}_2 - \bar{q}_1)\, sh\, k\varkappa_1 -$$
$$- \frac{ch\, k\varkappa}{sh\, kL} (\bar{q}_3 - \bar{q}_2)\, sh\, k(L - \varkappa_2);$$

$$I(\varkappa_1 < \varkappa_2 < \varkappa) = \frac{sh\, k(L - \varkappa)}{k\, sh\, kL} [(\bar{q}_2 - \bar{q}_1)\, sh\, k\varkappa_1 +$$
$$+ (\bar{q}_3 - \bar{q}_2)\, sh\, k\varkappa_2];$$

$$i(\varkappa_1 < \varkappa_2 < \varkappa) = \frac{ch\, k(L - \varkappa)}{sh\, kL} [(\bar{q}_2 - \bar{q}_1)\, sh\, k\varkappa_1 +$$
$$+ (\bar{q}_3 - \bar{q}_2)\, sh\, k\varkappa_2].$$

6. By induction we can derive recurrence relations for an arbitrary section between the (m - 1)-th and m-th jumps for a total number of jumps p:

$$I(\varkappa_{m-1} < \varkappa < \varkappa_m) = \frac{sh\, k(L - \varkappa)}{k\, sh\, kL} \sum_{1}^{m-1} (\bar{q}_{i+1} - \bar{q}_i)\, sh\, k\varkappa_i +$$
$$+ \frac{sh\, k\varkappa}{k\, sh\, kL} \sum_{m}^{p} (\bar{q}_{i+1} - \bar{q}_i)\, sh\, k(L - \varkappa_i); \qquad\qquad \text{(II.36)}$$

$$i(\varkappa_{m-1} < \varkappa < \varkappa_m) = \frac{ch\, k(L - \varkappa)}{sh\, kL} \sum_{1}^{m-1} (\bar{q}_{i+1} - \bar{q}_i)\, sh\, k\varkappa_i -$$

63

$$-\frac{\operatorname{ch} kx}{\operatorname{sh} kL} \sum_{m}^{p} (\bar{q}_{i+1} - \bar{q}_i) \operatorname{sh} k(L - x_i).$$ /62

7. Local perturbation at a section of limited extent is a special form of load of the cases considered. The case where local perturbation occurs at an edge of the transducer is the most interesting case for measuring practice. In the numerical example for which the plots are constructed in Fig. 35, the region of perturbation is confined to the value $\kappa = (0-0.9)\delta_2$, that is, in the symbols of Eqs. (II.32) and (II.33) $\kappa_1 = 0.1$ and $k = 1$. The scale of relative lengths in the perturbation region, for sake of clarity, is selected as being an order of magnitude greater than for the entire transducer field. When the arguments are small, the current density in the intermediate plate in the perturbation region remains practically the same. The current strength in the current-collecting plate increases linearly.
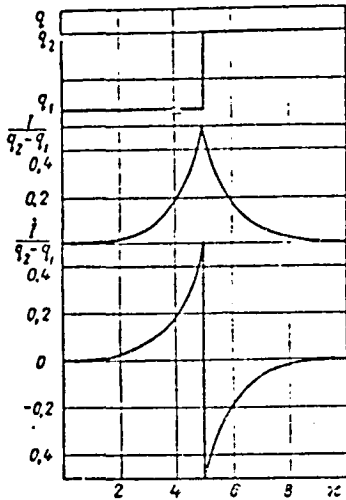
Fig. 34 Plots of transducer current when flux varies stepwise
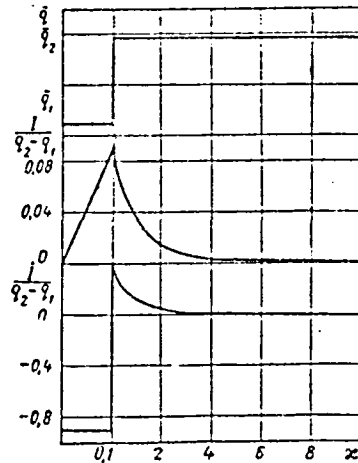
Fig. 35 Plots of transducer current when there is edgewise thermal perturbation

As the plot in Fig. 35 shows, the densities of transverse current induced by interference decrease rapidly with distance from the perturbation location. Tracing the variations in residual perturbations on the plot is hard, so they are presented below:

x	0.1	1.0	2.0	3.0	4.0	5.0	6.0
$\dfrac{i(x)}{q_2-q_1}$	0.032	0.037	0.0136	0.0070	0.0018	0.00070	0.00025
$\dfrac{i(x)}{i_{max}}$, %	100	40.5	14.9	5.5	1.96	0.8	0.3

Given the selected transducer dimensions with the relative /63 distance of the central leads from the edge equal to $\kappa = 5$ to the current-collecting conductors, only 0.8 percent of the initial perturbation is reached. Apparently, a further increase in the transducer directions in the x-direction is no longer advisable. Because of the foregoing, we can understand the considerable reduction in the perturbing influences observed when the mounting location of the current-collecting conductors is shifted from the transducer edge to its center.

The density of the transverse electric current at any point on the transducer, specifically, the mounting location of the current-collecting conductors, can be found by the above-considered methods, for a given flux distribution pattern in the transducer. Under Kirchhoff's law, the transverse current will weaken or strengthen the transducer working signal. Assuming a flux q and transverse current i that are known for the conductor mounting location, the effective recorded transducer signal is

$$e_{eff} = \frac{q}{k_t} + \delta_2 \rho_2 i \qquad (II.37)$$

where the directions shown in Fig. 31 are chosen as positive.

3. Interference and Noise in Signals of Self-Contained Heat Flux Transducers

The working coefficients of small self-contained heat flux transducers are close to $500 \cdot 10^6$ W/m$^2 \cdot$V. When the fluxes are measured in the 10^3-10^6 W/m^2 range, the transducer signal varies roughly from 2 to $2 \cdot 10^3$ μV; this corresponds to 0.05-50 deg of temperature difference at the intermediate layer. Along the current-collecting conductors, the temperature change as a rule turns out to be much larger. Under all known methods of reducing interference /205/, evidently suppression of the causes of interference in the transducers is most radical in the measuring circuits.

According to GOST 1790-63 and 6916-54, the error of thermocouples made of standard thermoelectrodes may exceed 1 percent of the measured value. This was due mainly to the inhomogeneity of materials both from lot to lot, as within a single conductor segment /91/.

As in the thermocouples, the interference source in self-contained heat flux transducer is the temperature difference along the thermoelectrodes. But the distinction here is that in thermocouples the working signal and the interference originate usually for the same reason, and in transducers the signal is caused by the measured flux that is not due to the temperature difference along the current-collecting electrodes.

As a rule, the temperature difference at the transducer is sometimes several orders of magnitude smaller than the temperature difference at the current-collecting conductors. Therefore, for the same tolerances for measurement error, the requirements /64 on the homogeneity of the thermoelectrodes must be much higher for transducers than for thermocouples.

To clarify the question of how suitable standard thermoelectrodes are for current-collecting conductors of self-contained heat flux transducers, a check was made for homogeneity by the customary method /92, 190/. It was found that wires of pure metals have much better thermoelectrical homogeneity than alloys. Pure platinum (99.99 percent) and silver (99.9 percent), as well as electrotechnical conductor copper (GOST 2112-62) exhibit the highest homogeneity. But interference in alloys, including standard thermoelectrode alloys, is ordinarily one order higher than in pure metals. The nickel and iron analyzed had more than 1 percent impurities; as to homogeneity they were between the alloys and the pure metals. It appears that we can expect all pure metals to have high homogeneity.

Requirements on the intermediate thermoelectrode are conventional, so it can be made of alloys.

All the foregoing about the requirements for homogeneity of transducer materials is valid also for materials in differential thermocouples for measuring small temperature differences. It must be noted that the system of selecting standard thermoelectrodes adopted in the USSR is inferior to the systems adopted in Western European countries (Great Britain, France, and the FRG). In our country pure platinum is used only in the platinum-rhodium alloy-platinum thermocouple, but in all the other thermocouples both thermoelectrodes are alloy; none of the noble pure metals (copper, iron, and nickel) have been adopted as standard materials. In France, for example, most thermocouples

have the following as the pure thermoelectrode: copper-constantan, iron-constantan, and nickel-nichrome /286/. As to composition, the last-named composition corresponds to our chromel.

Because all alloy conductors, in particular standard thermoelectrodes, have low homogeneity, usually wires of pure platinum and electrotechnical copper are commonly employed for the current-collecting conductors of transducers. Even when the transducer temperature is about 600° C, for a series-manufactured self-contained heat flux transducer, the interference from inhomogeneity in copper can lead to an error in the measured flux of no more than 30-40 W/m^2.

Perturbations and inhomogeneity in the measured flux (see Section 2 of this chapter) can be one of the main sources of stationary interference in the signal.

At temperatures other than 0° K, all physical parameters of the transducer suffer from fluctuational changes. As applied to self-contained heat flux transducers, this may end up in statistical variation in the transducer working signal. In some cases of measuring practice, this noise level determines equipment capability. In particular, at room temperature (20° C) in metals the fluctuational electron stream is as high as 10^{13} $/65$ A/cm^2 /243/. On the average this enormous current (existing instruments can measure only billionths of its value) is completely equilibrated by a current that is oppositely opposed for each area, to an accuracy of counted electrons per second (charge on the electron $e = 1.6 \cdot 10^{-19}$ A·s).

The equilibrium that is quasistationary on the average is disturbed owing to the quantum nature of energy exchange between the particles of the transducer materials. In a formal analysis, the fluctuational nature of the signal is manifested, on the one hand, in the inhomogeneity of the differential equations, and on the other--in the inhomogeneity of the boundary conditions. Even if there were certainty as to the correctness of the main representations from which the differential equations are derived and the boundary conditions are formulated, their solution would have to be limited to a number of simplifying assumptions /167/. Therefore let us dwell only on estimating the frequency spectrum of the fluctuational signal under conditions existing in the self-contained heat flux transducers, similar to what Rytov did for metal conductors /195/.

It is assumed that the period of the fluctuational oscillation is of the order of the mean free path length of electrons in the metal /5/, and that this time on the average is equal

to the ratio of the mean free path length s to the electron
thermal velocity v:

$$\tau = \frac{s}{v} \qquad\qquad (II.38)$$

The values of the quantities appearing in Eq. (II.38), in
the usual conditions of thermal experiments, are of the order of
magnitude $s \sim 10^{-8}$ m and $v = 10^6$ m/s. So the fluctuation period
of the transducer signal due to thermal fluctuation of the elec-
trons is of the order of $\tau \sim 10^{-14}$ s. So electron fluctuation
does not have to be taken into account since in ordinary tech-
nical measurements the time constant of the system can be mea-
sured in the range of a few seconds and only in exceptional situ-
ations reaches 10^{-4} s.

Fluctuation in the local temperature at the signal-acquisi-
tion points in the transducer can be the next cause of signal
fluctuations. For conventional thermoelectrode materials Geiling
/268/, based on Maxwell's distribution law, found the minimum
value of the recorded signal: it does not exceed in magnitude
the noise effect. For a thermoelectrical receiver, 1 mm^2 in
area, $P_{min} = 0.5 \cdot 10^{-10}$ W. These data agree well with Fell'zhe's
measurements. For a 1 cm^2 transducer--noting that the minimum
power is directly proportional to the square root of the trans-
ducer area, we found that the flux, reduced to the noise signal,
does not exceed $q_{noise} = 0.5 \cdot 10^{-5}$ W/m^2.

All the evaluations given are not marked by rigor of pro-
blem formulation and therefore permit determining just the order   /66
of the desired quantity.

4. Accounting for Distortions Introduced in Measurements Because
Transducers Were Present

Ordinarily it is assumed that the presence of a transducer
does not introduce appreciable distortions into the measured
flux values. For this purpose, all the heat-physical character-
istics (total thermal resistances, coefficients of absorption
and emission, and so on) in the flux path, when a transducer is
inserted, must remain unchanged. Often, however, these condi-
tions prove to be unfulfilled, and we have to reconcile ourselves
with the distortions introduced, by taking accounting of them
with appropriate corrections.

Below are given the necessary relations between the true
and the measured parameters in the most characteristic measure-
ment cases.

Transducer placed in infinite body. When measurements taken with plane electrothermal models (plane problem) were compared with calculation results using the finite-differences method for axisymmetric cases (three-dimensional problem), fairly good mutual agreement was obtained /62/. Because of this, in the following period the concentrating (or dissipating) effect of the transducer was studied only with plane electrothermal models made of electrically conducting paper, with a Fil'chakov-Panchishin integrator, model EGDA-9/61, by the method of orthogonal conversion of current functions into a potential and the conversion of the potential into a current function.

When the paper parts of the models were assembled with electrically conducting cement, a large scatter of data points resulted. Since in these problems the required accuracy is much higher than was adopted in the EDGA model, electrically conducting conducting cements had to be abandoned, because they inevitably introduced uncontrollable local inhomogeneities in the test fields. To reduce the effect of local inhomogeneities intrinsic to paper, the models were assembled of several layers dissimilarly oriented relative to the direction of the poles of the initial material. But cement use remained the main reason for inhomogeneity.

A solution was reached by using ordinary shot coated with a thin layer of electrical insulation. A layer of this shot, heaped on a model assembled without cement, did not change the local conditions of conductivity and only slightly impeded measurement. By the effect of gravity the shot evenly compressed individual model component elements, thereby ensuring reliable electrical contact without disturbing the resistance fields. All measurements showed good reproducibility and mutual agreement of results. The dependence of the correction factor /67
$k = \dfrac{q_{mea}}{q}$ on the ratio of the transducer thermal conductivity to the body conductivity, for different relative transducer dimensions, is shown in Fig. 36.

The correction factor k must be considered as the relative increase in the density of current lines caused by introducing the transducer.

Transducer placed on surface of semibounded body. Owing to the symmetry of the temperature field and the flux field in the body, the results are applicable to the case when the transducer is on the surface of a semibounded body, assuming a boundary condition of the first kind. Corresponding to identical conditions are transducers whose thickness is half the value for the transducers for which Fig. 36 was plotted.

69
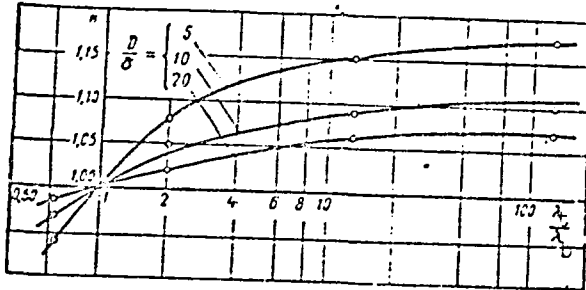
Fig. 36 Dependence of coefficient of flux concentration by transducer located in body on the relative thermal conductivity and relative transducer dimensions

Transducer placed on surface of heat-exchanger. When convective heat transfer is investigated, transducers are commonly placed on the wall surface; this causes local increase in thermal resistance, leading to distortion of the heat flux field.

For heat-exchangers on flat and curved walls characteristics such as total temperature head and thermal resistances of elements can be assumed independent of the fact of transducer placement. And under Ohm's law, the correction must be equal to the ratio of the corresponding total thermal resistances:

$$k = \frac{q_{mea}}{q} = \frac{R_{sys}}{R_{sys} + R_t} \qquad (II.39)$$

Here as earlier, the correction is the ratio of the flux signal measured by the transducer and recorded to the true flux that would have occurred if there were no perturbing effect of the transducer.

Using the main equation (II.39), we can easily find the values of the correction factors for different characteristic cases of transducer placement in industrial heat-power installations:

for a plane wall

$$k = \frac{\dfrac{1}{\alpha_1} + \dfrac{\delta_w}{\lambda_w} + \dfrac{1}{\alpha_2}}{\dfrac{1}{\alpha_1} + \dfrac{\delta_w}{\lambda_w} + \dfrac{1}{\alpha_2} + \dfrac{\delta_t}{\lambda_t}} \qquad (II.40)$$

70

for a cylindrical wall, when the transducer is placed on the outside,

$$k = \cfrac{\cfrac{1}{\alpha_1 d_1} + \cfrac{1}{2\lambda_w} \ln \cfrac{d_2}{d_1} + \cfrac{1}{\alpha_2 d_2}}{\cfrac{1}{\alpha_1 d_1} + \cfrac{1}{2\lambda_w} \ln \cfrac{d_2}{d_1} + \cfrac{1}{2\lambda_t} \ln \cfrac{d_2 + 2\delta_t}{d_2} + \cfrac{1}{\alpha_2 (d_2 + 2\delta_t)}} \qquad (II.41)$$

for a cylindrical wall, when the transducer is placed on the inside,

$$k = \cfrac{\cfrac{1}{\alpha_1 d_1} + \cfrac{1}{2\lambda_w} \ln \cfrac{d_2}{d_1} + \cfrac{1}{\alpha_2 d_2}}{\cfrac{1}{\alpha_1 (d_1 - 2\delta_t)} + \cfrac{1}{2\lambda_t} \ln \cfrac{d_1}{d_1 - 2\delta_t} + \cfrac{1}{2\lambda_w} \ln \cfrac{d_2}{d_1} + \cfrac{1}{\alpha_2 d_2}} \qquad (II.42)$$

for a spherical wall, when the transducer is placed on the outside,

$$k = \cfrac{\cfrac{1}{\alpha_1 d_1^2} + \cfrac{1}{2\lambda_w} \left(\cfrac{1}{d_1} - \cfrac{1}{d_2} \right) + \cfrac{1}{\alpha_2 d_2^2}}{\cfrac{1}{\alpha_1 d_1^2} + \cfrac{1}{2\lambda_w} \left(\cfrac{1}{d_1} - \cfrac{1}{d_2} \right) + \cfrac{1}{\lambda_t} \cdot \cfrac{\delta_t}{d_2 (d_2 + 2\delta_t)} + \cfrac{1}{\alpha_2 (d_2 + 2\delta_t)^2}} \qquad (II.43)$$

for a spherical wall, when the transducer is placed on the inside, -

$$k = \cfrac{\cfrac{1}{\alpha_1 d_1^2} + \cfrac{1}{2\lambda_w} \left(\cfrac{1}{d_1} - \cfrac{1}{d_2} \right) + \cfrac{1}{\alpha_2 d_2^2}}{\cfrac{1}{\alpha_1 (d_1 - 2\delta_t)^2} + \cfrac{1}{\lambda_t} \cdot \cfrac{\delta_t}{d_1 (d_1 - 2\delta_t)} + \cfrac{1}{2\lambda_w} \left(\cfrac{1}{d_1} - \cfrac{1}{d_2} \right) + \cfrac{1}{\alpha_2 d_2^2}} \qquad (II.44)$$

For the conditions of flow of the radiative components of the measured fluxes to be equivalent, it is necessary that the transducer. have a degree of blackness equal to that for the wall in the transducer placement location. The difference in the surface properties of the transducers allows us to distinguish convective from radiative components in complex heat transfer (see Section 3, Chapter 7).

5. Measuring Nonstationary Fluxes

The task of measuring heat fluxes with transducers amounts to finding the relation between the measured flux and the generated signal. Naturally, the transducer reacts to the flux penetrating it, so the effect of the transducer's presence on the measured flux must be reduced to a minimum. The extent of absorption or emission of the measuring element must be the same as the receiving surface, and the total thermal resistance in the heat flux circuit must remain unchanged (see Section 4 of this chapter). But even if the boundary conditions are kept totally identical, the transducer signal can markedly differ from the signal that, given stationary conditions of calibration, corresponds to uniform measured flux.

In the linear version, the heat-physical properties ($\lambda_1 =$ = const and a_1 = const) and the heat-transfer coefficient at the surface $x^1 = \delta_2$ are assumed to be independent of temperature. The coordinate x is read off from the plane of contact between the plates toward the side designated by the subscript 2 (see Fig. 38).

This effect can be described by a one-dimensional thermal conductivity equation:

$$\frac{\partial t(x, \tau)}{\partial \tau} = a_i \frac{\partial^2 t(x, \tau)}{\partial x^2} \quad (i = 1, 2) \tag{II.45}$$

where the coefficient of thermal diffusivity is selected as a function of the region for which the thermal conductivity equation is used (a_1 or a_2).

As per the foregoing, the boundary conditions can be written as:

$$\frac{\partial t(-\delta_1, \tau)}{\partial x} = -\frac{1}{\lambda_1} q(\tau); \quad \frac{\partial t(\delta_2, \tau)}{\partial x} = -\frac{\alpha_2}{\lambda_2} [t(\delta_2, \tau) - t_0(\tau)]$$

$$t(0 - 0, \tau) = t(0 + 0, \tau); \quad \frac{\partial t(0 - 0, \tau)}{\partial x} = \frac{\lambda_2}{\lambda_1} \cdot \frac{\partial t(0 - 0, \tau)}{\partial x}. \tag{II.46}$$

For convenience and conciseness of the subsequent manipulations, let us use the Laplace transform. In the images from Eq. (II.45) and conditions (II.46), we get

$$\frac{d^2 T(\varrho_i, s)}{d\varrho_i} - \frac{s\delta_i^2}{a_i} T(\varrho_i, s) = 0; \quad \varrho_i = \frac{x}{\delta_i} \quad (i = 1, 2) \tag{II.47}$$

$$\frac{dT(-1, s)}{d\varrho_1} = -\frac{\delta_1}{\lambda_1} Q(s); \quad \frac{dT(0-0, s)}{d\varrho_1} = \frac{\lambda_2\delta_1}{\lambda_1\delta_2} \cdot \frac{dT(0 \div 0, s)}{d\varrho_2} \qquad \text{(II.48)}$$

$$T(0-0, s) = T(0 \div 0, s); \quad \frac{dT(1, s)}{d\rho_2} = -\frac{\alpha\delta_2}{\lambda_2}[T(1, s) - T_0(s)]$$

where $\quad T(\varrho_i, s) = \int_0^\infty t(\varrho_i, \tau)e^{-s\tau}d\tau = L[t(\varrho_i, \tau)] \quad$ is the image of temperature

$t(\varrho_i, \tau); Q(s) = L[q(\tau)], T_0(s) = L[t_0(\tau)] \qquad$ are the images of flux $q(\tau)$

and temperature $t_0(\tau)$.

Equations and boundary conditions are reduced to dimensionless coordinates; in each region (1 and 2) the coordinates are related to the corresponding plate thickness.

The solutions to Eqs. (II.47) have the following forms:

$$T(\varrho_1, s) = A_1 \operatorname{sh} \beta_1\varrho_1 + B_1 \operatorname{ch} \beta_1\varrho_1$$

$$T(\varrho_2, s) = A_2 \operatorname{sh} \beta_2\varrho_2 + B_2 \operatorname{ch} \beta_2\varrho_2 \qquad \text{(II.49)}$$

where $\quad \beta_1^2 = \frac{s\delta_1^2}{a_1}; \quad \beta_2^2 = \frac{s\delta_2^2}{a_2}$.

Starting from the assumption made about the linearity of the conditions, the solutions (II.49) can be expressed in terms of the transfer functions:

$$T(\varrho_1, s) = Y_q(\varrho_1, s)Q(s) \div Y_t(\varrho_1, s)T_0(s)$$

$$T(\varrho_2, s) = Y_q(\varrho_2, s)Q(s) + Y_t(\varrho_2, s)T_0(s) \qquad \text{(II.50)}$$

where Y_q and Y_t are transfer functions linking the temperature images in the body with the images of heat fluxes $Q(s)$ and, thus, the temperature images of the medium $T_0(s)$.

When investigating the nonstationary conditions, it is best to apply the N. A. Yaryshev method; fundamentally, it permits solving the problem when there is arbitrary variation in time of both the incoming fluxes and the boundary temperatures /245/.

Among the diverse conditions of measurement, the following cases are technically meaningful:

the measured (positive or negative) flux is received by a transducer placed on the surface of a semibounded body (Fig. 37, a)

part of the heat-exchanger wall is replaced with a transducer (Fig. 37, b)

the transducer located on a section of the heat-exchanger surface receives the recorded flux, passing further through the wall and removed at the rate α toward a medium at a temperature $t_0(\tau)$ (Fig. 37, c)

the measured flux initially penetrates the bearing wall, and then passes through the transducer to the surrounding medium (Fig. 37, d).

In our case the measured flux $q(\tau)$ and temperature $t_0(\tau)$ of the receiving medium are arbitrarily specified functions of time. /71

All the variants enumerated can be reduced to particular solutions of the thermal conductivity problem for a two-layer wall. When evaluating the effects of nonstationary character, considering the results given in Section 2 of this chapter, we can neglect the distortions at the peripheral regions of the transducers and we consider them as infinite plates, just like the bearing wall (Fig. 38).
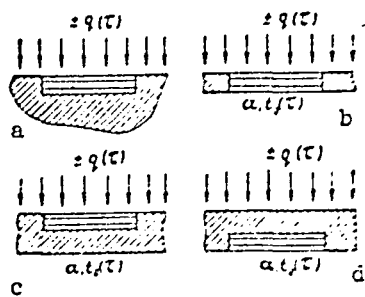
Fig. 37   Schematic representation of different cases of transducer operation
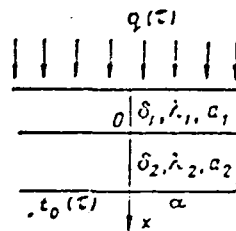
Fig. 38   Model of two-layer wall

Substituting Eqs. (II.49) and (II.50) in (II.48), we get:

$$Y_q(\varrho_1, s) = \frac{\delta_1}{\lambda_1 \Delta} [\beta_2 (\mathrm{ch}\beta_2 \,\mathrm{ch}\,\beta_1 \varrho_1 - \varkappa \,\mathrm{sh}\,\beta_2 \,\mathrm{sh}\,\beta_1 \varrho_1) \div$$

$$+ \zeta_2 (\mathrm{sh}\,\beta_2 \,\mathrm{ch}\,\beta_1 \varrho_1 - \varkappa \,\mathrm{ch}\,\beta_2 \,\mathrm{sh}\,\beta_1 \varrho_1)];$$

$$Y_q(\varrho_2, s) = \frac{\delta_1}{\lambda_1 \Delta} [\beta_2 \,\mathrm{ch}\,\beta_2 (1 - \varrho_2) + \zeta_2 \,\mathrm{sh}\,\beta_2 (1 - \varrho_2)];$$

$$Y_t(\varrho_1, s) = \frac{\varkappa \zeta_2 \beta_1}{\Delta} \,\mathrm{ch}\,\beta_1 (1 \div \varrho_1);$$

$$Y_t(\varrho_2, s) = \frac{\zeta_2 \beta_1}{\Delta} [\mathrm{sh}\,\beta_1 \,\mathrm{sh}\,\beta_2 \varrho_2 + \varkappa \,\mathrm{ch}\,\beta_1 \,\mathrm{ch}\,\beta_2 \varrho_2],$$

(II.51)

where $\Delta = \beta_1 [\beta_2 (\mathrm{sh}\,\beta_1 \,\mathrm{ch}\,\beta_2 \div \varkappa \,\mathrm{sh}\,\beta_2 \,\mathrm{ch}\,\beta_1) + \zeta_2 (\mathrm{sh}\,\beta_1 \,\mathrm{sh}\,\beta_2 \div \varkappa \,\mathrm{ch}\,\beta_1 \,\mathrm{ch}\,\beta_2)]$

$$\frac{\beta_2}{\beta_1} = \eta; \qquad \frac{\lambda_2 c_2 \gamma_2}{\lambda_1 c_1 \gamma_1} = \varkappa^2; \qquad \frac{\alpha \delta_2}{\lambda_2} = \zeta_2$$

From the solutions (II.51), we can determine—in particular—the values of the transfer functions for the above-considered cases.

Corresponding to Fig. 37, a is an unbounded increase in /72 the thickness of the supporting transducer of a plate ($\delta_2 \to \infty$). And the values $-\eta$ and ζ_2 increase without bound at the same time. After simple transformations and cancellations from the system of equations (II.51) for the transducer placed on the semibounded body (II.51), we find

$$Y_q(\varrho_1, s) = \frac{\delta_1}{\lambda_1 \beta_1} \cdot \frac{\mathrm{ch}\,\beta_1 \varrho_1 - \varkappa \,\mathrm{sh}\,\beta_1 \varrho_1}{\mathrm{sh}\,\beta_1 - \varkappa \,\mathrm{ch}\,\beta_1}$$

(II.52)

$$Y_t(\varrho_1, s) = 0$$

Corresponding to Fig. 37, b is a limited fall-off in the thickness of the supporting wall to zero ($\delta_2 \to 0$). And η and ζ_2 also falls off to zero.

As a result, from the system of equations (II.51) we get the following transfer functions for the heat-exchanger surface fulfilling the functions of a transducer, considering that

$$\zeta_2 \frac{\varkappa}{\eta} = \zeta_1 = \frac{\alpha \delta_1}{\lambda_1},$$

75

$$Y_q(\varrho_1, s) = \frac{\delta_1}{\lambda_1} \cdot \frac{\beta_1 \operatorname{ch} \beta_1 \varrho_1 - \zeta_1 \operatorname{sh} \beta_1 \varrho_1}{\beta_1 (\beta_1 \operatorname{sh} \beta_1 - \zeta_1 \operatorname{ch} \beta_1)}$$

$$Y_t(\varrho_1, s) = \frac{\zeta_1 \operatorname{ch} \beta_1 (1 + \varrho_1)}{\beta_1 \operatorname{sh} \beta_1 - \zeta_1 \operatorname{ch} \beta_1}$$

(II.53)

Finally, the second of each pair of Eqs. (II.51) are applicable to the case of Fig. 37, d.

The particular cases of Eqs. (II.52) and (II.53) coincide with N. A. Yaryshev's solutions /245/, obtained in individual derivations for a one-layer wall and a plate laid against a semibounded body. This derivation method in the general case with conversions to particular cases is more universal.

The solutions described allow us to evaluate the factors affecting the measurements and to classify them by degree of importance.

A transducer as such is a three-layer wall, which in conjunction with the supporting element must form a four-component system. In the one-dimensional representation, the thermal conductivity equation is retained in the form (II.45) and the boundary conditions are similar to (II.46). The method of constructing the solution is transparently clear, but so cumbersome that the conceptual extension of the results does not justify the means with which the results can be obtained. The effect of the presence of current-collecting plates can be estimated approximately with simpler relations derived in the preceding section.

Let us look at the case when the transducer is placed on a semibounded body that has heat-physical characteristics of the intermediate plate of the transducer. The effect of the current-collecting plates can be neglected, to the first approximation. Thermal conductivity in the transducer can be described by Eq. (II.52).

/73

To evaluate the effect of the nonstationary character of the regime, all we need to do is compare the flux entering the plate with the flux leaving it on the opposite face. Requirements on the value of the ratio of these fluxes in accordance with the uniqueness theorem can be formulated both in the originals and in the images. The latter is much more convenient, although it contains a certain incompleteness for the final numerical estimate.

76

The derivative with respect to the coordinate of the transfer function from the flux to the temperature is a measure of imaging the local heat flux. So from Eq. (II.52) we can derive the ratio of the flux images

$$\frac{Q(0, s)}{Q(-1, s)} = -\frac{\lambda_1}{\delta_1}\left[\frac{dY_2(\varrho_1, s)}{d\varrho_1}\right]_{\varrho_1 = 0} = \frac{1}{ch\,\beta_1 \div \frac{1}{\varkappa}\,sh\,\beta_1} \qquad (II.54)$$

In measurements, it is often necessary to know the measure of correspondence of the output signal of the sensitive part or the system as a whole to the steady-state value of the signal; but it does not mean, however, restricting oneself to the case of measuring the constant flux. The value of the right-hand side of Eq. (II.54) must be close to unity, to which small values of β_1 correspond. And in the expansions of the hyperbolic functions, we can limit ourselves to the first members:

$$\frac{Q(0, s)}{Q(-1, s)} \approx \frac{1}{1 + \frac{1}{\varkappa}\beta_1} \qquad (II.55)$$

So, the measure of the identical heat-measurement nonstationary character of a plate placed on a semibounded body in the images is determined by the ratio β_1/κ . In converting to the originals, since in the Laplace transform the product $s\tau$ must be kept dimensionless, the following expression can serve as a criterion of estimating nonstationary character, to the first approximation:

$$\frac{a_1\tau}{\delta_1^2}\varkappa^2 = \overline{\tau}\varkappa^2 \qquad (II.56)$$

For the above-described copper-constantan transducers, when the criterion $\overline{\tau}\kappa^2$ have identical values, the intrinsic times characterizing the inertia of the outermost and intermediate plates differ by two orders. So we can neglect the effect of the current-collecting plates being present and take into account only the intermediate plate.

The transfer functions of the heat flux and temperature of /74 the medium to the transducer signal in all the cases considered --assuming constancy of the thermoelectrical coefficients and the thermal conductivity coefficients--are equal to the

77

difference of the corresponding transfer functions of temperature at the coordinates of the receiving and emitting transducer faces:

$$Z_q(s) = (\alpha_1 - \alpha_2)[Y_q(-1, s) - Y_q(0, s)]$$

$$Z_t(s) = (\alpha_1 - \alpha_2)[Y_t(-1, s) - Y_t(0, s)]$$

(II.57)

where $Z_q(s)$ is the transfer function from flux to transducer signal, and $Z_t(s)$ is the transfer function from temperature of the medium to the transducer signal.

For a transducer placed on a semibounded body, from Eqs. (II.52) and (II.57) we find:

$$Z_q(s) = \frac{1}{k_t \beta_1} \cdot \frac{\operatorname{ch}\beta_1 - 1 + \varkappa \operatorname{sh}\beta_1}{\operatorname{sh}\beta_1 + \varkappa \operatorname{ch}\beta_1}$$

(II.58)

where $k_t = \frac{(\alpha_1 - \alpha_2)\delta_1}{\lambda_1}$ is the transducer coefficient, numerically equal to the stationary flux causing a unit transducer emf.

The inverse transforms for finding the originals--the transducer emf values--can be presented for specific cases of assigning the functions $q(\tau)$ describing the changes in the measured fluxes with time. In particular, for a suddenly begun exposure to a constant flux, we have

$$q(\tau) = q_0 = \operatorname{const}$$

(II.59)

$$Q(s) = \frac{q_0}{s}$$

Referring to Eqs. (II.58) and (II.59), the change in the transducer emf can be defined as:

$$\Delta u = L^{-1}[Z_q(s)Q(s)]$$

(II.60)

where L^{-1} is the inverse Laplace transform.

For a plate on a semibounded body, these transforms are easily obtained for the following particular cases.

1. The transducer heat-physical properties coincide with those for a semibounded body ($\kappa = 1$):

$$\Delta u(\tau) = \frac{q_0}{k_\lambda}\left\{\frac{2}{\sqrt{\pi}}\tau^{\frac{1}{2}}\left[1 - \exp\left(-\frac{1}{4\tau}\right)\right] \div \operatorname{erfc}\frac{1}{2\tau^{\frac{1}{2}}}\right\} \qquad (II.61)$$

2. The supporting surface is an ideal surface ($\kappa \to 0$):

$$\Delta u(\tau) = \frac{q_0}{k_t}\left[1 - \frac{8}{\pi^2}\sum_{n=1}^{\infty}\frac{1}{(2n-1)^2}\exp\left(-\frac{\pi^2(2n-1)^2}{4}\tau\right)\right] \qquad (II.62)$$

3. The supporting surface is an insulator

$$\Delta u(\tau) = \frac{1}{2}\frac{q_0}{k_t}\left\{1 - \frac{8}{\pi^2}\sum_{n=1}^{\infty}\frac{1}{(2n-1)^2}\times\exp\left[-\pi^2(2n-1)^2\tau\right]\right\} \qquad (II.63)$$

Graphically, the values

$$\vartheta = \Delta u(\tau)\frac{k_t}{q_0},$$ corresponding to Eqs. (II.61) - (II.63) for a series-manufactured transducer are presented in Fig. 39.

As the thickness of the supporting wall decreases to zero (see Fig. 37, b), the transfer functions of the measured flux and the temperature of the medium to the transducer signal are defined by Eqs. (II.53) and (II.57):
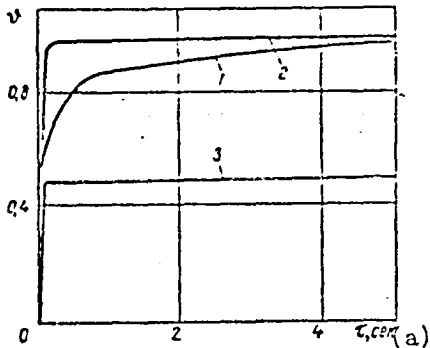
Fig. 39 Plot of variation in signals of transducers placed on semibounded body:

1. according to Eq. (II.62)
2. according to Eq. (II.63)
3. according to Eq. (II.64)

Key: a. seconds

$$Z_q(s) = \frac{1}{k_t}\cdot\frac{\beta_1(\operatorname{ch}\beta_1 - 1) + \zeta_1\operatorname{sh}\beta_1}{\beta_1(\beta_1\operatorname{sh}\beta_1 \div \zeta_1\operatorname{ch}\beta_1)}$$

$$Z_t(s) = \frac{\zeta_1(1 - \operatorname{ch}\beta_1)}{\beta_1\operatorname{sh}\beta_1 \div \zeta_1\operatorname{ch}\beta_1}. \qquad (II.64)$$

In the double wall variants (see Fig. 37, c and d) for the transfer functions (II.57), by referring to Eq. (II.51) we get

$$Z_{q_1}(s) = \frac{1}{k_t \Delta} \left[(\beta_2 \, ch\, \beta_2 + \zeta_2 \, sh\, \beta_2)(ch\, \beta_1 - 1) \div \varkappa (\beta_2 \, sh\, \beta_2 \div \right.$$
$$\left. \div \, \zeta_2 \, ch\, \beta_2) \, sh\, \beta_1 \right];$$

$$Z_{q_1}(s) = \frac{\eta}{\varkappa k_t \Delta} \left[\beta_2 (ch\, \beta_2 - 1) + \zeta_2 \, sh\, \beta_2 \right]; \qquad \qquad \text{(II.65)}$$

$$Z_{t_1}(s) = - \frac{\varkappa \zeta_2 \beta_1 (\alpha_1 - \alpha_2)}{\Delta} (ch\, \beta_1 - 1);$$

$$Z_{t_1}(s) = - \frac{\zeta_2 \beta_1 (\alpha_1 - \alpha_2)}{\Delta} \left[sh\, \beta_1 \, sh\, \beta_2 \div \varkappa \, ch\, \beta_1 (ch\, \beta_2 - 1) \right].$$

In the case of arbitrarily specified $q(\tau)$ and $t_0(\tau)$, their images $Q(s)$ and $T_0(s)$ are known, and the emf will be determined from the obvious symbolic equation:

$$u(\tau) = L^{-1} [Z_q(s) Q(s) + Z_t(s) T_0(s)] \qquad \qquad \text{(II.66)}$$

Exact values cannot always be found for the inverse transform (II.66), as--in contrast--has been done for the three cases of transducer placement on a semibounded body. But if the exact transform is not known, we can use any of the methods of getting the asymptotic values $/\,2\,/$. These operations require a certain caution, since not any asymptotic and even convergent expansions necessarily lead to valid results. Although from the Lerkh theorem it also follows that approximate originals correspond to the approximate images, a measure for this correspondence has not been established. Therefore each solution is best reduced to particular cases that have exact solutions or that have a representative confirmation of solution correspondence for each group.

For rational algebraic functions it is convenient to use the Vashchenko-Zakharchenko (Heaviside) expansion theorem, and for periodic functions, apparently, the allied Fourier or Hilbert transforms are more suitable.

So in any formulation a complete solution to the problem does not encounter fundamental difficulties. Cumbersomeness in computations now may no longer be much of an obstacle, thanks to successes in designing and developing high-speed digital computers. Let us turn to analyzing the particular cases.

To the first approximation, let us limit ourselves to the first powers of the parameter s in the expansions of the transfer function numerator and denominator (II.64) and (II.65). Then the transfer functions can be represented as the following rational fractions:

$$Z_q(s) \approx k\frac{s+n}{s+M}; \qquad Z_t(s) \approx K\frac{s+N}{s+M} \qquad (II.67)$$

As applied to the one-layer wall-transducer, the transfer functions can be described by Eqs. (II.64); the values of the coefficients in the approximate expansions (II.64) will be:

$$k = \frac{1}{3k_t}\cdot\frac{3+\zeta_1}{2+\zeta_1}; \qquad n = \frac{a_1}{\delta_1^2}\cdot\frac{6\zeta_1}{3+\zeta_1}$$

$$K = -\frac{\zeta_1}{2+\zeta_1}; \quad N = 0; \quad M = \frac{a_1}{\delta_1^2}\cdot\frac{2\zeta_1}{2+\zeta_1} \qquad (II.68)$$

Analogously, for the two-layer wall in Eqs. (II.65) we can /77 assume that in the expansion in the transfer function numerator and denominator it is acceptable to limit ourselves to the first power of parameter s, that is,

$$Z_{q1}(s) \approx k_1\frac{s+n_1}{s+M_1}; \qquad Z_{q2}(s) \approx k_2\frac{s+n_2}{s+M_1}.$$

$$Z_{t1}(s) \approx K_1\frac{s+N_1}{s+M_1}; \qquad Z_{t2}(s) = K_2\frac{s+N_2}{s+M_1} \qquad (II.69)$$

whence

$$M_1 = \frac{a_1}{\delta_1^2}\cdot\frac{\zeta_2\varkappa}{P}; \qquad k_1 = \frac{\eta}{2k_tP}\left[1+\zeta_2+\varkappa\eta(2+\zeta_2)+\frac{\varkappa\zeta_2}{3\eta}\right];$$

$$n_1 = \frac{a_1}{\delta_1^2\eta}\cdot\frac{2\zeta_2\varkappa}{1+\zeta_2+\varkappa\eta(2+\zeta_2)+\frac{\varkappa\zeta_2}{3\eta}};$$

$$k_2 = \frac{\eta^3}{2k_tP}\left(1+\frac{\zeta_2}{3}\right); \quad n_2 = 2\frac{a_1}{\delta_1^2\eta^2}\cdot\frac{3\zeta_2}{3+\zeta_2};$$

$$K_1 = -\frac{\varkappa\zeta_2(\alpha_1-\alpha_2)}{2P}; \qquad N_1 = 0;$$

$$K_2 = -\frac{\zeta_2\eta(2+\varkappa\eta)(\alpha_1-\alpha_2)}{2P}; \qquad N_2 = 0, \qquad (II.70)$$

81

where $P = \eta(1 + \varkappa\eta) + \zeta_2\left[\eta + \frac{1}{2}\varkappa(1 + \eta^2)\right]$

If the temperature of the cooling medium is constant and is equal to the temperature of the measuring system with which sudden exposure to constant heat flux is begun, $q(\tau) = q_0$, $t_0(\tau)$, and their images are

$$Q(s) = \frac{q_0}{s}; \quad T_0(s) = 0 \tag{II.71}$$

Referring to the system of equations (II.70) and substituting (II.67) - (II.69) and (II.71) in (II.66), we find the trends of the transducer signals with time for the cases shown in Fig. 37, b:

$$\Delta u(\tau)_b = q_0\left[\frac{1}{k_t}(1 - e^{-M\tau}) + ke^{-M\tau}\right] \tag{II.72}$$

$$-\quad \frac{\Delta u(\tau)}{\Delta u(\infty)}\bigg|_b = 1 - (1 - kk_t)e^{-M\tau} \tag{II.73}$$

in Fig. 37, c:

$$\Delta u(\tau)\big|_c = q_0\left[\frac{1}{k_t}(1 - e^{-M_1\tau}) + k_1 e^{-M_1\tau}\right] \tag{II.74}$$

$$\frac{\Delta u(\tau)}{\Delta u(\infty)}\bigg|_c = 1 - (1 - k_1 k_t)e^{-M_1\tau} \tag{II.75}$$

in Fig. 37, d:

$$\Delta u(\tau)\big|_d = q_0\left[\frac{1}{k_t}(1 - e^{-M_1\tau}) + k_2 e^{-M_1\tau}\right] \tag{II.76}$$

$$\frac{\Delta u(\tau)}{\Delta u(\infty)}\bigg|_d = 1 - (1 - k_2 k_t)e^{-M_1\tau}. \tag{II.77}$$

Eqs. (II.61) - (II.63), (II.72) - (II.77) establish the relation between between the measured and the true heat fluxes in the transient regime in different cases of practical interest. However, we must remember that in deriving Eqs. (II.72) - (II.77) small values of s were assumed, to which there correspond the time values that are large enough for the process to be viewed as a regular second-order regime.

From the derived equations we can determine the inertia for
different transducer operating conditions: the time constant is
equal to a quantity that is the inverse of M or M_1. Referring
to the corresponding equations in the systems (II.68) and (II.70),
it is easy to find the dependence of the transducer inertia on
parameters like the intrinsic transducer time δ_1^2/a_1 and the
intrinsic bearing wall time δ_2^2/a_2, their ratio η, the Biot
criteria ζ_1 and ζ_2, and the ratios of the heat-receiving capa-
bilities κ.

The values of the dimensionless time constants for the cases
shown in Fig. 37, b are

$$\frac{a_1}{M_1\delta_1^2} = \frac{2+\zeta_1}{2\zeta_1} \qquad (II.78)$$

in Fig. 37, c

$$\frac{a_1}{M_1\delta_1^2} = \frac{\eta(1-\kappa\eta) + \zeta_2\left[\eta + \frac{1}{2}\kappa(1+\eta^2)\right]}{\zeta_2\kappa} \qquad (II.79)$$

in Fig. 37, d

$$\frac{a_2}{M_1\delta_2^2} = \frac{\eta(1+\kappa\eta) + \zeta_2\left[\eta + \frac{1}{2}\kappa(1+\eta^2)\right]}{\eta^2\zeta_2\kappa} \qquad (II.80)$$

In particular, for a series-manufactured self-contained
copper-constantan transducer ($a_1 = 7\cdot10^{-6}$ m^2/s, $\delta_1 = 10^{-3}$ m),
when $\zeta_1 = \zeta_2 = 0.05$ ($\alpha = 1000$ W/m^2·deg) for the case in Fig. 37, /79
c, the time constant is 3 s. When the transducer is placed on
the wall surface with the same characteristics as the transducer
($\eta = 1$, $\kappa = 1$), the time constant is increased to 6 s.

6. Technology of Fabricating Series-Manufactured Self-Contained
Heat Flux Transducers

᱐ the fabrication technology of series-built self-con-
ta᱐   ᱐ transducers was under development, unitary
int᱐   ᱐ transducers were the goal. A nearly identical
eff᱐   ᱐ be achieved in welded and galvanic versions. Pre-
feren᱐᱐, obviously, must be given to the latter.

The process of making welded transducers includes the fol-
lowing main operations: blanking and machining the current-
collecting copper electrode-plates; making and machining the

intermediate constantan electrodes; making current-collecting conductors and welding them to the plates; welding one current-collecting plate to the intermediate electrode; filling the channel for the lead-out of the conductors with heat-resistant insulating compound and welding the second plate; external machining to remove welding defects and burrs, and decorative polishing; and nickel-plating.

Blanking the copper and constantan plates consisting in annealing the corresponding sheet material, rolling it to the required dimension, and stamping it. Then an 0.8 mm diameter opening was drilled in the constantan plates, in their center, and a channel was cut out for leading out the current-collecting conductors. The resulting products were cleaned free of burrs, straightened, annealed, etched in hydrochloric and nitric acids, and washed and dried. Constantan plates were ground on a grinder that gave a surface finish not worse than class ten. On one side the constantan plates were cemented to a polished fused quartz disk. The disk was mounted in a special holder that ensured parallelity of the surfaces of the quartz and working cast-iron disks during complex relative motion. The cast-iron disk was bathed with water containing abrasive additives. After one side had been machined, the plates were turned over and the other side was machined. About 50 plates were machined at the same time. The machining precision for the entire set was not lower than 10 μm.

Standard copper conductors in an enamel insulation 0.20 mm in diameter were used in making the current-collecting conductors. The conductors were 1.5-2 m long.

Conductor ends were carefully stripped of insulation to a length of 3 mm and bent into a loop 0.6 mm in diameter. The prepared copper and constantan plates and the conductor ends were etched in weak sulfuric acid, washed with water, ethanol /80 or carbon tetrachloride, and sent for welding. Welding a copper conductor with a copper plate was most tricky. Satisfactory results were realized with silver, tungsten, and molybdenum electrode-clamps. Carefulness in cleaning the contacts and preparing products to be welded is very important. Even so, the rejection rate in welding copper to copper is as high as 80 percent.

The copper plate with the soldered conductor is placed on the constantan plate in such a way that the conductor loop falls into the central drilled opening, and the conductor--in the channel. Welding begins at the center, extends around the edge of the cut with successive transitions with a spacing of about 1 mm, and gradually approaches the periphery of the blank. In conclusion, welding is done twice along the edge.

After the first copper plate has been welded on, the cut in the constantan plate is filled with silicate concrete /215/. The filler insulates the outgoing conductor from the plates and immobilizes it, protecting the welding location against bending. This latter feature is important owing to the unreliability of welding copper to copper. Welding the second plate is similar to welding the first. Next, the remaining part of the channel is filled with silicate concrete. Shallow pockmarks remain from welding at the external working surfaces in the welded transducer. To eliminate the welding defects and to ensure dimensional identity, the transducer working surfaces are ground, and the side surfaces are cleaned. The polished transducers are nickel-plated for protection against corrosion. The thickness of the ready-to-use transducers varies in the range 0.85-0.95 mm.

During successive calibrations, the welded transducers showed significant (to ±30 percent) scatter and variation in the calibration characteristics with time. The greatest deficiency was due to the inhomogeneity of the welding of copper plates to the constantan plate. The result was that additional thermal resistance was induced in the transition between the metals that was dissimilar in different transducers and varying in magnitude with time. This deficiency can be eliminated by the galvanic deposition of the current-collecting plates. The variation in the technology demanded some change in design: the conductors were led out through the drilled openings in the body of the intermediate thermoelectrode (Fig. 40).

Fabrication of the galvanic self-contained heat flux transducers can be subdivided into the following operations: preparing the plates for the intermediate thermoelectrode; drilling the openings in the body of the constantan plate from the edge to the middle; drilling the transverse openings; sinking the rims of the transverse openings; embedding of the collecting conductors; final grinding of the intermediate thermoelectrode; galvanic deposition of the current-collecting plates; machining of the excesses of galvanic deposition; grinding and polishing of the external transducer surfaces; and galvanic deposition of a protective coating.

Prepa ration of the constantan plates for galvanic trans-   /81
ducers does not differ in general outline from the preparation described for welded transducers. Constantan plate thickness in the finished product is usually 0.95 mm, with a tolerance of ±14 μm.

The openings were drilled in a special conductor that ensures a pairwise encounter of the openings in the plate body.

In series-manufactured transducers with intermediate plate thickness $\delta_2 = 0.95$ mm, the diameter of the longitudinal openings is 0.65 mm. When the transducer size is 10x10 mm^2, the depth of the longitudinal openings is 5.5 mm. The diameter of the transverse drilled openings is chosen as somewhat smaller--0.55 mm. This is so because when the drilling axes do not coincide (and this is unavoidable), upon entering the head-on opening the drill hooks on to the edge and fractures. When the drill diameter is chosen as smaller, the probability of fracture is reduced. Nonetheless, in short transverse openings the drills fracture more often than in long longitudinal openings.
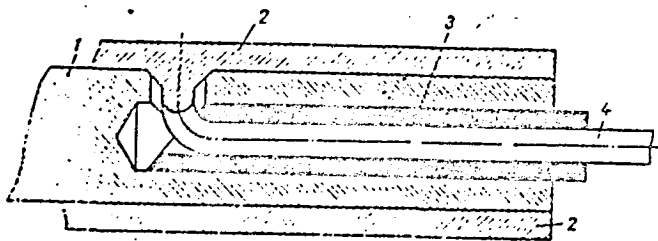
Fig. 40 Galvanic self-contained
heat flux transducer:

1. intermediate plate
2. current-collecting plate
3. insulation bushing
4. thermoelectrode

The transverse openings are countersunk using a tool at an angle of 120° to a depth of 0.1 mm.

The current-collecting conductors are made of grade PEL copper wire 0.2-0.25 mm in diameter and 1.5-2 m in length. One end of the wire is stripped, the second is threaded at first through a quartz bushing, and then through a drilled opening in the constantan plate. At the threaded end the conductor is fused into a bead 0.8- -0.9 mm in diameter. For fusion, the threaded end is lowered into a small bath of graphite powder and through the conductor is passed a current as was done in the fabrication of thermocouples /66/. During the fusion, insulation enamel is scorched to a distance of 2-2.5 mm from the bead. The bead is etched in sulfuric acid containing nitric acid, washed, then dried in a jet of warm air.

The technique of drawing out the insulation tubes was described in the study /214/. Quartz tubes are harder to draw than glass tubes; on the other hand, they are stronger and more convenient in subsequent handling. Blanks 200 mm in length are calibrated as to inner and outer diameters.

One end of the tube is cut off at an angle of about 45°   /82 on a diamond wheel. The tube is inserted into a special chuck and a bushing 5 mm long is broken off from it.

On the conductor the bushing is lubricated with silicate or organic cement and, with the required orientation of the oblique cutoff, is inserted into the drilled opening in the constantan plate up to the stop.

The etched bead on the conductor is drawn into the countersinker, flattened with a small residual deformation with a special screw clamp, and with several discharges on a capacitative welding machine it is welded to the plate. Similar operations are performed also on the other side of the plate.

The projecting parts of the copper beads are stripped off on a facing diamond wheel. After finish grinding, the transducer blanks are sent to be copper-plated. The technology of copper-plating and nickel-plating is conventional. Before the galvanic coatings begin to be applied, a reverse current is switched on for a short period. Checking the adherence of the galvanic coatings is done by bending the specimens at an angle of 180° and allowing them to straighten out. When this is done, constantan is observed to fracture at the drilled openings, while the copper coating does not flake.

Using a diamond tool permits such a careful machining of the surface that the finished transducers can be "glued" to each other by lapping, like Ioganson plates. Given this kind of machining, there is no chance of skewing of the measured flux because the transducer thermal resistance is nonuniform.

CHAPTER 3

BANKED TRANSDUCERS

Low sensitivity is a serious failing of self-contained transducers. The working coefficients of monolithic self-contained transducers, 1 mm thick, average approximately $500 \cdot 10^6$ $W/m^2 \cdot V$. The most sensitive series-manufactured measuring instruments (F-18, F-116, V-1-4, and V-2-11), at their lower limits, have scales designed for measuring 1.5-10 µV.

State-of-the-art capability of boosting dc signal strength is, practically speaking, applied in the instruments mentioned above. Now in custom-built instruments that have to be carefully insulated from external influences or that have to be deep-cooled sensitivities one to two orders greater have been attained. So the lower limit of measuring heat fluxes with self-contained transducers evidently lies at about 200 W/m^2.

The need to measure much smaller values comes up from time to time in technology and in the environment. For example, the flux through partitions between refrigeration chambers seldom is more than 1 W/m^2, but the geothermal flux averages about 0.03 W/m^2 and in some areas more than an order of magnitude smaller than this value. All of this leads to the necessity of improving sensitivity by four to five orders of magnitude. The simplest solution to the problem is in connecting together self-contained elements into series banked instruments. The transducers that result are called banked transducers (banked heat flux transducers

Following a brief look at common structural and technological features, in this chapter we present the results of theoretical studies of optimal transducer characteristics. Calculation formulas are derived from an amplified theory of similarity. Briefly described are the main technological processes of series manufacture of banked heat flux transducers. Concluding the chapter, we give the theory of a slant-layered banked transducer that pioneers new areas in heat measurement practice.

1. Designs of Banked Heat Flux Transducers and General   /84
Questions of Their Construction

The main concept of the banked heat-measuing instrument is
that the elements are connected in parallel with respect to the
measured flux and in series with respect to the generated signal.
The elements in one of the first transducers (1962) were self-
contained 2x2x1 mm^3 transducers. The outermost layers of the
elements were made of 0.1 mm copper foil. The intermediate
plates were stamped out of constantan ribbon. Intervals and
gaps between the elements were filled with insulating compound;
above and below the banked instrument thin mica wafer-sheets
were placed. The sensitive elements were fitted into a metal
housing of stainless steel; it was covered with a lid welded to
the housing. From technological considerations, round housings
were found more convenient. About 100 of these transducers
were made for different organizations.
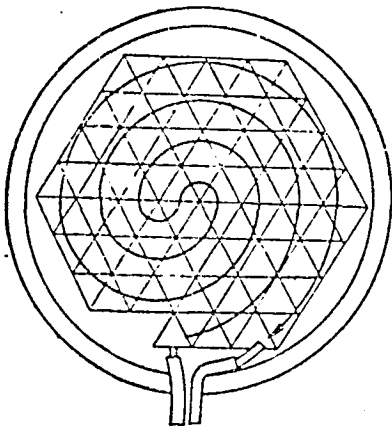
Fig. 41   Connection diagram
of triangular elements in
round banked heat flux trans-
ducer

The number of elements in
these transducer, called disk-
type transducers, was as high
as 114; sensitivity could thus
be boosted by two orders com-
pared to a self-contained
transducer /61/. Triangular
elements can fit much more com-
pactly in the round housings
(Fig. 41). Recently these
designs have found little use,
since more efficient versions
have been developed.

When sensitivity is pushed
even higher through added ele-
ments, element cross-sectional
areas must be reduced. Here
the ratio of element height to
element cross-section changes
considerably. These systems
can operate only in banks where
the neighboring elements each
perform for each other the func-
tions of shield devices, and the number of the outermost elements
is relatively modest.

One attempt was simply reducing the cross-sectional dimen-
sions of the disk-type transducer elements down to 0.1 mm. The
connection sites of the thermoelectrodes were arranged in two
parallel planes.

C-2

Because of the relatively high thermal conductivity,
thermoelectrodes carry nearly all the flux, so the transducer
readings, in contrast to a thermopile, depend little on the
cooling conditions of the cold junctions. These transducers,
like the self-contained versions, differ from ribbon calori-
meters, for example, the Shmidt calorimeters, by the fact that
the auxiliary wall of the former is formed mainly by thermo-
electrode materials. So they are more compact, have much lower
thermal resistance and, still, are more sensitive, generally
speaking.

Theoretically, more than 10^4 conductors, 0.1 mm in dia-
meter, can be fitted per square centimeter; this corresponds
to 5000 paired elements. In practice, the number of elements
in series manufacture only slightly exceeds 1000 per cm^2 and
only with especially careful fabrication can this number be
raised to 2000 per cm^2. Compared with the self-contained heat
flux transducers, banked heat flux transducers are more sensi-
tivity because of the larger number of junction pairs and the
high flux concentration /256/.

The transducer as a finished product must consist of a
tightly laid-out system of a set of thin wires welded at their
ends in a strict sequence of alternating materials. Each error
allowed in the welding sequence leads to a change in the sense
of polarity for the signal generated by the next part of the
banked instrument. Making a mistake just once in the middle
of the banked instrument is enough for the entire system sensi-
tivity to become near-zero. When there is a large number of
elements, even a slight probability of error in the element-
connection sequence makes operating the device meaningless.

Consecutive connection of short segments (1 mm) of dissimi-
lar materials is conveniently done in a network woven of paired
thermoelectrode wires in such a way that one of them serves as
the warp, and the other--as the weft. We weld the wire intersec-
tions. Then strips are cut out of the network so that they con-
sist of successively alternating segments of paired electrodes.
A miniature ribbon-ladder is insulated and compressed so that
the segments take on an alternating orientation. The ribbons
are welded into several pieces, fitted into a compact set of
rows, and pressed down. As to plan view, the banked instrument
becomes square-shaped. After pressing, the blank is filled with
epoxy resin or ceramic compound and is heat-treated /60/.

One deficiency of this transducer is that the operator must
pay attention to each junction several times. So manufacture
of banked heat flux transducers is laborious, fatiguing, and
low in productivity.

90

Galvanic thermocouples considerably simplify the manufacture of banked heat flux transducers, while only slightly lowering sensitivity.

Under the first technology, the transducer sensitive elements are made in the form of screw springs with outer diameter of about 1 mm, wound of 0.1 mm diameter constantan wire. Half of each turn is copper-plated. After copper-plating, a spring is coated with insulating varnish and one of the free ends of the wire is threaded through the inner cavity of the spring. The lead wires are together in this case, simplifying installation. The spring is fitted into the transducer along a spiral path in such a way that the transition sites of the copper-plated half-turns lie in the upper and lower transducer planes. From the kind of element placement, the transducers came to be called spiral-type transducers /59/. The transducer is placed into a metal housing and filled with several different setting compounds. /86

Shortcomings of the spiral transducers include the low density in filling the space occupied by sensitive elements; because of this the thermal resistance of the transducers is fairly high; another failing is that when the elastic springs are copper-plated, then fitted into the banked instrument, major technical difficulties must be faced.

Correcting these failings while retaining the advantages was achieved in sandwich-type transducers; their fabrication technology is given in section 5 of this chapter. The unquestioned advantage of sandwich-type transducers, compared with network transducers is that operator attention now does not have to be directed at individual elements.

In several cases the sensitivity of the sandwich-type transducer is found to be more than good enough. Here metal banked transducers with low thermal resistance can be used with good effect. A round channel 20 mm in diameter, 2 mm deep, and 1.5 mm wide, is bored in a 30 mm diameter metal housing. The channel walls are insulated with high-temperature enamel. The sensitive element, placed into the channel, resembles the blank for the sandwich-type transducer. Usually, chromel or nichrome with a galvanic nickel coating is the base.

Depending on the required thermal resistance, the housings are made of copper, brass, or stainless steel.

As applied to the operating conditions of electrolyzers for making alkali and alkaline-earth metals, a special round alundum transducer was developed, built with several specimens, and

91

tested in working conditions /81/. Its distinguishing feature
is that in it an "auxiliary" wall in cylindrical form is used;
along the generatrix of the cylindrical form the "hot" and
"cold" junctions of the differential thermocouple are depo-
sited on both sides. If the heat flux penetrates the "auxi-
liary" wall in such a way that it has a component that is per- /87
pendicular to the cylinder axis, some temperature difference
is formed along the cylinder generatrices in the plane of the
heat flux vector. This difference will be directly propor-
tional to the magnitude of the normal component of the heat
flux and can be measured with a banked differential thermo-
couple whose junctions lie on diametrally opposed generatrices.
The thermoelectrodes are fitted in a groove on the cylindrical
surface so that the surface of a cylinder with placed thermo-
couple is smooth. The output signal of the system, consisting
of an auxiliary cylindrical body with a banked thermocouple,
is directly proportional to the magnitude of the heat flux
component that is normal to the cylinder axis, and therefore
the system can serve as a heat flux transducer.

When the heat flux is being measured, the alundum trans-
ducer is placed tightly on the body in which the flux measure-
ment must be made. Owing to the round cylindrical shape, this
kind of transducer can be rotated about an axis. When the plane
of the banked thermocouple junctions coincides with the plane
of the heat flux vector, the signal value reaches a maximum.
Thus the transducer can determine not only the value of the
normal projection, but also the direction and magnitude of
the maximum value of the normal component of the heat flux.

The thermocouple spiral is made by galvanic deposition of
the paired material on a wound base (for example, nickel on
chromel or nichrome) or by preliminary welding of the blank
for a spiral of segments of calculated length of the paired
thermoelectrodes.

For protection against the corrosive halogenide atmosphere,
the prepared rod with the differential thermocouple on solidi-
fied clinker is inserted into an alundum sleeve and, after
drying, calcined.

Calibration is carried out on the wall of a hollow-body
graphite cylinder in conditions aproximating full-scale condi-
tions in an electrolyzer. When measurements are taken, the
transducer is placed with respect to the flux by rotation about
an axis.

2. Optimization of Design Parameters for Disk-Type and Network Transducers

A single element, replicated many times by successive connection into an electrical circuit for forming a banked transducer, is a combination of descending and ascending branches, shown in Fig. 42.

It is assumed that the regions of the junction areas are sufficiently small that their effect can be neglected. Part of flux measured flows along the insulation in the intervals between the columns. The total cross-sectional area of the insulation depends only slightly on the ratio between the branch cross-sections. The fraction of the flux accounted for by the insulation is small, so its variation need not be taken into account.

The Peltier and Thomson effects do not depend either on cross-sectional area, or on the perimeters of the thermoelectrodes. Both effects are directly proportional to the current strength. Below we examine the conditions of maximum yield with respect to the electric power, to which the maximum current generated corresponds. The value of the current near the maximum varies only slightly, and at the maximum the change in current is zero. So we can also neglect the Peltier and Thomson effects.

The electrical resistance of the matched load, as we know, is equal to the resistance to the generating unit. In this case the resistance of the load occurring on each element considered that is made up of two branch must equal the total resistance proper of these branches. The problem reduces to determining the ratio between the cross-sectional areas of the descending and ascending branches corresponding to the maximum power generated in the recording instrument.

As a unit of area measurement, let us use the total cross-sectional areas of the descending and ascending branches. The cross-sectional areas of the descending branch we designate by the desired quantity, x; then the value 1 − x is accounted for at the cross-section of the ascending branch.

Since the height of both branches δ and their temperature gradients are identical, the value of the flux flowing through the pair of branches is

$$q = [\lambda_1 x + \lambda_2 (1 - x)] \frac{\Delta t}{\delta} \qquad \text{(III.1)}$$

from which we have

$$\Delta t = \frac{q \delta}{\lambda_1 x + \lambda_2 - \lambda_2 x}$$

93

The electromotive force of an element under these conditions is

$$e = (\alpha_1 - \alpha_2)\Delta_* = \frac{(\alpha_1 - \alpha_2)q\delta}{\lambda_1 \cdots + \lambda_2 - \lambda_2 x} \qquad \text{(III.2)}$$

The intrinsic (internal) electrical resistance of the element is

$$R_e = \varrho_1\frac{\delta}{x} + \varrho_2\frac{\delta}{1-x} = \delta\frac{\varrho_1 - \varrho_1 x + \varrho_2 x}{x - x^2} \qquad \text{(III.3)}$$

When there is matched loading, the circuit resistance is 2R , and the current flowing through the instrument is

$$I = \frac{q(\alpha_1 - \alpha_2)}{2} \cdot \frac{x(1-x)}{[\lambda_1 x + \lambda_2(1-x)][\varrho_2 x + \varrho_1(1-x)]} \qquad \text{(III.4)}$$

On analyzing Eq. (III.4) as to the maximum I with respect to x, we find that it occurs given the condition that

Fig. 42 Element of disk-type banked transducer

$$\left(1 - \frac{\lambda_1\varrho_2}{\lambda_2\varrho_1}\right)x^2 - 2x + 1 = 0 \qquad \text{(III.5)}$$

to which there correspond the roots

$$x_1 = \left[1 - \left(\frac{\lambda_1\varrho_2}{\lambda_2\varrho_1}\right)^{\frac{1}{2}}\right]^{-1} \qquad \text{(III.6)}$$

$$x_2 = \left[1 + \left(\frac{\lambda_1\varrho_2}{\lambda_2\varrho_1}\right)^{\frac{1}{2}}\right]^{-1} \qquad \text{(III.7)}$$

Both roots are symmetrical relative to the subscripts, that is,

94

$$x_i\left(\frac{\lambda_1 c_2}{\lambda_2 c_1}\right) = 1 - x_i\left(\frac{\lambda_2 c_1}{\lambda_1 c_2}\right) \qquad (III.8)$$

where $i = 1$ or 2.

The dimensionless argument $\dfrac{\lambda_1 c_2}{\lambda_2 c_1}$ can only be positive,

therefore both roots of Eq. (III.5) are real.

When the arguments are positive, the first root has two domains of existence: $1 < x_1 < \infty$ and $0 > x_1 > -\infty$. In both domains the values of the roots are meaningless.

So only the second root has a practical application (III.7).

The information about the thermal, electrical, and thermoelectrical properties of the materials used that is needed for subsequent calculations and manipulations is given in Table 2.

If the values of the argument $\dfrac{\lambda_1 c_2}{\lambda_2 c_1}$ are small, it is best to use Eq. (III.8); with the same calculation errors, the calculation result turns out to be more exact.

Below are presented the optimal ratios of the cross- /90 sectional areas for the most common thermoelectrode materials (the order of listing corresponds to the subscripts):

Materials	f_2/f_1 opt
Silver-constantan	0.044
Copper-constantan	0.047
Chromel-alumel	0.650
Chromel-nickel	0.870
Nichrome-constantan	0.660
Iron-constantan	0.230
Nickel-nichrome	0.100
Platinum-platinorhodium (10 percent Rh)	0.360

In the ideal case of measurements based on the compensation arrangement, the effective resistance of the load increases without limit, and the current passing through the emf source must be zero. A transducer resistance matched with the load must also increase without bound. Under these ideal conditions, the optimization task breaks down.

95

Table 2

Материалы (a)	(b) e, мкв/град	(c) λ, вт/м·град	(d) $\varrho \times 10^8$, ом·м
Серебро (e)	7,5	420	1,7
Медь (f)	7,5	390	1,8
Золото (g)	7,8	310	2,5
Железо (h)	20	70	12
Никель (i)	15	87	8
Сурьма (j)	49	18	49
Висмут (k)	−73	8	130
Платина (l)	0	70	12
Германий (m)	340	60	$0,9 \cdot 10^5$
Кремний (n)	−415	80	$1,0 \cdot 10^5$
Теллур (o) (p)	500	1,5	$1,6 \cdot 10^5$
Константан (p)	−35	25	48
Копель (q)	−40	23	50
Хромель (r)	28	19	76
Нихром (s)	11,5	14	103
Платинородий (t) (10% Rh)	6,5	38	20,5
Алюмель (u)	−13	23	32

Key:

a. Materials
b. µV/deg
c. W/m·deg
d. ohms·m
e. Silver
f. Copper
g. Gold
h. Iron
i. Nickel
j. Antimony
k. Bismuth
l. Platinum
m. Germanium
n. Silicon
o. Tellurium
p. Constantan
q. Copel
r. Chromel
s. Nichrome
t. Platinorhodium (10 percent Rh)
u. Alumel

But in practice, the compensation system has a specific effective resistance, which depends on the insensitivity zone of the null galvanometer. So Eq. (III.7) turns out to be valid even for this method of measurement.

3. Optimization of Design Parameters for Galvanic Sandwich-Type Transducers

The situation is somewhat different with transducers made galvanically; the technology is described in section 5 of this chapter.

The specific features of the manufacturing technology grow
out of the constancy of the cross-sectional area of the main
wire. To analyze the optimal relations in these transducers,
information is needed concerning the thermoelectrical properties
of wires electrolytically coated with the paired thermoelectrode
material. Differential banked thermocouples, composed of gal-
vanically coated sections, of the thermoelectrode in a pair with
the uncoated sections have a number of obvious advantages and
have found fairly wide application. One of the first studies
of the galvanic thermocouples was undertaken by Wilson and
Epps /331/. Initially the authors started from the fact that
when there is relatively low electrical resistance of the gal-   /91
vanically deposited material, the effect of the base will be
minor. Results of experiments in which pure constantan con-
ductor formed a thermocouple with its extension galvanically
coated with a thick copper layer showed that the thermo-emf
of this thermocouple will be practically the same as the value
for the copper-constantan thermocouple. But in experiments
with constantan coated with iron and, especially, antimony,
marked deviations are observed: the thermo-emf was lower than
expected. The authors of the study /331/ found that short-
circuited current loop originate in the bimetallic part of the
galvanic thermocouples when there is a longitudinal component
of the temperature gradient. To understand the nature of these
short-circuit currents and to determine their qualitative effect,
Wilson and Epps arranged the following ingenious experiment.

Measurements were made on a wooden cylinder; along its gene-
ratrix a heating rod, forming a region of hot junctions, was laid
in a chiseled-out channel. Because the ribbon was stretched,
the strips along the periphery were pressed against the cylinder
surface in such a way that the junction location was near the
heating rod. On the one side the copper and constantan strips,
beginning from the junction, were insulated from each other over
their entire extent. They were used as a copper-constantan ther-
mocouple to measure the temperature of the hot-junction region.

On one side the copper strip reached only to the cold-junc-
tion region. Here the strips could be commutated in the interval
between the regions of the hot and cold junctions in two ways.
Under the first method, they were placed one on the other, form-
ing a continuous contact with each other and simulating a bi-
metallic thermoelectrode. Under the second, a thin capacitor
paper, for reliable electrical insulation with relatively good
thermal contact, was fitted in the interval between the regions
of the hot and cold junctions. The paper insulation was made
a little shorter than the copper strip; because of this, the tip
of the copper strip gain made contact with the constantan. The
potential difference between the constantan branches was the
signal of the second thermocouple.

97

Numerous measurements showed that insulation in the entire interval between the hot and the cold junctions did not affect the thermo-emf of the composite thermoelectrode. From this follows the conclusion that the bimetallic thermoelectrode can be replaced with an equivalent system of two conductors that have the same cross-section, length, resistivity, and thermo- /92 electrical coefficients as in the base and galvanically deposited thermoelectrodes.

In the equivalent system, the conductors simulating the bimetallic section must be connected only at their ends. This system can be easily calculated from Kirchhoff's laws and all the thermoelectrical characteristics can be found.

If subscripts 1 and 2 stand for the characteristics of the base and the deposited material, the following equation can be written for the thermoelectrical coefficient of the bimetallic section /64, 68/:

$$\alpha_{bi} = \alpha_1 - \frac{\alpha_1 - \alpha_2}{1 + \frac{\varrho_2 l_1}{\varrho_1 l_2}} \qquad (III.9)$$

Later the properties of the galvanic thermocouples were repeatedly the object of studies by a number of authors. The best investigation in the domestic literature is that by S. A. Sukhov, S. Ya. Kadlets, and G. D. Pavlyuk /216/. Since this problem was an urgent one, the author of the present monograph carried out a large series of measurements to verify the properties of the bimetallic galvanic thermoelectrodes. These thermoelectrodes were obtained by galvanic copper-plating of the constantan and copel bases. The diameters of the bases were varied in the range 0.1-1.0 mm, and the relative cross-sectional areas of the coating--from 0 to 0.5. The measurement results confirmed Eq. (III.9), within the limits of possible accuracy.

Similar to what was described in Section 2 of this chapter, let us look at a single element consisting of an ascending and a descending branch. One branch was the base conductor, and the other was the galvanically coated section.

If heat flux Q was passed through each element, the temperature difference

$$\Delta t = \frac{Q\delta}{2\lambda_1 l_1 + \lambda_2 l_2 + \lambda_3 l_3} \qquad (III.10)$$

was induced in the elements, where the subscripts 1, 2, and 3 correspond to the base material of the conductor, galvanically coated material, and the intermediate insulating compound.

Referring to Eq. (III.9), for the thermo-emf generated by an element we can write the following equation:

$$e = \frac{Q\delta(\alpha_1 - \alpha_2)}{(2\lambda_1 f_1 + \lambda_2 f_2 + \lambda_3 f_3)\left(1 + \dfrac{\varrho_2 f_1}{\varrho_1 f_2}\right)}$$

(III.11)

When the signal was measured in a compensation circuit, the current through the transducer was zero, and the resistivity did not affect the value of the generated signal. By inspecting Eq. (III.11) for the maximum with respect to the ratio f_2/f_1, let us find the optimal cross-section of the coating:

$$\frac{f_2}{f_1}\bigg|_e = \left[\frac{\varrho_2 \lambda_1}{\varrho_1 \lambda_2}\left(2 + \frac{\lambda_3 f_3}{\lambda_1 f_1}\right)\right]^{\frac{1}{2}}$$

(III.12)

In these same cases, when the transducer operated with a matched load, the optimal ratio of the cross-sectional area of the galvanic coating with respect to the base cross-section must be selected with allowance for the effect of coating thickness on the intrinsic transducer resistivity.

But the resistance of the branches of an elementary transducer is

$$R_e = \frac{\delta \varrho_1}{f_1} \cdot \frac{2 + \dfrac{\varrho_1 f_2}{\varrho_2 f_1}}{1 + \dfrac{\varrho_1 f_2}{\varrho_2 f_1}}$$

(III.13)

When there is a matched load, the total resistance of a circuit must be twice the transducer resistance. Taking note of Eqs. (III.11) and (III.13), let us define the transducer current:

$$I = \frac{e}{2R_e} = \frac{Q(\alpha_1 - \alpha_2)}{2\lambda_1 \varrho_2} \cdot \frac{\dfrac{f_2}{f_1}}{\left(2 + \dfrac{\lambda_2}{\lambda_1}\cdot\dfrac{f_2}{f_1} + \dfrac{\lambda_3}{\lambda_1}\cdot\dfrac{f_3}{f_1}\right)\left(2 - \dfrac{\varrho_1 f_2}{\varrho_2 f_1}\right)}$$

(III.14)

By analyzing the current value at the maximum with respect to f_2/f_1 in Eq. (III.14), we find that in this case the optimal ratio of cross-sections is

$$\left.\frac{l_2}{l_1}\right|_l = \left[2\frac{\varrho_2\lambda_1}{\varrho_1\lambda_2}\left(2 \div \frac{\lambda_3 l_3}{\lambda_1 l_1}\right)\right]^{\frac{1}{2}} \qquad \text{(III.15)}$$

From a comparison of Eqs. (III.12) and (III.15), it is clear that when there is matched load, the coating thickness must be $2^{\frac{1}{2}}$ times larger than in the limiting case of measurement with an unmatched high-ohmic load at the output.

It was of interest to verify the functions derived, experimentally. These measurements were repeated a number of times and the optimal mode of the galvanic coating was always observed to correspond to Eq. (III.12).

When there was identical density of element placement and constant thickness of the sandwich-type transducer, the emf of a self-contained element from Eq. (III.11) can be obtained:

$$e = C\Phi\frac{\delta q}{\left(2 \div \frac{\lambda_2 l_2}{\lambda_1 l_1} \div \frac{\lambda_3 l_3}{\lambda_1 l_1}\right)\left(1 \div \frac{\varrho_2 l_1}{\varrho_1 l_2}\right)} \qquad \text{(III.16)}$$

where $\quad C = \frac{\alpha_1 - \alpha_2}{\lambda_1}; \quad \Phi = \frac{2l_1 \div l_2 \div l_3}{l_1}$

Taking note of the fact that the number of elements in the transducer equals the ratio of the area of the entire transducer f_t to the element area $2f_1 + f_2 + f_3$, we find the following expression for the working coefficient of the transducer from Eq. (III.16):

$$k_t = \frac{1}{C}\left(2 \div \frac{\lambda_2 l_2}{\lambda_1 l_1} \div \frac{\lambda_3 l_3}{\lambda_1 l_1}\right)\left(1 \div \frac{\varrho_2 l_1}{\varrho_1 l_2}\right)\frac{l_1}{f_t\delta} \qquad \text{(III.17)}$$

Since for most practical cases f_2/f_1 is close to optimally small compared with 2 and f_3/f_1 in Eq. (III.17), we can neglect the effect of f_2 on f_3.

The measurements were conducted on series-manufactured sandwich-type transducers with the following characteristics: $\delta = 1.2 \cdot 10^{-3}$ m; $\lambda_1 = 25$ W/m·deg; $\lambda_2 = 380$ W/m·deg; $\lambda_3 = 0.3$ W/m·deg;

$\rho_1 = 0.48 \cdot 10^{-6}$ ohm·m; $\rho_2 = 0.018 \cdot 10^{-6}$ ohm·m; $\alpha_1 - \alpha_2 = 43 \cdot 10^{-6}$ V/deg; and $f_1 = 0.8 \cdot 10^{-8}$ m^2.

For the series density of placement of about 100 junction pairs per cm^2 and with a standardized transducer size of 17x17 mm^2 for transducers with the described characteristics, Eq. (III.17) can be described in the following abridged form:

$$k_t = 13.4 \cdot 10^3 \left(2.7 \div 15.2 \frac{f_2}{f_1} \div 0.08 \frac{f_1}{f_2} \right) \qquad \text{(III.18)}$$

In the plot in Fig. 43, the points reflect the measured values of the working transducer coefficients for different relative galvanic coating thicknesses, and the curve was plotted according to Eq. (III.18). The experimental results agree quite satisfactorily with the theoretical results. The scatter of points is accounted for by the large number of factors affecting the individual stages of the technical process of transducer fabrication. When $f_2/f_1 > 0.04$, the variance of the measurements relative to the theoretical curve is 0.0068; this corresponds to a mean-square-root error of 8 percent. Eq. (III.15) was not experimentally verified, since it was derived on the same grounds as Eq. (III.12), and its verification technique is much more involved.

As we can see in Fig. 43, when the relative coating thick- ness is less than the optimal thickness, the transducer sensitivity falls off sharply, while at the same time when there is an increase after the optimal value, there is a gradual fall-off in sensitivity. Because of this and referring to the operating conditions to which Eq. (III.15) correspond, and also the possibility of reducing the coating thickness owing to corrosion, the working coating thickness must be selected as 50 percent higher than follows from Eq. (III.12). In particular, for series-manufactured sandwich-type transducers made of 100 µm diameter constantan wire, the copper-plating thickness was chosen as equal to 3-3.5 µm. Below are given the optimal values of the cross-sectional areas of the galvanic coatings for different pairs of materials when the measurements were made in the compensation schemes calculated according to Eq. (III.12). The first is called the base material, the second--the paired material of the galvanic coating. The correction for thermal conductivity of the filler was not taken into account:

Материалы (a)	$\frac{f_2}{f_1}\big|_e$	Материалы (a)	$\frac{f_2}{f_1}\big|_e$
Константан-серебро (b)	0.065	Нихром-никель (j)	0.158
Константан-медь (c)	0.070	Хромель-никель (k)	0.21
Копель-серебро (d)	0.061	Хромель-висмут (l)	2.85
Копель-медь (e)	0.066	Платинородий-платина (m)	0.79
Копель-золото (f)	0.086	Алюмель-сурьма (n)	2.18
Копель-сурьма (g)	1.58	Копель-теллур (o)	>200
Алюмель-железо (h)	0.55	Копель-германий (p)	>30
Копель-железо (i)	0.40	Хромель-кремний (q)	>20

Key:

a. Materials	j. Nichrome-nickel
b. Constantan-silver	k. Chromel-nickel
c. Constantan-copper	l. Chromel-bismuth
d. Copel-silver	m. Platinorhodium-platinum
e. Copel-copper	n. Aluminum-antimony
f. Copel-gold	o. Copel-tellurium
g. Copel-antimony	p. Copel-germanium
h. Alumel-iron	q. Chromel-silicon
i. Copel-iron	
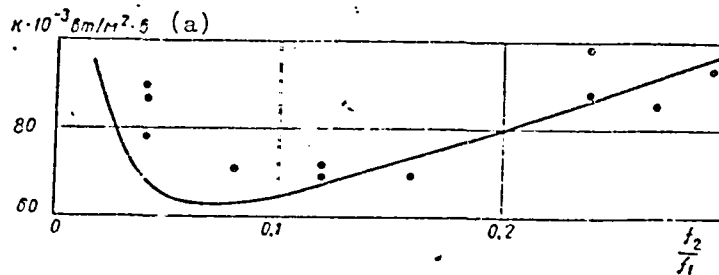
Fig. 43 Dependence of coefficient of sandwich-type transducer on relative thickness of galvanic coating

Key: a. watts/meter^2·volt

4. Theory of Similarity and Calculation Formulas

From the foregoing we can make a number of general conclusions determining the general principles of designing galvanic banked transducers such as was done, for example, for hydraulic jet machines.

Transducers are considered as geometrically similar transducers when their ratio of any dimension of one transducer (denoted by the subscript m) to the corresponding dimension of the other (n) is a constant. The materials of which the transducers were made are also assumed to be identical.

Since the signal from each element, for a fixed value of the measured flux, is proportional to its height δ (III.16), the emf generated by similar transducers are proportional to their linear dimensions:

$$\frac{e_m}{e_n} = \frac{\delta_m}{\delta_n}$$

(III.19)

The resistance of an element is proportional to its height and inversely proportional to its cross-sectional area, that is, to the wire diameter squared. The total effect is that the electrical resistances are inversely proportional to the geometrical dimensions:

$$\frac{R_m}{R_n} = \frac{\delta_n}{\delta_m}$$

(III.20)

When the loads are matched, the currents in the measurement circuits must be directly proportional to both the emf and the conductivity of the transducers. As a result, from Eqs. (III.19) and (III.20) it follows that the transducer currents are directly proportional to the squares of the characteristic dimensions:

$$\frac{I_m}{I_n} = \left(\frac{\delta_m}{\delta_n}\right)^2$$

(III.21)

and the power generated--to their cubes:

$$\frac{P_m}{P_n} = \left(\frac{\delta_m}{\delta_n}\right)^3$$

(III.22)

103

The power of the measured flux is directly proportional to the transducer area, and the transducer area is directly proportional to the linear dimensions. So the transducer efficiencies are directly proportional to transducer size:

$$\frac{\eta_m}{\eta_1} = \frac{\delta_m}{\delta_n}$$

(III.23)

Eq. (III.23) is found in accordance with the results from analyzing the elementary Carnot cycle, since the temperature differences are also directly proportional to the linear dimensions.

When the external transducer dimensions are unchanged, we can modify internal transducer dimensions with the preservation of the geometrical similarity in the cross-sections. The height /97 of the individual elements is assumed to be unchanged, as is the total transducer height. As an argument, let us take the number of elements making up the bank. The emf generated by the transducer and the total length of the elements are directly proportional to the number of elements. The element cross-section and the current strength are inversely proportional to the number of elements, and the resistance is directly proportional to the square of the number of elements. The transducer power and efficiency, with the external transducer dimensions kept unchanged and with variation in the internal dimensions while the geometrical similarity is preserved, remain unchanged. Here the power is directly proportional to the transducer volume and the transducer efficiency to transducer height.

Further variations in the structural elements are possible by changes in external geometry (thickness and area) with the geometry of the internal sections unchanged. When there was variation in the total external dimensions, the emf and the power of the transducer are directly, and the resistance --inversely proportional to transducer volume. The transducer current strength, for matched load, does not depend on these external transformations. The efficiency, as before, is directly proportional to the height δ and does not depend on the area.

When there is tight placement, a change in the form factor (Φ < 20) practically ceases to affect the fraction of the flux passing through the inter-turn insulation filling. So when the external dimensions of the transducer and the supporting cross-section of the wire f_1 are kept the same, the transducer emf depends only slightly on the form factor: the resistance is directly, and the power, current, and efficiency are inversely

proportional to the number of elements. The dependence of the thermal resistance on the form factor is close to an inverse proportionality. Since the thermal resistance determines the extent of perturbation introduced by the measuring part, we must try to get the minimum value of the form factor attainable from technological conditions.

In general, when there is variation in the form factor, the meaningfulness of the similarity theory is lost to a large extent. Therefore it is best to compare the transducers with the identical form factor values. The quantity that is the reciprocal of the form factor uniquely determines technological ideality.

Usually the designers know the conditions in which the device built must operate. As applied to heat flux transducers, the conditions are characterized by a measured flux and by an instrument used in measuring the electrical signal. These conditions determine the required values of the transducer working coefficient k_t and its electrical resistance R_e. The problem is to determine all the structural elements of the transducer that would exhibit the necessary characteristics.

The expression for the transducer coefficient (III.17) can be rewritten in the following form:

$$k_t = \frac{A}{C\Phi} \cdot \frac{1}{z\delta} \qquad \text{(III.24)}$$

where $A = \left(2 + \frac{\lambda_2 l_2}{\lambda_1 l_1} + \frac{\lambda_3 l_3}{\lambda_1 l_1}\right)\left(1 + \frac{\varrho_2 l_1}{\varrho_1 l_2}\right);$ $z = \frac{l_t}{2l_1 + l_2 + l_3}$ is the number of /98 elements in the transducer.

Transducer electrical resistance is an important characteristic, also necessary for matching the measuring circuit elements. Taking note of Eq. (III.13), the resistance of the entire transducer can be represented as the product of the resistance of one element by the number of elements in the transducer:

$$R_e = \frac{\delta \varrho_1}{l_1} Bz \qquad \text{(III.25)}$$

where $B = \dfrac{2 + \frac{\varrho_1 l_2}{\varrho_2 l_1}}{1 + \frac{\varrho_1 l_2}{\varrho_2 l_1}}$

Table 3

Наименование пары (a)	A	B	$C \times 10^4$
(b) Константан-медь	4,86	1,35	1,72
(c) Константан-сереб- ро	4,94	1,35	1,72
(d) Копель-медь	4,93	1,35	2,07
(e) Копель-серебро	4,85	1,36	2,07
(f) Копель-железо	5,30	1,37	2,61
(g) Нихром-никель	4,58	1,33	1,89
(h) Кромель-никель	4,58	1,33	2,27
(i) Платинородий- платина	6,19	1,43	0,17
(j) Алюмель-железо	5,80	1,40	1,18
(k) Алюмель-сурьма	5,93	1,41	2,21

Key:

    a. Name of pair
    b. Constantan-copper
    c. Constantan-silver
    d. Copel-copper
    e. Copel-silver
    f. Copel-iron
    g. Nichrome-nickel
    h. Chromel-nickel
    i. Platinorhodium-platinum
    j. Alumel-iron
    k. Alumel-antimony

For geometrically similar transducers, the constancy of the coefficients A and B in Eqs. (III.24) and (III.25) is obvious. It is important that even for large deviations from the laws of similarity, but with the optimal values of the ratios of the metal sections kept the same (Eqs. (III.12) or (III.15), A varies only slightly, and B remains constant. When there is a change in the arguments within limits that are meaningful in practice, the ratio $\dfrac{\lambda_3 f_3}{\lambda_1 f_1}$ remains small compared with

$2 + \dfrac{\lambda_2 f_2}{\lambda_1 f_1}$, and all the remaining members of these equations depend only on the ratio of the metal cross-sections and the thermophysical characteristics of the metals.

So for any pair of thermoelectrode materials, A, B, and C (Eq. (III.16)) can be determined ahead of time. The values of these coefficients are given in Table 3 for promising pairs. Optimal values of the relative cross-sections are determined according to Eq. (III.15).

The form factor in series manufacture can be relatively easily kept at about 12-13; with special care in transducer production, its value can be lowered to 6-7.

By cancelling $z\delta$ from Eqs. (III.24) and (III.25), we can find the initially required wire diameter: /99

$$d = \left(\frac{4AB\rho_1}{\pi C\Phi R_e^4 t} \right)^{\frac{1}{2}} \qquad \text{(III.26)}$$

and then the product $z\delta$ necessary for the required coefficients k_t and resistance R_e is

$$z\delta = \frac{A}{k_t C\Phi} \qquad \text{(III.27)}$$

If we assume that the transducer diameter D is 20-40 times greater than transducer height δ, that is,

$$\frac{D}{\delta} = \frac{d\sqrt{\pi z \Phi}}{\delta} = 20 - 40 \qquad \text{(III.28)}$$

and if we substitute Eqs. (III.26) and (III.27) into (III.28), we can find

$$z = (5 - 7)\left(\frac{AR_e}{BC\Phi^2 \rho_1 k_t} \right)^{\frac{1}{3}}$$

$$\delta = (0.22 - 0.14)\frac{A^{\frac{2}{3}} B^{\frac{1}{3}} \rho_1^{\frac{1}{3}}}{C^{\frac{2}{3}} \Phi^{\frac{1}{3}} R_e^{\frac{1}{3}} k_t^{\frac{2}{3}}} \qquad \text{(III.29)}$$

Since A, B, and Φ vary in fairly narrow limits, for approximate calculations Eqs. (III.26) - (III.28) can be simplified:

$$\left. \begin{aligned} d &= 0.85 \sqrt{\frac{\rho_1}{C k_t R_e}}; \\ \delta &= 0.24 \sqrt[3]{\frac{\rho_1}{C^2 k_t R_e}}; \\ z &= 1.7 \sqrt[3]{\frac{R_e}{C \rho_1 k_t}}; \\ D &= 3.1 d\sqrt{z}. \end{aligned} \right\} \qquad \text{(III.30)}$$

107

5. Technology of Sandwich-Type Transducer Manufacture

At the present time, galvanic sandwich transducers are made by winding the base-wire on a soluble celluloid ribbon. Nitrocellulose cord motion picture film, 35 mm wide and 0.17 mm thick, is used as the initial material for the celluloid mandrel. Strips with perforations are slit along the sides with a special roller shears in a single pass of the ribbon; the middle part is unwound for 20 identical strips 1 mm wide. Usually a 20 m long ribbon is used in the unwinding. The resulting strips are successively cemented with motion picture cement and wound on an approximately 400 m magnetic tape spool.

The middle part of the ribbon is unwound for wider strips for transducers that are thicker.

The machine for winding the wire on a celluloid strip resembles the machines for winding wires with filament insulation. The strip is fed by rubber rolls from a Warren mini-motor via reduction gearing with a variable transmission ratio.

The wire is wound from a spool spinning evenly around a celluloid strip traveling slowly across a hollow axis. The winding spacing is chosen to be 1.5-2 times the wire diameter. The length of the continuously wound intermediate product (15-25 m) is limited by spool capacity. Machine productivity is about 5 m of strip an hour.

After winding, for reduced elastic unwinding the intermediate product is rolled out between the rolls of a manual rolling mill, and then for convenience in storage it is wound on the spool.

As necessary, segments as long as required are sliced off from the intermediate product. The length of a cut intermediate product for 17x17 mm^2 transducers is 600 mm; this corresponds to $(3-3.5)\cdot10^3$ pairs of elementary junctions.

Operation-by-operation monitoring at all the next stages is executed mainly in terms of the electrical resistance of the wound wire. The resistance values are entered in the transducer rating plate.

Strips on one segment side are twice coated with cellulose nitrate varnish (GOST 5236-50); the strips are allowed to dry for an hour after each coating and are placed on a special frame for copper-plating. On the frame the strip is dipped into the galvanic bath. Copper is deposited in accordance with recommendations in electroplating handbooks /27/. During

108

copper-plating in an acidic electrolyte, it is best to add about 1 percent ethanol to the bath; this does much to improve coating density and strength. The coating thickness is selected in accordance with the calculated recommendations (see Section 3 of this chapter). The coating thickness is 3-3.5 μm for an 0.1 mm diameter constantan wire. /101
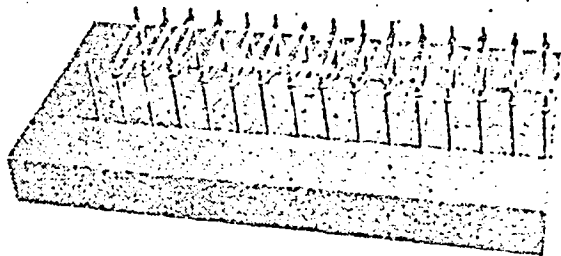
Fig. 44   Hackle for forming and drying intermediate products for sandwich-type transducer
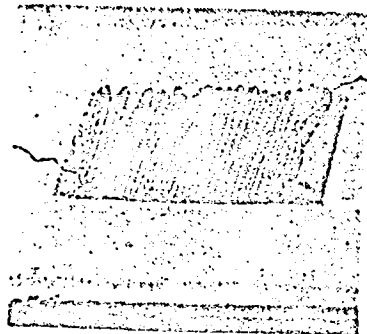
Fig. 45   Teflon-type press mold for "pebbles"

Deposits from cyanide electrolytes are better than from acidic electrolytes, but their use means greater production-line toxicity.

When copper-plating ends, the celluloid base and the cellulose nitrate varnish are dissolved out in acetone; the spiral is coated with AK-20 varnish and kept in the air at room temperature for 3-5 min. The varnish-coated spiral is fitted in zigzag fashion on a special hackle (Fig. 44), placed in a drying cabinet, and kept there 2 hr at 80-90° C. Depending on the required transducer size, hackles of different widths are employed.

When the varnish polymerizes, the zigzag spiral is coated with epoxy resin mixed with curing agent, placed in a teflon-type press mold (Fig. 45), squeezed on all sides, heated with the press mold in a thermostat to 100° C, kept there 2 hr, and allowed to cool in air down to room temperature. What results is a compact sandwich-type rectangular paralleliped--"pebbles."

"Pebble" quality is evaluated on a calibration stand; on it the preliminary value of the transducer working coefficient is determined.   /102

Next, the product can be used as an intermediate product --as "pebbles" for different purposes applicable to local

conditions. Generally the "pebbles" are mounted in a stainless
steel ring (Fig. 46) with an internal groove and are filled over
with epoxy resin to which lampblack had been added for better
absorptivity. This transducer is shown in finished form in
Fig. 47.
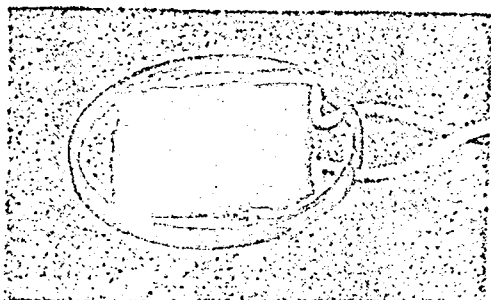
Fig. 46   Preliminary placement of
"pebble" in ring before epoxy
resin filling

Fig. 47   General view of
finished 1.5 mm thick
transducer

Transducers made as per the technology described, using
grade ED-4 epoxy resin, can function at temperatures to 100° C.
When ED-6 resin or FAED-13 furan-epoxy resin is used, the work-
ing temperature of the transducer can be raised to 120 or 150° C,
respectively. The rated upper temperature limits for these
resins are $30-40^\circ$ C higher.

For functioning at temperatures to 300° C, after being
insulated with AK-20 varnish the copper-constantan intermediate
products are filled over with enamel capable of enduring higher
temperatures. During heat treatment of the enamel the varnish
burns up.

Enamels that have not been brought to the glaze condition
are gas-permeable. So at temperatures higher than 300° C active
oxidation of the copper coating commences, leading to a rapid
change in the calibration characteristic of the transducer.

At temperatures up to 700° C, chromel wire is recommended /103
as the base, and nickel is recommended as the coating. In
high-temperature cases, the transducer service life is shortened
to tens of hours. Measurements with sodium electrolyzers con-
ducted at the Berezino Titanium-Magnesium Combine showed that

110

transducers withstood up to 1000 measurements with no change in characteristics and broke down mainly from mechanical damage.

6. Theory of Slant-Layer Transducers

The sensitive element of a slant-layer transducer is a plate consists of successively alternating layers of paired thermoelectrode materials (for example, copper with constantan). The layers are arranged obliquely at an angle of 20-45° to the basal surface on which the transducer is placed (Fig. 48).
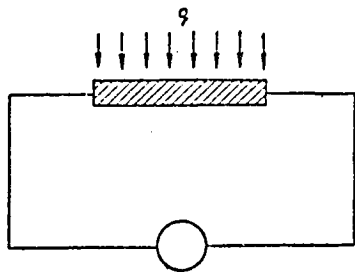
Fig. 48 Diagram of slant-layer transducer

When the measured heat flux penetrates the transducer, a temperature difference is induced between the upper and the lower transducer surfaces; the temperature difference excites a thermo-emf capable of accumulating along the transducer ribbons. Because of this, the transducer designed in this way is suitable for measuring heat fluxes /268/.

In the horizontal direction (along the basal surface), individual transducer elements are connected in series; this leads to a summing of the signal. That is why this transducer can be classed with the banked transducers.

The qualitative and, to a sufficient extent, quantitative pattern of distribution of current lines and isotherms was obtained on a model EGDA-9-61 electrical integrator /229, 241, 242/.

Fig. 49 presents the distribution of equipotentials and current lines for copper-constantan transducers that have a ratio of constantan layer thickness to copper layer thickness of 16 and 8, respectively. The slope of the layer is chosen as 45°. The boundary conditions on the lower basal face are of the first kind, and on the upper face--of the second kind. This corresponds to use of the transducer as a radiative-energy receiver (for example, in a pyrometer) with its mounting on a surface of a semibounded body with high thermal conductivity.

Paper being inhomogeneous, the equipotential lines on the /104 were recorded with irregularities not intrinsic to the solution of the Laplace equation for piecewise-linear domains--models of slant-layer transducers. The fields recorded on the electrical integrator were corrected by successive approximations using

Cauchy-Riemann conditions similar to what is done in hydro-
mechanics when solutions are constructed for different cases
of potential flows /189/. The model length is selected so that
a further increase in length does not alter the field pattern
in the middle area.

a

b
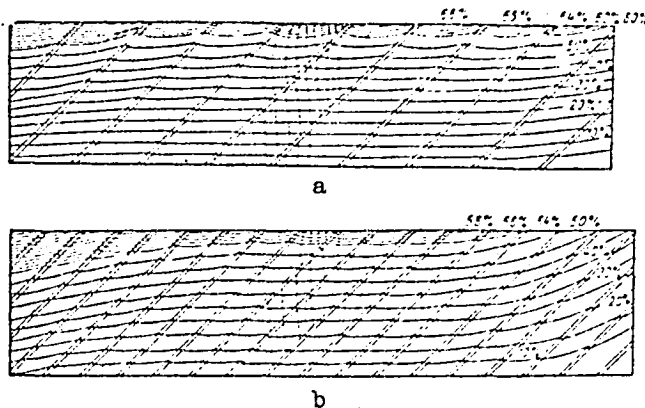
Fig. 49   Distribution of isotherms and
current lines in a slant-layer transducer
when

$$k_\lambda = \frac{\lambda_2}{\lambda_1} = 0.07, \quad k_Q = \frac{Q_2}{Q_1} = ?, \quad k_\delta = \frac{\delta_2}{\delta_1} = 16 \quad \text{(a)}$$

$$k_\lambda = \frac{\lambda_2}{\lambda_1} = 0.07, \quad k_Q = \frac{Q_2}{Q_1} = ?, \quad k_\delta = 8 \quad \text{(b)}$$

In all cases the slant-layer design promotes the sloping of
the current lines in the direction of layer slope. This causes
distortions in the end sections. With the adopted orientation
of transducer layers in the left part of the field, clumping
results, and when the orientation is in the right part, thin-
ning out of the current lines.

The size of the region of these end perturbations is equal
to the transducer thickness. As can be seen in Fig. 49, the
end perturbation no longer is detectable at a distance of two
transducer thicknesses. Readily visible in this figure are the
regions of rearrangement of the current lines at the upper and
lower faces. A uniformly incident flux concentrates in the more

conductive layers. In the less-thermally conductive layers, the current lines and the isotherms thin out with deeper penetration of the flux in the transducer body; corresponding to this situation is the positive curvature of the equipotentials. In the more-thermally conductive layers the reverse phenomenon is observed, but the scale of the model does not let us observe it.

The domain of current line rearrangement is determined /105 by the thickness of the less-conductive layer. At a depth that is greater than this thickness, the field becomes uniform and the equipotentials within the sections with identical conductivity straighten out. At the inter-layer boundaries the equipotentials and the current lines undergo an inflection.
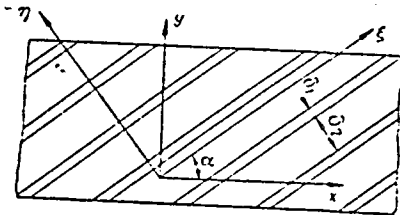
Fig. 50 Designation of dimensions and axes in slant-layer transducer

The problem of thermal conductivity in the slant-layer transducer is a particular case of thermal conductivity in anisotropic media; exemplifying these, besides the artificial sandwich-type compositions, are many crystals and natural layered formations (wood, sedimentary shales, and so on).

Equipment for analytical investigation in this field was brought by G. Lame, G. Stokes, W. Roentgen, and T. Boussinescu /124/ to such a state of advancement that it was just about unchanged for nearly a century.

The fundamental generalizing assumption of the thermal conductivity theory of anisotropic bodies is that each component of the heat flux vector at a point is a linear function of all components of the temperature gradient at this point, that is,

$$\left. \begin{aligned}
-q_1 &= \lambda_{11}\frac{\partial t}{\partial x_1} + \lambda_{12}\frac{\partial t}{\partial x_2} + \lambda_{13}\frac{\partial t}{\partial x_3}; \\
-q_2 &= \lambda_{21}\frac{\partial t}{\partial x_1} + \lambda_{22}\frac{\partial t}{\partial x_2} + \lambda_{23}\frac{\partial t}{\partial x_3}; \\
-q_3 &= \lambda_{31}\frac{\partial t}{\partial x_1} + \lambda_{32}\frac{\partial t}{\partial x_2} + \lambda_{33}\frac{\partial t}{\partial x_3},
\end{aligned} \right\} \qquad \text{(III.31)}$$

where in the subscripts 1 stands for x or ξ; 2--y or η; and 3--z or ζ.

113

The thermal conductivity values λ_{rs} are components of a second-rank tensor. Important to further exposition is a translation of the components of the thermal conductivity tensor from one system of orthogonal coordinates to another. The direction cosines between the axes are designated in the matrix below:

Axes	x	y	z
ξ	α_{11}	α_{12}	α_{13}
η	α_{21}	α_{22}	α_{23}
ζ	α_{31}	α_{32}	α_{33}

where $\alpha_{11} = \cos(x,\xi)$, $\alpha_{21} = \cos(x,\eta)$, and so on.

The primary formulas for translating the tensor components in converting from one coordinate system to another can be written as follows /142/:

$$\lambda'_{kl} = \sum_{r=1}^{3} \sum_{s=1}^{3} \alpha_{kr}\alpha_{ls}\lambda_{rs} \qquad \text{(III.32)}$$

As applied to a slant-layer transducer, considerable simplifications can be introduced into the system presented above.

The transducer flux and temperature fields can be examined in a two-dimensional coordinate system (Fig. 50). Since both coordinate systems are orthogonal and lie in the same plane, the number of direction cosines can be reduced to two: $\cos\alpha$ and $\cos\left(\dfrac{\pi}{2}+\alpha\right)$. As the initial system let us adopt the

$\xi-\eta$ system. For it all cross-coefficients of the thermal conductivity are equal to zero: $\lambda_{\xi\eta}=\lambda_{\eta\xi}=0$; only the principal coordinates of thermal conductivity remain nonzero.

Assuming the heat flux field to be continuous in the stationary mode, we can find the principal thermal conductivities:

$$\lambda_\xi = \frac{\lambda_1\delta_1 + \lambda_2\delta_2}{\delta_1 + \delta_2}$$

$$\lambda_\eta = \frac{\lambda_1\lambda_2(\delta_1+\delta_2)}{\delta_1\lambda_2 + \delta_2\lambda_1} \qquad \text{(III.33)}$$

or, on converting to the dimensionless values $k_\delta = \dfrac{\delta_2}{\delta_1}$ and $k_\lambda = \dfrac{\lambda_2}{\lambda_1}$

114

$$\lambda_\xi = \lambda_1 k_\xi \quad \text{and} \quad \lambda_\eta = \lambda_1 k_\eta \qquad (III.34)$$

where

$$k_\xi = \frac{1 + k_\lambda k_\delta}{1 + k_\delta}; \quad k_\eta = \frac{1 + k_\delta}{1 + \frac{k_\delta}{k_\lambda}}$$

If the initial system chosen is one in which the thermal conductivity coefficients along the coordinate axes are the principal coefficients, as occurs in the system $\xi-\eta$, all the initial cross-thermal conductivities become equal to zero. In this case Eq. (III.32) becomes simplified:

$$\lambda'_{kl} = \alpha_{k1}\alpha_{l1}\lambda_{11} + \alpha_{k2}\alpha_{l2}\lambda_{22} \qquad (III.35)$$

from whence we get

$$\left. \begin{aligned} \lambda_{11} &= \lambda_{xx} = \lambda_1(k_\xi \cos^2\alpha + k_\eta \sin^2\alpha); \\ \lambda_{22} &= \lambda_{yy} = \lambda_1(k_\xi \sin^2\alpha + k_\eta \cos^2\alpha); \\ \lambda_{12} &= \lambda_{21} = \lambda_{xy} = \lambda_{yx} = \frac{\lambda_1}{2}\sin 2\alpha (k_\xi - k_\eta). \end{aligned} \right\} \qquad (III.36)$$

The thermal diffusivity formulas are similar to the thermal /107 conductivity formulas. Corresponding projections of the heat fluxes are determined according to Eq. (III.31), with reference to Eq. (III.36):

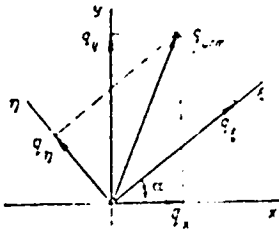A vector diagram of the heat fluxes in the coordinate systems adopted is shown in Fig. 51.

Fig. 51 Vector diagram of
        fluxes

Fig. 52 Diagram of short-
        circuited heat loops

The flux skews within the transducer (toward the layer slope) and because of this its density increases. The flux component along the y-axis is equal to the flux received by the transducer.

The temperature gradient vector, in contrast to the principal flux vector, coincides with the y-axis. The temperature difference between the ends of the metal strips forming the transducer leads to the origination of short-circuited current loops caused by the presence of a thermo-emf (Fig. 52). By their nature they resemble currents in bimetallic galvanic thermocouples described in Section 3 of this chapter. The value of the thermoelectrical coefficient of the bimetallic compositions along the layers is determined by Eq. (III.9). When the heat flux transversely enters into the slant-layer transducer the longitudinal accumulation of the thermo-emf takes place. To investigate the value of this thermo-emf, we can examine longitudinal transitions in the form of step changes: initially perpendicular to the layers, and then along the layers.

Let us select a material denoted by subscript 1 as the base material, that is, as the material used in making the pickups of signal from the slant-layer transducer ends.

The value of the thermoelectrical coefficient when there is transverse passage is determined from the relation

$$(\alpha_1 - r)_\perp = (\alpha_1 - \alpha_2)\frac{k_\delta}{k_\delta + k_\lambda} \qquad \text{(III.37)}$$

which can easily be derived if we cancel out the temperature drops at the base layers δ_1 not participating in generating the thermo-emf.

If the perpendicular passage coincides with the positive projection of the temperature gradient, the subsequent passage parallel to the layers will occur opposite to the corresponding gradient projection. The inequality of the thermoelectrical coefficients in the perpendicular and longitudinal directions in the sandwich composition is the only formal cause of signal origination in the slant-layer transducer.

For this case the difference between the temperatures of the upper and lower transducer faces is

$$\Delta t = \frac{q\lambda}{\lambda_{yy}} = \frac{q\lambda}{\lambda_1 (k_\xi \sin^2 \alpha + k_\eta \cos^2 \alpha)} \qquad \text{(III.38)}$$

116
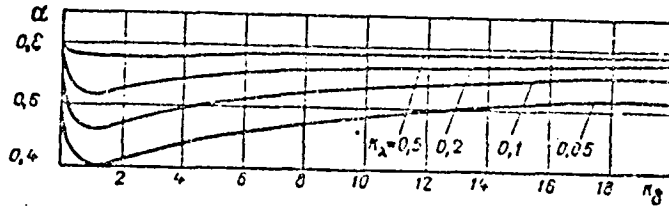
Fig. 53 Dependence of optimal slope of
transducer layers on transducer design
parameters

The signal in the interval equal to one pair of passages
is

$$e_{ca} = \frac{q(\alpha_1 - \alpha_.)\Delta}{h_1(k_\xi \sin^2\alpha + k_\eta \cos^2\alpha)}\left(\frac{k_\delta}{k_\delta - k_\varrho} - \frac{k_\delta}{k_\delta + k_\lambda}\right) \qquad (III.39)$$

To get the signal generated per unit transducer length,
let us divide the right-hand side of Eq. (III.39) by the length
of the paired passage section equal to $\dfrac{\Delta}{\sin\alpha\cos\alpha}$. Then

$$\frac{e}{l} = q\frac{\alpha_1 - \alpha_.}{h_1}\left(\frac{k_\delta}{k_\delta - k_\varrho} - \frac{k_\delta}{k_\delta + k_\lambda}\right)\frac{1}{k_\xi \operatorname{tg}\alpha + k_\eta \operatorname{ctg}\alpha} \qquad (III.40)$$

Characteristically, the signal generated per transducer
length does not depend on transducer thickness. This opens up
the theoretically possibility of reducing, without limit, the
transducer inertia by reducing transducer thickness, without
lowering sensitivity /26d7.

From Eq. (III.40) it is clear that the sensitivity is at
a maximum when the sum $k_\eta\operatorname{tg}\alpha + k_\eta\operatorname{ctg}\alpha$ is at a minimum; corres-
ponding to this sum is

$$\operatorname{tg}^2\alpha_{opt} = k_\eta / k_\xi \quad \text{or}$$

$$\alpha_{opt} = \operatorname{arctg}\sqrt{\frac{k_\eta}{k_\xi}} \qquad (III.41)$$

117

By analyzing Eq. (III.34) we see that $\frac{k_\eta}{k_i} \leq 1$ and there-fore, $\alpha_{opt} = \pi/4$. Plotted in Fig. 53 are the α_{opt} values for different k_δ and $k\lambda$. As we can see in Fig. 53, in agreement /109 with Gayling's recommendations ($\alpha_{opt} = \pi/4$) are only the limit-ing values when $k_\delta = 0$, $k_\delta = \infty$; and $k_\delta = 1$. The two first values correspond to the monolithic bodies incapable of gene-rating any signal. When $k_\lambda = 1$, the signal differs from zero only if $k_\rho \neq 1$. Since the Wiedemann-Franz law is obeyed appro-ximately in all metals, when $k_\lambda = 1$, k_ρ cannot differ appre-ciably from unity. Therefore in the latter case the slant-layer transducer signal is near-zero.
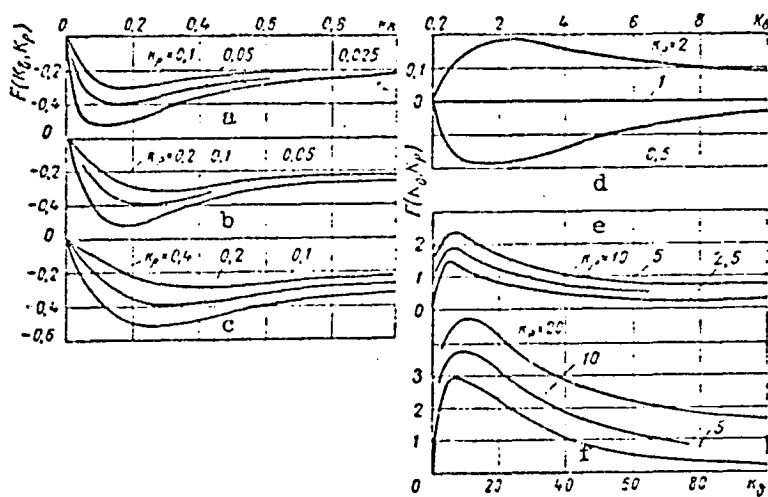
Fig. 54 Dependence of slant-layer transducer characteristics on design parameters:

a. $k_\lambda = 20$ c. $k_\lambda = 5$ e. $k_\lambda = 0.2$

b. $k_\lambda = 10$ d. $k_\lambda = 1$ f. $k_{\lambda\lambda} = 0.1$

For all real cases, the optimal values of the angle $\alpha_{opt} < \pi/4$ reach 0.4 ($23°$) even in the case of materials that are contrasting in thermal conductivity and electroconductivity and that are promising for slant-layer transducer fabrication.

By substituting Eq. (III.31) into (III.40), we find.

$$\frac{e}{l} = \frac{\alpha_1 - \alpha_2}{2l_1} qF(k_\delta, k_\varrho, k_\lambda)$$ (III.42)

where

$$F(k_\delta, k_\varrho, k_\lambda) = \frac{k_\delta(k_\lambda - k_\varrho)}{(k_\delta \div k_\varrho)(k_\delta \div k_\lambda)} \left\} \sqrt{\frac{k_\delta \div k_\lambda}{1 \div k_\delta k_\lambda} \cdot \frac{1}{k_\lambda}}$$ (III.43)

Shown in Fig. 54 are the plots of the dependences of the function $F(k_\delta, k_\varrho, k_\lambda)$ on all its arguments. From these plots we can evaluate the effect of the individual design factors and find the optimal relations.

The tabulation regions of the functions $F(k_\delta, k_\varrho, k_\lambda)$ /110 were selected with reference to the departures from the Wiedemann-Franz law that are possible for metals.

Summing up, we can state the following: the specific signal of a Gayling transducer does not depend on its thickness; the signal in transducers with thermal conductivity ratios equal to the electrical resistance ratios does not accumulate lengthwise --the transducer shuts off; the maximum signal values are characteristic of contrasting pairs of materials that have high values of relative thermal and electroconductivity; optimal ratios exist for all structural characteristics of slant-layer transducers.

ABSOLUTE CALIBRATION MEASUREMENTS OF RADIATIVE FLUXES
AT LOW AND MODERATE TEMPERATURES ($\pm 200^\circ$ C)

Calibrating an instrument, all things considered, amounts to measuring a standardized parameter. Of the three classificatory kinds of heat transfer--convection, conduction, and radiation--the last-named kind lends itself to the most exact standardization.

Calibrating transducers by the radiative method means, on the one hand, providing a standardized stable radiative flux, and on the other--providing metrological information about this flux.

Moderate-density radiators were developed with standard incandescent bulbs and infrared lamps, and for high-density fluxes--blackbody mirror models with graphite or silicon carbide heaters.

The designs worked out for absolute radiometers were based on Angstrom actinometers, inertial radiometers, and instruments with successive-replacement compensation. They are all adapted to transducer calibration conditions when the measured flux densities differ.

A method of calibrating series-manufactured transducers by the radiation method is presented at the end of this chapter.

1. Radiators of Low-Intensity Fluxes

The present-day theory of radiative heat transfer has in its arsenal means of calculating the flux that is incident on the instrument under calibration in specific geometrical and

temperature conditions, for known blackness values. The system of logical assumptions formally is found to be closed, but some of its elements are not fully validated. Many authors, lacking better opportunities, have resorted to this method.

Not trusting geometrical calculations, Kheydzher used absolute blackbody models in the form of hollow isothermal cones placed near the receiving surfaces of the radiometers undergoing calibration /232, 233/. Even in this case there was no certainty that calibration was correct. So it is best /112 to simultaneously measure the fluxes with absolute and calibrated instruments placed in identical conditions as to geometry and blackness value. The blackness value is easier to make identical for two objects than it is to determine its absolute value. No longer is monitoring spectral composition then necessary.
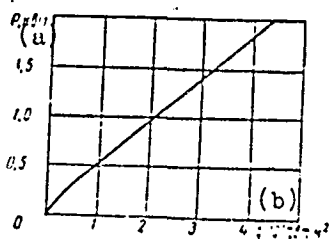
Fig. 55 Characteristic of quartz radiator with two NIK-220-1000 lamps

Key:

    a. kilowatts
    b. watts/meter^2

The author of this monograph used general-purpose incandescent lamps (GOST 2239-60) as low-flux radiators, and for fluxes to 10 kW/m^2---industrial lamps, type ZS, for infrared drying.

A heavy disadvantage of tungsten filament lamps is that in the region where the spiral image forms the incident flux changes abruptly. One or several matte glass units are placed on the path of the incident flux in order to equalize the density in the illumination fixture. Maulard /285/ used this procedure in heat-measurement calibration. This procedure is inseparably associated with large energy losses owing to absorption in the glass and contaminants.

For a pure low-absorption matte surface, the bulb envelope was coated with a thin layer of fine halite crystals (NaCl). The coating technology is relatively simple: a concentrated solution of chemically pure salt in distilled water was applied by sprayer on the surface of the bulb envelope functioning in the mode of approximately 40 percent load.

Test results showed that the nonuniformity of the incident flux is not worse than 1 percent, and the flux density can be brought to 10 kW/m^2 on an area up to 50 mm in diameter when the distance from the incandescent filament is 200 mm. These same fluxes were obtained in a muffle furnace at much larger outlays of materials, energy, and time $\underline{/50, 51}$.

NIK-220-1000 lamps regularly produced commercially are convenient to use in building up fluxes to 60 kW/m^2. They are resistant to "thermal shocks" (an incandescent lamp can be sprayed with water) and short-term overloading with doubled power (to 2 kW) can be tolerated.

To produce an oriented flux two NIK-220-1000 lamps were placed within a cooled copper reflector. The characteristic of this unit with respect to flux is presented in Fig. 55 for a distance of 100 mm from the plane of the lamp bulb axes.   /113

Fluxes to 200 kW/m^2 can be obtained when NIK-220-1000 lamps can be tightly laid out in a continuous panel in the short-term forcing mode.

Although the intrinsic inertia of electrical lamps with tungsten filaments is measured in the seconds, the above-described units, owing to heating of the reflectors and the associated parts, actually reach the steady-state mode in 5-10 min.

2. High-Intensity Flux Radiators

There is no standard, series-manufactured equipment for generating fluxes with densities greater than 200 kW/m^2.

In 1961 a radiator of fluxes with densities to 300 kW/m^2 was developed in 1961 in the Laboratory for Methods of Heat Measurements (LMTI); this radiator is designed for calibrating different calorimeters and thermometric devices $\underline{/32}$, 58, 69/. It differs by its low inertia and high stability. Graphite was selected as the radiator material. Graphite begins vigorously burning up in an oxidizing medium even at 800° C. Applied as protection was a graphite coating with an approximately 1 mm thick silicon carbide layer. To do this, products were lowered into a slip of a mixture of carborundum, silicon, and glycerine and, after drying, they were subjected to heat treatment in a neutral atmosphere. The silicizing technology was worked out in detail in the Institute for Problems of Materials Science, Ukrainian SSR Academy of Sciences, by G. G. Gnesin.

122

Carbon and silicon from silicon carbide, in an oxidizing atmosphere, burn up, liberating carbon dioxide gas and with the formation on the surface of a stable protective film in the form of some silica modification.

The radiator was made in the form of a hemisphe_cal dish with a diameter twice the diameter of the furnace port hole. The furnace longitudinal cross-section (modification I) is shown in Fig. 56.

Electric energy is fed the heater from a welding transformer through brass water-cooled connections. The resistance of the element in finished form is approximately 0.1 ohm.

When the thermal insulation lowering the temperature from 1600-2000° C to 20-30° C was selected, comparative calculations were made of the design variants. The cold reflecting insulation was found to be best. Copper walls surrounding the heat were internally polished and gilded, and externally chrome-plated. Channels for the inflow of cooling water were provided in the body of the walls. As to design, the insulation was molded in the form of a hemisphere covering the front wall with the port hole.

For determining the optimal gap between the reflector and the heater, variant calculations were made of heat trans- /114 fer through the spherical gas interlayer owing to radiation and thermal conductivity.

Provided in the cooling system was an interlocking arrangement, including an emergency signal and a furnace disconnection when there is an impermissible lowering in the pressure of the cooling water.

The radiator instability depended only on fluctuations in the line voltage. Conditioning of the heating elements was not long--after 200 h operation the resistance went up by 8 percent. When the port hole was 50 mm in diameter, the radiator efficiency was approximately 25 percent. As the port hole diameter was increased to 100 mm, the efficiency was lowered to 60 percent, but the density of the radiated flux was somewhat reduced and nonuniformity of the flux field at the edges showed up. The results of measuring the flux field for a furnace with a 50 mm diameter port hole are shown in Fig. 57.

One drawback of the silicized heaters is that they rapidly break down, operating at temperatures under 1400° C.

123

The protective ability of the coating film is just as distinctive as many other properties of silica. P. Bridgman and his students studied the properties of silica at pressures from $1.8 \cdot 10^{10}$ N/m² and temperatures to 2000° C. But much information about the properties of silica under ordinary conditions is contradictory.

In nature silica is encountered usually as quartz--a transparent or colored crystalline mineral in the trigonal system with a density of 2.655 g/cm³. When the temperature increases, its physical properties undergo changes, of which the most substantial is the transition from the α-state to the β-state at 572±5° C, with a 2 percent drop in density.

Subsequently, at 867°, quartz passes over into β-tridymite in the rhombic system, with a 15 percent decrease in density; at 1470° C there is a transition to β-cristoballite, with a 3 percent gain in density.

The transitions quartz-to-tridymite, tridymite-to-cristoballite, and all reversible forms of transitions are slowly executed. Factors affecting their rates are not known. All three main crystalline forms exist at low temperatures and are observed at temperatures exceeding the corresponding critical transition values.

Fig. 56 Low-inertia furnace (variant I):

1, 7. inflow of cooling water
2. installation plate
3. port hole
4. heating element
5. cooling channels
6. current-conducting buses

The melting points of each of the forms are individual: according to some sources quartz does not melt /42/, but other authorities say that with rapid heating its melting point is 1550° C /1/; tridymite melts at 1670±10° C, and cristoballite --at 1710±10° C.

No references are in the literature concerning the preservation in the liquid of information telling about from what crystalline form the liquid is obtained, and without this information we cannot understand the features of the existence of

liquid silica in the 1550-1710° C range. So the crystalline
forms of silicon dioxide are an interesting object for inves-
tigating thermophysical properties in this temperature range.
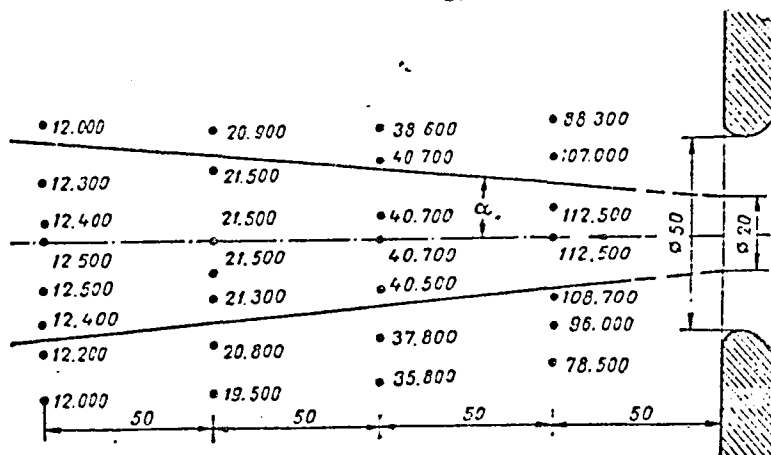
Fig. 57   Field of fluxes in variant I furnace

Applied in the equipment is amorphous silica--quartz glass
or fused quartz, exhibiting nearly the same small coefficient
of thermal expansion ($0.42 \cdot 10^{-6}$ deg^{-1}) and melting at 1620° C.

Molten silica boils only at 2590° C, but even after
1600° C the vaporization rate increases markedly with increase
in temperature.

Even from the solid state at 1600° C, sublimation occurs
so rapidly that the heating element can withstand only 3-5 h.
Heaters operated in the 1400-1550° C range for more 300 h each,
and the number of switchings exceeded 100.

Audible crazing of the graphite coating can be heard   /116
during cooling after disconnection (in the 900-800° C range).
Even when there are subsequent reconnections, the heater tem-
perature exceeds 1400° C, evidently there is "healing" of the
cracks in the solid state and the heater can function for long
periods. The heater crack can be explained by the partial or
full conversion of tridymite to quartz, accompanied by a large
change in density.

The reflecting insulation was packed in a furnace constructed under variant II, and the port hole was covered with quartz glass (Fig. 58). The internal furnace volume was filled with argon. When this was done there was no need for special processing of the heaters and the heater temperature could be substantially raised.

This kind of furnace was designed for fluxes greater than 1000 kW/m^2, but it was not brought to the design power rating because the packing burned up in the quartz window. The power rating of the resulting fluxes exceeded 500 kW/m^2.

To grow monocrystals of refractory oxides and to heat-treat them, a radiative furnace with thermally transparent cooled partitions was built; molten corundum (2050° C) /72/ was melted in an oxygen atmosphere. From calculations confirmed by experiments with a small model, it follows that in the case when the dimensions of these furnaces were increased, the temperature at which objects were heated in corrosive media (O_2, HCl, and HF) can be brought to 2600° C.

Fig. 58 Low-inertia furnace (variant II):

1. quartz window
2. sleeve for gas cooling of window
3. heater
4. front wall
5. cooling connection
6. spherical reflector
7. clamp-current conductor
8. cover
9. installation plate

In developing heavy-duty radiators, the designers often start from the false assumption that with a reflector a beam of rays can be formed whose flux density depends only slightly on the distance between the radiating system and the receiving body. So an erroneous view took form, to the effect that the density of the incident flux can be increased by moving away the radiators with the reflectors and increasing their number. The erroneousness of this approach could be easily deduced from the Manzhen-Chikolev formula: the density of a flux incident at the optical image of a source is inversely proportional to the square of its distance /117 tance from the lens or mirror.

The surface of the tungsten spiral radiates a flux with a density of about $2 \cdot 10^6$ W/m^2; the laws of geometrical optics provide the opportunity of acquiring up to 30 percent of this flux in the image. Evidently in practice a little more than 10 percent of the source flux density, to which 200 kW/m^2 corresponds, can be obtained in the image.

Black plasma in xenon lamps developed by the Moscow Plant of Electrovacuum Instruments has a temperature of as high as 6000° K. As to spectral composition, the radiation of these lamps is close to solar composition. The density of radiation from the surface of the plasma in these lamps can extend to $80 \cdot 10^6$ W/m^2; this makes possible a flux density of up to $10 \cdot 10^6$ W/m^2 in optical systems with high luminosity.

Interestingly, flux density was as high as $50 \cdot 10^3$ W/m^2 /208/ in an instrument built in 1747 by Buffon; in it, solar reflected light spots from 168 mirrors each 150x200 mm^2 in size were directed at a target 47 m away.

So using standard incandescent radiators, in commercial series-manufacture, uniform stable fluxes can be obtained whose density is smoothly regulated in the range from 0 to 200 kW/m^2. Flux densities to 500-1000 kW/m^2 can be obtained in specially developed incandescent units. The densities of the incident fluxes in the compact plasma images, in the natural state (the Sun) or the artificially obtained state can be increased by one order of magnitude.

3, Compensation Type Radiometers

In radiometer development the concept of building Angstrom compensation type radiometers was utilized (see Section 9, Chapter 1). The first radiometer design (1957) was calculated for measuring fluxes to 20 kW/m^2 /51/. Measuring plates, made of 40x10x0.05 mm^3 manganin strips, were mounted on copper forks; through their teeth direct current was supplied from a storage battery. The power was regulated with a double rheostat.

Together with the forks, the plates were secured in a massive copper block so that their facing blackened surfaces projected from the port holes, facing in opposite directions. In this way, when one of the plates was heated with the radiation flux being measured, the second was in shadow. The plates and the block were cooled through free convection.

To measure fluxes with a power rating to 300 kW/m^2, in 1961 a radiometer design was developed that was based on forced

cooling of the working plates /55, 57, 71/ (Fig. 59). Nichrome
plates 1 are the sensitive elements of the head of the compensation radiometer; the plate edges are secured in current-conducting buses 2. Heat arriving at the plates as radiative or electrical energy is removed from the internal plate surfaces by forced convection of air. The air is fed by a compressor into the channel formed by the buses, with a head of about 10^4 N/m²; corresponding to this value is a theoretical flow rate of up to 120 m/s. The real air flow rate in the narrowest place reaches 100 m/s at the working plate level. The junctions of differential thermocouple 3 are attached in the middle of each plate; thermal conditions are monitored as to identical values by the thermocouple.

A longitudinal cross-section of this radiometer is shown in Fig. 60. Buses 2 in the upper part of the head form a square channel, gradually intergrading into a round channel in its lower area. This bus configuration is due to the fact that when the radiometer operates, the places of the irradiated and shadowed plates must be interchanged--this is easily done by turning the head about the axis of symmetry with handle 4. The internal dimensions of the square channel in the upper part of the head are 22x22 mm². Externally, the buses are polished and gilded to reduce heating from absorbed radiation. The buses are separated along the channel generatrix by 0.5 mm thick mica insulating lining.

Cut into the buses in the upper part of the radiometer
head are windows for 16x8x0.2 mm³ radiometer plates. The plate ends are inserted into grooves cut into the buses and are carefully soldered in. Since excess solder on the plates can make the boundary conditions nonidentical, the excess is carefully removed--mechanically at first, and then by electrolytical dissolution. The external sides of the plates are coated with lampblack. In the lower part of the radiometer head the copper buses are clamped between cylindrical ebonite and steel bushings 3, 5, and 7. When assembled, the buses and the bushings form a unified system that can be rotated about the axis of symmetry. Ball detent 8 immobilizes the rotary system in three positions differing by a quarter-turn. Screw 6 prevents longitudinal displacements and limits the rotation about the axis to no more than half a turn.

The radiometer plate is the most critical element of the instrument. That is why all the design dimensions of plate and all associated are selected from a thorough analysis and variant calculations.
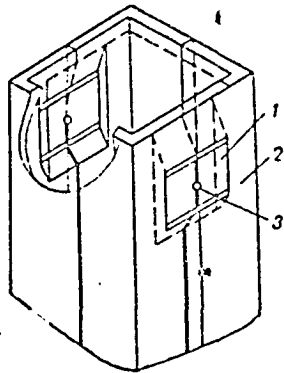
Fig. 59 Head of compensa-
tion radiometer:

1. working plate
2. bus
3. thermocouple junction
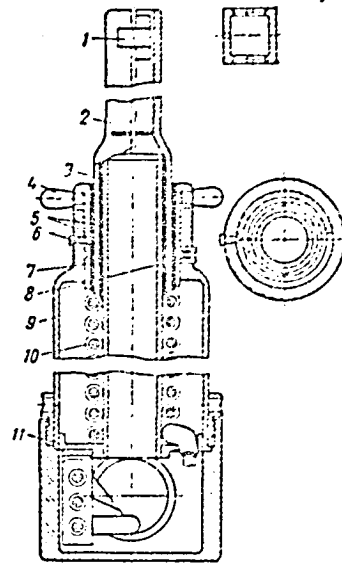
Fig. 60 Longitudinal cross-
section of compensation radio-
meter:

1. working plate
2. buses
3. internal bushing
4. handle
5. insulating bushing
6. set screw
7. external bushing
8. detent
9. support
10. power supply conductor
11. centering disk

In painstaking fabrication, nonidentity in energy supply
conditions can be the only source of error in the method.

The working plate is heated with radiative flux through
the lampblack coating, and the compensation plate—by electric
current throughout its volume. Heat is removed, mostly, from
the internal swept side. And the heat flux of the working
plate overcomes the thermal resistance of the lampblack coating,

the plates proper, and the heat transfer from the swept surface. But the flux of the compensation plate overcomes only about half the plate resistance and all the resistance to heat transfer.

For the plate operating conditions to be made sufficiently identical, the thermal resistance of the lampblack coating and the plates proper must be small compared with the resistance to heat transfer.

With maximum flow sweeping the plates, the measured heat transfer coefficient on the internal plate side was 780 $W/m^2 \cdot deg$. The true value must be somewhat smaller, since part of the heat is removed by thermal conductivity into the supporting buses.

When the conditions are identical, the ratio of the total thermal resistances of both plates must differ only slightly from unity:

/δ.p = blackened plate/

$$\frac{\frac{\delta_{b.p}}{\lambda_{b.p}} + \frac{\delta}{\lambda} + \frac{1}{\alpha_2}}{\frac{1}{2}\frac{\delta}{\lambda} + \frac{1}{\alpha_2}} = 1 \div \Delta \qquad (IV.1)$$

The coating blackness no longer changes when $\delta_{b.p} \geq 8$ μm.

If $\delta_{b.p} < 4$ μm, the coating proves to be heat-transparent /120 to some extent, and the amount of radiative energy absorbed begins to depend on thickness. The thermal conductivity of the coating $\lambda_{b.p}$ can be 1 W/m·deg. For a nichrome plate $\delta_{b.p} =$ = 0.2 mm and λ = 20 W/m·deg. The coefficient of nonidentity Δ in Eq. (IV.1) is 1 percent.

In actinometric Angstrom compensation instruments, heat transfer occurs by free convection and its thermal resistance is two orders of magnitude larger.

Deviations lead to violated symmetry are inescapable in parts fabrication and instrument assembly. So the design elements of the instrument are best selected to that the effect of the errors tolerated on measurements is small.

The possible nonidenticalness of the embedding of the working plate ends can lead to a fictitious balance in measurements. The plate dimensions must be selected so that the effect of end embeddings on the middle-area temperature is not appreciable. The plate is a uniformly heated rod with heat removed

130

from the surface by convection and in the mounting area--by
thermal conductivity. The thermal conductivity equation
for this case has the following form:

$$\frac{d}{dx}\left(\delta \lambda \frac{dt}{dx}\right) \div W - a_2 t = 0 \qquad (IV.2)$$

where W is the power supplied per unit rod area; the temperature
t is read off from the cooling air temperature.

The boundary conditions at the mounting areas when x = 0
and x = ℓ and in the middle of the plate, when x = $\ell/2$ will be,
respectively, as follows:

$$t = 0$$

$$\frac{dt}{dx} = 0 \qquad (IV.3)$$

If we neglect the effect of the temperature on the coef-
ficient of thermal conductivity, Eq. (IV.2) can be reduced to
the following dimensionless form:

$$\frac{d^2 \vartheta}{dx^2} - k^2 (\vartheta - 1) = 0, \qquad (IV.4)$$

where

$$\vartheta = \frac{t a_2}{W}; \quad \varkappa = \frac{x}{l}; \quad k^2 = \frac{\alpha_2 l^2}{\lambda \delta}$$

and the boundary conditions are as follows:

when $\varkappa$ = 0 and $\varkappa$ = 1, ϑ = 0

when $\varkappa$ = 1/2, $d\vartheta/d\varkappa$ = 0 $\qquad (IV.5)$

Given conditions (IV.5), the general solution to Eq. (IV.4)
has the form

$$1 - \vartheta = \frac{e^{k\varkappa}}{1 + e^k} \div \frac{e^{-k\varkappa}}{1 + e^{-k}} \qquad (IV.6)$$

For the middle of the plate where the differential thermo-
couple heads are attached, $\varkappa$ = 1/2 and Eq. (IV.6) takes on the
form:

$$\vartheta_m = 1 - \operatorname{sch} \frac{k}{2} \qquad (IV.7)$$

131

In order for the end embeddings of the plates not to more than slightly affect the temperature in the plate middle, k must be large enough--this can be seen from Eq. (IV.7). If, for example, $1 - \partial_m = 0.03$, the strongest perturbation on one end of the plate or at both its ends leads to no more than a 3 percent temperature change at the middle of the plate. Corresponding to this is k = 7, selected as the base in determining the design dimensions of the radiometer described.

The actual embedding conditions can differ only slightly from the ideal conditions, therefore the expected deviation must be much smaller than this figure (3 percent).

The nonidenticalness of the mounting of the differential thermocouple heads on the working plates can also be a source of error. The thermocouples are fabricated of chromel and alumel wires, 0.15 mm in diameter. Welding is conducted in a crucible filled with graphite powder, according to the technology that is fairly widely described in a number of publications (for example, /66/). After annealing, the junction locations are cleaned and the thermoelectrodes are drawn out so that one of them is a direct extension of the other. Then the junction location is rolled out on rolls or pulled apart to a thickness of 0.03 mm.

The resulting strip is lined with 10 µm mica wafers and is cemented to the surface of the radiometer working plate. And the total resistance to the passage of heat from the plate to the thermocouple junction does not exceed 5 percent of the resistance of the subsequent passage in heat transfer to the cooling flow.

To reduce heat outflow through the thermoelectrodes they must be arranged along an isothermal line, that is, across the plates. Nonetheless, since the transverse plate dimension is limited, the heat outflow can occur and the problem consists of finding the dimensions of the thermoelectrodes; here their effect will not outreach the allowable limits.   /122

When the thermal conductivity equation is set up for a thermoelectrode, we must allow for the inflow of heat through the electrical insulation between the plate and the electrode, and also the transfer of heat to the sweeping air. In an approximate evaluation, the problem must be viewed as a one-dimensional problem and the temperatures of the cooling air t_2 and of the plate at which the thermoelectrode is cemented t_1 must be assumed as constant. We can also neglect the dependence of the thermal conductivity of the thermoelectrode on temperature.

In this case the dimensionless equation of thermal conductivity for the thermoelectrode becomes

$$\frac{d^2\vartheta}{dx^2} - k_1^2\vartheta = -k_2$$

Here $\vartheta = \dfrac{t}{t_1}$ is the instantaneous temperature of the

thermoelectrode in the cross-section with coordinate κ , related to the plate temperature t_1 = const; all temperatures are read off from the cooling air temperature, that is, $t_2 = 0, \kappa = x\lambda$;

$$k_1^2 = \frac{(\alpha_1 + \alpha_2)l^2}{\delta\lambda}; \quad k_2 = \frac{\alpha_1 l^2}{\delta\lambda}$$

where α_1 is the conditional coefficient of heat transfer from plate to thermoelectrode; α_2 is the coefficient of heat transfer from electrode to cooling air; and l is plate width.

This equation is identical to the earlier-solved Eqs. (II.11) and (IV.4). With the right-hand side kept constant, it corresponds to the case presented in section 2 of Chapter 2. As Fig. 33 makes clear, when $k_1 > 7$, the edge perturbations practically speaking do not yet reach the plate middle (κ = 1/2; $k_1\kappa$ = 3.5).

The measured heat transfer coefficient α is 780 $W/m^2\cdot$deg on the radiometer plate. Corresponding to this value, given the condition of suppression of perturbations, is the thermoelectrode thickness $\delta \leq$ 0.07 mm.

When the instruments are assembled, attention must be given to the identicalness of the measuring arms; this identicalness is monitored in experiments with simultaneous electrical heating of both plates. Here the error of the measurements must be of the same order as in the Angstrom pyrheliometers, that is, must not exceed 1 percent of the measured value.

The blackened surface of the receiving plate does not receive all the energy of the incident flux. The blackness of the coating determined with an error of 1-2 percent is 0.93-0.95, which must be taken into account in absolute measurements. But in relative measurements, when the receiving plates of the radiometer and the calibrated transducers are coated with identical blackness, the latter situation is not significant.

The radiometer is powered from line current through a stabilizer, a system of regulating autotransformers, and a selenium rectifier in the six-phase rectification scheme.
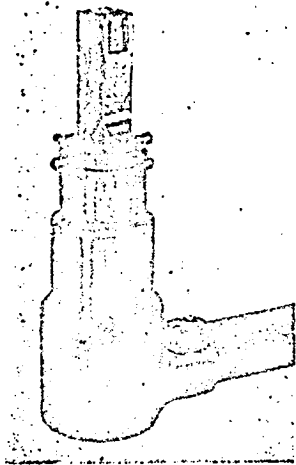
Fig. 61 General view
of radiometer
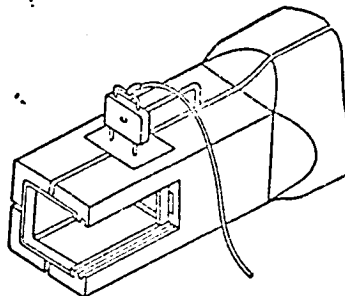
Fig. 62 Head of radiometer
with small yokes for monitoring
voltage drop

The strength of the current flowing through the plates is measured with calibrated shunts. Somewhat more complex is the situation in _determining the specific voltage drop, dependent in the case of nichrome also on temperature. In the more heated central part of the plate the density of release of electric power is greater than along the edges. So the voltage drop is measured along a short section in the middle, nearly isothermal part of the plate using special small yokes with a base of about 4 mm. The distance between the needles is determined to within 0.01 mm with a microscope with a micrometer stage.

The external appearance of the radiometer described, installed on a coordinate spacer around a radiation furnace, is shown in Fig. 61. The head of a radiometer with small yokes installed on it for monitoring the voltage drop is shown in Fig. 62.

Finally, after installation the identicalness of the radiometer plates is verified in the self-calibration mode, when both plates are heated only by electric current. Self-calibration calls for independent systems of power supply and measurement for each plate. Assuming careful execution, the deviation between the flux densities at the plates in

in the self-calibration mode does not exceed 1 percent in the balanced state. Interestingly enough, the power difference /124 between plates with increasing power changes sign several times.

One face of the radiometer head has a recess for a case housing the transducer under calibration.

4. Inertial Radiometers

In inertial radiometers, a massive copper cylinder one of whose faces is subjected to irradiation is the main element for measuring high-density fluxes /53/. All the remaining surfaces are thermally insulated (Figs. 63 and 64). Six 0.15 mm diameter chromel-alumel thermocouples·are embedded into a block for determining the temperature trend. One junction is at a depth equal to $1/3^{1/2}$ of the cylinder height. With constant density of the received flux, the temperature trend at this point coincides with the temperature that is mean-integrated over the block /150/. The block temperature trend is recorded with an electronic recording potentiometer.

The lateral surface and the rear block face are carefully polished and chrome-plated. When possible, they must be gilded. The gilding cost is modest, and the quality of insulation and stability of the insulation properties in this instance show marked improvement.

Around the block is fitted an aluminum "jigger" with a 1 mm gap. The diameter of the receiving area of the block is chosen as equal to the diameter of the radiator port. Because of this, the lateral surfaces of the "jigger" are blocked against radiation. The internal and external surfaces of the "jigger" are polished. The "jigger" is mounted in the center of a supporting ring with six 0.2 mm diameter steel cords. The copper block rests on sharp needles mounted in the bottom of the "jigger" and stretched on three cords. The electrodes of the thermocouples extend through a drilled opening in the stem of the "jigger."

The mass of the block M is determined by weighing it before installation, and the heat capacity c--from tables /6, 11, 12/.

Heat losses after the curve of the block temperature trend during the exposure has been recorded are determined by recording the temperature trend during cooling t_{co}, with all the other conditions kept the same as they were during the exposure period. The flux is determined by the formula

$$q = \frac{Mc}{f}\left(\frac{dt_{ex}}{d\tau} - \frac{dt_{co}}{d\tau}\right)$$

(IV.8)

in which the values of the derivatives are taken at identical temperatures $t_{ex} = t_{co}$ by the graphical differentiation of the recorder traces or with special equipment /235/.

For a comparison of the inertial radiometer with the compensation radiometer, it was placed on the coordinate spacer of the latter in such a way that by a simple rotation the radiometers can be made to change places in 1 s. The receiving surfaces of both instruments were simultaneously coated with lampblack of the identical composition. The discrepancy did not exceed 2 percent in measurements at high flux values. For fluxes weaker than 20 kW/m², the discrepancy reached 5 percent and was caused mainly by the error in the inertial instrument: differentiation of the experimental data always leads to a considerable increase in error.
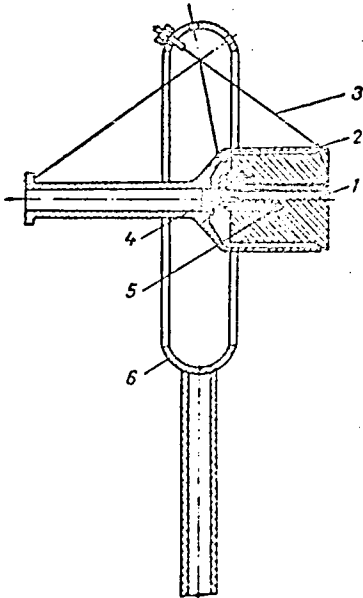
Fig. 63 Inertial radiometer:
1. block
2. protective "jigger"
3. cords
4. needles
5. thermocouples
6. supporting ring

Fig. 64 General view of inertial radiometer

136

Fluxes to 300 kW/m^2 were measured with the inertial radio-
meter; there was the full option of measuring the fluxes whose
power ratings exceeded the values named. A number of altera-
tions is needed to measure fluxes stronger than 600 kW/m^2.

A similar radiometer with a relative small mass of the
receiving body /84/ was developed for measuring fluxes to
2 kW/m^2.

5. Absolute Compensation Radiometers with Energy Substitution /126

Low sensitivity of the differential thermocouple is a short-
coming of radiometers built as per the Angstrom arrangement.
F. Ye. Voloshin /178/ increased the number of junctions to four,
slightly raising thermocouple sensitivity.
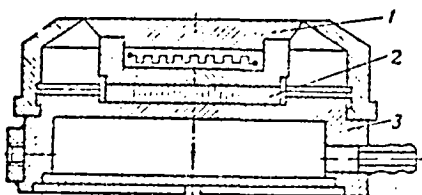
Fig. 65   Absolute radiometer
    with energy substitution:

1. radiation receiver
2. sandwich transducer
3. cooled housing

A cardinal improvement was
achieved by using as the sensi-
tive elements sandwich-type heat
flux transducers in which the
number of junction pairs is
greater, by three orders, than
the values given above. A dia-
gram of this instrument is
shown in Fig. 65 /74/.

The radiation receiver was
made of material with high ther-
mal conductivity (copper) and
was mounted on the cooled hous-
ing so that the energy absorbed
inevitably passed through the
transducer.

Thermal resistance to removal of absorbed heat at the trans-
ducer was two orders of magnitude higher than for the receiving
body. So it was a matter of practical indifference in what part
of the receiving body the measured energy was directed--a fact
permitting mutual substitution of the absorbed radiative energy
by the energy of the electrical heater. The primary concept
and the design execution of the instrument belong to V. G. Kar-
penko.

Mounted in the receiving body was a heater; it power can be
measured with high accuracy customary for electrical measurements.
The gap between the receiving body and the shielding blind was
approximately 0.3 mm. In order for the radiation flux penetra-
ting this gap (its area extends to 2 percent of the receiving
area) to by-pass the body, its surface was polished and gilded,

137

and the remaining surfaces of the cavity under the blind were covered with lampblack. By this the leakage of heat to the receiving body through the gap evidently does not exceed 2 percent of the quantity measured.

The diameter of the receiving surface was measured three times with a micrometer at $60°$ angles; its area was determined by the arithmetic mean. The housing and the blind were also of copper; their external surfaces were polished to reduce absorption. Since the housing was cooled with water at the ambient air temperature, the errors introduced by convection and background radiation can be reduced to a minimum.

These radiometers are made in two modifications: one with /127 a plane receiving surface, and the second--with a geared V-shaped surface.

The experimentally confirmed Psarouthakis function exists between the absorption coefficients of the plane (a_p) and the V-shaped geared (a_g) surfaces /309/:

$$a_g = \left[1 + \left(\frac{1}{a_p} - 1\right)\sin\frac{\vartheta}{2}\right]^{-1}$$ (IV.9)

where ϑ is the angle between the gear tooth sides.

The working coefficients of the geared and plane radiometers when they are used in measuring the incident radiation flux q_p will be

$$k_g = \frac{q_{c}a_g}{e_g}$$ (IV.10)

$$k_p = \frac{q_p a_p}{e_p}$$ (IV.11)

and their values with an error not exceeding 1 percent are determined in experiments when the absorbing body receives energy from the built-in electrical heater.

By dividing Eq. (IV.10) and Eq. (IV.11), we find that

$$\frac{q_g}{q_p} = \frac{k_g a_g}{k_p a_p}$$ (IV.12)

By jointly solving Eqs. (IV.9) and (IV.12), we get

138

$$a = \frac{1 - \frac{k_{BB}\varepsilon_{BB}}{k_p \varepsilon_p} \sin \frac{\vartheta}{2}}{1 - \sin \frac{\vartheta}{2}} \qquad (IV.13)$$

$$a_p = \frac{\frac{k_p \varepsilon_p}{k_{BB}\varepsilon_{BB}} - \sin \frac{\vartheta}{2}}{1 - \sin \frac{\vartheta}{2}}$$

So by exposing the plane and the geared radiometers, with identical coating of the receiving surfaces, to the same incident flux, we can determine their absorptivity and the magnitude of the incident flux. For blackened coatings, the value of the effective extent of absorption approaches unity so closely that the receiving surface of the geared radiometer can be assumed to be a satisfactory model of an absolute blackbody /132, 133/.

When the surface was covered with lampblack paint with an absorption a_p = 0.95, the geared surface absorbed more than 99 percent of the incident energy. A 1 percent error can be either allowed for, or neglected, assuming that the geared surface receives all the incident flux. /128

Measured with the plane radiometer was the received flux, which permits calculating the absorption of paint and varnish coatings and foil and film materials by depositing them on the receiving surface /87/.

To verify this type of absolute instruments, in 1968 at the biev Geophysical Laboratory tests were conducted in which the results of simultaneous measurements of solar activity were compared with the substitution radiometer described and a reference standard Angstrom pyrheliometer. The radiometer always showed a larger value of the measured flux than did the pyrheliometer; the difference between the values did not exceed 1 percent.

6. Radiation Calibration Method

The main task of the method is to provide the conditions under which the calibrating flux wholly traverses the transducer. To do this, the receiving side of each transducer must be covered with the same lampblack as was used in blackening the reference standard radiometer. At the Zagorsk Opticomechanical Plant, for example, the following lampblack formulation ("blackbody grade") is used: office silicate cement (90 g) is mixed with carefully screened, dried lampblack (10 g).

The heat absorbed must be removed so that not less than 99 percent of the heat flux penetrated the transducer.

During calibration in a compensation radiometer (see Section 3 of this chapter), the transducer is molded into a porcelain plate; the plate thickness is equal to the transducer thickness. The transducer is pressed against the dry gypsum mold and porcelain slip is allowed to pour over the mold. Before the pouring commences, around the transducer is fitted with a tweezers a small loop of gauze thread (lint) so that the plate does not craze during drying and shrinkage. A thickened welt is provided in the upper part, at the place where the transducer leads exit into the plate: for compensation of the weakening of strength using the transducer conductors and for convenience in manipulation during calibration.

Gypsum molds differ as to their mechanical model. Finished porcelain plates are made with a tolerance of about 0.2 mm; this gives them tight fitting in the window on the blank face of the radiometer head. The transducer is placed at the same height as the working and the compensation plates of the radiometer.

Using the radiometer coordinate spacer, the head can be positioned at ten fixed points spaced 50 mm apart opposite the port hole of the radiation source. By rotating the head around its own axis for 1 s, exposures can be changed for the plates of the radiometer and of the transducer under calibration. On the /129 inner side the transducer is open to a cooling air flow, just like the radiometer plates.

When calibrating is done with a plane radiometer, the painted transducer is rubbed with vacuum grease (Ramsay type) against the surface of a copper condenser similar in design to the radiometer housing and cooled with water at a temperature equal to the cooling air temperature.

The electrical signal of the transducer in all cases is recorded with a potentiometer. The working coefficients are defined as the ratio of the calibrating flux to the emf generated by the transducer.

A general view of the unit for radiation calibration is shown in Fig. 66.

All the units described showed good mutual agreement of results.
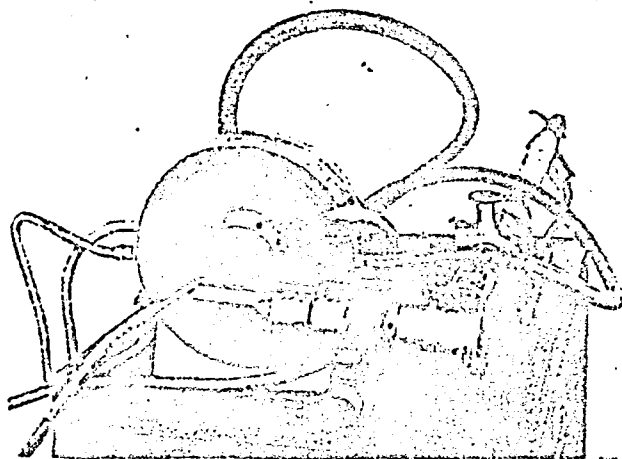
Fig. 66 Stand for radiation cali-
        bration

CHAPTER 5

CALIBRATION MEASUREMENTS OF CONDUCTIVE FLUXES AT LOW AND MODERATE TEMPERATURES ($\pm 200^\circ$ C)

Among the various systems for calibrating heat flux transducers, next most promising after radiation type transducers are the conductive transducers. The above-described absolute calibration instruments have shortcomings that are eliminated to some extent in the corductive transducers. Specifically, fluxes that have densities stronger than 150 kW/m^2 are more easily generated and more easily monitored.

An independent variation of fluxes and working temperatures is also more easily executed in this case. Combining different independent calibration methods makes measurements more trustworthy. This is particularly important because in heat measurements it is extremely hard to fully allow for all causes of error.

To generate a calibration conductive flux, three groups of instruments were developed: in one group the electrical heater, made of a good heat conductor, is pressed against the transducer under calibration and on all the other sides is surrounded with insulation provided with compensatory heating. The losses can be reduced to a negligibly small value.

In the second group of instruments it was possible to achieve a replacement of the measured energy with electric energy amenable to more exact monitoring.

Classed with the third group is an instrument that is a combination of two electrical substitution systems assembled

142

in a differential scheme, and the transducer under calibration
is positioned at the interface of the systems.

1. Electrical Calorimeters with Compensatory Insulation

A schematic diagram of this calorimeter is shown in Fig. 67.
The heat flux transducer to be calibrated is placed between the
heat source core and a condenser. In the steady-state heat
regime, the power directed to the core must be fully (without   /131
losses) removed through the transducer to the condenser. To
prevent heat losses, the copper block 5, performing the func-
tions of an adiabatic shell, is kept at the central heater tem-
perature. The temperature of block 5 is regulated automatically
with a thermoregulator of an EPD-12 electronic potentiometer.
Serving as the null indicator monitoring the absence of heat
losses and generating a command signal to the potentiometer is
the sensitive element of a series-manufactured sandwich-type
transducer-calorimeter (see Chapter 3).

The element is heated to 120° C, deformed on a cylindrical
mandrel, and after cooled it is placed in the circular gap be-
tween blocks 1 and 5. The large number of thermojunctions in
the indicator-calorimeter helps keep the temperature drop be-
tween the central and the protective blocks at approximately
0.01 deg. And the heat losses (positive or negative) do not
exceed 0.1-0.2 percent of the power fed to the central core.

The contact surfaces of the core and the condensers have
dimensions corresponding to the working planes of the trans-
ducer. During calibration, special attention must be given to
the quality of machining and assembly of the contiguous sur-
faces, since distortion of the heat flux field with contact
energy supply can lead to calibration errors. In addition,
the quality of contact affects also the thermal inertia of the
system.

The time constant of the calorimeter for 10x10x1 mm^3 trans-
ducers usually does not exceed 200 s when calibration relies on
a copper condenser.

During calibration, the transducer temperature is assumed
to be equal to the arithmetic mean of the readings of the thermo-
couples placed in the core of the heater and the condenser near
the surfaces abutting the transducer.

Calorimeters with compensation insulation were used in both
calibrating individual transducers and calibrating transducers
embedded in products /83/. A typical characteristic of one   /132
transducer recorded with this calorimeter is given in Fig. 58.
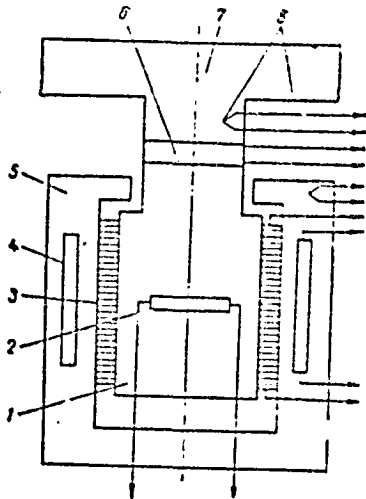
Fig. 67 Calorimeter with compensatory insulation:
1. core
2. heating element
3. indicator-calorimeter
4, 5. protective block containing heater
6. calibrated transducer
7. condenser
8. thermocouples

Fig. 69 Miniature calorimeter for calibrating sandwich-type transducers:
Key: 1. protecting housing
2. compensatory heater
3. indicator-calorimeter
4,6. elements of central heater housing
5. central heater
6. calibrated transducer
8. condenser

Fig. 68 Typical calibration characteristic of self-contained transducer recorded with a unit that has compensatory insulation

Key: a. e, microvolts
b. watts/meter^2

A compensatory calorimeter similar in layout, but differently designed, developed for calibrating high-sensitivity banked heat flux transducers, is shown in Fig. 69. Typical of this instrumental design is the alternation of materials with high and low thermal conductivity.

Much of the gap between the heat-protective housing and the central heating housing is filled with an indicator-calorimeter in the form of a series-manufactured sandwich-type heat flux transducer.

The compensatory heater is assembled from two windings; the power of one is hand-set during heater adjustment to compensate for scattering power losses, with a slight understatement. But the second heating coil is

144

energized with allowances from an automatic control system
that maintains the signal strength of the indicator-calori-
meter at about zero. The temperature is regulated with a
standard EPD-12 electronic potentiometer. The operating con-
ditions are selected so that the energy of the positive fluxes
passing through the indicator is equal to the energy of the
negative fluxes, and the amplitude of the power loss, alter-
nating with the influxes, did not exceed 5 percent of the
central heater power. Since the identicalness of the influxes
and the losses is monitored with an accuracy no worse than
10 percent, we can expect that in the system the unaccounted-
for loss will not exceed 0.5 percent.

A large part of the errors comes from the nonuniformi-
ties of local flux densities in the calibrated transducer.
So in repeated calibrations with repositioning of the trans-
ducer, a discrepancy in results was recorded, as much as 1.4
percent.

The calibrated banked transducer, just like the case of
the calorimeter for self-contained transducers, is placed be-
tween the central heater housing and the condenser.

Simplicity and independence of readings from boundary con-
ditions, especially for large heat fluxes penetrating the trans-
ducer, is an advantage of electrical calorimeters with compen-
satory insulation. In some sense, this type of calorimeter is
an absolute type, does not need calibration, and can be used
successfully for calibrating not only high-sensitivity banked,
but also low-sensitivity self-contained transducers.

The calibration temperature can be easily varied in com-
pensatory calorimeters; the upper temperature limit goes up to
350-400° C, thanks to the thermal resistance and heat stability
of the parts.

To determine the change in the transducer coefficients
when the temperature changes in the -180 to 100° C range, this
calorimeter is placed on a metal rod-condenser, then put into
a Dewar flask filled with liquid nitrogen. As the nitrogen
boils, the thermal resistance of the rod-condenser increases
and the calibration temperature rises. After all the nitrogen
has vaporized, calibration continues in the monotonic heating
regime. Heat accumulated in the transducer body and the cen-
tral heater is taken into account from the rate of temperature
rise.

For calibrations in the 0 to 100° C range no changes were
detected in the values of the sandwich-type transducer

145

coefficients. When the temperature goes up, and especially when it goes down beyond the indicated limits, a marked rise in the values of the working coefficients was observed.

2. Contact Type Thermoelectric Calorimeters with Substitution

For low-temperature contact calibration of transducers a series of thermoelectric calorimeters was developed; in operating principle these calorimeters are analogous to the absolute compensatory calorimeter described in Section 5 of Chapter 4 (Fig. 70).

The dimensions of the receiver and the thermopile of element 5 were selected with consideration of the required sensitivity and inertia of the calorimeter. The calorimeter body is conveniently cooled with water at the ambient temperature. The /134 thermal resistance to heat flux through the sensitive element is two or three orders of magnitude less than the thermal resistance to heat transfer by free convection. So when there are small differences between the ambient temperature and the cooling water temperature, heat losses can be neglected.
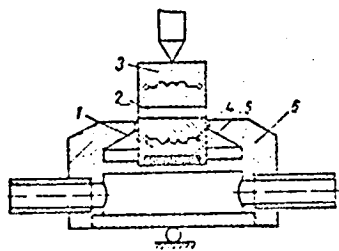
Fig. 70. Contact calibrated
substitution unit:

1. receiving body
2. calibrated transducer
3. heat source
4. substitution heater
5. sensitive element
6. condenser housing
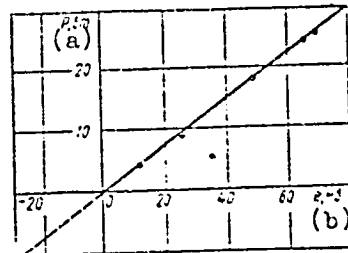
Fig. 71 Calibration charac-
teristic of substitution
calorimeter

Key:
   a. watts
   b. millivolts

For calorimeter calibration, the signal of the sensitive element was plotted as a function of the power of the heater of the heat flux receiver in steady-stage regimes. Heater 3

146

operated at low power levels; this made it possible to record a zero signal in the transducer under calibration in each regime. A typical low-temperature calibration characteristic is given in Fig. 71.

The measurement data were plotted along a line extending through the origin of coordinates, with a scatter no greater than 0.5 percent. Thus, the unambiguous dependence of the signal of the sensitive element on the power supplied the receiver was established.

When the thermal conductivity of the receiving body was large, the sensitive element of the calorimeter reacts the same to energy coming from the substitution heater, or to the energy passing through the transducer under calibration. This makes it possible from the plotted characteristic to determine the value of the flow penetrating the transducer under calibration in the following cases.

1. When the substitution heater was disconnected, all the flux recorded by the signal of the sensitive element flowed through the transducer under calibration and was calculated from the earlier-plotted characteristic located in the first quadrant.

2. When the heater was replaced with a condenser, the sig- /135 nals of the calibrated transducer and the sensitive element of the calorimeter changed sign; the flux passing through the transducer was determined from the extrapolated extension of the characteristic in the third quadrant.
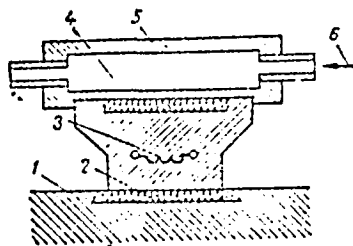
Fig. 72 Arrangement of elements when transducers secured to product were calibrated:

1. product
2. calibrated transducer
3. calorimeter heater
4. substitution heater
5. sensitive element
6. condenser housing

3. In both the cases above it can be found convenient to direct to the substitution heater some positive power; its value must be substracted from the value corresponding to the signal of the sensitive element found from the characteristic or its extension in the third quadrant. Other variants are not of practical interest.

In the third case, the calorimeter operates in the regime of excess simultaneous substitution and, thus, serves as a calibrated source of additional thermal energy.

147

These units have been used a number of times in calibrating self-contained and banked transducers directly attached to products (Fig. 72).

3. Twin Calorimeters

Based on the above-presented first and third regime variants, a twin thermoelectric calorimeter was constructed; it was developed for contact calibration of transducers at temperatures to 400° C. Essentially it comprises two substitution calorimeters; one operates in the source mode, and the other-- as a receiver of the energy penetrating the transducer undergoing calibration (Fig. 73).

To extend the temperature range of calibrations between the core 4 and sensitive element 2, a lining 3 was placed; it had a relatively high thermal resistance and was made of heat-resistant concrete.

The field of heat fluxes in the interval between calibrated transducer 2 and sensitive element 4 (see Fig. 72) changed considerably in the self-contained calorimeter when there was a transition from the substitution regime to the calibration regime.

Since the thermal conductivity of the receiving body is limited, confirming that the heat fields were completely identical in these regimes beyond the receiving body was difficult, in particular, the calibrated transducer 2 and sensitive element 4. This nonidenticality must be manifested most strongly when the calorimeter is converted from the sink mode to the source mode.

The imperfection of each of two constituent calori- /136
meters can be experimentally determined with a twin calorimeter. When there were substantial internal resistances during measurements of a flux identical in value in the source and sink modes, the calorimeter readings must differ from each other. This difference in all the measurements made did not exceed the scatter of points from the calibration curve.

Calibration can be conducted with both calorimeters, but usually only one is used after conversion to a different mode has been confirmed.

The calibration characteristic shown in Fig. 74 differs from a straight line. This is due to the rise in the receiving body temperature with increase in power transferred through lining 3 (see Fig. 73) and, therefore, with an increase in radiative losses.
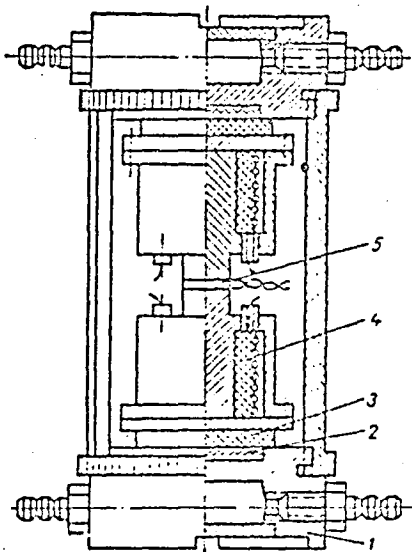
Fig. 73   Twin thermoelectric
          calorimeter:

1. condenser
2. sensitive element
3. lining
4. core with heater
5. transducer being calibrated
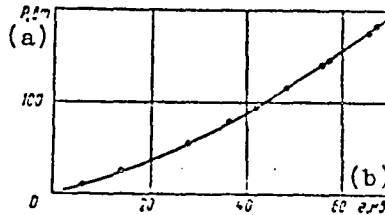
Fig. 74   Calibration charac-
          teristic of twin calorimeter

Key:
  a. watts
  b. millivolts

The density of the heat flux penetrating the transducer
that is being calibrated is defined as the difference between
the total heat from the receiver P_0 recorded by the sensitive
element and the heat release of the built-in heater P_b, per
transducer area:

$$q = \frac{P_0 - P_b}{f_t} \qquad (V.1)$$

The quantity P_0 is found from the calibration character-
istic (see Fig. 74), and P_b--from the readings of a wattmeter
incorporated in the heater circuit.

149

Chromel-alumel thermocouples were calked into the receiving bodies of the upper and lower calorimeters for measuring the calorimeter temperatures. The transducer temperature was assumed equal to the arithmetic mean of the receiving body temperatures of the upper and lower calorimeters.

Self-contained copper-constantan heat flux transducers were calibrated using the above-described unit in an air atmosphere at temperatures to 300° C. At higher temperatures, intensive oxidation of copper was observed and the transducers broke down rapidly.

Later an attempt was made to calibrate with the twin calorimeters at more elevated temperatures in a protective argon atmosphere. But the copper conductors and parts started oxidizing quickly--evidently associated with the voids in the cooling system and with argon contamination. Since it was not possible to remedy the causes of the malfunctions, the investigators limited themselves to calibration results at temperatures to 380° C.

Results of calibrating one of the copper-constantan transducers are shown in Fig. 75.
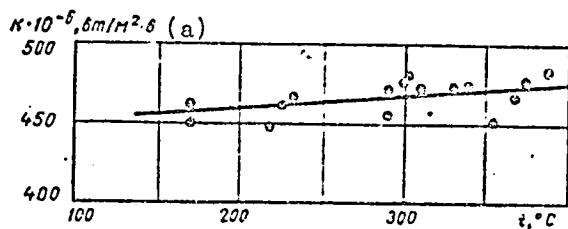
Fig. 75   Temperature characteristic of copper-constantan transducer

Key:

    a. watts/meter^2·volt

CHAPTER 6

CALIBRATION AT ELEVATED TEMPERATURES
(TO 600° C)

From analyzing the nature of signals of thermoelectric heat flux transducers it follows that transducer sensitivity must depend on temperature. So, naturally, the challenge of independent calibration over a wide temperature range emerged. In practice, the need for meeting this challenge appeared in 1965 owing to the development of a number of new electric energy sources and the investigation of high-temperature electrolyzers for molten salts.

One proposed variant involved generating a reference-standardized heat flux by bombarding the transducer being calibrated with head-on electron beams (the heat was removed by radiation). Unfortunately, this attempt was unproductive.

A second variant--use of the twin calorimeter described in the preceding chapter--made it possible to bring the calibration temperature to 380° C.

And finally, a third variant--applying a contact stack of high-temperature heaters--permitted extending calibration to 600° C.

1. Operating Principle of Calibration Stack

The calibration stack consists of successively alternating transducers and heaters whose power can be measured accurately enough. Projection of the heater on the transducer plane must not overshoot the transducer outline in order for the heaters not to "see" each other and in order that the energy interchange among the heaters to occur only through the transducers undergoing calibration (Figs. 76 and 77).

151

The external surface of each heater consists of end sur-
faces covered with the transducers being calibrated and a
lateral surface through which energy is scattered to the ambi-
ent medium. During calibration in vacuo with residual pres-
sure less than 10^{-2} N/m^2, scattering of heat occurs virtually
only by radiation.

Each heater gives off to the stack conductive fluxes di-
rected upward and downward. So all the intermediate transducers
are in a regime of head-on heat fluxes, when the sums of heater
power under the given scattering conditions ensure the corres-
ponding temperature, and their differences--the values of the
calibration fluxes passing through the transducers.

The heat balance equation for each heater has the follow-
ing form:

$$f_t(k_i e_i - k_{i+1} e_{i+1}) = P_{hi} - P_{si} \qquad (VI.1)$$

Here the left-hand side shows the difference of the fluxes
recorded by the upper and the lower transducers for the given
heater, and the right-hand side--the quantity that is the re-
mainder of the heater power P_h after part of the energy P_s has
been scattered by the side walls of the heater into the ambient
space.

For a stack that has the cross-section f_t, consisting of
n heaters and n + 1 transducers, the energy balance can be
described by the following system of equations:

$$\left. \begin{array}{l} f_t(k_1 e_1 - k_2 e_2) = P_{h1} - P_{s1} \\ \cdots \cdots \cdots \cdots \cdots \\ f_t(k_n e_n - k_{n+1} e_{n+1}) = P_{hn} - P_{sn} \end{array} \right\} \qquad (VI.2)$$

It is assumed that all the heaters and transducers assem-
bled in the stack have the same areas.

If we know the scattering power values P_{si} from some indi-
rect indicators, for example, from temperature, and if the
transducer signals e_i and the power levels required by the
heaters P_{hi} have been measured, only the transducer coeffici-
ents k_i in the system of equations (VI.2) remain unknown.

The number of transducers with unknown coefficients, as we
can see, is greater by one than the number of equations equal
to the number of heaters. So the system is not closed. To

solve the system, all we need to do is insert in the stack one transducer with a known working coefficient or with a variation in the stack operating conditions, and then bring the signal of one of the transducers to zero ($e_m = 0$).

Then we cancel out the coefficient of this transducer k_m from the system and the system becomes solvable with respect to all the working coefficients k_1, k_2, ..., k_n, which essentially was what we se. out to do.

2. Stand for High-Temperature Calibration in Vacuo

The stand was designed for general service in conducting experiments with strong-current (1000 A) heating to high (2700° C) temperatures in vacuo, with residual pressure to 10^{-4} N/m². The capacity of the working chamber under the glass hood was 0.15 m³. The potentialities of the stand have been realized only in part in the experiments related to our subject of interest.

A steel chrome-plated plate is the central assembly of the stand; the plate is placed on a support welded of steel angle bars. The upper surface of the support is used for accommodating the instrumentation and auxiliary equipment. Openings are provided in the plate for four strong-current and two banked weak-current hermetic lead-ins of 27 lines each.

Secured to the lower side of the plate on a flange is a VA-05 diffusion pump. The fore-vacuum is provided with a VN-2 pump. The pump under the hood is monitored with a standard VIT-1A measuring unit.

Above, the plate is covered with a glass hood with epoxy resin poured in a massive chrome-plated steel flange. On the outside the hood is protected with a steel screen, behind which the flange together with the hood is suspended on a cable by means of a /‾-shaped support to a counterweight. By means of a wedge stop the counterweight can be disconnected from the hood in the position when the flange linings adjoin the pl surface. The weight of the hood and the flange provides the initial clamp and the corresponding seal at the beginning of the evacuation of the internal space.

The parts and assemblies operating in vacuo are installed in accordance with the recommendations given in vacuum technology literature /98. 106, 249/.
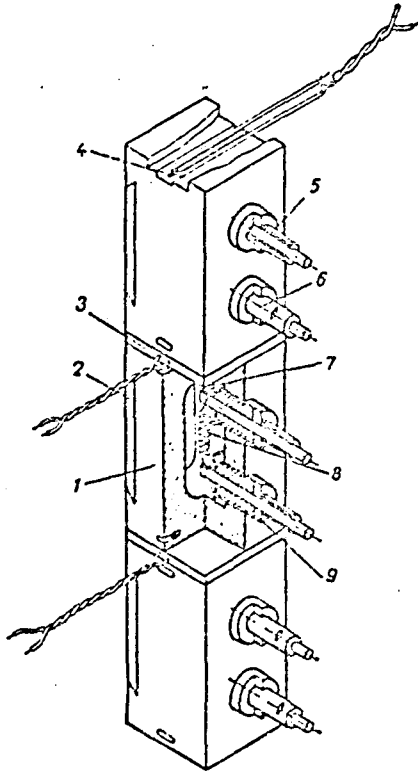
Fig. 76 General view of
calibration stack:

1. housing
2. cover
3. transducer
4. thermocouple
5. heater current lead-in
6. stepped bushing
7. reflecting panel
8. spiral
9. insulator
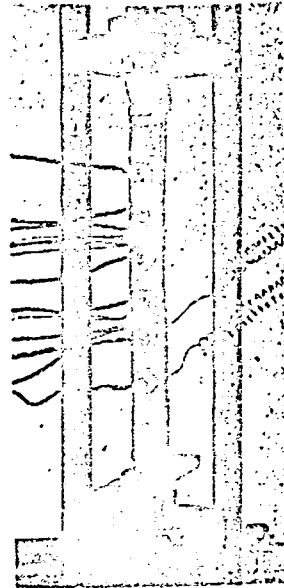
Fig. 77 General view of stack
in clamping accessory

154

The measuring stack is assembled in a clamping accessory (Figs. 77 and 78). The clamping is done with a screw that is screwed into a graphite architrave-nut. The upper belt is connected with the base by connecting rods along which a slide driven by the screw travels.

Direct contact of metal with metal was prevented in all the loaded matings in order to avoid diffusion welding /116, 117/. So the architrave was made of graphite and a graphite shell was press-fitted into the slide. Later it was found that rubbing graphite over the mated surfaces was enough to preventing seizing.

The stack parts 7, 8, 9, and 10 were pressed with slide 6 against support 11, resting on elastic washers made of vacuum rubber and overlain with metal washer. The base was placed on an installation plate using three adjustable support screws so that connecting rods 3 stood vertically. Owing to the elasticity of the support during heating of the stack, there were practically no additional stresses induced in the parts of the installation.

/142

The height of the elastic support was continuously measured with a dial type indicator--0.01 mm scale divisions--to monitor the compressive force. In the preliminary experiments the indicator was calibrated with respect to the stresses existing in the system. Usually the heaters operate at a force of about 1000 N (100 kg).

Fig. 78 Clamping device for calibration stack:

1. screw
2. architrave-nut
3. connecting rods
4. shell
5. thrust bearing
6. slide
7, 8, 9, 10. stack parts
11. lower support
12. elastic washers
13. rigid washer
14. base
15. support screws

Uniform fitting of the transducers over the entire surface long could not be achieved in the adjustment experiments. This was attributed to the fact that the tolerance for nonparallelity

155

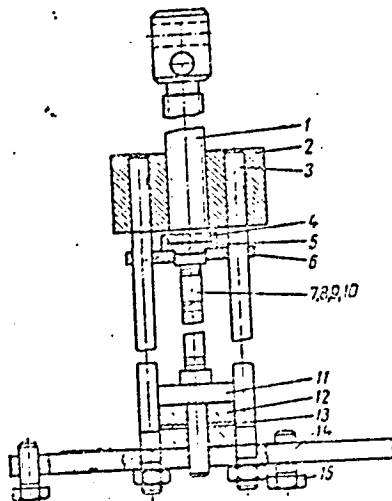of the working faces of the heaters was 100 µm, that is, two orders greater than the value of the possible elastic deformations of the heaters under compressive forces. Use of the rotary supports in ball form afforded a practical solution to the problem. Assuming the given tolerances, the practical deviation of the axial compression line from the transducer centers did not exceed 0.3 mm and was mainly due to the errors in installing the heaters and the transducers in the stack (displacements). The freedom of the ends ensured the freedom of mating over the entire contact mating planes of the stack elements.

The heater is the most significant part of the stack. High thermal loads (more than 50 W/cm³) at temperatures higher than 600° C occasioned certain difficulties. An increase in the dimensions of the heater and a lowering of the working temperature made operation meaningless. A satisfactory solution could be gained only in the third design attempt. Although in scientific experiments an unsuccessful attempt is no less instructive than a successful attempt, let us limit ourselves here only to the last variant.

The main distinction in the heaters assembled into the stack (see Fig. 76) from the preceding designs is that graphite was selected in place of copper as the housing material. The cover does not extend to the face surfaces (they pertain completely to the housing) and therefore all the parts can be subjected to final machining in the preparations. A layout of the placement of the current lead-in insulators is shown in Fig. 79.

Fig. 79   Twin insulator:

1. current lead
2. spiral
3. reflective disk insulator
4. cylindrical insulator
5. stepped bushing

In the first designs, the condensation of metals on the insulator led to a rapid drop in resistance. In the variant adopted, the deposition rate of /143 the conductive coatings in the interval between the disk and the main insulators was much lower than in the exposed surfaces.

Pyrophillite was selected as the insulator material /321/. It is easily worked in the crude form by all known methods.

156

After heating to 1100° C, pyrophillite is not inferior in strength and insulating properties to kilned porcelain. On a par with talc, pyrophillite is best used as a finishing material in insulator manufacture.
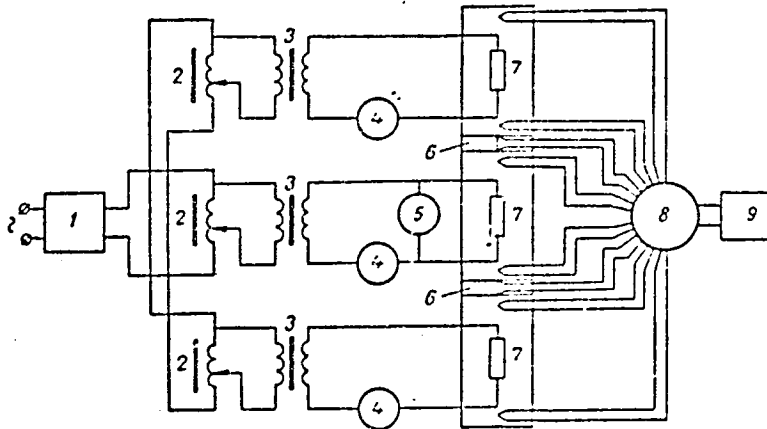
Fig. 80 Electrical diagram of vacuum stand for calibrating transducers in stack:

1. voltage stabilizer
2. autotransformers
3. cutoff transformers
4. ammeters
5. voltmeter
6. calibrated transducers
7. incandescent spirals
8. selector switch
9. potentiometer

At first, special stops opposing rotation were provided in the insulators, in the event of possible weakening of the interference fit between the housing and the insulator with respect to threading. This weakening was observed relatively rarely; this is evidently associated with the gradual increase in the dimensions of the pyrophillite products upon successive calcining. Sometimes in spite of this weakening sets in and can be eliminated only in two ways:

1) by building up the graphite in the contact area using 40 percent glucose. Coating with glucose was conducted three

157

or four times. As this was done, the insulator was firmly
cemented to the housing. Later, during heating in vacuo the
glucose decomposed and spongy coke remained, bonding well to
the rough surfaces of insulator and housing.

The property of glucose, when heated in vacuo, of coking
with the formation of ashless carbographite was repeatedly used
by us in experiments. In particular thermocouple junctions
(see Fig. 76) in the housing cavities were lubricated with
grease consisting of finely ground, low-ash graphite and 40
percent glucose.

2) by buildup of insulators by slip coating of an enamel
(for example, Ts-5). The enamel penetrated the gap and after
kilning bonded to the insulator and the housing, reliably secur-
ing the threaded connection.

To keep the current lead-in from rotating, on the projec-
ting part of the insulator was made a recess into which enters
a projection on the bushing 5, gripped against the nickel
current lead-in (see Fig. 79). The spiral in the current lead-
in was secured just as in the electric lamps with the bending
of the flattened current lead-in by 180°.

The heater was connected to the circuit with miniature plug
connectors. An electrical diagram of the measuring circuits
and the power supply of the stack heaters is shown in Fig. 80.
The heaters were powered from an alternating current line through
a stabilizer and a common regulating autotransformer, beyond
which the power supply circuit branches into autotransformers
for individual regulation of the heater power levels. Further,
voltage was fed through cutoff step-down transformers, ammeters,
or current coils of wattmeters and vacuum-tight conduits to
heater spirals.

Signals from the transducers and thermocouples were fed
through a banked hermetic lead-in and a selector switch to an
R-307 potentiometer.

3. Theory of Thermal Conductivity for Stack. Scattering Losses

In the design adopted all the energy from the spiral fed
to the heater was transferred to the housing and the cover by
radiation. Only a small part was transmitted through the cur-
rent lead-ins by thermal conductivity. In the simplest repre-
sentation we can assume that the power P absorbed by the
housing was uniformly distributed along the housing length ℓ
with the intensity

$$q_s = \frac{P}{l} \qquad \text{(VI.3)}$$

158

If we assume that the transverse thermal conductivity of the stack is infinitely large, this case can be reduced to the one-dimensional problem /124/.

When experiments are conducted in vacuo, the external surface of the stack can lose energy only through radiation at the rate

$$q_{s.1} = p\varepsilon\sigma(T^4 - T_{am}^4) \qquad (VI.4)$$

where p is the perimeter of the cross-section and T_{am} is the effective ambient temperature. The model adopted was formulated with simplifying concessions. The most substantive of these concessions are associated with the assumption that the problem is one-dimensional and that the supplied energy is uniformly distributed across the heater length.

The thermal conductivity equation for the steady-state regime of the stack heater is

$$f_t\lambda\frac{d^2T}{dx^2} - p\varepsilon\sigma(T^4 - T_{am}^4) + q_s = 0 \qquad (VI.5)$$

In the general case, from this equation we can formulate the integral equation of the stack heat balance in the 0 - x interval:

$$-f_t\lambda\frac{dT}{dx} = \int_0^x q_s\,dx - \int_0^x p\varepsilon\sigma(T^4 - T_{am}^4)dx - q_0 f_t \qquad (VI.6)$$

The left-hand side of Eq. (VI.6) is the heat flux penetrating the cross-section f_t with the longitudinal coordinate x; the right-hand side has $\int_0^x q_s\,dx$, which is the thermal power supplied the section 0 - x; $\int_0^x p\varepsilon\sigma(T^4 - T_{am}^4)dx$ is the power scattered owing to side losses; and $q_0 f_t$ is the flux through the cross-section from which the coordinate x is read off.

If we place the transducer to be calibrated in some fixed cross-section, the problem can be reduced to determining the right-hand side of Eq. (VI.6). The calibration regime in the stack is conveniently maintained when $q_0 = 0$. Then the principal part of the problem reduces to finding the side power losses:

$$Q_{s.1} = \int_0^l p\varepsilon\sigma(T^4 - T_{am}^4)dx \qquad (VI.7)$$

In this case, knowing the distribution T = f(x) is most essential

1

Neglecting the temperature change along the heater led to appreciable errors that were detected in the experiments.

The thermal conductivity equation (VI.5) can be rewritten this way:

$$\frac{d^2T}{dx^2} - aT^4 + b = 0 \tag{VI.8}$$

where

$$a = \frac{p\varepsilon\sigma}{f_t\lambda}; \quad b = \frac{p\varepsilon\sigma T_{am}^4}{f_t\lambda} + \frac{q_s}{f_t\lambda}$$

Given the boundary conditions

$$x = 0 - T = T_{1-0} \tag{VI.9}$$
$$x = l - T = T_l$$

the solution of Eq. (VI.8) is

$$x = \int_{T_{1-0}}^{T} [a_1(T^5 - T_l^5) - b_1(T - T_l)]^{-\frac{1}{2}} dT \tag{VI.10}$$

where

$$a_1 = \frac{2p\varepsilon\sigma}{5f_t\lambda}; \quad b_1 = \frac{q_s}{f_t\lambda} + \frac{2p\varepsilon\sigma T_{am}^4}{f_t\lambda}$$

Likewise, when x = 1, we have

$$l = \int_{T_{1-0}}^{T_l} [a_1(T^5 - T_l^5) - b_1(T - T_l)]^{-\frac{1}{2}} dT \tag{VI.11}$$

In principle, given a know stack geometry (p, f_t, ℓ), stack properties (λ, ε), and external and internal boundary conditions (q_p, T_{am}, T_{1-0}), from Eq. (VI.11) we can find T_ℓ, and from Eq. (VI.10)--the temperature in any cross-section with coordinate x.

But integrals (VI.10) and (VI.11) cannot be expressed in terms of elementary functions. The problem is too narrow for introduction of one more special function, but has fairly wide applied significance /277, 282, 287, 297, 308/.

The study /277/ examines closely problems associated with the temperature distribution in rods heated with electrical current in vacuo, over a wide range of design parameters. Like many earlier investigators, the authors of the study /277/ expand the integrand function in series; they were able to divide

160

the rod into characteristic regions, for which rapidly converging expansions were found. Given in /277/ are the interesting results of the authors' own measurements--they convincingly justify the assumptions made concerning the simplifying of the problem.

Following Jain and Krishnan, let us introduce the concept of maximum temperature T_{max} up to which the rod can be heated in its middle section when there is an infinite extension of its length. In this case all the heating energy is expended in compensating for the losses into the ambient medium. So the temperature T_{max} uniquely characterizes the possibility of heating in the conditions given. By definition we have

$$q_3 = \rho c \sigma (T_{max}^4 - T_{am}^4)$$

Taking note that $b_1 = 5a_1 T_{max}^4$ and denoting $T_\ell - T = t$, /147/ from Eq. (VI.10) we get

$$x \sqrt{a_1} = \int_t^{t_1} [5(T_{max}^4 - T_\ell^4)t + 10T_\ell^3 t^2 - 10T_\ell^2 t^3 + 5T_\ell t^4 - t^5]^{-\frac{1}{2}} dt$$

or

$$x_1 [5a_1(T_{max}^4 - T_\ell^4)]^{\frac{1}{2}} = \int_0^t t^{-\frac{1}{2}}(1 + y)^{-\frac{1}{2}} dt. \qquad (VI.12)$$

where

$$x_1 = \ell - x; \quad y = \frac{2T_\ell^3 t}{T_{max}^4 - T_\ell^4}\left[1 - \frac{t}{T_\ell} + \frac{t^2}{2T_\ell^2} - \frac{t^3}{10T_\ell^3}\right]$$

Since in our conditions $T_\ell > t$ and $T_{max} - T_\ell >> t$, y must always be positive, but much less than unity. And the expansion for $(1 + y)^{-\frac{1}{2}}$ will be rapidly converging. By integrating Eq. (VI.12), we find that

$$x_1 [5a_1(T_{max}^4 - T_\ell^4)]^{\frac{1}{2}} = 2\sqrt{t}(1 - s) \qquad (VI.13)$$

where

$$s = \frac{1}{2\sqrt{t}}\left[\int_0^t \frac{1}{2} t^{-\frac{1}{2}} y \, dt - \int_0^t \frac{3}{8} t^{-\frac{1}{2}} y^2 \, dt + \int_0^t \frac{5}{16} t^{-\frac{1}{2}} y^3 \, dt + \ldots\right]$$

Plotted in the graph in Fig. 81 is this function, reduced to the dimensionless argument t/t_{cr}, where $t_{cr} = \frac{T^4_{max} - T'_i}{2T'_i}$.

In the range $0 < \frac{t}{t_{cr}} < 0.2$ we used the sum s does not exceed 0.03. So in this case we can neglect s, which is small compared with unity. Then from Eq. (VI.13) we get

$$x_i^2 = \frac{4t}{5a_1(T^4_{max} - T'_i)}$$

or

$$t = \frac{5}{4} a_1 (T^4_{max} - T'_i) x_i^2 = A x_i^2 \tag{VI.14}$$

Importantly, the trend of the temperature along the rod is well approximated by a quadratic parabola and for completeness of information all we need to know is three parameters (temperature in three cross-sections, temperature in two cross-sections, and the derivative in one of them, and so on). The case when /148 the apex of the parabola of the temperature curve lies on one of the transducers corresponds to calibration with the experimental exclusion of the coefficient of this transducer from the system of equations (VI.2) by reducing its signal strength to zero.

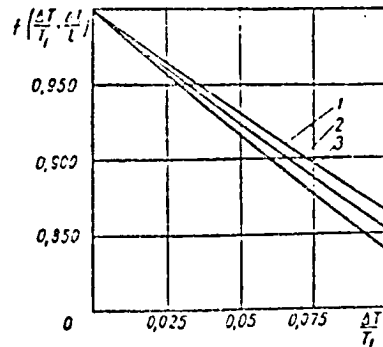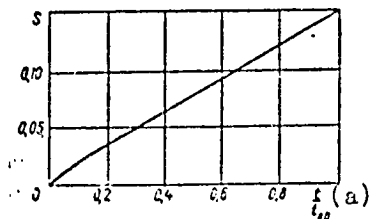Fig. 81 Plot of the function

$$s(t/t_{cr})$$

Key:

   a. t/t_{cr}

Fig. 82 Plot of the function of the correction $f(\Delta T/T_1; \Delta \ell/\ell)$:

1. $\Delta \ell/\ell = 0.05$
2. $\Delta \ell/\ell = 0.1$ 3. $\Delta \ell/\ell = 0.15$

The minimum number of heaters with which independent temperature and flux regulation is still possible is three.

Let $\Delta\ell$ stand for the embedding depth of thermocouples from the heater face; let T_1 and T_2 stand for the temperatures measured with the thermocouples $T_1 - T_2 = \Delta T$.

According to Eq. (VI.14), we have

$$T_1 = T_l - A\Delta l^2; \quad T_2 = T_l - A(l - \Delta l)^2$$

from which we get

$$T = T_1 \left| 1 \div \frac{\Delta T}{T_1} \cdot \frac{1}{1 - 2\frac{\Delta l}{l}} \left[\left(\frac{\Delta l}{l}\right)^2 - \left(\frac{x_l}{l}\right)^2 \right] \right|$$

In what follows we can neglect the products containing $\Delta T/T$ and $\Delta\ell/\ell$ three or more times. Physically this is equivalent to the assumption that $T_\ell = T_1$. In practice, the value of $\Delta\ell/\ell$ and especially $\Delta T/T$ is smaller than 0.1. Therefore, the error --if we assume that $T_1 = T_\ell$--cannot exceed 0.1 percent.

So we can assume that

$$T = T_1 \left[1 - \frac{\Delta T}{T_1} \cdot \frac{1}{1 - 2\frac{\Delta l}{l}} \left(\frac{x_l}{l}\right)^2 \right] \tag{VI.15}$$

Substituting Eq. (VI.15) into Eq. (VI.7) and neglecting, /149 as before, the products of three or more relatively small quantities, we find

$$Q_{3,1} = f\left(\frac{\Delta T}{T_l} ; \frac{\Delta l}{l}\right) \int_0^l p\varepsilon\sigma T_1^4 \, dx - \int_0^l p\varepsilon\sigma T_{am}^4 \, dx \tag{VI.16}$$

where

$$f\left(\frac{\Delta T}{T_1} ; \frac{\Delta l}{l}\right) = 1 - \frac{4}{3} \frac{\Delta T}{T_1}\left(1 \div 2\frac{\Delta l}{l}\right) + \frac{6}{5}\left(\frac{\Delta T}{T_1}\right)^2 \tag{VI.17}$$

Here the function $f\left(\frac{\Delta T}{T_l} ; \frac{\Delta l}{l}\right)$ can be easily tabulated. Its values are given in the plot in Fig. 82 for the cases that are of practical significance.

As a rule, we can neglect the second integral in Eq. (VI.16). But it is difficult to take the first integral since near the insulators and the current lead-ins it suffers from a determinacy /sic/ of the integrand, in particular, the product $p\varepsilon$. This

indeterminacy can be easily circumvented by direct measurement of the side losses $Q_{d.r}$ /d.r = dry run/ in "dry run" experiments --by which is meant the regime when both transducers abutting the heater display a zero flux. And the measured heater power is wholly expended in compensating for the side losses, and the correction function $f(\Delta T/T_1; \Delta \ell/\ell) = 1$.

Thus, the side losses

$$Q_{s.l} = f\left(\frac{\Delta T}{T_1}; \frac{\Delta l}{l}\right) Q_{d.r}(T_l) \qquad (VI.18)$$

can be determined by measurements in the "dry run" at different heater temperatures.

4. Methods of High-Temperature Calibration

In the simplest case, the calibration stack is assembled from three heaters separated by two heaters. In preliminary experiments, the "dry run" characteristic of the central heater is constructed from several points. In practice, in both the "dry run" regimes and during calibration it is difficult to maintain the operating conditions of the outermost heaters such that the transducer signals are exactly zero. So we have to be reconciled to the presence of several small signals, measuring their values, and introducing a correction for the heat sink or heat source, by using in the first approximation the working coefficients obtained earlier during dry run calibrations. In the second and subsequent calibrations we can more exactly allow for the temperature dependence of the transducer coefficients, but there is no longer any need for this when there are small residual fluxes, since the second approximation no longer dif- /150 fers from the first. This is so because the error in the small correction cannot strongly affect the result.

An important cause of systematic error is the zero drift of the galvanometer caused by the nonuniform heating of the frame parts because of illumination of the rotating mirror. For familiarity with this phenomenon, all we need do is switch on the illumination of the reflected spot on an electrically arrested galvanometer, for example, an M195/2 model, and observe the behavior of the reflected spot for 2 or 3 h. In some instruments the drift is as large as 15 scale divisions, corresponding to the appearance in the measuring circuit of a constant emf of about 7 µv, which cannot be neglected. This drawback is typical of both new galvanometers and, to a much greater extent, of frame suspensions that have undergone second soldering during repair.

164

Two transducers are calibrated in successive in a single
assembly. When heated the transducers malfunction to the extent
that they are suitable for extended operation only in this
single assembly. Because of this only transducers selected
from the batch are calibrated in advance.

The calibration conditions are organized in such a way
that the value of the flux passing through one of the trans-
ducers is close to zero; this transducer is called the "dry
run" transducer in contrast to the calibrated transducer
through which the principal flux passes.

From the heat balance it follows that the power penetra-
ting the transducer being calibrated, is

$$P_{cal} = P_h \div f_t k_d e_d - P_s \qquad (VI.19)$$

where P_h is heater power; $f_t k_d e_d$ is the power of the flux through
the "dry run" transducer; P_s is the scattering power, deter-
mined from the experimentally obtained graphical dependence of
the side losses on temperature in the isothermal regime ($P_{d.r}$),
with allowance for the nonisothermality correction:

$$P_s = f\left(\frac{\Delta T}{T_1} : \frac{\Delta l}{l}\right) P_{d.r} \qquad (VI.20)$$

In accordance with the foregoing in Section 3 of this
chapter, when determining $P_{d.r}$ from the plot, the reading of
ther thermocouple (T_1) placed near the "dry run" transducer is
chosen as the argument.

The nonisothermality correction $f(\Delta T/T_1; \Delta l/l)$ is deter-
mined as a function of the relative temperature difference in
the heater ($\Delta T/T_1$) and the relative coordinate of the embedding
of the thermocouple functions from the nearest working planes   /151
($\Delta l/l$) based on Eq. (VI.17) or the plot in Fig. 82.

The temperature of the transducer under calibration in each
regime is assumed equal to the arithmetic mean of the readings
of the thermocouples closest to it in the upper and lower heaters.
In the following, the working coefficient of the transducer at a
given temperature can be found from the expression

$$k_t = \frac{P_{cal}}{f_t e_t} \qquad (VI.21)$$

Fig. 83 Temperature characteristic of
copper-constantan transducers

The calculated functions, plotted from tabulated data, are given in Fig. 26.

During calibration in the stack, at low temperatures the fluxes prove to be small and the measurement errors increase. Using the results of the calculations given in the tables and the measurements with the twin calorimeter (see Section 3 of Chapter 5), we can conclude that in the 0-200° C range there is a minor reduction in the values of the working coefficients of the copper-constantan transducers, following by an increase.

Plotted in Fig. 83, based on the data in Sections 1 and 3 of Chapter 5 and this section, is the temperature dependence of the relative change in the working coefficient of the copper-constantan transducers in the -180 to 600° C range.
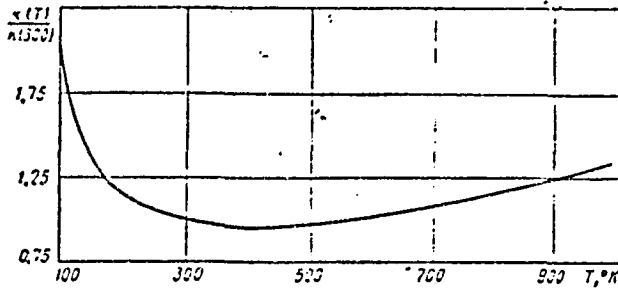
166

CHAPTER 7

DERIVED INSTRUMENTS AND SOME CASES OF APPLYING
HEAT MEASUREMENTS IN SCIENTIFIC RESEARCH

Solving a number of problems in the theory and technology
of fabricating the above-described transducers made it possible
to develop special-purpose derived instruments. Though the
area of use of each of these instruments is limited, the overall
range of their use is quite broad.

Use of sandwich-type banked heat flux transducers for their
direct purpose led to building a series of efficient heat-loss
meters, finding broad use industrially and in heat power engi-
neering.

Direct measurement of local fluxes can significantly sim-
plify the techniques of determining the coefficients of thermal
conductivity. From generalizing the operating experience with
prototypes in which each of the quantities determining the ther-
mal conductivity was obtained by direct measurement, a new instru-
ment for finding the thermal conductivity of insulation and con-
struction materials was designed and is in production in small
series.

Partially or wholly closed heat-measuring surfaces make it
possible to measure the energy effects of different phenomena.
On this basis a calorimeter was developed for biomedical inves-
tigations, along with the so-called thermal diverger--a calori-
metric variant of a dosimeter for measuring the energy of absorp-
tion of nuclear radiation in nuclear reactors.

As applied to nonstationary operating regimes of heat-insu-
lating enclosures, calorimeters make it possible to build a
system for direct measurement of their effective thermal conduc-
tivity and heat capacity in working conditions.

Miniature sandwich-type heat-measuring designs are applied as sensitive elements of pyrometric instruments, used industrially for measuring, monitoring, and automatic control.

In all the instruments and methods described in this chapter, standardized heat-measuring elements made it possible to simplify measurements, making them at the same time more reliable and accurate.

1. Heat-Loss Meters

After development of the technology of series production of sandwich type banked heat flux transducers, it appeared possible to introduce them widely in different sectors of the national economy.

A most promising application of banked transducers in heat power engineering may prove to be an instrument for monitoring losses through the heat insulation of pipelines, power generating facilities, process installations, and the like.

Annually about 3 million tons of asbestos, 0.5 million tons of vermiculite, and 0.2 million tons of magnesia are extracted; up to 3 million tons of mineral fiber and 0.5 million tons of perlite and claydite are produced. The proportions for the USSR are one-fourth to one-sixth of these quantities, and these indicators are continually increasing. Most of these materials go into thermal insulation. Even so, information about their performance is extremely scanty because of the low responsiveness of the available instruments. So constructing a responsive instrument based on sandwich-type transducers for measuring heat losses is an urgent problem $\underline{/52}$, 63, $6\underline{7}/$.

The series-manufactured 17x17x1 mm^3 transducer has the following characteristics:

Working coefficient, k_t, W/m$^2 \cdot$V	50,000
Ohmic resistance, R_e, ohms	300
Thermal resistance, R_t, m$^2 \cdot$deg/W	0.001
Time constant, μ, s	15

Heat is usually removed from the external surface of the thermal insulation by free convection with a thermal resistance of about 0.1 m$^2 \cdot$deg/W; the resistance of the insulation proper is usually one or two orders higher. In these conditions the thermal resistance intrinsic to the transducer can be neglected.

168

When the heat flux circuit has a low thermal resistance, the effect of the presence of the heat-measuring transducer can be taken into account by the method described in Section 4, Chapter 2.

By virtue of the particular working conditions, the instrument must be undemanding and must be immune to dampness, contaminations, overheating, and overcooling. All series ITP instruments possess these qualities to a good extent.

Relatively crude indicating type M-24 electrical instruments are used in the ITP-3, ITP-4, and ITP-4A instruments; the floating system is suspended on core bearings in these type M-24 instruments. The deficiency in the sensitivity of the indicating instrument is compensated by a built-in transistor amplifier assembled in the two-cascade differential scheme. The amplifier is powered from a KBSL-0.5 standard replaceable battery or a built-in dry battery cell that provides continuous operation of the amplifier for 10 h. In the ITP-4 and ITP-4A instruments the chargers are installed in the housings. The dry batteries are charged from an illumination line circuit.   /154

More sensitive transducers and indicating instruments are used in the ITP-5 meters. Owing to the augmented sensitivity of the elements there was no longer any need of using amplifiers and the corresponding power supply system. In addition, an attenuation system is used in ITP-5 instruments for varying the ranges of the heat-loss densities measured (1000, 2000, and
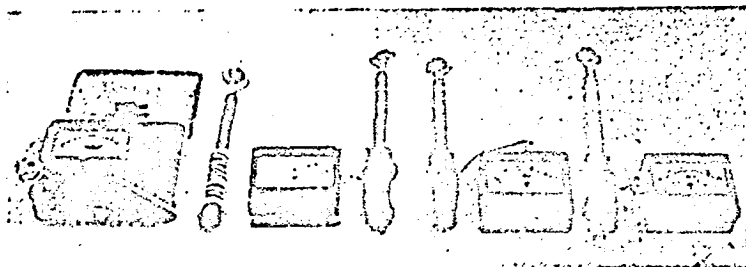
Fig. 84   General view of ITP series instruments

5000 W/m^2). For convenience in measurements the transducer is mounted on a telescoping rod; its length can be varied stepwise from 300 to 900 mm.

Improvements in instrument modifications for heat-loss measurements are continuing.

Operational monitoring of heat-insulation quality fosters, on the one hand, the purposeful use of expensive materials, and on the other--savings in heat and this means in fuel as well.

A general view of the ITP-4 and ITP-4A instruments is shown in Fig. 84.

2. Instruments for Determining the Coefficient of Thermal Conductivity

The ratio of the heat flux density to the temperature field intensity is the definition of the coefficient of thermal conductivity:

$$\lambda = \frac{q}{-\operatorname{grad} t} \qquad (VII.1)$$

Use of heat-measuring transducers makes it possible to determine directly the numerator in Eq. (VII.1), considerably simplifying the instrumental part of determining the coefficient of thermal conductivity.

The first and very simple device for determining the coefficient of thermal conductivity was tested in 1963. With it studies were made of the temperature dependence of thermal conductivity for steel foil and foamed silicate /62/:

for steel foil

$$\lambda = 0.014 + 0.000056\,t \qquad (VII.2)$$

for foamed silicate

$$\lambda = 0.175 + 0.00045\,t \qquad (VII.2a)$$

Later the instrument was improved with the adaptation of the method to mass measurements /77, 85, 191/. The instrument was intended for determining the coefficients of thermal conductivity of solids, liquids, and gases by the plane-plate method. The action of the instrument is based on direct measurements of the heat flux penetrating the specimen, the temperature difference between the planes of the test material, and the thickness of the material (Fig. 85).
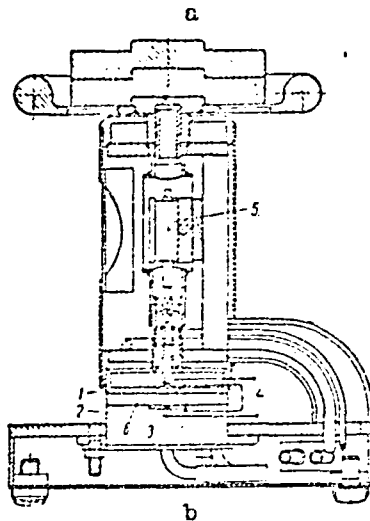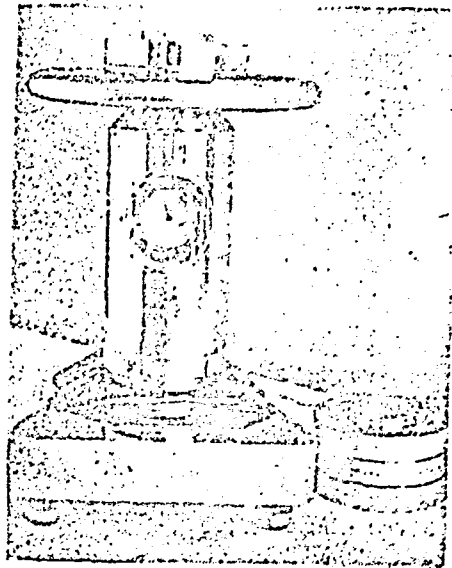
Fig. 8; General view (a) and structural diagram (b) of series-manufactured instrument for determining the coefficient of thermal conductivity:

1. heater
2. condenser
3. heat-flux transducer
4. thermocouples
5. specimen-thickness indicator
6. specimen

The heat flux is measured with a miniature plane high-sensitivity transducer, placed in the middle part of the condenser plane. This makes it possible not only to significantly simplify the experimental procedures, but also to avoid the conventional protective calorimeters or compensatory heaters, since the transducer directly records the heat fluxes penetrating the specimen of the test material.

A conventional R-307 high-ohmic potentiometer is used as the instrument for recording the transducer and thermocouple signals.

Below are presented the technical characteristics of the instrument for determining the coefficient of thermal conductivity:

Measurement limits,
    W/m·deg   0.02- 5
Specimen thickness,
    mm   0.2 -10
Temperature range,
    °C   20 -100
Error of measurement,
    percent   ±   5
Time for instrument
    to arrive at regime,
    min   60
Total instrument weight,
    kg   17

The sandwich-type transducer is cemented to the condenser with epoxy resin, and then its entire facing surface is potted with the same resin. After the resin sets, the facing surface is carefully machined, by hand at first, and then on a grinder. Thermocouples /70/ were installed on the first specimens for measuring the temperature difference in the surfaces of the condenser and the heater. In spite of careful machining the contacts with the specimen failed to be reliable, so later the thermocouples were embedded in elastic rubber linings that were laid on the specimen from both sides. The former method of attaching thermocouples to the body of the condenser and the heater was found to be effective enough for measurements on friable, liquid, and gaseous bodies.

The heater is a massive copper body that is grooved; a nichrome spiral is laid in the grooves on chamotte-kaolin grease.

The results of numerous verifications showed the correctness of measuring heat fluxes with the sandwich-type transducer. So the instrument was calibrated not with reference standards, as initially proposed and carried out, but by direct radiometric calibration following the method described in Section 6, Chapter 4. So the thermal conductivity measurements are absolute.

To measure the temperature field intensity, the specimen surfaces were carefully prepared by grinding the faces on a face grinding machine. The junctions and the electrodes of the thermocouples were burnished to a thickness no greater than 0.05 mm and were embedded in an elastic rubber sheet so that the junction location was on the surface in the central part. When the rubber sheets were clamped together, a good contact of thermocouple junction with test specimen surface was ensured /175/.

Instrument verification was done systematically on specimens differing in thickness, made of fused quartz and polymethylmethacrylate. These materials have been recommended by a number of authors as reference standard materials /115, 186/.

Table 4 gives the results of our thermal conductivity /157 measurements of fused quartz and polymethylmethacrylate in comparison with data from different sources. The tabulated data show that the measurements with the instrument developed are reliable.

Exposure at exhibits and press reports made the instrument widely known /77, 79, 85/. On requests from different organi- zations, about 1000 measurements were made in the LMTI on more /158 than 100 specimens of new materials and composite coatings.

Table 4

Источник (a)	Температура t, (b) °C	Теплопроводность λ, вт·м·град (c)
Полиметилметакрилат(d)		
[4]	20	0.184
[45]	—	0.197
[174]	—	0.177—0.00007 t
[186]	—	0.18 – 3.3·10⁻⁴
[40]	0—50	0.197—0.198
Наши измерения (e)	20—40	0.180±0.006
Плавленый кварц (f)		
[4]	0—100	1.35—1.42
[45]	14	1.19
[45]	42	1.17
[101]	—	1.38 – 0.0016 t
Наши измерения (e)	20—40	1.21±0.01

Key:

    a. Source
    b. Temperature
    c. Thermal conductivity, λ, watts/meter·deg
    d. Polymethylmethacrylate
    e. Our measurements
    f. Fused quartz

Table 5 gives the measurements of several electrical insulating materials used commercially.

Insulating materials in electrical machine building are used in combinations with each other and in impregnations with different varnishes. The measured values of the effective thermal conductivities for these compositions are shown in Table 6.

Staff members at the Knar'kov Aviation Institute proposed a most promising electrical machine building material: ferromagnetic dielectric compound, consisting of a magnetically conducting finely dispersed filler, bonded with furan-epoxy compound /31/. Epoxy resin envelopes the bonded grains of the powders and ensures good insulating qualities of the compound as a whole. The combination of enhanced relative magnetic permeability (approximately 80) with good electrical insulating qualities (approximately 10^3 ohms·m), high strength ($\sigma_v = 10^4$ N/cm²), thermal stability (to 180° C), and thermal conductivity

Table 5

Материал (a)	(b) Температура t, °C	Теплопроводность λ, $\frac{вт}{м\cdot град}$ (c)	(d) Примечание
Электрокартон (e)	28	0.15	ГОСТ 2824-60 (k)
Электронит (f)	30	0.31	Пропитан лаком ПФЛ-86 (l)
Пленкоасбокартон (g)	30	0.12	
Пленкоасбокартон (h)	30	0.15	Пропитан лаком КП-18 (m)
Пленка «Лумиррор» (i)	27	0.11	z>15; δ=0.05 mm, Фирма «Melinex» (n)
Терефталатная пленка (j)	30	0.13	0.05 mm
Асбокартон (r)	35	0.31	Электротехнический (o)
Стеклолакоткань ЛСБ (s)	35	0.21	ГОСТ 10156-61 (p)
Стеклолакоткань ЛСК (t)	35	0.20	То же (q)
Стеклолакоткань ЛСЭ (u)	35	0.18	То же (q)
Стекломиканит Г2ФГП (v)	30	0.15	
Эскапон (w)	40	0.21	
Прессшпан (x)	40	0.16	
Гетинакс (y)	40	0.28	
Текстолит (z)	40	0.34	
Стеклотекстолит (aa)	40	0.32	Электротехнический (o)

Key:
    a. Material
    b. Temperature
    c. Thermal conductivity, λ,
       watts/meter·deg
    d. Remark
    e. Electrical grade cardboard
    f. Electronite
    g. Film-asbestos cardboard
    h. Film-asbestos cardboard
    i. Lumirror film
    j. Terephthalate film
    k. GOST 2824-60
    l. Impregnated with PFL-86 varnish
    m. Impregnated with KP-18 varnish
    n. Melinex Company
    o. Electrotechnical
    p. GOST 10156-61
    q. As above

174

Table 6

Состав компизиции (a)	(b) Температура t, °C	Теплопроводность λ (c)	(d) Примечание
Электрокартон+пленка «Лумиррор» (e)	30	0.13	Пропитан лаком ПФЛ-8э (n)
Стекломиканит Г2ФГП (δ=1 мм)+стеклолакоткань ЛСБ (1 слой) (f)	35	0.13	Пропитан лаком МГМ-8 (o)
Стекломиканит Г2ФГП (δ=1 мм)+стеклолакоткань ЛСК (1 слой) (g)	35	0.09	Пропитан лаком К-47-к (p)
Стекломиканит Г2ФГП (δ=4 мм)+стеклолакоткань ЛСЭ (1 слой) (h)	35	0.11	Пропитан лаком ПФЛ-8б (q)
Электронит (δ=0.3 мм)+стеклослюдинит (δ=0.2 мм)+стеклолакоткань ЛСБ (δ=0.15 мм) (i)	39	0.49	Пропитан лаком 321-Т (r)
Электрокартон (δ=0.3 мм)+лавсан (δ=0.05 мм) (j)	40	0.12	То же (s)
Микалента ЛМ-4 (0.17×23 мм²) 7 слоев в полнахлеста склеено лаком БТ-95 (k)	40	0.17	Изоляционная обмотка (t)
Стеклослюдинитовая лента (0.13×20 мм²) 9 слоев в полнахлеста склеено лаком 88 (l)	40	0.19	То же (s)
Электрокартон ЭВ (δ=0.1 мм)+миканит ГФС (δ=0.2 мм)+стеклолакоткань ЛСБ (m)	40	0.20	Пропитан лаком 321-Т (r)

Key:

a. Composition
b. Temperature
c. Thermal conductivity, λ, W/m·deg
d. Remarks
e. Electrical grade cardboard + Lumirror film
f. Steklomikanit G2FGP (δ = 1 mm) + glass-varnish-reinforced cloth LSB (one ply)
g. Steklomikanit G2FGP (δ = 1 mm) + glass-varnish-reinforced cloth LSK (one ply)
h. Steklomikanit G2FGP (δ = 4 mm) + glass-varnish-reinforced cloth LSE (one ply)
i. Elektronit (δ = 0.3 mm) + stekloslyudinit (δ = 0.2 mm) + glass-varnish-reinforced cloth LSB (δ = 0.15 mm)
j. Electrical grade cardboard (δ = 0.3 mm) + lavsan (δ = 0.05 mm)
k. Mikalenta LM-4 (0.17x x23 mm²) 7 plies in half-lapping cemented with BT-95 varnish
l. Stekloslyudinit tape (0.13x20 mm²) 9 plies in half-lapping cemented with varnish 88
m. Electrical grade cardboard ЭВ (δ = 0.1 mm) + mikanite GFS (δ = 0.2 mm) + glass-varnish-reinforced cloth LSB

n. Impregnated with PFL-8v varnish
o. Impregnated with MGM-8 varnish
p. Impregnated with K-47-k varnish
q. Impregnated with PFL-8v varnish
r. Impregnated with 321-T varnish
s. As above
t. Insulation winding

(to 0.7 W/m·deg) accounts for the wide use of ferromagnetic
dielectric compound as connection and closure parts in magnetic
conductors.

Thermal conductivity measurements of ferromagnetic dielec-
tric compound of different compositions are given in Table 7:
here PEPA stands for polyethylene polyamine; FAED--furan-epoxy
resin; GMDM--hexmethylenediamine; PZh2M2--iron powder; and
NB--boron nitride powder.

On the suggestions of staff members of the Dnepropetrovsk
and Donetsk mining institutes, series of thermal conductivity
measurements were made for specimens of sedimentary rock from
the Donbass; the results are in Table 8.

Also subjected to similar measurements were many materials /160
with known properties. Our data agree with literature values.
An exception is represented by soft dry chrome leather; its
measured thermal conductivity was λ = 0.07-0.08 W/m·deg. Tabu-
lated data /3, 47 are markedly higher and, evidently, refer to
a more compact leather.

The measured thermal conductivity values of nonsystematic
materials are presented in Table 9.

The dependence of the thermal conductivity of two kinds of
glass-reinforced plastic electrical insulation on temperature
is shown in Fig. 86. Polypropylene was found to exhibit a
practically linear dependence of thermal conductivity on the
content of the customarily used filler--calcium silicate
(Fig. 87).

A number of physical properties of substances have a quality
in common and therefore it is not surprising that they are inter-
related /192, 226/. On the suggestion and with the participa-
tion of V. F. Zinchenko, we determined the correlation between
thermal conductivity and the strength of glass-reinforced plas-
tics based on epoxy resin when the binding agent is present in

Table 7 REPRODUCIBILITY OF THE ORIGINAL PAGE IS POOR   /159

| (a) Компоненты* | | | | (f) Толщина образца, мм | (g) Теплопроводность λ, вт/м·град | | |
(b) отвердитель (c)	весовых частей (c)	(d) наполнитель	весовых частей (e)		(h) 1 серия измерений	(i) 2 серия измерений	Среднее значение (j)
ПЭПА (k)	10	—	—	5.20	0,205	0,204	0,20
ПЭПА	15	—	—	4.05	0,199	0,196	0,20
ПЭПА	10	(m)НБ	10	5.35	0,271	0,266	0,27
ПЭПА	10	НБ	15	6.30	0,303	—	0,30
ПЭПА	10	НБ	20	6.45	0,407	0,408	0,41
ГМДМ**(l)	10	—	—	5.20	0,207	0,205	0,21
ГМДМ**	15	—	—	5.70	0,210	0,202	0,21
ГМДМ***	10	(n)—	—	5.48	0,212	0,201	0,21
ГМДМ***	15	—	—	3.10	0,168	0,168	0,17
ГМДМ**	15	ПЖ2М2	250	5.80	0,540	0,557	0,55
ГМДМ***	15	ПЖ2М2	250	3.98	0,610	0,593	0,60
ГМДМ**	15	ПЖ2М2	250	3.30	0,657	0,645	0,65
ГМДМ***	15	ПЖ2М2	250	4.05	0,688	0,675	0,68

* Gravimetric content of FAED in all compositions was assumed to be 100
** Alcoholic solution
*** Melt

Key:

a. Constituents*
b. curing agent
c. parts by weight
d. filler
e. parts by weight
f. Specimen thickness, mm
g. Thermal conductivity, λ, W/m·deg

h. first measurement series
i. second measurement series
j. Mean value
k. PEPA
l. GMDM**
m. NB
n. PZh2M2

different proportions (d). The existence of this dependence was indicated by N. A. Krylov /149/. Measurements taken on 24-ply specimens are presented in Fig. 88.

Similar functions were obtained also for specimens of dif- /161 ferent thicknesses; however, when the thickness was reduced to 10 plies (2.5 mm), the correlation becomes poorly defined. This evidently is due to the fact that with decrease in thickness the relative effect of edge effects begins to rise. The total number of measurements supporting this correlation exceeds 1000. Most of these measurements were obtained in the Institute of Polymer Mechanics, Latvian SSR Academy of Sciences, by V. F. Zinchenko.

Table 8

(a) Порода	(b) t, °C	(c) λ, вт/(м·град)
Песчаник кварцевый среднезернистый, содержит до 15% мусковита, сидерита и обломков аргиллита (d)	31	1,72
Песчаник крупнозернистый, состоит из кварца и обломков кремнистых пород на известково-глинистом цементе (e)	32	1,80
Песчаник серый разнозернистый, плохоотсортированный (f)	~	1,50
Песчаник Никитского ртутного месторождения (g)	30	2,80
Алевролит темно-серый, содержит ориентированные включения мелкочешуйчатого мусковита (h)	31	2,70
Мрамор белый массивной текстуры (i)	34	1,75
Мрамор серый массивной текстуры (j)	35	1,85
Аргиллит темно-серый плотный (k)	32	1,13
Бетон (цемент + крупнозернистый песок, 1:2,8) воздушно-сухой (k)	33	0,80
То же, высушенный при 100° С (l)	33	0,60

Key:

a. Rock
b. Temperature
c. Thermal conductivity, λ, W/m·deg
d. Sandstone, quartz, medium-grain, contains up to 15 percent muscovite, siderite, and argillite detritus
e. Sandstone, coarse-grain, consists of quartz and detritus of silicaceous rock with limestone-clay cement
f. Sandstone, gray, inequigranular, poorly graded
g. Sandstone of Nikitskoye ore deposit
h. Aleurolite, dark-gray, contains oriented inclusions of fine-platy muscovite
i. Marble, white, massive texture
j. Marble, gray, massive texture
k. Argillite, dark-gray, compact
l. Concrete (cement + coarse-grain sand, 1:2.8), air-dried
m. As above, dried at 100° C

Table 9

Материал (a)	Темпе-ратура t, °C (b)	Теплопровод-ность λ, вт/м·град (c)
Мебельные плиты из пеноэпоксида и наполнителя (опилки) в отношении 1:1 (d)	30	0,12
Ткань Петрянова (e)	35	0,035—0,045
Карборундовая композиция на связке Б1 [130] (f)	42	1,26
Отвержденный пульвербаке-лит — связка ПБ (ГОСТ 3552-63) (g)	40	0,23
Связка № 1 (на основе алюми-ния) [130] (h)	40	0,80
Связка БР (ПБ + резиновая му-ка) (i)	30	0,24

Key:
a. Material
b. Temperature
c. Thermal conductivity, λ, W/m·deg
d. Furniture slabs of foamed epoxide and filler (shavings) in a 1:1 ratio
e. Petryanov cloth
f. Carborundum composition with B1 binder /130/
g. Cured sprayed bakelite-- with PB binder (GOST 3552-63)
h. Binder No. 1 (aluminum-based) /130/
i. BR binder (PB + rubber flour)
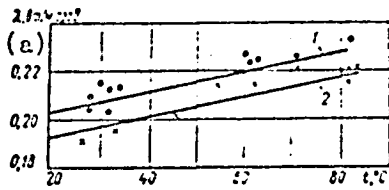
Fig. 86 Dependence of
thermal conductivity of
glass-reinforced plastic
electrical insulation on
temperature:

1. EK-20 binder
2. ED-6 binder

Key:
    a. λ, W/m·deg
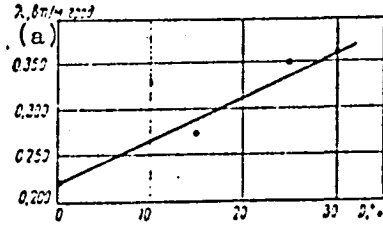
Fig. 87 Dependence of thermal
conductivity of polypropylene
on filler content--calcium
silicate

Key:
    a. λ, W/m·deg
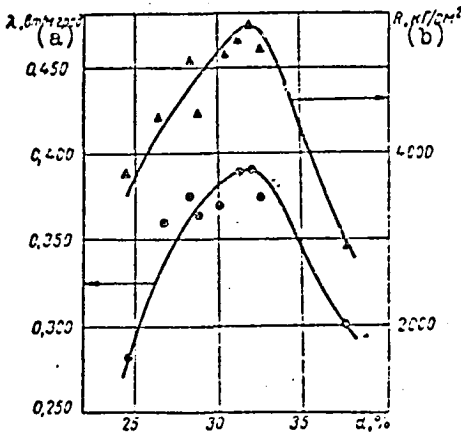
Fig. 88 Correlation between
conductivity and
strength of 24-ply
glass-reinforced plastic
for different bonder content
Key: a. λ, W/m·deg b. kg/cm^2
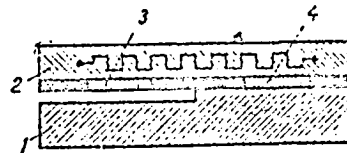
Fig. 89 Arrangement of instru-
ment for determining the
thermal conductivity of a
liquid:
1. heat receiver
2. heat source 3. temperature
  difference transducer
4. heat flux density transducer

180

The correlation found between thermal conductivity and the strength of glass-reinforced plastics allows us to determine the strength properties directly in products without taking out specimens. Similar correlations must be considered as the primary uses of strain gage flaw detection.

In systems intended for determining thermal conductivity coefficients the strain gage transducers are applied not just to measure the heat flux density, but also the gradient of the temperature field in the test body. This is done most simply in a special instrument used for finding the thermal conductivity of liquids in field conditions (Fig. 89).

The transducers were connected in a bridge arrangement /162
and were positioned between flat bodies exhibiting high thermal conductivity. Mounted in the upper body was an electric heater; when it is energized, in spite of significant losses into the ambient space, some temperature difference is established between receiver 1 and source 2. The temperature difference ensures that heat flows from the upper body to the lower in two parallel paths: through the first transducer 3 in contact with both bodies, and also through the second transducer 4 and the gap filled with the test liquid.

The values of the fluxes passing through the transducers are directly proportional to the temperature difference between the bodies and inversely proportional to the thermal resistances of the corresponding circuits of heat fluxes:

$$q_1 = k_1 c_1 = \frac{\Delta t}{R_1}; \quad q_2 = k_2 c_2 = \frac{\Delta t}{R_2 \div \frac{\delta}{\lambda}} \qquad \text{(VII.3)}$$

Cancelling out Δt, we find that the thermal conductivity of the liquid filling the gap is an unambiguous function of the ratio of transducer emf values:

$$\lambda = \frac{\delta}{\frac{R_1 c_1 k_1}{c_2 k_2} - R_2} = \frac{A}{\frac{c_1}{c_2} - B} \qquad \text{(VII.4)}$$

where the instrument constants A and B are determined from the measurements taken with reference standard liquids.

3. Determination of Convective and Radiative Components of Complex Heat Transfer

Heat transfer by conduction and by convection is so closely interrelated that sometimes dividing them is very different. This is due to the commonality of the principles of the effects

studied. At the same time the nature of radiation differs sig-
nificantly from thermal conductivity and convection and there-
fore its proportion in overall heat transfer is best considered
separately.

Nusselt made one of the first attempts in this direction:
he simulated heat transfer in the working chambers of internal
combustion engines with spherical calorimetric bombs of differ-
ent diameters and different blackness values of internal sur-
faces /300/. Later, the method of heat measurements on surfaces
with different absorptivities as applied to open-hearth furnaces
was developed by V. S. Kocho /143/, and for fireboxes of boiler
installations by S. S. Filimonov, B. A. Khrustalev, and V. N.
Adrianov /228/. The presence of compact heat-measuring trans- /163
ducers with high sensitivity made improvements in this method
possible.

In most of the known methods of heat transfer investigation
the heat-flux densities are estimated indirectly from measure-
ments of other parameters, mainly temperature. Efficient heat-
measuring instrumentation makes it possible, from heat-flux
values, to determine all the remaining quantities characterizing
heat transfer. In principle, measurements of only flux densities
can be sufficient to get complete information. Naturally, we
must have additional sources--transducers whose readings are
not linearly interrelated--to get the additional information.

In the general case, the heat flux density measured by some
i-th transducer

$$q_i = q_{ki} + A_{ii}q_n - q_{ini}$$ (VII.5)

where q_{ki} is the convective fraction of the flux measured with
the given transducer; A_{ii} is the blackness value of its receiv-
ing surface; q_n is the incident radiative flux; and q_{ini} is the
intrinsic radiation from the receiving surface of the given
transducer.

The flux direction in which the heat is received by the
wall is taken as the positive direction.

Corresponding to each of the principal equations of the
form (VII.5) are the additional following equations:

$$q_{ki} = \alpha [T_{nv} - T_i]$$ (VII.6)

$$q_{ini} = \varepsilon_{ii}\sigma T_i^4$$ (VII.7)

$$q_i = \frac{1}{R_i}(T_i - T_a) \qquad\qquad (VII.8)$$

where T_{av} is the temperature of the sweeping medium, T_i is the temperature of the receiving surface of the given transducer; and R_1 is the thermal resistance of the transducer.

Usually the surface temperature T_s of the surface on which the transducer is placed is a function of the flux measured and can be specified in analytical form. This function gives us one more equation in the system. To make things simpler, let us dwell on the special case when the transducers were placed on a surface made of material that has a high thermal conductivity, when we can assume T_s = idem.

Eleven quantities enter into a system of four equations. Of these only three can be obtained in the preliminary calibrations (A_{11}, ε_{11}, and R_1). Therefore, there is not enough information about four quantities in order for complete information to be arrived at; these four quantities can be found only by measurement. When there is one calorimeter (i = 1), three more parameters must be measured, for example, T_s, T_{av}, and q_s.

Each additional heat-measuring transducer, when brought into the measuring situation, leads to the appearance of four additional equations and only three extra unknowns. We assume that quantities like α, T_{av}, T_s, and q_s remain the same for all transducers. It is important that the transducer readings are not linearly interrelated, that is, that no repetitions must be made of transducers with the same values of absorption, radiation, and thermal resistance. Introduction of each additional transducer makes it possible to exclude one of the direct measurements of any other parameter. So we can manage with just thermal measurements; from these, by calculation we can determine all temperatures, components of complex heat transfer, and the heat transfer coefficient. It is best to combine heat-measurement transducers with other measuring instruments.

For instrumental implementation of the method, individual transducers have been designed and built with different fixed absorption levels, and also two-, three-, and four-section transducers, two of which are schematically shown in Fig. 90. Each section differs from the neighboring sections only by the absorption level or by thermal resistance. Since when systems of the kind (VII.5)-(VII.8) are solved, the measured flux values are subtracted and the sections are connected in opposition in order to directly measure the difference signal. Since all

183

sections of one integrated transducer for direct measurement of a difference signal must have a strictly identical sensitivity, which is quite difficult to do, the measurements are taken with individual transducers that have characteristics precluding the possibility of linear dependence of readings in the selected measurement conditions.
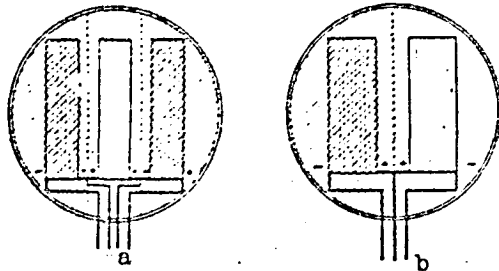
Fig. 90   Arrangement of three-
(a) and two-sectional (b)
combined transducers

Surfaces with a high absorption level are prepared using carbon black paints. If the paint formulations are identical, the absorption levels are replicated quite well.

For low-absorption surfaces, tests were made of transducer foil coatings of gold, silver, aluminum, brass, bronze, and nickel. The initial absorption levels were ranked in the order in which these materials are listed. In accordance with /16 the tabulated data, best reflection was recorded from gold, silver, and aluminum surfaces, but in operating conditions they rapidly lost their initial qualities. Most stable are the values of surface properties for nickel foil.

In the order in which the proposed method of distinguishing the components of complex heat transfer was introduced, a large number of measurements were made during the baking of full-sized products in industrial bakery ovens of different types /89, 155, 156/. The transducers were pressed into the dough surface when the experiment started and during the whole baking process yielded information about the heat transfer trend. These measurements in bread-baking were the first of their kind and made it possible for specialists to arrive at conclusions about individual stages of the technological process.

4.   Microcalorimetry

In 1923 A. Tian proposed a calorimeter design in which the thermal intensity of a process studied can be measured by relying on compensation by the Peltier and Joule-Lenz effects Essentially, the time derivative of the calorimetric effect was recorded. The device should have been named "differential calorimeter," but this name was already in use, so a less apt name--microcalorimeter--was settled on.

184

Measurements of the derived parameter were developed extensively in studies by A. Tian /121, 320/. Considerable attention was given to studies in microcalorimetry in the United States, Canada, and France. Through the efforts of students of A. Tian and E. Calvier, a special center for studies in microcalorimetry and thermochemistry was founded in Marseilles. In the USSR investigations in this area came to be called thermographic calorimetry /14, 23-26, 28, 54, 56, 122, 193, 244/.

The absolute error of measurement does not exceed 1 µW in the most sensitive devices. For purposes of microcalorimetry it is convenient to use wholly or partially closed shells made of series of specially prepared transducers. In the case of a closed heat-measurement shell, the power released in the internal volume is associated with the heat flux density, the working coefficient of the transducer, and the emf generated by the transducer by the following relations:

$$P = q f_t = k_t e f_t \qquad \text{(VII.9)}$$

Typically, for the selected type and elementary dimensions $k_t f_t = k_c$ = const and does not depend on transducer area. For the above-described sandwich-type copper-copel transducers, $k_c \approx$ 15 W/V when the transducer is 1 mm thick and when the wire diameter is 0.1 mm.

If the error of the most sensitive instruments (M-195 and F-116) is 0.1-0.2 µV, we can expect an absolute error of measurement of about 3-4 µV for series-manufactured sandwich-type transducers. How transducer sensitivity can be augmented is described in Section 4, Chapter 3.

Making direct measurements of the heat balance items of individual body organs was of much interest. The kidney is an organ that is most convenient in this respect. Complete heat balances of a cat kidney in different regime conditions were formulated in the department of normal physiology of the Kiev Medical Institute /147/. In acute experiments heat-measuring transducers were sewn to different areas of the kidney surface. A total of more than 200 experiments were conducted; as a result, complete energy balances of the kidney were arrived at for the administration into the organism of pituitrine, urea, and ascorbic and dehydroascorbic acids. About 90 percent of the thermal energy released in the kidney was removed by the bloodstream, 8-10 percent--through thermal conductivity, and only 1-2 percent--with the products of the organism's vital activity. Characteristic is the presence of a heat flux transiting through the kidney from the liver located nearby--the liver is an organ with high heat release.

185

A quantitative dependence between the effective thermal conductivity of kidney tissue and blood circulation was determined in the Institute of Physiology, Ukrainian SSR Academy of Sciences, based on heat measurements using a miniature transducer /47, 48/. More than 70 acute experiments were conducted on cats and rabbits as an indirect comparison of the data of thermoelectric measurements with direct methods of blood circulation recording, as well as in direct experiments with perfusion (by pumping) of blood from the isolated organ in situ with a pump that has capacity calibrated as a function of the rpm value.

The same measurements were conducted on a spleen, small intestine, liver, skin, and muscles of the extremities. From the data recorded for the change in effective thermal conductivity with the perfusion tempo, curves of mutual dependence of these quantities were plotted for each organ.

Acute experiments, naturally, are excluded as applied to the human organism. But heat measurements of the organism as a whole can be obtain from surface measurements. In air these measurements were found to be poorly effective owing to the large effect on the boundary conditions of random factors (drafts, solar radiation, and so on).

But in water boundary conditions have a much stronger effect. Special measurements with a surface resistance thermometer established that even in 60 s after immersion the surface temperature of the swimmer's skin is practically no different /167 from the water temperature. In the principal experiments a heat flux transducer was cemented on different parts of the swimmer's body; the readings were fed through a 20 m conducting halyard to an M95 instrument. The following conclusions were reached on the basis of measurements made on more than 30 swimmers at a water temperature of 15 to 27° C:

a) at the instant when the swimmer was immersed, in a nonstationary cooling regime, the heat losses are proportional to the initial difference between the skin surface temperature and the water temperature and in some cases exceeded 10 kW

b) arriving at the stationary regime of heat release occurs in 7-10 min; the density of the stationary flux now falls in the range 250-800 W/m^2 and depends on the water temperature, the thickness of the subcutaneous fatty tissue, and the personal mental and nervous qualities of the subject

C-3

c) under identical conditions (water temperature and body build), the heat loss densities can differ by more than twofold; typical of persons of choleric temperament is a greater tendency to heat release; trained swimmers are less prone to heat losses

d) based on heat measurements, an objectively sound selection can be made of persons predominantly suited for athletic and occupational activities in which systematic or random long-term presence in water is inevitable (for example, marine aviation, underwater divers, and so on)

e) when there is an increase in physical load, the stationary heat release climbs by 30 to 50 percent; the towing speed of an immobile swimmer does not affect heat release.

A twin microcalorimeter was built for analyzing individual animal organs; it was based on series-manufactured sandwich-type transducers (Fig. 91). The object of study was placed in a sleeve 12 mm in diameter and 80 mm long. A controllable flow of heat occurs through a thickness made in the middle part of the sleeve, into a receiving insert and a massive housing through a transducer and a tapered bushing. The sensitive element was assembled of three series-manufactured sandwich-type transducers connected in series with respect to signal.

Openings were drilled in the intervals between the transducers and a threading was cut; in it were screwed heat shunts leading part of the flow past the transducers.

Because of the threading, the thermal resistance of the heat shunts can be regulated over a wide range and with high accuracy.

A variable electrical shunt was installed in the external part of the transducer circuit of each microcalorimeter; the shunt is capable of regulating the sensitivity of the system of transducers independently of their thermal resistance. This system has the possibility of independently regulating the sensitivity and inertia of each microcalorimeter and, thus, with <u>/168</u> high accuracy these characteristics can be established for both microcalorimeters identically.

Both elements were placed in symmetric recesses in a massive (40 kg) block, thermally insulated externally. All the parts were made of copper; the contact locations were carefully wiped and lubricated to reduce the thermal resistances.

187

The microcalorimeter sensitivity in the arrangement described can be regulated in the range $(10-40) \cdot 10^{-3}$ V/W, and the time constant is 120-300 s.

The instrument was intended for calorimetric and microcalorimetric measurements in direct, differential, and compensation regimes. The negative thermoelectrical compensation due to the Peltier effect was practically not provided for.

When necessary, this effect can be replaced with positive compensation due to the Joule-Lenz effect in the differential regime during a nonisothermal process.

After preliminary tests, the microcalorimeter described was transferred to the department of normal physiology of the Kiev Medical Institute (N. I. Putilin), where it was used for studies of the dynamics of the energy balance in the static and dynamic functioning of frog muscles.

One method in the dosimetry of ionizing radiation consists of measuring the heat intensity of the dose absorbed by a specimen. Generally, simplified calorimetric systems are used, and a curve of the trend of energy release in the specimen with time was graphically differentiated to determine the intensity /36/. Classical microcalorimeters are rarely used because of their cumbersomeness.

Closed heat-measurement sheaths in whose internal cavity the irradiated specimens were placed were found to be very effective (S. S. Ogorodnik and A. V. Nikonov).

By early 1969 four types of thermal nuclear dosimeters were placed in regular production; the number of these installations operating in different organizations exceeds 40.

5. Use of Heat-Measurement Transducers in Radiation Pyrometry

Essentially, the sensitive elements of radiation pyrometry instruments are heat-measurement transducers /199/. So it was natural to try to use the sensitive elements designed in the field of pyrometry.

In the first of this series of instruments the circular sandwich-type transducer, 10 mm in diameter, was mounted on a copper plug screwed into the instrument body /66, 80/ (Fig. 92).

A number of diaphragms was bored into the pyrometer body /169 to increase the absorption of the internal cavity and reduce

188

possible convection. All the internal cavity surface, including the transducer, was blackened with "blackbody grade" lampblack. The imaging of the of the irradiating object on the transducer was obtained with standard Gelios-40 or Yupiter-6 objectives. The external surface of the copper body was protected with insulation for protection against external thermal perturbations.
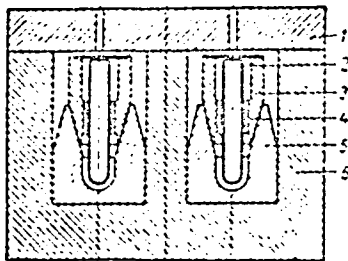
Fig. 91 Layout of twin microcalorimeter for sandwich type transducers:

1. cover
2. lining
3. tapered bushing
4. sensitive element
5. receiving insert
6. body
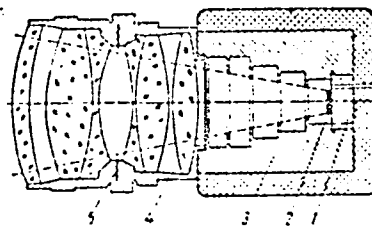
Fig. 92 Structural diagram of radiometric pyrometer with sandwich-type transducer:

1. copper plug
2. transducer
3. body
4. diaphragm

Results of extended tests showed that the equipment functions stably. When radiation from a small incandescent lamp was measured, the instrument reacted cleanly to the slightest (0.1 percent) change in supply voltage. This system, evidently, can prove to be useful for measuring the voltage drop in alternating current circuits. Calibration of the system to high accuracy can be done with direct current.

In many cases of commercial and research practice there is a need for contactless measurement of the temperature of semitransparent gases, their effective absorptivity and radiativity, as well as a number of radiative characteristics of different solid and gaseous objects. Ordinarily in these measurements use is made of standard radiation pyrometers exhibiting some shortcomings: cumbersomeness, sensitivity to inevitable contaminations of optical system components, selectivity of reception, complexity of manufacture and operation, high cost, and the like.

A narrow-angle total-radiation radiometer-probe was developed in the Institute of Gas, Ukrainian SSR Academy of Sciences /181/ (Fig. 93). The total radiative heat flux from the object measured was received by the sandwich-type transducer 3, which was placed on the face of massive copper plug 4. A characteristic feature of the instrument is that it has no condenser elements (lenses or mirrors). A diaphragming device 1 is used as an optical system delimiting the sighting angle of the transducer. To prevent the entrance of hot gases, condensation of water vapor, and solid-particle contamination of the internal cavity of the radiometer, use was made of an air seal (purging of the forward part of the diaphragming device through a system of openings). Conductors from the transducer were inserted into the secondary instrument in internal tubing 7 through which the purging air was directed. The radiometer was sighted on the measured object using an alignment sighting device 5. Cooling water was directed and removed through connection 6.

Owing to the absence of condenser elements, the spectral composition of the received heat flux is not distorted, the instrument is simple to make and operate, does not require adjustments, is not in need of temperature compensation devices, and is nearly insensitive to contaminants. Owing to the purging system and water cooling, the instrument can function in corrosive media. The radiometer-probe has small transverse dimensions (30 mm diameter) and, when necessary, any length and configuration of the support rod (from 0.250 m to several meters). So it can be used for measurements in hard-to-get-at places, can be introduced in a furnace inside the flame, and used near an object of electron-beam melting of metals. Any reading or recording potentiometer, in series production commercially (EPP, PSR, N-373, and others), can be employed as the secondary instrument.

When surface temperatures are measured--for which the radiativity is not known, to the end of the instrument is attached a semiclosed fitting made of material that has high reflectivity according to an arrangement proposed by T. Land and R. Barber /92/. Below are given the specifications of the radometer-probe:

Sensitivity, $W/m^2 \cdot V$	$570 \cdot 10^6$
Flare angle	1:12 or $5°$
Minimum dimension of sighting area, mm^2	12x12
Inertia, s	10-15
Diameter, mm	30
Length, m	0.25-4
Weight (as a function of length of supporting rod), kg	from 0.3
Flow rate of cooling water, cm^3/s	2-10
Purging air pressure, N/m^2	$(1-5) \cdot 10^3$
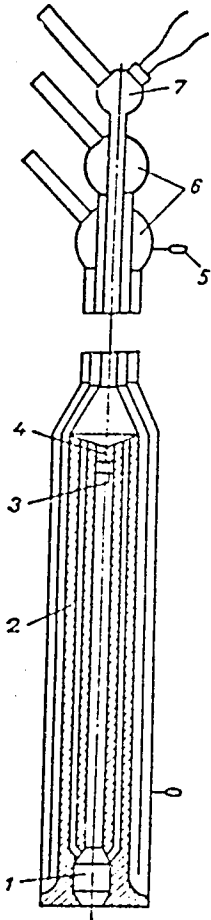
Fig. 93 Narrow-
angle radiometer-
probe:
1. entrance diaphragm
2. body with air channels
3. transducer
4. plug
5. sighting device
6. cooling water connec-
   tion
7. sealing air tubing

For glass industry conditions
a number of special-purpose instru-
ments were made for measuring the
temperatures of rolling mill rolls,
glass ribbon, glass bath, furnace
crown, gas burners, and so on. The
insensitivity to contaminants makes
it possible to place these instru-
ments in close proximity to points
bearing control instruments. The
transducer signals are fed to a
computer monitoring the operating
regime of the entire process com-
plex.

It appeared of interest to
combine the narrow long sandwich-
type transducer with a system of
slit diaphragms /88, 141/. This
unit is polarized in terms of sen-
sitivity and generates a minimum
signal when there is coincidence
of the transducer plane and the
plane of the slit diaphragm with
the normal to the isotherm at the
nonisothermal radiator.

6. Heat-Measurement Determination
of Properties in Nonstationary
Regimes

Several methods of determin-
ing heat-physical characteristics
are founded on solutions to problems
in nonstationary thermal conducti-
vity. Some of these methods serve
in determining the heat-physical
characteristics of rocks, construc-
tion materials, and so on in-place,
without resorting to extracting
materials and making specimens
/169/.

In the physical formulation,
the problem under consideration
can be represented as follows.
Some finite body, exhibiting high
thermal conductivity and temperature

diffusivity, with initial temperature T_0, is brought into contact through a heat-measuring transducer with the test mass (a semibounded body). The temperature of the mass $t(r, \tau)$ at the initial instant is assumed identical and, naturally, differing from the probe body temperature $t(r, 0) = 0$. If the reading is done from the initial mass temperature, then $t(r, 0) = 0$. After contact, the temperatures are equalized at a rate that is dependent on the heat-physical characteristics of the test mass. If we neglect heat transfer at the free (noncontacting) surfaces /17 of bodies, the differential equation of thermal conductivity for this case can be written as follows:

$$\frac{\partial t(r,\tau)}{\partial \tau} = a\left[\frac{\partial^2 t(r,\tau)}{\partial r^2} + \frac{2}{r}\cdot\frac{\partial t(r,\tau)}{\partial r}\right] \qquad (VII.10)$$

under the boundary conditions

$$t(R,\tau) = T(\tau); \quad \lambda f\frac{\partial t(R,\tau)}{\partial r} = c\frac{dT(\tau)}{d\tau} \qquad (VII.11)$$

The solutions to Eqs. (VII.1) are as follows:

$$\frac{t(R,\tau)}{T_0} = \frac{\beta}{\beta-\alpha}\exp(\beta^2 a\tau)\,\mathrm{erfc}(\beta \sqrt{a\tau}) - \frac{\alpha}{\beta-\alpha}\exp(\alpha^2 a\tau)\,\mathrm{erfc}(\alpha\sqrt{a\tau})$$

$$(VII.12)$$

$$-\frac{\partial t(R,\tau)}{\partial r}\cdot\frac{R}{T_0} = \frac{R}{\sqrt{\pi a\tau}} + a(\alpha R - 1)\exp(\alpha^2 a\tau)\,\mathrm{erfc}(\alpha\sqrt{a\tau}) -$$

$$-\beta(\beta R - 1)\exp(\beta^2 a\tau)\,\mathrm{erfc}(\beta\sqrt{a\tau}).$$

For convenience in practical measurements, Eqs. (VII.12) were tabulated and the plots shown in Fig. 94 were constructed for the equations. In each experiment measuring temperatures and fluxes twice is sufficient for determining thermal conductivity and temperature diffusivity.

Heat capacity can also be determined in these experiments, but this is not sensible, since there are more advanced methods for heat capacity measurements.

The potentialities of local heat-measurements permit also the effective determination of integrated heat-physical characteristics of complex heat-insulating enclosures in full-scale conditions. In some cases (for example, heat measurements of enclosures packed with fibrous or porous friable material), the method described below appears to be hardly the only effective approach /75/. At first, we select the section of the complex enclosure in which the heat flux is normal to the external and

192

internal enclosure surfaces. This operation is carried out with two heat flux transducers installed along the same normal to both sides of the wall. The absence of heat leakage along the wall /173 is estimated from the equality of the readings of the external and internal transducers in a steady-state regime. Then by disturbing the stationary conditions a transient regime is produced in which the effective heat capacity of the enclosure is determined from changes in the enthalpy of the enclosure and its temperature.
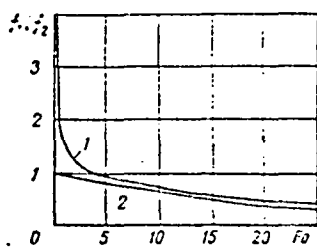
Fig. 94 Plot of the functions

$$\frac{\partial t}{\partial r} \cdot \frac{R}{T_0} = f_1(\tau) \quad \text{(curve 1)}$$

and $\frac{t}{T_0} = f_2(\tau)$ (curve 2)

The change in enthalpy is established on the basis of the recording readings c_1 and c_2 of the transducers installed on different sides of the enclosure,

$$Q = \int_{\tau_1}^{\tau_2} (q_1 - q_2) d\tau \qquad \text{(VII.13)}$$

In practice, integral (VII.13) is determined by planimetry of the area bounded by curves $q_1(\tau)$ and $q_2(\tau)$ (Fig. 95).

The effective volume heat capacity is calculated by the familiar formula:

$$\text{6ff} = \frac{Q}{6\Delta t} \qquad \text{(VII.14)}$$

Ordinarily, in formulas of the type (VII.14) the temperature change is customarily taken as averaged so that the scalar essentially of the heat capacity did not depend on the direction of thermal action. For convenience in measurements and for processing experimental data and calculations, it is best to relate the change in enthalpy to the temperature change at the enclosure surface. It is of interest to note that for enclosure components that are not symmetrical by arrangement, the heat capacity can depend substantially on which side the thermal action on the insulation occurs. In particular, for a home refrigerator door heat capacity for external action (change in room temperature) turns out to be about 50 percent higher than for internal action (change in operating regime of refrigerator) /76, 82/. The /174 thermal conductivity of the enclosure is determined in a steady-state regime according to Eq. (VII.1). Measurements for the walls of home refrigerators are given in Table 10.

193
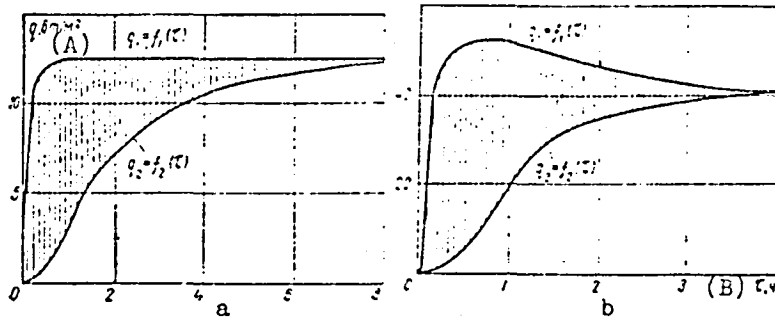
Fig. 95 Heat-measurement characteristics of
of transient regime of enclosure at constant
power (a) and temperature (b) of room

Key:

    A. W/m^2

    B. hours

Table 10

Компоненты ограждения (a)	δ, m	$t_{огр}$, (b)	q, кдж/м² (c)	(d) $c_{эфф}$, кдж/м³·град	(e) λ, вт/м·град
Стиропор (45 кг/м³) (f)	0.07	35	77	107	0,036
Сополимер СНП (g) Стиропор (35 кг/м³) (h)	0.003 0.077	10	175	148	0,042
Сополимер СНП (g) Стекловата (i) Сталь (j)	0.002 0.054 0.001	40	116	155	0,054
Сополимер СНП (g) Стиропор (35 кг/м³) (h) Сталь (j)	0.003 0.026 0.001	12	182	356	0,042

Key: a. Enclosure components
    b. $t_{enclosure}$
    c. kJ/m^2
    d. c_{eff}, $kJ/m^3 \cdot deg$
    e. $W/m \cdot deg$
    f. Expanded polystyrene (45 kg/m³)
    g. SNP copolymer

    h. Expanded polystyrene (35 kg/m³)
    i. Glass wool
    j. Steel

194

7. Direct Application of Transducers

Besides the above-described instruments, systems were developed in the LMTI for studies of the correlations of heat transfer in equipment and processes of new technology. Brief reports of some of these developments are the content of this present, concluding text section.

In the departments of thermal conductivity and dynamics of thermal processes, Institute of Technical Thermophysics, Ukrainian SSR Academy of Sciences, self-contained and banked heat flux transducers are used for investigating heat transfer through surfaces bounding interblade channels from above and from below. Here the heat transfer effect is significantly complicated by the presence of the so-called steaming eddy.

Sections of sandwich-type transducers were mounted in the surfaces of internally heated spheres for studies conducted in the department of combustion and two-phase nonisothermal systems, Institute of Technical Thermophysics, Ukrainian SSR Academy of Sciences. With these devices heat transfer was measured from the sphere to the boiling layer. The investigations are continuing and their results have been published in part /22/. In the same department probes with dissimilarly oriented heat-measurement receiving surfaces were prepared for measuring radiation characteristics of muffle heaters.

Fairly widespread use is made of a structure based on a compact refrigerator bearing a sandwich-type transducer on its facing surface. More than 40 of these structures were built. They are in service in the heat and mass transfer department, Institute of Technical Thermophysics, Ukrainian SSR Academy of Sciences and in the heat-physics laboratory, Scientific Research Institute of the Construction Industry (NIISP), for determining /175 the radiation characteristics of infrared drying equipment with flameless gas combustion.

Calorimeters made the following operations simpler:

a) balance tests of industrial electrolyzers for making alkali metals; owing to the high working temperature (to 800° C) nichrome-nickel sandwich-type transducers with enamel potting were built for these experiments

b) since 1965 processes of aging of the thermal insulation of heating networks buried underground have been studied in full-scale conditions

c) investigat'ons of heat transfer from heated walls to viscofriable materials (for example, sunflower, peanut, and other oilcakes)

d) investigations of the radiative characteristics of low-temperature electrical heaters and, based on a sandwich-type banked heat flux transducer, the development of a new instrument for these investigations

Let us look more closely at one of these investigations--study of heat transfer for the removal of ice glaze formations on the ground and on roads. This problem is particularly urgent for airfields, where ice glaze formations considerably complicates operating landing and takeoff strips. Ordinarily, during ice glazes the landing and takeoff strips are swept with hot jets from a jet engine mounted on a mobile chassis. During the jet sweeping periods with a virtually transparent jet at below-1000° C temperatures, the ice crust melts only at the surface, and evaporation considerably reduces the thermal effectiveness of the action taken. In regions with unstable meteorological conditions, combatting ice glaze sometimes becomes an object of continual concern, and fuel consumption is measured in the hundreds of tons a day.
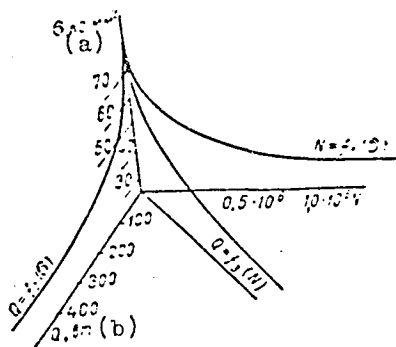
Fig. 96   Results of heat-measurements of heat losses during fatigue tests of glass-reinforced plastics

Key: a. kg/mm^2
     b. watts

It was noted that on sunny days the crust readily separates from concrete and is swept off landing strips in the solid state. Melting and evaporation are reduced and the capacity of the cleaning system increases by several-fold. So in the Riga laboratory of the State Scientific Research Institute of Civil Aviation (A. A. Mogutnov), a method was developed that provides for a combination of jet action with treatment of the surface with short-wave thermal radiation, for which the ice crust is transparent, to a large extent. Much of the radiant energy is absorbed at the ice-concrete interface; the ice melts and is easily separated and removed by the gas-air jets. /176

Through use of elements of the sandwich-type banked heat flux transducers, it was possible in full-scale conditions to determine the radiative characteristics of the ice glaze

coatings on concrete foundations, to analyze in detail all heat balance items, to find the optimal working regimes, and to set up a method of thermal calculation of necessary installations.

Casting and formation of steel ingots was investigated with heat-measurement equipment in the Institute of Casting Problems, Ukrainian SSR Academy of Sciences. Heat losses from the metal surface in the casting heads of large forged ingots can be measured with a unit developed on the basis of a sandwich-type transducer. The measurement results permitted deriving the correlations of the thermal functioning of the casting head and finding ways of improving the conditions of ingot formation. A batch of self-contained transducers was also installed on several of the most stressed elements of the installation for continuous steel casting.

Heat-measurement transducers were attached to specimens later subjected to fatigue failure in the Institute of Mechanics, Ukrainian SSR Academy of Sciences. It was thus possible to measure the energy of dissipation directly (Fig. 96).

The following quantities were laid out along the coordinate axes: maximum stress in the cycle σ_{max}, number of cycles to failure of the specimen N, and total heat losses Q during the test period.

The three-dimensional curve represents the locus of points at which specimen failure occurs. Noteworthy is the projection of this curve onto the Q vs. N plane. As the plot shows, the projection turns out to be a straight line; this means that the energy of dissipation in one cycle does not depend on the stress to which the specimen was loaded.

Investigations were begun on heat measurements of cold and hot treatment of food products in storage and processing conditions in the Kiev Technological Institute of the Food Industry, the Ukrainian Scientific Research Institute of the Meat and Dairy Industry, and in a number of other organizations, by V. G. Fedorov.

Sandwich-type transducers were embedded in drip pans for sublimation drying in the refrigeration installations department (V. I. Karpov) in the Kaliningrad Technological Institute of the Fishing Industry; as a result, the heat balance and temperature conditions of this new and promising kind of drying were investigated.

These examples do not exhaust the actual and prospective potentialities of heat-measurements. Experience shows forward-looking trends both in formulating new tasks and in solutions.

REFERENCES

1. Bol'shaya Sovetskaya Entsiklopediya /Great Soviet Encyclo-   /177
   pedia/, 2nd ed., Izd-vo BSE, Moscow, 1949-1958.

2. Korn, G., and Korn, T., Spravochnik po matematike /Handbook
   on Mathematics/, Izd-vo "Nauka," Moscow, 1968.

3. Entsiklopedicheskiy spravochnik /Encyclopedic Handbook/,
   Vol. 4, Izd-vo "Mashinostroyeniye," Moscow, 1947.

4. Spravochnik mashinostroitel'ya /Machinebuilder's Handbook/,
   Vol. ?, Mashgiz, Moscow, 1960.

5. Fizicheskiy entsiklopedicheskiy slovar' /Encyclopedic Physics
   Dictionary/, GNI "Sovetskaya entsiklopediya," Moscow,
   1960-1966.

6. Chaylds, U., Fizicheskiye postoyannyye /Physical Constants/,
   Fizmatgiz, Moscow, 1961.

7. Chirkin, V. S., Teplofizicheskiye svoystva materialov yader-
   noy tekhniki /Heat-Physical Properties of Nuclear Engineer-
   ing Materials/, Atomizdat, Moscow, 1968.

8. Der Grosse Brockhaus, 15 volumes, Leipzig, 1929-1933.

9. Encyclopedia Britannica, Chicago-London-Toronto, 1957.

10. Handbuch der Physik /Handbook of Physics/, Springer Verlag,
    1956-1961.

11. Handbook of Thermophysical Properties of Solid Materials,
    Vols. 1-5, Oxford, London-New York-Paris, Pergamon Press.
    1962.

12. Landolt-Bornstein, Physikalisch-chemische Tabellen /Physico-
    chemical Tables/, 5th ed., Springer Verlag, Berlin, 1936.

13. McGraw-Hill Encyclopedia of Science and Technology, US,
    McGraw-Hill Book Company, 1960.

14. Aydaraliev, A. A., Gerashchenko, O. A., and Putilin, M. I.,
    Metodika teplometrichnikh doslidzhen' organiv i tkanin
    /Methods of Heat-Measurement Studies of Organs and Tissues/,
    DAN URSR, Series B, No. 12, 1968.

15. Alad'yev, I. T., "Experimental determination of local and mean heat transfer coefficients for turbulent flow in tubes," Izv. AN SSSR, OTN, No. 11, 1951.

16. Alekseyev, N. I., and Shestopalov, L. M., "Optical mirror calorimeter," PTE, No. 1, 1968.

17. Amirkhanov, Kh. I., and Kerimov, A. M., "Study of heat capacity of water and water vapor near the bounding curve, including critical region," Teploenergetika, No. 9, 1957.

18. Angerer, E., Tekhnika fizicheskogo eksperimenta /Techniques of Physical Experiments/, Fizmatgiz, Moscow, 1962.

19. Armisted, R., and Keyes, D., "Film transducer for studying turbulence near wall," PNI, No. 1, 1968.

20. Astaymer, R. V., and Bakli, R. Ye., "Pyroelectric calorimeter for measuring energy and intensity of laser radiation," PNI, No. 12, 1967.

21. Babikova, Yu. F. et al, "Recording of heat fields in semiconductor instruments using photoemulsions," PTE, No. 1, 1968.

22. Babukha, G. L. et al, "Experimental study of heat transfer between immersed surfaces and fluidized bed," in the book: Teplo- i massoperenos /Heat and Mass Transfer/, Izd-vo "Nauka i tekhnika," Minsk, 1968.

23. Barskiy, Yu. P., Fridman, N. G., and Ivanitskaya, R. B., "Thermographic calorimetry in simplest formulation," in the book: Trudy 1-go soveshchaniya po termografii /Proceedings of the First Conference on Thermography/, Izd-vo AN SSSR, Moscow-Leningrad, 1955.

24. Barskiy, Yu. P., "Theory of diathermic heat measurements in nonstationary temperature conditions," in the book: Trudy NIIStroykeramiki /Transactions of the Scientific Research Institute of Construction Ceramics/, No. 18, Gosstroyizdat, Moscow, 1961. /178

25. Barskiy, Yu. P., "Method and instrument for simultaneous measurement of heat-physical coefficients and heats of reactions of phase transformations in a wide temperature range," in the book: Trudy NIIStroykeramiki, No. 20, Gosstroyizdat, Moscow, 1962.

26. Barskiy, Yu. P., "Determination of heat capacity and heats of reaction using heat analysis," in the book: Trudy NIIStroykeramiki, No. 20, Gosstroyizdat, Moscow, 1962.

27. Bakhvalov, G. R., Birkman, L. N., and Labutin, V. P., Spravochnik gal'vanostera /Electroplating Handbook/, Metallurgizdat, Moscow, 1954.

28. Berg, L. G., Vvedeniye v termografiyu /Introduction to Thermography/, Izd-vo "Nauka," Moscow, 1969.

29. Bogdanov, G. B., "Potentialities of ferrites in solving problems of measurement techniques," Izmeritel'naya tekhnika, No. 1, 1963.

30. Bogdanov, G. B., and Bokrinskaya, A. A., Ferritovyye termistory /Ferrite Thermistors/, Izd-vo "Tekhnika," Kiev, 1964.

31. Borzyak, Yu. G. et al, "Ferromagnetic dielectric compound," Avt. svid. /Author's Certificate/, No. 169706 (Byulleten' Izobreniya, No. 7, 1965).

32. Borovikov, S. I., Gerashchenko, O. A., and Fedorov, V. G., "Radiation furnace," in the book: Teploobmin ta gidrodinamika /Heat Transfer and Hydrodynamics/, Izd-vo AN URSR, Kiev, 1962, No. 12.

33. Borkhert, R., and Yubitts, V., Tekhnika infrakrasnogo nagreva /Infrared Heating Techniques/, Gosenergoizdat, Moscow-Leningrad, 1963.

34. Bocharov, V. V., Katulin, V. A., and Smirnov, V. G., "Calorimeters for measuring short light pulses with low energy," PTE, No. 1, 1967.

35. Braun, Pitts, and Leppert, "Heat transfer in forced convection from a uniformly heated medium," Trudy AOIM-Teperedacha (Seriya S), Vol. 84, No. 2, 1962.

36. Briksman, B. A. et al, "Calorimetric dosimetry of mixed reactor of VVR-Ts reactor," in the book: Trudy 2-go koordinatsionnogo soveshchaniya po dozimetrii bol'shikh doz /Transactions of the Second Coordination Conference on Large-Dose Dosimetry/, Izd-vo "Fan," Tashkent, 1966.

37. Buravoy, S. Ye., "Low-inertia radiation calorimeter," Izv. vuzov. Priborostroyeniye, Vol. 10, No. 2, 1967.

38. Buravoy, S. Ye., Platunov, Ye. S., and Shramko, Yu. P., "Methods of investigating heat-physical properties of solid materials in regime of monotonic temperature change," in the book: Teplo- i massoperenos, Izd-vo "Nauka i tekhnika," Minsk, 1968, No. 7.

39. Burshteyn, A. I., Fizicheskiye osnovy rascheta poluprovodnikovykh termoelektricheskikh ustroystv /Physical Fundamentals in Calculating Semiconductor Thermoelectric Devices/, Fizmatgiz, Moscow, 1962.

40. Vasil'yev, L. L., and Frayman, Yu. Ye., Teplofizicheskiye svoystva plokhikh provodnikov tepla /Heat-Physical Properties of Poor Heat Conductors/, Izd-vo "Nauka i tekhnika," Minsk, 1967.

41. Vekshinskiy, S. A., Novyy metod metallograficheskogo issledovaniya splavov /New Method of Metallographic Investigation of Alloys/, Gostekhizdat, Moscow-Leningrad, 1944.

42. Vinchell, A., Opticheskaya mineralogiya /Optical Mineralogy/, IL, Moscow, 1954.

43. Vitte, N. K., Teplovoy obmen cheloveka i yego gigiyenicheskoye znacheniye /Heat Transfer of Man and Its Hygienic Significance/, Gosmedizdat, Kiev, 1956.

44. Volokhov, G. M., "Substantiation of several methods of determining heat-physical characteristics based on analysis of two-dimensional temperature fields," in the book: Teplo- i massoperenos, Izd-vo "Nauka i tekhnika," Minsk, 1968, No. 7.

45. Voronkova, Ye. M. et al, Opticheskiye materialy dlya infrakrasnoy tekhniki /Optical Materials for Infrared Techniques/, Izd-vo "Nauka," Moscow, 1965.

46. Vrolik, I., "Heat flux receiver for rocket engine," in the book: Izmereniye nestatsionarnykh temperatur i teplovykh potokov /Measuring Nonstationary Temperatures and Heat Fluxes/, Izd-vo "Mir," Moscow, 1966.

47. Vishatina, O. I. et al, "Quantitative estimation of variation in tissue blood circulation recorded thermoelectrically," Fiziologichniy zhurnal, Vol. 14, No. 1, 1968.

48. Vyshatina, A. I., and Gerashchenko, O. A., "Possibility of quantitative estimation of variation in tissue blood circulation by thermoelectric method," in the book: Fiziologiya serdechnogo vybrosa /Physiology of Cardiac Output/, Izd-vo "Naukova dumka," Kiev, 1968.

201

49. Gerashchenko, O. A., "Designing and building a heat flux   /179
        detector," Udostovereniye o registratsii No 5552 s pri-
        oritetom 5 fevralya 1957 g. /Registration Certificate
        No. 5552 with Priority as of 5 February 1957/, Committee
        on Inventions and Discoveries under the USSR Council of
        Ministers.

50. Gerashchenko, O. A., and Fedorov, V. G., "Instrument for
        measuring local heat fluxes," Teploenergetika, No. 6,
        1958.

51. Gerashchenko, O. A., and Fedorov, V. G., "Heat flux trans-
        ducer," Perevodoy nauchno-tekhnicheskiy i proizvodstvennyy
        opyt, No. P-58-80/3, VINITI, Moscow, 1958.

52. Gerashchenko, O. A., and Fedorov, V. G., "Problem of inves-
        tigating heat transfer between wall and granular material,"
        in the book: Zbirnik prats' ITE /Collection of Articles
        of the ITE/, Izd-vo AN URSR, Kiev, 1959, no. 16.

53. Gerashchenko, O. A., and Fedorov, V. G., "Instrument for
        measuring local values of intense heat fluxes," Avtomatika
        i priborostroyeniye, No. A-28(173), ITI, Kiev, 1961.

54. Gerashchenko, O. A., Khrizman, S. S., Dekhtyarenko, P. I.,
        and Karpenko, V. P., "Selecting automatic control scheme
        of a differential calorimeter," in the book: Voprosy mag-
        nitnykh izmereniy /Problems of Magnetic Measurements/,
        Izd-vo AN URSR, Kiev, 1961.

55. Gerashchenko, O. A., and Fedorov, V. G., "Instrument for
        measuring radiative heat fluxes of high intensity," Pere-
        dovoy nauchno-tekhnicheskiy i proizvodstvennyy opyt,
        No. P-62-45/4, GOSINTI, Moscow, 1962.

56. Gerashchenko, O. A., Dekhtyarenko, P. I., and Karpenko, V. P.
        V. P., "Analysis of automatic control schemes of differen-
        tial calorimeter," in the book: Novyye metody i apparatura
        dlya ispytaniya ferromagnitnykh materialov /New Methods
        and Equipment for Testing Ferromagnetic Materials/,
        No. 64 (124), Standartgiz, Moscow, 1962.

57. Gerashchenko, O. A., and Fedorov, V. G., "Compensation radio-
        meter," Avtomatika i priborostroyeniye, No. 2, 1962.

58. Gerashchenko, O. A., and Fedorov, V. G., "Low-inertia radia-
        tor of intense heat fluxes," Avtomatika i priborostroyeniye,
        No. 2, 1962.

59. Gerashchenko, O. A., and Fedorov, V. G., "Spiral heat flux transducer," Peredovoy nauchno-tekhnicheskiy i proizvodstvennyy opyt, No. 26-64-1028/54, GOSINTI, Moscow, 1964.

60. Gerashchenko, O. A., Lebedev, A. D., and Fedorov, V. G., "Sandwich-type heat flux transducer," Peredovoy nauchno-tekhnicheskiy i proizvodstvennyy opyt, No. 26-64-1162/57, GOSINTI, Moscow, 1964.

61. Gerashchenko, O. A., and Fedorov, V. G., "Disk type heat flux transducers," Peredovoy nauchno-tekhnicheskiy i proizvodstvennyy opyt, No. 26-64-1029/55, GOSINTI, Moscow, 1964.

62. Gerashchenko, O. A., and Fedorov, V. G., Tekhnika teplotekhnicheskogo eksperimenta /Techniques of Heat-Measurement Experiments/, Izd-vo "Naukova dumka," Kiev, 1964.

63. Gerashchenko, O. A., Dekhtyarenko, P. I., Karpenko, V. P., and Khrizman, S. S., "Automatic differential calorimeter for magnetic measurements in a wide frequency range," in the book: Avtomaticheskiy kontrol' i metody elektricheskikh izmereniy /Automatic Control and Methods of Electrical Measurements/, Izd-vo SO AN SSSR, Novosibirsk, 1964, No. 2.

64. Gerashchenko, O. A., and Ionova, N. N., "Study of thermal emf of galvanic thermocouples," in the book: Avtomaticheskiy kontrol' i metody elektricheskikh izmereniy /Automatic Control and Methods of Electrical Measurements/, Izd-vo SO AN SSSR, Novosibirsk, 1965, No. 2.

65. Gerashchenko, O. A., and Fedorov, V. G., "Thermoelectric heat flux measuring elements," in the book: Avtomaticheskiy kontrol' i metody elektricheskikh izmereniy, Izd-vo SO AN SSSR, Novosibirsk, 1965, No. 2.

66. Gerashchenko, O. A., and Fedorov, V. G., Teplovyye i temperaturnyye izmereniya. Spravochnoye rukovodstvo /Thermal and Temperature Measurements, a reference guide/, Izd-vo "Naukova dumka," Kiev, 1965.

67. Gerashchenko, O. A., and Fedorov, V. G., "Study of high-temperature processes using heat flux transducers," in the book: Eksperimental'naya tekhnika i metodika vysokotemperaturnykh izmereniy /Experimental Techniques and Methods of High-Temperature Measurements/, Izd-vo "Nauka," Moscow, 1966.

68. Gerashchenko, O. A., and Ionova, N. N., "Thermal emf of galvanic thermocouples," Izmeritel'naya tekhnika, No. 1, 1966.

69. Gerashchenko, O. A., and Fedorov, V. G., "Radiation furnace for temperatures to 1700° C with inertialess reflective insulation," in the book: Eksperimental'naya tekhnika i metody vysokotemperaturnykh izmereniy, Izd-vo "Naukova dumka," Moscow, 1966. /180

70. Gerashchenko, O. A., and Ionova, N. N., "New instrument for determining coefficients of thermal conductivity," in the book: Teplofizicheskiye svoystva veshchestv /Heat-Physical Properties of Substances/, Izd-vo "Naukova dumka," Kiev, 1966.

71. Gerashchenko, O. A., and Fedorov, V. G., "Absolute instruments for measuring high-intensity radiative fluxes," in the book: Eksperimental'naya tekhnika i metody vysokotemperaturnykh izmereniy, Izd-vo "Nauka," Moscow, 1966.

72. Gerashchenko, O. A. et al, "High-temperature electric furnace," Avt. svid. No. 180271 (Byull. izobr., No. 7, 1966).

73. Gerashchenko, O. A., "Strength of signal of cross-grained heat flux transducers," Zbornik radova YUREMA-67 /Collection of Articles at the YUREMA-67 Conference, Zagreb, 1967.

74. Gerashchenko, O. A., Karpenko, V. G., and Sazhina, S. A., "Determination of absorptivity by method of two radiometers and calorimeter," Energetika i elektrofikatsiya, No. 1 (37), 1968.

75. Gerashchenko, O. A., Karpenko, T. G., Pilipenko, A. M., and Fedorov, V. G., "Applications of heat flux transducers," in the book: Teplo- i massoperenos, Izd-vo "Nauka i tekhnika," Minsk, 1968, No. 7.

76. Gerashchenko, O. A., Grishchenko, T. G., Pilipenko, A. M., and Fedorov, V. G., "Heat-measurement determination of heat-physical characteristics," in the book: Teplo- i massoperenos, Izd-vo "Nauka i tekhnika," Minsk, 1968, No. 7.

77. Gerashchenko, O. A., Grishchenko, T. G., Rolik, A. I., and Yakovlev, A. I., "Thermal conductivity of ferromagnetic dielectric compound with fillers," Elektrotekhnicheskaya promyshlennost', No. 208, 1968.

204

78. Gerashchenko, O. A., Karpenko, V. G., and Chimisov, Yu. M., "Allowing for the effect of transducer thermal resistance in the measurement of convective heat fluxes," in the book: Konvektivnyy teploobmen /Convective Heat Transfer/, Izd-vo "Naukova dumka," Kiev, 1968.

79. Gerashchenko, O. A., Yakovlev, A. I., and Grishchenko, T. G., "Thermal conductivity of insulation materials," Energetika i elektrifikatsiya, No. 4/40, 1968.

80. Gerashchenko, O. A., "Problems of the applications of heat-measurement methods," Zbornik radova YUREMA-68, Zagreb, 1968.

81. Gerashchenko, O. A., and Dmitriyev, V. I., "Heat flux transducer," Avt. svid. No. 218493 (Byulleten' izobreteniy, No. 17, 1968).

82. Gerashchenko, O. A., Fedorov, V. G., and Pilipenko, A. M., "Method of determining heat capacity of insulation enclosures," Avt. svid. No. 215564 (Byulleten' izobreteniy, No. 13, 1968).

83. Gerashchenko, O. A., Karpenko, V. G., and Tatarinov, E. A., "Adiabatic calorimeter for contact calibration of heat flux transducers," in the book: Teplofizika i teplotekhnika, Izd-vo "Naukova dumka," Kiev, 1968, No. 16.

84. Gerashchenko, O. A., Karpenko, V. G., and Chimisov, Yu. M., "Inertial radiometer for measuring radiative heat fluxes," in the book: Voprosy tekhnicheskoy teplofiziki /Problems of Engineering Heat Physics/, Izd-vo "Naukova dumka," Kiev, 1968.

85. Gerashchenko, O. A., and Grishchenko, T. G., "Determination of thermal conductivity of new materials," in the book: Voprosy tekhnicheskoy teplofiziki, Izd-vo "Naukova dumka," Kiev, 1968.

86. Gerashchenko, O. A., Karpenko, V. G., and Gorshunova, N. N., "Separate measurement of radiative and convective components of heat flux using heat flux transducer," in the book: Voprosy tekhnicheskoy teplofiziki, Izd-vo "Naukova dumka," Kiev, 1968.

87. Gerashchenko, O. A., Karpenko, V. G., and Sazhina, S. A., "Determination of absorptivity by method of two radiometers and calorimeter," in the book: Voprosy tekhnicheskoy teplofiziki, Izd-vo "Naukova dumka," Kiev, 1968.

88. Gerashenko, O. A. et al, "Method of determining direction of isothermal lines, heat flux vector, and temperature field gradient of nonisothermal objects," Avt. svid. No. 246120 (Byull. izobr., No. 20, 1969).

89. Gerashchenko, O. A., Lisovenko, A. T., and Karpenko, V. G., /181 "Heat flux transducer," Avt. svid. No. 243902 (Byulleten' izobreteniy, No. 17, 1969).

90. Golovanov, A. B., "Method of determining coefficients of thermal conductivity of insulation materials for different mechanical loads and a unit for this purpose," Avt. svid. No. 162688 (Byulleten' izobreteniy, No. 10, 1964).

91. Gordov, A. N., and Ergardt, N. N., "Some sources of error in measuring temperatures with thermocouples," Zavodskaya laboratoriya, No. 12, 1953.

92. Gordov, A. N., Osnovy pirometrii /Essentials of Pyrometry/, Izd-vo "Metallurgiya," Leningrad-Moscow, 1964.

93. Grishin, V. A., "Method of instantaneous compensation in heat measurements and its theory," IFZh, Vol. 4, No. 10, 1966.

94. Grishin, V. A., "Heat measurements by instantaneous compensation method," in the book: Teplo- i massoperenos, Izd-vo AN BSSR, Minsk, 1962, No. 1.

95. Grishin, V. A., "Compensation method of determining local coefficient of thermal conductivity," Avt. svid. No. 183436 (Byull. izobr., No. 13, 1966).

96. Gumener, P. I., Izucheniye termoregulyatsii v gigiyene i fiziologii truda /Study of Thermoregulation in Hygiene and Work Physiology/, Medgiz, Moscow, 1962.

97. Gutarev, V. V., "Heat transfer in initial section of straight tube for different entrance shapes," in the book: Trudy Moskovskogo instituta khimicheskogo mashinostroyeniya /Transactions of the Moscow Institute of Chemical Machine Building/, Vol. 15, No. 1, Syaz'izdat, Moscow, 1958.

98. Gutri, A., and Uokerling, R., Vakuumnoye oborudovaniye i vakuumnaya tekhnika /Vacuum Equipment and Vacuum Technology/, IL, Moscow, 1951.

99. Gukhman, A. A., and Ilyukhin, N. V., *Osnovy ucheniya o teploobmene pri bol'shikh skorostyakh* /Essential Concepts of Heat Transfer at High Rates/, Mashgiz, Moscow, 1951.

100. Dvernyakov, V. S., and Pasichniy, V. V. "Determination of parameters with a special solar unit (SGU)," *DAN URSR*, No. 6, 1966.

101. Devyatkova, Ye. D. et al, "Fused quartz as a specimen material in thermal conductivity measurements," *Fizika tverdogo tela*, Vol. 2, No. 4, 1960.

102. Dzhemison, Dzh. E. et al, *Fizika i tekhnika infrakrasnogo izlucheniya* /Physics and Technology of Infrared Radiation/, Izd-vo "Sovetskoye radio," Moscow, 1965.

103. Dobrokhotov, A. N., *Rychazhnyye vesy* /Beam Balances/, 2nd ed., Mashgiz, Moscow-Leningrad, 1939.

104. Dudnik, D. M., "Calculations of low-inertia heat flux meter," in the book: *Trudy Odesskogo tekhnologicheskogo instituta pishchevoy i kholidil'noy promyshlennosti* /Transactions of the Odessa Technological Institute of the Food and Refrigeration Industry/, Oblizdat, Odessa, 1962, No. 2.

105. Dushin, I. F., and Nikolayevskiy, A. P., "Method of determining thermal conductivity of materials," *Avt. svid.* No. 76265 (*Svod izobreteniy*, No. 8, 1949).

106. Deshman, S., *Nauchnyye osnovy vakuumnoy tekhniki* /Scientific Essentials of Vacuum Technology/, Izd-vo "Mir," Moscow, 1964.

107. Yermolin, V. K., "Intensification of convective heat transfer in tube in curved flow conditions," *IFZh*, No. 11, 1960.

108. Zhukovskiy, V. S., Kireyev, A. V., and Shamshev, L. P., "Optical method of studying the distribution of heat transfer coefficient in a forced flow," *ZhTF*, Vol. 4, No. 10, 1934.

109. Zalkind, I. Ya., Anan'in, A. V., and Kormer, I. M., "Low-inertia calorimeter of ORGRES," *Teploenergetika*, No. 7, 1960.

110. Zalkind, I. Ya. et al, "Instrument for determining the co-efficients of thermal conductivity by stationary flow method," Avt. svid. No. 160341 (Byulleten' izobreteniy, No. 3, 1964).

111. Ivanov, N. S., "Calorimeter installations for field studies," in the book: Teplo- i massoobmen v pochvakh i gornykh po-rodakh /Heat and Mass Transfer in Soils and Rock/, Izd-vo AN SSSR, Moscow, 1961.

112. Ivanov, N. S., "Methods of measuring heat fluxes in rock," in the book: Teplo- i massoperenos v merzlykh pochvakh i gornykh porodakh /Heat and Mass Transfer in Frozen Soils and Rock/, Izd-vo AN SSSR, Moscow, 1961.

113. Ivanov, G. P., Teploobmen mezhdu slitkom i izlozhnitsey /Heat Transfer Between Ingot and Ingot Mold/, Metallur-gizdat, Moscow, 1951.

114. Iordanishvili, Ye. K., Termoelektricheskiye istochniki pitaniya /Thermoelectric Power Supplies/, Izd-vo "Sovet-skoye radio," Moscow, 1968.

115. Ipatov, Yu. S. et al, "Instruments for thermal conducti-vity measurements," in the book: Issledovaniya v ob-lasti teplovykh i temperaturnykh izmereniy /Studies in Thermal and Temperature Measurements/, No. 63 (123), Standartizdat, Moscow-Leningrad, 1962.

116. Kazakov, N. F., Diffuzionnaya svarka v vakuume metallov, splavov i nemetallicheskikh materialov /Diffusion Weld-ing in Vacuo of Metals, Alloys, and Nonmetallic Mater-ials/, Izd-vo MVO, Moscow, 1965.

117. Kazakov, N. F., Diffuzionnaya svarka v vakuume /Diffusion Welding in Vacuum/, Izd-vo "Znaniye," Moscow, 1966.

118. Kalitin, N. N., "New type of actinometer for measuring voltage of solar radiation," Meteorologicheskiy vestnik, No. 1, 1927.

119. Kalitin, N. N., "New type of Arago-Davy actinometer." Mete-orologicheskiy vestnik, No. 5, 1927.

120. Kalitin, N. N., Aktinometriya /Actinometry/, Gidrometeoiz-dat, Leningrad-Moscow, 1938.

121. Kal've, E., and Prat, A., Mikrokalorimetriya /Microcalori-metry/, IL, Moscow, 1963.

/18

122. Kapustinskiy, A. F., and Barskiy, Yu. P., "Thermographic calorimetry," in the book: Trudy 1-go soveshchaniya po termografii /Transactions of First Conference on Thermography/, Izd-vo AN SSSR, Moscow-Leningrad, 1955.

123. Karandeyev, K. B., and Shtamberger, G. A., Obobshchennaya teoriya mostovykh tsepey peremennogo toka /Generalized Theory of Alternating-Current Bridge Circuits/, Siberian Division, USSR Academy of Sciences, Novosibirsk, 1961.

124. Karslou, G., and Yeger, D., Teploprovodnost' tverdykh tel /Thermal Conductivity of Solids/, Izd-vo "Nauka," Moscow, 1964.

125. Kats, N. V., Metallizatsiya raspyleniyem /Metallizing by Sputtering/, Izd-vo Khar'kovskiy Dom Tekhniki, 1940.

126. Kedrolivanskiy, V. N., and Sternzat, M. S., Meteorologicheskiye pribory /Meteorological Instruments/, Gidrometeoizdat, Leningrad, 1953.

127. Kimmitt, M., Prior, A., and Roberts, V., "Measurements in the far infrared region," in the book: Diagnostika plazmy /Plasma Diagnostics/, Izd-vo "Mir," Moscow, 1967.

128. Kintsi, F., and Sosa, S., "Characteristics of output voltage of axial heat flux transducers," PNI, No. 5, 1966.

129. Kirpichev, M. V., "Study of heat transfer in individual areas of a cylindrical body in an air current," in the book: Trudy Leningradskoy fiziko-tekhnicheskoy laboratorii /Transactions of the Leningrad Engineering Physics Laboratory/, No. 2, Lenizdat, Leningrad, 1926.

130. Kovalev, S. N. et al, Abrazivnyy instrument iz sinteticheskikh almazov /Synthetic Diamond Abrasive Tool/, Izd-vo "Tekhnika," Kiev, 1966.

131. Kozdoba, L. A., Elektromodelirovaniye temperaturnykh poley v detalyakh sudovykh energeticheskikh ustanovok /Electrical Modeling of Temperature Fields in Parts of Marine Power Plants/, Izd-vo "Sudostroyeniye," Leningrad, 1964.

132. Kozyrev, B. P., and Buznikov, A. A., "Multichamber blackbody," Izv. LETI, No. 15, 1966.

133. Kozyrev, B. P., and Buznikov, A. A., "Model of a black-body," Avt. svid. No. 164077 (Byulleten' izobreteniy, No. 14, 1964).

134. Kokorev, D. T., "Compensation radiometer," in the book: Voprosy teploperedachi i metody opredeleniya teplofizicheskikh kharakteristik. Trudy MIKhM /Problems of Heat Transfer and Methods of Determining Heat-Physical Characteristics, Transaction of the Moscow Institute of Chemical Machine Building/, Svyaz'izdat, Moscow, 1958, No. 15.

135. Kolenko, Ye. A., Termoelektricheskiye okhlazhdayushchiye pribory /Thermoelectric Cooling Instruments/, Izd-vo "Nauka," Leningrad, 1967.

136. Kolesnikov, A. G., and Speranskaya, A. A., "Instrument for Determining Heat Fluxes," Izv. AN SSSR, Ser. geofiz., No. 11, 1958.

137. Kondrat'yev, G. M., Pribory dlya skorostnogo opredeleniya teplovykh svoystv materialov /Instrument for Rapid Determination of Thermal Properties of Materials/, Mashgiz, Moscow-Leningrad, 1949.

138. Kondrat'yev, G. M., Regulyarnyy teplovoy rezhim /Regular Thermal Regime/, Gostekhizdat, Moscow, 1953.

139. Konozenko, I. D., and Zaika, Zh. A., Pribory infrakrasnoy radiometrii na osnove poluprovodnikovykh bolometrov /Instruments of Infrared Radiometry Based on Semiconductor Bolometers/, Izd-vo "Naukova dumka," Kiev, 1969.

140. Kononko, V. P. et al, "Radiation pyrometer of the reflector type," Informatsionnoye pis'mo, No. 12 (99), Izd-vo "Naukova dumka," Kiev, 1969.

141. Kononko, V. P. et al, "Radiation pyrometer for measuring the temperature of nonisothermal objects," Avt. svid. No. 219247 (Byulleten' izobreteniy, No. 18, 1968).

142. Kochin, N. Ye., Vektornoye ischisleniye i nachala tenzornogo ischisleniya /Vector Calculus and Principles of Tensor Calculation/, Izd-vo AN SSSR, Moscow, 1951.

143. Kocho, V. S., "Study of heat transfer in the working space of open-hearth furnaces," Stal', No. 3, 1950.

144. Kremenchugskiy, L. S., Mal'nev, A. F., and Samoylov, V. P., /183
"Large-area pyroelectric radiation receiver," PTE, No. 6,
1966.

145. Kriksunov, L. Z., and Usol'tsev, I. F., Infrakrasnyye sis-
temy obnaruzheniya, pelengatsii i avtomaticheskogo so-
provozhdeniya dvizhushchikhsya ob"yektov /Infrared Sys-
tems for Detecting, Direction Finding, and Automatic
Tracking of Moving Objects/, Izd-vo "Sovetskoye radio,"
Moscow, 1968.

146. Kruzhilin, G. N., and Shvab, V. A., "New method of deter-
mining heat transfer coefficient field at surface of a
body swept by a liquid flow," ZhTF, Vol. 5, No. 3, 1935.

147. Kruzhilin, G. N., and Shvab, V. A., "Study of alpha-field
at the surface of a right cylinder swept by a transverse
air flow," ZhTF, Vol. 5, No. 4, 1935.

148. Krylov, A. N., O nekotorykh differentsial'nykh uravneniyakh
matematicheskoy fiziki /Some Differential Equations of
Mathematical Physics/, Gostekhizdat, Moscow-Leningrad,
1950.

149. Krylov, N. A., Radiotekhnicheskiye metody kontrolya kaches-
tva zhelezobetona /Radiotechnical Methods of Reinforced
Concrete Quality Control/, Stroyizdat, Leningrad-Moscow,
1966.

150. Kudryavtsev, Ye. V., Chakalev, K. N., and Shumakov, N. V.,
Nestatsionarnyy teploobmen /Nonstationary Heat Transfer/,
Izd-vo AN SSSR, Moscow, 1961.

151. Kuznetsov, L. A., "Heat transfer of a circular air jet
streaming in a crack," Energomashinostroyeniye, No. 11,
1959.

152. Lebedev, P. D., Sushka infrakrasnymi luchami /Drying with
Infrared Rays/, Gosenergoizdat, Moscow, 1955.

153. Lekont, Zh., Infrakrasnoye izlucheniye /Infrared Radia-
tion/, GIFML, Moscow, 1955.

154. Lel'chuk, V. L., "Heat transfer and hydraulic drag during
high-speed flow," ZhTF, Vol. 9, No. 9, 1939.

155. Lisovenko, A T. et al, "Studies of thermal operating
regime of working chamber of a breadbaking oven," Khlebo-
pekarnaya i konditerskaya promyshlennost', No. 12, 1957.

211

156. Lisovenko, O. T. et al, "Role of radiative and convective heat transfer in blind-end and through-type conveyor breadbaking ovens," in the book: 34-a naukova konferentsiya /34th Scientific Conference/, Izd-vo KTIPP, Kiev, 1968.

157. Lykov, A. V. et al, "Method and equipment for integrated study of heat-physical characteristics of materials in a broad temperature range," in the book: Teplo- i massoperenos, Izd-vo "Nauka i tekhnika," Minsk, 1966, No. 7.

158. Mal'tsev, V. A., "Study of movement of gases and heat transfer in rotating rotors," Vestnik elektropromyshlennosti, No. 11, 1962.

159. Manko, G., Payka i pripoi /Soldering and Solders/, Izd-vo "Mashinostroyeniye," Moscow, 1968.

160. Margolin, I. A., and Rumyantsev, N. P., Osnovy infrakrasnoy tekhniki /Essentials of Infrared Equipment/, Voyenizdat, Moscow, 1957.

161. Markov, M. N., "Amplifier for infrared spectrophotometer," ZhTF, Vol. 24, No. 10, 1954.

162. Markov, M. N., "Bi-Pb alloy-based bolometers," DAN SSSR, Vol. 108, No. 3, 1956.

163. Markov, M. N., Priyemniki infrakrasnogo izlucheniya /Infrared Radiation Receivers/, Izd-vo "Nauka," Moscow, 1968.

164. Meyerovich, I. G., and Kertselli, I. Yu., "Nonstationary method of measuring contact thermal resistances and coefficients of thermal conductivity," in the book: Teplo- i massoperenos, Izd-vo "Nauka i tekhnika," Minsk, 1966, No. 7.

165. Mendeleyev, D. I., "Exact weighing procedures," Sochineniya /Collected Works/, Vol. 22, Izd-vo AN SSSR, Leningrad-Moscow, 1950.

166. Mirlin, D. N., "Semiconductor bolometers," in the book: Poluprovodniki v nauke i tekhnike /Semiconductors in Science and Technology/, Izd-vo AN SSSR, Moscow-Leningrad, 1957, No. 1.

167. Mirlin, D. N., "Electrical fluctuations in semiconductors," in the book: Poluprovodniki v nauke i tekhnike, Izd-vo AN SSSR, Moscow-Leningrad, 1958, No. 2.

168. Mikhel'son, V. A., "New V. A. Mikhel'son actinometer,"
Meteorologicheskiy vestnik, Vol. 18, No. 4, 1906.

169. Morachevskiy, I. I., Spektor, B. V., and Ryazantsev, V.
I., "Method and instrument for determining heat-physical
characteristics of materials--nondestructive approach,"
in the book: Teplo- i massoperenos, Izd-vo AN BSSR,
Minsk, No. 1, 1962.

170. Mullakhmetov, R. Kh., and Khorn, Ye. A., "Solving inverse
problem of thermal conductivity for case of unbounded
plate by least-squares method," in the book: Gidroaero-   /184
dinamika /Hydro-aerodynamics/, Izd-vo Khar'kovskiy gosu-
darstvennyy universitet, Khar'kov, 1967, No. 5.

171. Meyts, B., and Perls, T., "Transducer for measuring heat
intensity," PNI, Vol. 32, No. 3, 1961.

172. Nerele, and Stikford, "Thin-walled radiative heat flux
transducer," Raketnaya tekhnika i kosmonavtika, Vol. 2,
No. 9, 1964.

173. Ozhigov, G. Ye., Smirnov, V. G., and Sokovishin, Yu. A.,
"Fabrication of thermopile and method of experimental
detemination of its time constant," IFZh, Vol. 4, No. 10,
1961.

174. Oleynik, B. N., "Studies in the measurement of thermal
quantities," in the book: Nauchno-issledovatel'skiye
raboty v oblasti metrologii /Scientific Research Studies
in Metrology/, No. 76 (136), Standartgiz, Moscow-Lenin-
grad, 1965.

175. Oleynik, B. N., Chadovich, T. Z., and Kirichenko, Yu. A.,
"Device for determining coefficient of thermal conducti-
vity," Avt. svid. No. 156323 (Byulleten' izobreteniy,
No. 15, 1963).

176. Pankratov, N. A., "Ratio of specific and threshold sensi-
tivity of chamber of nonselective opticoacoustic receiver
with its time constant," Optiko-mekhanicheskaya promysh-
lennost', No. 2, 1957.

177. Pereleshina, A. P., "Results of experimental studies of
thermal emf in thermistors," IFZh, No. 4, 1960.

178. Perren De Brishambo, Sh., Solnechnoye izlucheniye i radi-
atsionnyy obmen v atmosfere /Solar Radiation and Radia-
tion Exchange in the Atmosphere/, Izd-vo "Mir," Moscow,
1966.

179. Petukhov, B. S., Opytnoye izucheniye protsessov teploperedachi /Experimental Study of Heat Transfer Processes/, Gosenergoizdat, Moscow-Leningrad, 1952.

180. Petukhov, B. S., Detlaf, A. A., and Kirillov, V. V., "Experimental study of local heat transfer of a plate in a subsonic air flow," ZhTF, Vol. 24, No. 10, 1954.

181. Pikashov, V. S. et al, "Narrow-angle full-radiation radiometer-probe," TFVT, No. 2, 1969.

182. Piskunov, A. A., and El'ke, I. N., "Full-radiation calorimeter," Stal', No. 8, 1964.

183. Platen, B., "Multipiston high-pressure and high-temperature equipment," in the book: Sovremennaya tekhnika sverkhvysokikh davleniy /Modern Equipment of Ultrahigh Pressures/, Izd-vo "Mir," Moscow, 1964.

184. Platunov, Ye. S., and Kurepin, V. V., "Device for high-speed measurement of coefficients of thermal conductivity of materials in the 150 to 400° C range," Avt. svid. No. 168500 (Byulleten' izobreteniy, No. 4, 1965.).

185. Platunov, Ye. S., and Kurepin, V. V., "Method of determining heat-physical characteristics of materials," Avt. svid. No. 219259 (Byulleten' izobreteniy, No. 4, 1965).

186. Poverka priborov dlya temperaturnykh i teplovykh izmereniy /Verification of Instruments for Temperature and Thermal Measurements/, Standartgiz, Moscow, 1965.

187. Pol', R. V., Vvedeniye v fiziku /Introduction to Physics/, Vols. 1-3, Fizmatgiz, Moscow, 1957-1965.

188. Polyak, B. G., Geotermicheskiye osobennosti sovremennogo vulkanizma /Geothermal Characteristics of Current Volcanism/, Izd-vo "Nauka," Moscow, 1966.

189. Prandtl', L., Gidroaeromekhanika /Hydroaeromechanics/, IL, Moscow, 1949.

190. Preobrazhenskiy, V. P., Teplotekhnicheskiye izmereniya i pribory /Heat-Engineering Measurements and Instruments/, Gosenergoizdat, Moscow-Leningrad, 1953.

191. "Instrument for determining coefficients of thermal conductivity (Institute of Technical Thermophysics, Ukrainian SSR Academy of Sciences)," Pribory dlya nauchnykh issledovaniy /Instruments for Scientific Research/, Vol. 5, Izd-vo "Nauka," Moscow, 1967.

192. Rzhevskiy, V. V., and Novik, G. Ya., "Mutual correlation of physical properties of rock," in the book: Fizika gornykh porod i protsessov /Physics of Rock and Processes/, Izd-vo "Nedra," Moscow, 1967, No. 55.

193. Rivin, O. V., "Calorimetric determinations based on heat flux measurements," in the book: Uchenyye zapiski Kazanskogo universiteta /Scientific Notes of Kazan' University/, Izd-vo Kazan'skiy gosudarstvennyy universitet, Alma-Ata, 1957, No. 33.

194. Rozenshtok, Yu. L., and Kaganov, M. A., "Device for measuring heat fluxes," Avt. svid. No. 162981 (Byulleten' izobreteniy, No. 11, 1964).

195. Rytov, S. M., Teoriya elektricheskikh fluktuatsiy i teplo- /18 vogo izlucheniya /Theory of Electrical Fluctuations and Thermal Radiation/, Izd-vo AN SSSR, Moscow, 1953.

196. Savinov, S. I., "Arago-Davy actinometer," Meteorologicheskiy vestnik, No. 7, 1928.

197. Savinov, S. I., "Savinov thermoelectric actinometer," Meteorologicheskiy vestnik, No. 11, 1928.

198. Savinov, S. I., "Theory of Michel'son strip-type actinometer," in the book: Trudy glavnoy geofizicheskoy observatorii /Transactions of Main Geophysical Observatory/, No. 14 (76), Gidrometeoizdat, Leningrad, Leningrad.

199. Svet, D. Ya., Ob"yektivnyye metody vysokotemperaturnoy pirometrii pri nepreryvnom spektre izlucheniya /Objective Methods of High-Temperature Pyrometry for Continuous Radiation Spectrum/, Izd-vo "Nauka," Moscow, 1968.

200. Sellers, D. P., "Thermocouple receivers for estimating local coefficients of heat transfer in rocket engines," in the book: Izmereniye nestatsionarnykh temperatur i teplovykh potokov /Measurement of Nonstationary Temperatures and Heat Fluxes/, Izd-vo "Mir," Moscow, 1966.

201. Semikin, I. D., Kostogryzov, V. S., and Tsygankov, O. L., "New instrument for measuring radiation heat fluxes," Avtomatika i priborostroyeniye, No. 2, 1961.

202. Sergeyev, A. S., "Device for heat flux measurement," Avt. svid. No. 125927 (Byulleten' izobreteniy, No. 3, 1960).

203. Sergeyev, A. S., "Device for heat flux measurement," Avt. svid. No. 185094 (Byulleten' izobreteniy, No. 16, 1966).

204. Sergiyevskaya, T. G., "Heat transfer of stator of electrical machines," Vestnik elektropromyshlennosti, No. 11, 1962.

205. Ser'yeznov, A. N., and Tsapenko, M. P., Metody umen'sheniya vliyaniya pomekh v termoelektricheskikh tsepyakh /Methods of Reducing the Effect of Interference in Thermoelectric Circuits/, Izd-vo "Energiya," Moscow, 1968.

206. Sivkov, A. A., and Gud, V. V., "Pneumatic receiver of radiative energy with strain gage transducer," PTE, No. 1, 1967.

207. Sinel'nikov, A. S., and Chashchikhin, A. S., "Heat transfer of right cylinder as a function of angle of attack," ZhTF, Vol. 2, Nos. 9-10, 1932.

208. Slyusarev, G. G., O vozmozhnom i nevozmozhnom v optike /Possible and Impossible in Optics/, Fizmatgiz, Moscow, 1960.

209. Smirnov, D. A., "Problem of selecting best actinometer," Meteorologicheskiy vestnik, Vol. 18, No. 9, 1908.

210. Smit, R., Dzhons, F., and Chesmer, R., Obnaruzheniye i izmereniya infrakrasnogo izlucheniya /Detection and Measurement of Infrared Radiation/, IL, Moscow, 1959.

211. Smit, R., Poluprovodniki /Semiconductors/, IL, Moscow, 1962.

212. Sterman, L. S., and Styushin, N. G., "Effect of circulation rate on heat transfer in boiling," in the book: Teploperedacha i aerogidrodinamika /Heat Transfer and Aerohydrodynamics/, No. 5, Gosenergoizdat, Leningrad, 1951.

213. Stil'bans, L. S., Fizika poluprovodnikov /Physics of Semiconductors/, Izd-vo "Sovetskoye radio," Moscow, 1967.

214. Strong, D., Tekhnika fizicheskogo eksperimenta /Techniques of Physical Experiments/, Lenizdat, Leningrad, 1948.

215. Subbotkin, M. I., and Kuritsyna, Yu. S., Kislotoupornyye betony i rastvory /Acid-Resistant Concrete and Mortar/, Stroyizdat, Moscow, 1967.

216. Sukhov, S. A., Kadlets, S. Ya., and Pavlyuk, G. D., "Study of electrolytical thermocouple," Izmeritel'naya tekhnika, No. 1, 1959.

216

217. Schastlivyy, G. G., "Device for determining local heat transfer coefficients," Avt. svid. No. 147009 (Byulleten' izobreteniy, No. 9, 1962).

218. Schastlivyy, G. G., Nagrevaniye zakrytykh asinkhronnykh elektrodvigateley /Heating Closed Asynchronous Electric Motors/, Izd-vo "Naukova dumka," Kiev, 1966.

219. Temkin, A. G., "Inverse problems in thermal conductivity," IFZh, Vol. 4, No. 10, 1961.

220. Tikhonov, A. N., and Samarskii, A. A., Uravneniya matematicheskoy fiziki /Equations of Mathematical Physics/, Izd-vo "Nauka," Moscow, 1966.

221. Tkachev, A. G., "Experimental study of heat transfer in melting," in the book: Voprosy teploobmena pri izmenenii agregatnogo sostoyaniya veshchestva /Problems of Heat Transfer with Change in State of Aggregation of Matter/, GEI, Moscow-Leningrad, 1953.

222. Tret'yakov, V. D., "Monometallic actinograph," in the book: Trudy Glavnoy geofizicheskoy observatorii, No. 5 (67), Gidrometeoizdat, Leningrad, 1947.

223. Usov, P. G., Popova, G. N., and Voronova, N. F., "Low-iron talc of Alguyskoye deposit," in the book: Izv. Tomskogo politekhnicheskogo instituta /News of the Tomsk Polytechnic Institute/, Vol. 148, Izd-vo TPI, Tomsk, 1967.

224. Faerman, G. P., Sintsov, V. N., and Popova, K. B., "Evaporography," Optiko-mekhanicheskaya promyshlennost', No. 11, 1962.   /186

225. Fedorov, V. G., and Gerashchenko, O. A., "Transducer for measuring local heat fluxes," Avt. svid. No. 159048 (Byulleten' izobreteniy, No. 23, 1963).

226. Fedoseyev, G. P., "Relations of dielectric and mechanical properties in Mycalex," in the book: Trudy GIPRONIINemetallorud, No. 3, Stroyizdat, Moscow, 1958.

227. Fedot'yev, N. P., Elektroliticheskiye splavy /Electrolytic Alloys/, Mashgiz, Moscow-Leningrad, 1962.

228. Filimonov, S. S., Khrustalev, B. A., and Adrianov, V. N., "Measuring convective and radiative components by the two-radiometer method," in the book: Konvektivnyy i luchistyy teploobmen /Convective and Radiative Heat Transfer/, Izd-vo AN SSSR, Moscow, 1960.

229. Fil'chakov, P. F., and Panchishin, V. I., <u>Integratory EGDA</u> /Electrohydrodynamic Analogy Integrators/, Izd-vo AN USSR, Kiev, 1961.

230. Fingerson, L., and Blekshir, P., "Heat flux receiver for dynamic measurements in high-temperature gases," in the book: <u>Izmereniye nestatsionarnykh temperatur i teplovykh potokov /Measurement of Nonstationary Temperatures and Heat Fluxes/</u>, Izd-vo "Mir," Moscow, 1966.

231. Finkel'shteyn, I. D., <u>Tal'k /Talc/</u>, Promstroyizdat, Moscow, 1952.

232. Kheydzher, N., "Absolute differential radiometer," <u>PNI</u>, No. 9, 1963.

233. Kehydzher, N., "Thin-film heat flux meter," <u>PNI</u>, No. 11, 1965.

234. Tsoglin, Yu. L. et al, "Absolute dosimetry of reactor radiation in reactor core and near reactor core," in the book: <u>Trudy 2-go koordinatsionnogo soveshchaniya po dozimetrii bol'shikh doz /Transactions of the Second Coordinating Conference on High-Dose Dosimetry/</u>, Izd-vo "Fan," Tashkent, 1966.

235. Chervenka, "Instrument for continuous differentiation of experimental curves," <u>PNI</u>, No. 5, 1966.

236. Chernogolov, A. I., "Instruments for measuring heat fluxes in high-temperature furnaces," <u>Zavodskaya laboratoriya</u>, Vol. 15, No. 2, 1949.

237. Chirkin, V. S., <u>Teploprovodnost' promyshlennykh materialov /Thermal Conductivity of Commercial Materials/</u>, Mashgiz, Moscow, 1962.

238. Shabanov, V. V., and Galyamin, Ye. P., "Calorimeter for determining heat fluxes in soil," <u>Avt. svid.</u> No. 147819 (<u>Byulleten' izobreteniy</u>, No. 11, 1962).

239. Shatenshteyn, V. G., "Method of calibrating calorimeters and calibration unit," <u>Avt. svid.</u> No. 163395 (<u>Byulleten' izobreteniy</u>, No. 12, 1964).

240. Shatenshteyn, V. G., "Calibration of high-temperature calorimeters in laboratory set-up," <u>Zavodskaya laboratoriya</u>, Vol. 31, No. 1, 1965.

241. Shvets, I. T., Gerashchenko, O. A., and Dyban, Ye. P.,
"Study of temperature fields in zone of shafts of
turbine blades in electrical models," Teploenergetika,
No. 7, 1957.

242. Shvets, I. T., Dyban, Ye. P., and Gerashchenko, O. A.,
"Study of temperature fields in rims of turbine rotors
by electrothermal analogy method," in the book: Trudy
In-ta teploenergetiki AN USSR /Transactions of the Insti-
tute of Heat-Power Engineering, USSR Academy of Sciences/,
Izd-vo AN UkSSR, Kiev, 1958, No. 14.

243. Yum-Rozeri, V., Atomnaya teoriya dlya metallurgov /Atomic
Theory for Metallurgists/, Metallurgizdat, Moscow, 1955.

244. Yagfarov, M. Sh., and Berg, L. G., "Principles of compara-
tive thermographic method of simultaneous determination
of heat capacity, thermal conductivity, and heats of
reaction," in the book: Trudy 2-go soveshchaniya po
termografii, Izd-vo AN SSSR, Kazan', 1961.

245. Yaryshev, N. A., Teoreticheskiye osnovy izmereni a nesta-
tsionarnykh temperatur /Theoretical Essentials of Measure-
ment of Nonstationary Temperatures/, Izd-vo "Energiya,"
Leningrad, 1967.

246. Yanishevskiy, Yu. D., Aktinometricheskiye pribory i metody
nablyudeniy /Actinometric Instruments and Observation
Methods/, Gidrometeoizdat, Leningrad, 1957.

247. Alpher, R., Gamow, G., and Herman, R., "Thermal cosmic rad-
iation and the formation of protogalaxies," Proc. of the
Nat. Acad. of Sci. of the USA, Vol. 58, No. 6, 1967.

248. Angstrom, K., "Absolute determination of heat with elec-
trical compensation pyrheliometer," Wied. Ann. der Physik,
No. 67, 1899.

249. Ardenne, M. von, Tabellen der Elektronenphysik, Ionenphysik
und Ubermikroskopie /Tables of Electron Physics, Ion
Physics, and Ultramicroscopy/, Deut. Verl. d. Wissen-
schaften, Berlin, Vol. 2, 1956.

250. Bauck, R. H., and Thring, M. W., "A heat-flow meter for use /18
in furnaces," J. Iron and Steel Inst., Vol. 153, No. 1,
1946.

251. Bennet, S. H., Sweet, W. H., and Bassett, D. L., "A heated thermocouple flowmeter," *Journ. Clin. Invest.*, No. 23, 1944.

252. Born, M., "On quantum theory of pyroelectricity," *Rev. mod. phys.*, Vol. 17, No2. 2-3, 1945.

253. Boussinesq. T. V., *Theorie analytique de la chaleur* /Analytical Theory of Heat/, Paris, 1901.

254. Bracht, J., "On the heat conductivity of the earth and snow and heat exchange within the ground," publication of the Geophysical Institute of the Univ. of Leipzig, 14, 1949.

255. Buttner, K., "Physical bioclimatology," *Proleme d. kosm. Physik*, No. 18, Berlin, 1938.

256. Cermak, I., "Thermoelectric measurements of heat flux," *Automatisace*, No. 10, 1958.

257. Cox, M., "Thermal and electrical conductivities of tungsten and tantalum," *Phys. Rev.*, Vol. 64, No. 7, 1943, p. 8.

258. Czerny, M., "Measurement in the rotation spectrum of HCl in the low wave infrared," *Zeitschrift für Physik*, Vol. 37, No. 3, 1926.

259. Czerny, M., "Infrared photography," *Zschr. f. Phys.*, Vol. 53, No. 1, 1929.

260. Debye, P., "Calculation of molecular dimensions from radiometer observation," *Physikalische Zeitschrift*, Vol. 11, 24, 1910.

261. Einstein, A., "On the theory of radiometer forces," *Zeitschrift für Physik*, Vol. 27, No. 1, 1924.

262. Falcenberg, G., "Instrument for the determination of the momentaneous nocturnal heat exchange between earth and air," *Meteorologische Zeitschrift*, Vol. 47, 1930.

263. Fischer, F., Dehn, K., Sustmann, H. "On the increase in thermal forces of oxygen resulting from the use of complex oxides," *Annales der Physik*, Tome 5, Vol. 15, Nos. 5-6, 1932.

264. Fransilla, M., and Huovila, S., "on the measurement of the heat flux into the soil," *Geophysica (Helsinki)*, No. 5, 1957.

265. Garden, R., "An instrument for the direct measurement of intense thermal radiation," *RSI*, Vol. 24, No. 5, 1953.

220

266. Gardon, R. A., "A transducer for the measurement of heat-flow rate," Transact. ASME (Ser. C), Vol. 82, No. 5, 1960.

267. Geiger, R., The Climate of the Air Layer Near the Ground, 3rd Edition, F. Vieweg und Sohn, 1950.

268. Geiling, L., "The thermoelement as a radiation meter," Zschr. f. angew. Phys., Vol. 3, 12, 1951.

269. Gibbs, F. A., "A thermoelectric blood flow recorder in the form of a needle," Proc. Soc. Exper. Biol. Med., Vol. 31, 1933.

270. Hardy, R. G., and Paddock, D. A., "A new thermal radiative flux gage," ISA Trans., Vol. 6, No. 1, 1967.

271. Hatfield, H. S., and Wilkins, F. I., "A new heat-flow meter," J. Sci. Instr., Vol. 27, No. 1, 1950.

272. "Heat-flow detector," RSI, Vol. 26, No. 2, 1956.

273. Hencky, K., "The economic conduction and distribution of steam over large distances," VDI Zschr. Vol. 69 No. 16, 1925.

274. Henning, F., Temperature Measurement, Leipzig, Johan Ambrosius Verlag, 1955.

275. Hensel, H., "A flowcalorimeter for any given points on the body," Zschr. ges. exper. Med., 117, 1951.

276. Hool, J. N., "Local coefficients of skin friction and heat transfer for turbulent boundary layers in two-dimensional diffusors," Aeronaut. Res. Council. Report and Memoranda, London, Oxford University, 1957.

277. Jain, S. C., and Krishnan, K. S., "The distribution of temperature along a thin rod electrically heated in vacuo," Proc. Roy. Soc., I. Theoretical, Vol. 222, No. 1149; II-IV. Theoretical and experimental, Vol. 225, No. 1160, pp. 1-32; V. Time, 1955, Vol. 227, No. 1169, pp. 141-154; VI. End losses, 1955, Vol. 229, No. 1179, pp. 439-444.

278. Jespersen, H. B., "Heat conduction of damp substances and its determination," Gesundheits-Ingenieur, Vol. 74, 1953.

279. Jones, R. C., "Phenomenological description of the response and detecting ability of radiation detectors," Proc. IRE, Vol. 47, No. 9, 1959.

280. Knudsen, M., "An absolute manometer," _Annales der Physik_, Vol. 32, No.4, Item 9, 1910.

281. Koitzsch, R., "Experiments for the determination of water content of the earth on a thermal basis," Proceedings of the Meteorological and Water Service of the GDR, Vol.8 No. 54, 1960.

282. Langmuir, I., "Incandescent lamps and tungsten," _The Collected Works_, Vol. 2, London, Pergamon Press, Oxford, 1960.

283. Lawton, R. W., Prouty, L. R., and Hardy, J. D., "A calorimeter for rapid determination of heat loss and heat production in laboratory animals," _RSI_, Vol. 25, No. 4, 1954.

284. Levy, L., Graichen, H., Stolwijk, J., and Calabresi, M., "Evaluation of local tissue blood flow by continuous direct measurement of thermal conductivity," _J. of Appl. Physiology_, Vol. 22, No. 5, 1967.

285. Maulard, J., "Measurement of high thermal flows by means of sampling," _Rech. aeronaut_, 93, 1963.

286. MECI, _Conversion Tables for Standardized Thermocouples_, Paris, 1962.

287. "Measuring heat flow detectors for attachment to any material," _Engineering_, Vol. 178, No. 4615, 1954.

288. "Measuring the flow of heat," _Engineering_, Vol. 181, No. 4707. 1956.

289. Moll, W.J.H., Burger, H.C., "The thermal relay," _Zeitschrift für Physik_, Vol. 34, 1925.

290. Moll, W.J.H., Burger, H.C., "Senistivity and capability of a galvanometer," _Zeitschrift für Physik_, Vol. 34. 1925.

291. Moll, W. J. H., and Burger, H. C., "The thermo-relay," _Phil. Mag._, Vol. 50, No. 6, 1925.

292. Moll, W. J. H., and Burger, H. C., "The sensitivity of galvanometer and its amplification," _Phil. Mag._, Vol. 50, Series 6, 1925.

293. Moll, W. J. H., and Burger, H. C., "A new vacuum thermoelement," _Phil. Mag._, Vol. 50, Series 6, 1925.

294. Moran, J. P., "Radiant energy measurement," Instrum. and Control Syst., Vol. 38, No. 7, 1965.

295. Morris, L. G., Trickett, E. S., and Moulsley, L. J., "The measurement of heat flow on soil with reference to glass-house heating," Wrest Park, National Institute of Agricultural Engineering, 1955.

296. Musial, N. T., "Heat flux measuring device," U.S. Patent No. 3123996, Off. Gas, Vol. 800, No. 2, 1964.

297. Nagai, M., "Graphical solution of linear heat flow with radiation," Journ. Phys. Soc. Japan, Vol. 11, No. 3, 1956.

298. Niedzialek, B., Chomiak, J., "Simple method for measuring surface temperature by means of total radiation sensors," Prace Institutu Lotnictwa, 31, 1967.

299. Nunner, W., "Heat transfer and pressure decay in rough pipes," VDI-Forschungsheft, Vol. 22, p. 455, 1940.

300. Nusselt, W., "The heat transfer in the combustion engine," VDI-Zeitschrift, Vol. 67, 28, 1925.

301. Ostald,-Luther, Physiochemical Measurements, Leipzig Academy Verlagsgesellsch, 4th Edition, 1925.

302. Pellan, C. M., and Bradley, C. B., "A rapid heat-flow meter thermal conductivity apparatus," Res. a. Stand., Vol. 2, No. 7, 1962.

303. Perls, T. A., Diesel, T. J., and Dubrov, W. I., "Primary pyroelectricity in barium titanate ceramics," J. Appl. Physics, Vol. 29, No. 9, 1958.

304. Perry, K. P., "Heat transfer by convection from a hot gas jet to a plane surface," Proc. Inst. Mech. Engrs., Vol. 168, No. 30, 1954.

305. Petritz, R. L., "Fundamentals of infrared detectors," Proc. IRE, Vol. 47, No. 9, 1959.

306. Powell, W. B., Howell, C. W., and Irving, J. P., "A method for the determination of local transient heat flux in uncooled rocket motors," Jet Propulsion Lab. T.R., 32-257, Pasadena, Calif., 1962.

223

307. Powell, W. B., and Price, T., "A method for the determination of local heat flux from transient temperature measurements," _ISA Trans._, Vol. 3, No. 3, 1964.

308. Prescott, C. H., and Hincke, W. B., "The true temperature scale of carbon," _Phys. Rev._, Vol. 31, No. 1, 1928.

309. Psarouthakis, J., "Apparent thermal emissivity from surfaces with multiple V-shaped grooves," _AIAA Journal_, Vol. 1, No. 8, 1963.

310. Rall, D., and Stempel, F., "A discussion of the standardized procedure for calibrating heat flux transducers," 19th Annual ISA Conference Proceedings, New York, Vol. 19, No. 2, 1964.

311. Rose, P. H., and Stark, W. J., "Stagnation point heat transfer measurement in dissociated air," _JAS_, Vol. 25, No. 2, 1958.

312. Shücke, H., "A quantitative experimental determination of condensation on walls," _Gesundheits-Ingenieur_, 74, 1953.

313. Schmidt, E., _A New Heat Flow Meter and its Practical Significance in Heat Saving Technology_, Munich, 1923.

314. Scmudde, P., "Radometer effect on thin plates of varying temperatures at high pressures (Test of Einstein theory)," _Zeitschrift für Physik_, Vol. 53, No. 5, 1930.

315. Seban, R. A., "The influence of free stream turbulence on the local heat transfer from cylinders," _Transact. ASME_, Series C, Vol. 82, No. 2, 1960.

316. Sprinks, T., "Influence of calorimeter heat transfer gages on aerodynamic heating," _AIAA Journal_, Vol. 1, No. 2, 1963.

317. Stair, R., Schneider, W., Waters, W., and Jackson, J., "Some factors affecting the sensitivity and optical response of thermoelectric (radiometric) detectors," _Appl. Optics_, Vol. 4, No. 6, 1964.

318. Stempel, F. C., and Rall, D. L., "Direct heat transfer measurements," _ISA Journal_, Vol. 11, No. 4, 1964.

319. Storke, P., "Heat transfer measuring apparatus," USA Patent No. 3256734.

320. Swietoslawski, W., _Microcalorimetry_, New York, Reinhold, 1946.

321. Taggart, A. F., _Handbook of Mineral Dressing of Ores and Industrial Minerals_, London, John Wiley, 1960.

322. Treharne, R. W., and Trolander, H. W., "Wavelength-independent direct-reading radiometer," _Journ. Sci. Instr._, Vol. 42, No. 9, 1965.

323. Tunmore, B. G., "A simple radiometer for the measurement of radiative heat exchange between buildings and their environment," _Journ. Sci. Instr._, Vol. 39, No. 5, 1962.

324. De Waard, R., and Wormser, E. M., "Description and properties of various thermal detectors," _Proc. IRE_, Vol. 47, No. 9, 1959.

325. Warmbt, W., "Heat flow measurements for physiological purposes by using foil heat flow meters," _Zeitschrift ges. inn. Med. u. Grenzgeb_, 19, 1963.

326. Warmbt, W., "Comparative investigations with heat flow meters to determine momentaneous cooling values," _Zeitschrift für angew. Meteor._, 4, 1961.

327. Warmbt, W. "On the use of heat flow mearurement proceedures in bioclimatology," _Wiss. Zschr. f. techn. Univ. Dresden_, Vol. 13, No. 5, 1964.

328. Watts, D., "Heat flux responsive device," USA Patent No. 3238775, _Official Gazette_, March 8, 1966.

329. White, R. G., _Handbook of Industrial Infrared Analysis_, New York, Plenum Press, 1964.

330. Willaughby, A. B., "Absolute water flow calorimeter for measurement of intense beams of radiant energy," _RSI_, Vol. 25, No. 7, 1954.

331. Wilson, W. H., and Epps, T. D., "The construction of thermocouples by electrodeposition," _Phys. Soc. Proc._, Vol. 32, Part 5, 1921.

332. Witte, A., and Harper, E., "Experimental investigation of heat transfer in rocket thrust chambers," _AIAA Journal_, Vol. 1, No. 2, 1963.

333. Wolf, R. W., "A selected bibliography on IR techniques and applications," _Proc. IRE_, Vol. 47, No. 9, 1959.

225

END

DATE

FILMED

DEC 26 1979